



Bacterial Removal of Iron Impurities to Increase the Quality and Value of Industrial Minerals

A thesis submitted to the Newcastle University in partial fulfilment of the requirements for the degree of Doctor of Philosophy in the Faculty of Science,
Engineering and Agriculture

Sani YAHAYA

School of Civil Engineering & Geosciences
Newcastle University, UK

September, 2011

DECLARATION

Except where acknowledgment has been given, this thesis is the work of the author. No part of the material offered has been submitted previously for a degree or other qualification in this, or any other University.

Sani YAHAYA, September, 2011.

ACKNOWLEDGEMENTS

I would like to sincerely thank my supervisor Professor David Manning not only for the supervisory role but also for the fatherly role he served throughout my studies. Thank you so much. My thanks also to Professor Ian Head for the advice he gave me. I would like to acknowledge Dr. Claire Fialips for initiating the project and Dr. Asfaw Zegeye for all the laboratory skills I have acquired through him, your assistance will never be forgotten.

Special thanks to Mr. Rob Hunter for fabricating my bioreactor and Mr. Phil Green for his useful advices. I am also grateful to Mr Graham Patterson for all the computing support he has offered. My appreciation goes to Maggie White for conducting the XRD analysis. I will specially extend my acknowledgment to Mrs Margaret Wardley and Mrs Yvonne Hall.

I am extremely grateful to my parents and all my family members for their tireless effort and continuous support in my entire life. I thank you all. Special appreciation to Ahmed Umar, Bashar Bature, Aminu Bature, Salisu Yahaya, Abdullahi Abubakar, Mustapha Bature, Shafi'u Isah Gwadabawa, Abdulhamid Bature, Abba, Jabir, Sale and Buhari. I also wish to acknowledge Hajiya Balkisu Ajiya and Rukayya, Fatima, Zainab and Hafsatu. I am especially grateful to my fiancée (Farida) for all her advices, supports and encouragements. Thank you for standing behind me, I really count on you so much.

I would like to thank my colleagues who have in one way or the other contributed to the success of this piece of research; Musa Bashir, Bello Adamu, Kasim Muhammad, Bello Imam, Umar Ba, Aminu Muhammad Bayawa, Sani Mua'zu Makarfi, Waziri Galadima, Ojuigo Okafor, Uzochukwu Ugochukwu, Nikky Allen, Hilmi Senin and the entire staffs of the School of Civil Engineering and Geosciences.

I would like to finally extend my sincere appreciation to Imerys Minerals Ltd, OMYA Ltd, and WBB Minerals/Sibelco UK, for their kind support at every time needed during the course of this research.

Thank you all
Sani YAHAYA

DEDICATION

I dedicated this thesis to my uncle Alhaji Bature Muhammad Shinkafi for all the support he has been offering toward successful completion of this piece of research. Thank you.

ABSTRACT

Kaolin, silica sand and high grade carbonates are industrial minerals widely and extensively used as fillers and coating agents in the manufacture of paper, ceramics, glass, paint and cosmetics. When mined, kaolin and silica sand are generally not pure, often associated with iron hydroxide and oxy-hydroxide impurities (ranging between 0.074 up to 44.2mg Fe per gram of mineral) usually in the form of Fe^{3+} -phases adsorbed onto the mineral surface, covering the entire mineral surface, or admixed as a separate iron bearing phase. The iron-bearing impurities associated with calcium carbonate are mostly ferrous (Fe^{2+}) in the form of siderite (FeCO_3). In all cases, the presence of iron affects the colour and the physical properties of the mineral, and so lowers the industrial value and limits the application and uses. Due to the environmental, economic and operational disadvantages associated with conventional physical and chemical refining processes, this thesis considers a microbial refining process in a closed non-growth system as an alternative for iron removal from these minerals.

Bioreduction was initially optimised using 80ml microcosm batch experiments and subsequently up-scaled to a 4.5L closed system bioreactor with continuous monitoring of pH, Eh and temperature. The anaerobic removal of Fe(III)-bearing impurities from these minerals was investigated using different iron-reducing *Shewanella* strains (*S. putrefaciens* CIP8040, *S. putrefaciens* CN32, *S. oneidensis* MR-1, *S. algae* BrY and *S. loihica*) in the presence of anthraquinone 2,6 disulphonate (AQDS) serving as electron shuttling mediator. The efficiency of natural organic matter (NOM) was also investigated as a substitute for AQDS.

In the microcosm experiments, up to 4.4% of the insoluble Fe(III) in kaolin (as determined by XRF) was successfully reduced to more soluble and leachable Fe(II) by the five different iron reducing bacteria (except *S. loihica*) after 5 days. This was equivalent to 46.6mg of bioreducible Fe_2O_3 per 100g of kaolin. After bioreduction, the colour value of the biotreated kaolin mineral improved, with a substantial increase in brightness from 76.1% to 79.7% and whiteness from 57.7% to 67.8%. For the silica sand, up to 17.6% of the iron bearing impurities (~117mg of bioreducible Fe_2O_3 per 100g of silica sand) was successfully removed

after 15 days. In both cases, addition of AQDS as electron transport mediator enhanced the rate and extent of bioreduction by facilitating the exchange of electrons between the iron-reducing bacteria and the iron-bearing phase in the mineral. Natural organic matter also increased the rate and extent of Fe(III) reduction when compared with experiments without electron shuttling mediators.

Because iron-bearing impurities present in the carbonate (chalk) were mostly ferrous, biotreatment by iron reduction was unable to improve significantly the iron content and colour properties in this mineral. Another microbial bioleaching method was tested for the carbonate using *Desulfovibrio desulfuricans*. *Desulfovibrio desulfuricans*, which is a sulphate reducing bacterium, was able to leach Fe from the chalk but the Fe immediately precipitated as a different iron phase (probably iron sulfide) giving a dark coloration to the chalk. The colour properties did not improve, with the colour value decreasing below the initial value after sequential centrifugation.

The 4.5L batch bioreactors designed to upscale the bioleaching process successfully supported the bioreduction of Fe(III)-oxide in both kaolin and silica sand. Up to 5.9% of the total iron bearing impurities of the same kaolin material was removed (equivalent to 62.2mg of bioreducible Fe₂O₃ per 100g of kaolin material) with appreciable improvement in brightness from 75.79% to 79.06% and whiteness from 55.69% to 66.01%), similar to what was observed in the small scale microcosm study. Bioleaching of silica sand (King's Lynn) in the batch reactors successfully removed up to 53.9% of Fe-bearing impurities (~89.03mg of Fe₂O₃ per 100g of silica material) on day 4. The bioreduction did not cause any unfavourable modification in the mineralogy of either kaolin or silica sand, and no apparent crystalline by-product was formed after biotreatment.

TABLE OF CONTENT

DECLARATION	ii
ACKNOWLEDGEMENTS	iii
DEDICATION	iv
ABSTRACT	v
TABLE OF CONTENT	vii
LIST OF FIGURES	xi
LIST OF TABLES	xvi
APPENDIX	xix
CHAPTER 1 : INTRODUCTION AND LITERATURE REVIEW	1
1.1: INTRODUCTION	1
1.2: OCCURRENCE, SUPPLY AND MARKET CONSUMPTION OF THE MINERALS	3
1.2.1: Kaolin	3
1.2.2 Silica sand	4
1.2.3: Calcium carbonate (Chalk)	5
1.3: Trade and values of the minerals	6
1.4: Current conventional iron leaching process	9
1.4.1: Froth flotation	9
1.4.2: Selective flocculation	9
1.4.3: Magnetic Separation	10
1.5: CHEMICAL AND STRUCTURAL COMPOSITION OF THE MINERALS	10
1.5.1: Mineral composition and structure of kaolinite	10
1.5.2: Silica minerals and their chemical composition	11
1.5.3: Calcium carbonate minerals and their chemical composition	12
1.6: THE IRON OXIDES AND OXYHYDROXIDE IMPURITIES	12
1.6.1: Iron oxy-hydroxide minerals	12
1.6.2: Reduction of Fe(III) oxides in soils and sediments	13
1.7: BIOMINERALISATION OF IRON BY REDUCING MICROORGANISMS	15
1.7.1: Role of bacteria in biomineralisation of iron	15
1.7.2: Diversity of dissimilatory iron-reducing bacteria in the environment	16
1.8: MECHANISMS OF DISSIMILATORY IRON REDUCTION PROCESSES AND ROLE OF ELECTRON SHUTTLES	21
1.8.1: Reduction via direct contact with insoluble iron (III) oxide	22
1.8.2: Reduction of insoluble iron via an external electron shuttle	23
1.9: PREVIOUS STUDIES ON THE BIOLEACHING OF CLAY AND IRON CONTAINING MINERALS	25
1.10: Aim and objectives	27
CHAPTER 2 : MATERIALS AND METHODS	29
2.1: INTRODUCTION	29
2.2: SAMPLE DESCRIPTION	29
2.2.1: Kaolin samples	29
2.2.2: Silica sand samples	31

2.3: NATURAL ORGANIC MATTER.....	33
2.4: BIOREDUCTION CULTURES	34
2.4.1: Procurement of <i>Shewanella</i> pure cultures	34
2.4.3: Preparation of <i>Shewanella</i> inoculum	35
2.4.4: Bacterial plate count using serial dilution	37
2.4.5: Bioreduction cultures.....	37
2.5: PREPARATION OF TITRATION SOLUTION	38
2.5.1: Fe(II) standard	38
2.5.2: 1, 10-Phenanthroline monohydrate	39
2.5.3: Glycine.....	39
2.5.4: Nitrilotriacetic acid (NTA).....	39
2.5.5: Preparation of titration mixture.....	39
2.5.6: Measurement of standard calibration curve	39
2.5.7: Analysis of HCl-extractable Fe(II) using the phenanthroline technique	40
2.6: Soxhlet extraction of Natural Organic Matter	41
2.7: ANALYTICAL METHODS.....	41
2.7.1: Total Carbon Nitrogen and Hydrogen analysis	41
2.7.2: Total Organic Carbon analysis	41
2.7.3: Colour analysis using Colour Touch PC analyser	42
2.7.4: X-ray Fluorescence spectrometry	43
2.7.4.1: X-ray Fluorescence (kaolin samples)	43
2.7.5: Infrared spectroscopy	43
2.7.6: Electron Microscopy.....	44
2.7.7: X – Ray Diffraction	46
2.7.8: Mössbauer spectroscopy	47
2.7.9: Pyrolysis - Gas Chromatography – Mass Spectroscopy	48
2.8: BIOREACTOR EXPERIMENTS	49
2.8.1. Design of bioreactor	49
2.8.2: Reactor bioreduction experiments	49
CHAPTER 3 : BIOREDUCTION OF KAOLIN PART I: OPTIMISATION AND MECHANISM OF REACTION ...	52
3.1: INTRODUCTION.....	52
3.2: METHODOLOGY.....	53
3.3 RESULTS	54
3.3.1: Selection of the most suitable iron reducing bacteria.	54
3.3.2: Effect of temperature on the bioreduction of Fe(III) in kaolin	57
3.3.3: Effect of solid/liquid ratio on bioreduction of Fe(III) in kaolin.....	58
3.3.4: Effect of cell/solid ratio on Fe(III) bioreduction	61
3.3.5: Effect of different concentrations of electron donor.	63
3.3.6: Effect of microcosm re-amendment on Fe(III) bioreduction	64
3.3.7: Influence of electron donor concentration and re-inoculation of cells for Fe(III) bioreduction in kaolin.	66
3.4: STOICHIOMETRY AND MASS BALANCE OF MINERAL FE(III) RESPIRATION.....	68

3.4.1: Total organic carbon analyses.....	69
3.4.2: Stoichiometry of lactate oxidation couple to Fe(III) reduction in kaolin	70
3.5: BACTERIAL FE(III) REDUCTION KINETICS IN KAOLIN	72
3.5.1: Rates of reaction	72
3.5.2: Integrated rate order kinetics for Fe(III) reduction in kaolin.	75
3.5.3: Rate of Fe(II) production and substrate consumption using Michaelis-Menten kinetics..	77
3. 6: DISCUSSION	79
CHAPTER 4 : BIOREDUCTION OF KAOLIN PART II: PROPERTIES OF SOLID PRODUCTS	85
4.1: INTRODUCTION.....	85
4.2: RESULTS	85
4.2.1: Bioreduction of kaolin-bound Fe(III) in the presence of AQDS, NOM or absence of electron shuttle	85
4.2.2: Bioreduction of kaolin Fe(III): relative importance of biogenic and abiotic factors	88
4.2.3: Investigation and assessment of possible AQDS Sorption on the surface of Kaolin 3.....	91
4.3: PERCENTAGE REMOVAL OF FE- BEARING IMPURITIES FROM INITIAL KAOLIN	93
4.4: EFFECT OF BIOREDUCTION ON THE MINERALOGY AND TEXTURE OF KAOLIN.	94
4.5: DISCUSSION	102
CHAPTER 5 : BIOLEACHING OF SILICA SAND USING BATCH MICROCOSM	107
5.1: INTRODUCTION.....	107
5.2: METHODOLOGY	108
5.3: RESULTS	109
5.3.1: Selection of the most suitable iron reducing bacteria	109
5.3.2: Effect of cell density on the rate and extent of Fe(III) reduction.....	110
5.3.3: Effect of electron shuttling system on the initial rate and extent of Fe(III) reduction	111
5.3.4: Bioreduction of silica sand bound Fe(III) in the presence of AQDS, NOM or absence of electron shuttle.	114
5.3.4: Effect of electron donor concentration and re-inoculation of cells for Fe(III) reduction in silica sand	115
5.3.4: Reaction kinetics	118
5.3.5: Integrated rate order kinetics	120
5.4: EFFECT OF BIOREDUCTION ON THE MINERALOGY OF SILICA SAND	121
5.5: DISCUSSION	127
CHAPTER 6 : BIOLEACHING OF KAOLIN AND SILICA SAND USING 4.5L BATCH BIOREACTOR.....	132
6.1: INTRODUCTION.....	132
6.2: METHODOLOGY	134
6.3: RESULTS	135
6.3.1: Preliminary investigation and optimisation	135
6.3.2: Batch bioreactor experiment with Kaolin 2	137
6.3.3: Batch bioreactor experiment with Kaolin 3	140
6.3.4: Batch bioreactor experiment with Kaolin 4	142
6.4: Bioleaching of silica sand.....	144
6.5: EFFECT OF BIOREDUCTION ON THE MINERALOGY.....	146
6.6: DISCUSSION	154

CHAPTER 7 : BIOLEACHING OF CALCIUM CARBONATE (CHALK).....	158
7.1: INTRODUCTION.....	158
7.2: METHODOLOGY.....	160
7.2.1: Carbonate sample:	160
7.2.2: Selection of commercially available bacteria for the bioleaching of carbonate.....	160
7.2.3: Microcosm experiment using <i>Desulfovibrio desulfuricans</i>	161
7.2.4: Bioleaching experiment using <i>Pseudomonas mendocina</i>	162
7.2.5: Microcosm experiments with Iron reducing bacteria.....	162
7.2.6: Mineralogical assessment.....	163
7.3: RESULTS	163
7.3.1: Batch scale microcosm studies using iron-reducing bacteria	163
7.3.2: Bioleaching of chalk using <i>Pseudomonas mendocina</i>	166
7.3.3: Bioleaching of chalk using <i>desulfovibrio desulfuricans</i>	167
7.4: EFFECT OF BIOLEACHING ON THE MINERALOGY	168
7.5: Effect of bioleaching process on the mineral type	170
7.6: DISCUSSION:	172
CHAPTER 8 : GENERAL DISCUSSION	176
8.1: Optimisation of bioleaching process using small scale microcosm	177
8.2: Effect of multiple cell injection during bioreduction	179
8.3: Effect of electron transfer mediators on the rate and extent of bioreduction	180
8.4: Bioleaching of chalk using <i>Pseudomonas mendocina</i> and <i>Desulfovibrio desulfuricans</i>	182
8.5: Comparison of iron removed from kaolin silica sand and carbonate (chalk)	183
8.6: Batch scale bioreactor experiments.....	184
8.7: Impact of bioleaching on mineralogy.....	185
CHAPTER 9 : GENERAL CONCLUSION AND FUTURE WORK	187
9.1: GENERAL CONCLUSION	187
9.2: FUTURE WORK.....	190
REFERENCES.....	193

LIST OF FIGURES

CHAPTER 1

Figure 1.1: Granite outcrops and kaolin clay deposit of south-western England. Source: The ball clay heritage society (www.clayheritage.org/pages/whatisballclay.htm).

Figure 1.2: Locations of silica sand quarries in England, active in 1990, according to geological age of extracted deposit. Source (Department et al., 1996)

Figure 1.3: Distribution of principal industrial chalk resources in the United Kingdom. Source (online image access from (<http://openlearn.open.ac.uk/mod/oucontent/view.php?id=399847§ion=6>))

Figure 1.4: Diagrammatic sketch showing crystal structure of kaolinite mineral. The Al in the silicate structure may be substituted by Fe. Source (Dr. Claire Fialips lecture slides 2008)

Figure 1.5: Iron cycling in natural environment. Source from Luu and Ramsay, (2003).

Figure 1.6: Mechanism of iron reduction via direct contact with the insoluble iron (III) oxide minerals.

Figure 1.7: model for AQDS serving as an electron shuttle between iron (III)-reducing microorganisms and insoluble iron oxides

CHAPTER 2

Figure 2.1 : Picture showing sampling of freshly exposed rock of (a) kaolin 1 and (b) the anaerobic jar use to transport the sample under anoxic condition. (Photos from Asfaw Zegeye).

Figure 2.2: Picture of Oakamoor quarry site used to sample silica sand 1 and silica sand 2. (Photo from Claire Fialips)

Figure 2.3: Picture of the sampling site for silica sand 3 (King's Lynn Quarry)

Figure 2.4: Diagrammatic illustration of bacterial culturing method.

Figure 2.5: Illustration of experimental set up for the small scale bioleaching of kaolin and silica sand.

Figure 2.6: General illustration of the 4.5 litre batch bioreactor designed for the up-scaling of bioleaching experiment.

CHAPTER 3

Figure 3.1 Line plots showing extractable Fe(II) concentration from 20g kaolin 2 (Remblend) as a function of time obtained to compare different iron-reducing *Shewanella* strains in the presence of 10mM lactate and 100µM AQDS at 20°C.

Figure 3.2: Bar chart showing the optical property of raw and bio-treated kaolin (A) % ISO Brightness (B) % Yellowness (C) % Whiteness using different iron-reducing *Shewanella* strains for 5 days at 20°C.

Figure 3.3: Line plots showing extractable Fe(II) concentration at different temperature using *S. putrefaciens* CIP8040.

Figure 3.4: Bioreduction of kaolin bound-Fe(III) by *S. putrefaciens* CN32 and *S. putrefaciens* CIP8040 using 10g or 20g mineral mass in 80ml of solution. Experiments were run at 30°C.

Figure 3.5: Colour analyses of kaolin after bioreduction with *S. putrefaciens* CN32 and *S. putrefaciens* CIP8040 using 10g or 20g at 30°C.

Figure 3.6: Bioreduction of Fe(III) from 10g and 20g kaolin using different injection of *S. putrefaciens* CIP8040 cell suspension ($1.2 \pm 0.4 \times 10^8$ CFU/mL) at 30°C.

Figure 3.7: Bioreduction of 20g Kaolin under varying lactate concentrations (0.1 – 1mM) in the absence of electron shuttling system. Experiment was conducted at 30°C.

Figure 3.8: Bioreduction of 10g Kaolin 2 amended with acetate, kaolin and fresh cells at 192 hours with one of the treatment left unamended since the start of experiment. Experiment was run under 30°C using *S. putrefaciens* CIP8040.

Figure 3.9: Bioreduction of kaolin under different concentration of electron donor (5–20mM) and multiple inoculations of *S. putrefaciens* CIP8040 at 30°C. Error bars represent standard error for three replicates

Figure 3.10: Correlation between TOC measured over time and Fe(II) leached after bioreduction of kaolin in experiment added with 5, 10, 15 and 20mM lactate. Equations and coefficients of regression (r^2) values determined from linear regression analysis are given from each lactate concentration.

Figure 3.11: Semi-log plot of Fe(II) concentration against time for different concentration of lactate (0.1 – 1mM) predicting reaction kinetic order of Fe(III) reduction in kaolin.

Figure 3.12: TOC equivalent of lactate depleted over time during bioreduction of kaolin under varying concentration of lactate. Equations and coefficients of regression (r^2) values determined from linear regression analysis are given for each lactate concentration.

Figure 3.13: Plot of rate of Fe(III) reduction overtime against concentrations of lactate (0.1 -0.5) showing first order rates and linear increase of Fe(II) production between 2 to 18 hours. Equations and coefficients of regression (r^2) values determined from linear regression analysis are given for 4, 6 and 8 hours.

Figure 3.14: Plot of rate of Fe(III) reduction over time against concentrations of lactate (0.1 -1mM) linear increase of Fe(II) production and possible saturation point. Equations and coefficients of regression (r^2) values determined from linear regression analysis are given for 4 and 12 hour.

Figure 3.15: Plot of rate of Fe(II) production overtime against concentrations of lactate (0.1 -1mM) using Michaelis-Menten kinetic.

CHAPTER 4

Figure 4.1: Comparison of rate and extent of microbial Fe(III) reduction from Kaolin 4 in the presence of either AQDS, NOM 1 or absence of electron shuttle at 30°C using 20g kaolin mineral.

Figure 4.2: Comparison of rate and extent of microbial Fe(III) reduction from Kaolin 3 in the presence of either AQDS, NOM 1, NOM 2 or absence of electron shuttle at 30°C using 10g kaolin mineral.

Figure 4.3: Rate and extent Fe(III) bioreduction from Kaolin 4 (Melbur Yellow MGP, a bleached kaolin) as a function of microbial cell suspension added. The experiment was run at 30°C.

Figure 4.4: Rate and extent Fe(III) bioreduction from Kaolin 3 (Melbur Yellow HCP, an unbleached kaolin) as a function of microbial cell suspension added. The experiment was run at 30°C.

Figure 4.5: Colour analysis of biotreated Kaolin 4 (Melbur Yellow MGP, a bleached kaolin) after 10 days incubation using *Shewanella putrefaciens* CIP8040.

Figure 4.6: Colour analysis of biotreated Kaolin 3 (Melbur Yellow HCP, an unbleached kaolin) after 10 days incubation using *Shewanella putrefaciens* CIP8040.

Figure 4.7: Investigation of adsorption of AQDS and lactate on different surface area of Kaolin 3 (Melbur Yellow HCP, an unbleached kaolin).

Figure 4.8: XRD pattern of Kaolin 2 (Remblend) before and after bioreduction using *S. putrefaciens* CIP8040 at 30°C.

Figure 4.9: FTIR spectra of Kaolin 2 (Remblend) before and after bioreduction using *S. putrefaciens* CIP8040 at 30°C.

Figure 4.10: Scanning electron micrographs showing the morphology of Kaolin 2 (Remblend) before and after bioreduction using *S. putrefaciens* CIP8040 at 30°C.

Figure 4.11: Mössbauer spectra (4.5K) of biotreated and blank Kaolin 3 (Melbur Yellow HCP) in the presence of AQDS using *S. putrefaciens* CIP8040 at 30°C.

Figure 4.12: Room Temperature (RT) Mossbauer spectra of biotreated and blank Kaolin 3 (Melbur Yellow HCP) in the presence of AQDS using *S. putrefaciens* CIP8040 at 30°C.

Figure 4.13: Mössbauer spectra (290K) of Kaolin 2 (Remblend) before and after bioreduction using *S. putrefaciens* CIP8040 at 30°C in reflection mode.

Figure 4.14: Mössbauer spectra (6.5K) of Kaolin 2 (Remblend) after bioreduction using *S. putrefaciens* CIP8040 at 30°C in transmission mode.

CHAPTER 5

Figure 5.1: Line plot showing extractable Fe(II) concentration from 2.5g Silica Sand 2 as a function of time to compare different iron-reducing *Shewanella* strains in the presence of 10mM lactate and 100µM AQDS at 20°C

Figure 5.2: Bioreduction of Fe(III) from 2.5 g Silica Sand 3 using different injection of *S. putrefaciens* CIP8040 cell suspension ($1.2 \pm 0.4 \times 10^8$ CFU/mL) at 30°C. Error bars represent standard error for three replicates.

Figure 5.3: Rate and extent of microbial reduction of Fe(III) using Silica Sand 3 in the presence and absence of AQDS at 30°C with the injection of 4ml of *S. putrefaciens* CIP8040 cell suspension at 1.2×10^8 CFU/mL.

Figure 5.4: Impact of electron potential of AQDS and NOM 2 on the Fe(III) reduction rate of Silica Sand 2 with variable injection of *S. putrefaciens* CIP8040 at 30°C.

Figure 5.5: Comparison of rate and extent of microbial Fe(III) reduction from Silica Sand 3 in the presence of either AQDS, NOM 1, NOM 2 or absence of electron shuttle at 30°C with the injection of 4ml cell suspension of *S. putrefaciens* CIP8040.

Figure 5.6: Bioreduction of Silica Sand 3 under different concentration of electron donor (1 – 15mM lactate) and multiple inoculations of *S. putrefaciens* CIP8040 at 30°C. Error bars represent standard error for three replicates.

Figure 5.7: Individual plots for the bioreduction of Silica Sand 3 under different concentration of electron donor (1 – 15mM lactate) showing different inoculations time of *S. putrefaciens* CIP8040 at 30°C. Error bars represent standard error for three replicates.

Figure 5.8: Semi-log plot of Fe(III) concentration against time for different concentration of lactate (1 – 15mM) predicting reaction kinetic order of Fe(II) production in silica sand. Equations and

coefficient of regression (r^2) values determined from linear regression analysis are given for each lactate concentration.

Figure 5.9: Plot of rate of reduction overtime against concentrations of lactate (1 – 15mM) showing zero order rate of Fe(II) production. Equations and coefficient of regression (r^2) values determined from linear regression analysis are given for 2 and 6 hour.

Figure 5.10: XRD pattern of Silica Sand 3 before and after bioreduction with *S. putrefaciens* CIP8040 at 30°C.

Figure 5.11: FTIR spectra of Silica Sand 3 after biotreatment with *S. putrefaciens* CIP8040 at 30°C.

Figure 5.12: FTIR spectra of initial, blank and biotreated Silica Sand 3 using *S. putrefaciens* CIP8040 at 30°C.

Figure 5.13: Scanning electron micrographs showing the morphology of Silica Sand 3 before bioreduction.

Figure 5.14: Scanning electron micrographs showing the morphology of Silica Sand 3 after bioreduction with *S. putrefaciens* CIP8040 at 30°C.

Figure 5.15: Mössbauer spectra of un-treated Sand 3 in transmission mode.

CHAPTER 6

Figure 6.1: Bioleaching of Fe(III) in Kaolin 2 (Remblend) in a batch bioreactor experiment as function of time. Error bars represent standard error for two replicates.

Figure 6.2: Time profile of pH and redox potential (E_h) in biotreated and blank reactor during bioleaching of Kaolin 2 (Remblend) using *Shewanella putrefaciens* CIP8040 from 19/Jan/2011 to 24/Jan/2011.

Figure 6.3: Time profile of temperature plot in biotreated and blank reactor during bioleaching of Kaolin 2 (Remblend) using *Shewanella putrefaciens* CIP8040 from 19/Jan/2011 to 24/Jan/2011.

Figure 6.4: Colour analysis of Kaolin 2 (Remblend) before and after bioreduction with *S. putrefaciens* CIP8040 at 30°C.

Figure 6.5: Bioleaching of Fe(III) in Kaolin 3 (Melbur Yellow HCP) in a batch bioreactor experiment as function of time. Error bars represent standard error for two replicates.

Figure 6.6: Colour analysis of Kaolin 3 (Melbur Yellow HCP) on day 5 and 10 before and after bioreduction with *S. putrefaciens* CIP8040 at 30°C.

Figure 6.7: Bioleaching of Fe(III) in Kaolin 4 (Melbur Yellow MGP) using batch bioreactor experiment as function of time. Error bars represent standard error for two replicates.

Figure 6.8: Bioleaching of Fe(III) in 140g Silica Sand (Oakamoor) using batch bioreactor experiment as function of time. Error bars represent standard error for two replicates.

Figure 6.9: Bioleaching of Fe(III) in 70g Silica Sand 3 (Oakamoor) in a batch bioreactor experiment as function of time. Error bars represent standard error for two replicates.

Figure 6.10: Scanning electron micrograph showing the morphology of Kaolin 3 (Melbur Yellow HCP) before and after bioreduction using *S. putrefaciens* CIP8040.

Figure 6.11: Scanning electron micrograph showing the morphology of Silica Sand 3 (Oakamoor) after bioreduction using *S. putrefaciens* CIP8040.

Figure 6.12: Scanning electron micrograph showing the morphology of blank Silica Sand 3 (Oakamoor).

Figure 6.13: XRD pattern of Kaolin 3 (Melbur Yellow HCP) before and after batch bioreactor experiment using *S. putrefaciens* CIP8040.

Figure 6.14: XRD pattern of Kaolin 4 (Melbur Yellow MGP) before and after batch bioreactor experiment using *S. putrefaciens* CIP8040.

Figure 6.15: XRD pattern of Silica Sand 3 (King's Lynn) before and after batch bioreactor experiment using *S. putrefaciens* CIP8040.

Figure 6.16: FITR spectra of Kaolin 3 (Melbur Yellow HCP) before and after batch bioreactor experiment in the presence of *Shewanella putrefaciens* CIP8040.

Figure 6.17: FITR spectra of Silica Sand 3 (Oakamoor) before and after batch bioreactor experiment in the presence of *Shewanella putrefaciens* CIP8040.

CHAPTER 7

Figure 7.1: Production of Fe(II) from chalk (W41723) at 20°C using *Shewanella loihica* suspension in the presence of ADQS and/or NTA.

Figure 7.2: Production of Fe(II) from 10 and 20g chalk (W41723) at 30°C using *Shewanella putrefaciens* CIP8040 suspension in the presence of ADQS

Figure 7.3: Bioleaching of chalk (W41723) using aerobic *Pseudomonas mendocina*. Experiment was run at 30°C for 15 days.

Figure 7.4: Picture of chalk (W41723) on day 1 and day 15 during bioleaching with sulfur-reducing *Desulfovibrio desulfuricans* at 30°C.

Figure 7.5: FTIR spectra of chalk (W41723) after biotreatment with *P. mendocina* and *D. desulfuricans*.

Figure 7.6: XRD pattern of chalk (W41723) before and after bioleaching with *Pseudomonas mendocina*.

Figure 7.7: Amount of Fe(II) removed in aqueous solution (80mL) between kaolin (20g), silica sand (2.5g) and carbonate (20g) leached in the presence of *S. putrefaciens* CIP8040.

Figure 7.8: Amount of Fe₂O₃ removed in gram per 100g of kaolin, silica sand and carbonate in the presence of *S. putrefaciens* CIP8040.

LIST OF TABLES

CHAPTER 1

Table 1.1: English production of silica sand in 2007 (British Geological Survey, 2009a).....	5
Table 1.2: England production of calcium carbonate (chalk) in 2004 (British Geological Survey, 2006).	5
Table 1.3: Prices (per tonne) of Kaolin, silica sand and chalk (Industrial Mineral, 2009).....	7
Table 1.4: United Kingdom summary of total annual exports and imports of silica sand, chalk and kaolin between 2005 -2009 with the total commodity prices based on the tonnage produced (Bide et al., 2010)	8
Table 1.5: Examples of oxides and oxyhydroxide irons in the environment, from Cornell and Schwertmann, (2003).....	13
Table 1.6: Lactate oxidation couple to the reduction of some iron oxide.....	15
Table 1.7: Summary of literature on some Iron reducing bacteria	19

CHAPTER 2

Table 2.1: Initial XRF, surface area, particle size and colour index data provided by Imerys Minerals Ltd. (kaolin) and WBB/Sibelco (silica sand) for the different mineral materials supplied for the experiments.	31
Table 2.2: Illustration of dilutions of Fe(II) standard solutions and absorbance values measured.....	40

CHAPTER 3

Table 3.1: Colour analyses of kaolin after bioreduction with different injection of <i>S. putrefaciens</i> CIP8040 on day 5.	63
Table 3.2: Colour analyses of biotreated kaolin re-amended with acetate, <i>S. putrefaciens</i> CIP8040 cells and kaolin after 192 hours.	66
Table 3.3: Colour analyses of biotreated kaolin using different concentration of electron donor and re-injection of <i>S. putrefaciens</i> CIP8040 at different interval.	68
Table 3.4: Analyses of organic and inorganic carbon from different standard solutions of lactate	69
Table 3.5: Analyses of organic and inorganic carbon from different standard solutions of lactate and acetate	69
Table 3.6: Total organic carbon data in microcosm after 130 hours under varying lactate concentration.....	70
Table 3.7: Rate of Fe(III) reduction determined in microcosms amended with 0.1 – 1mM lactate.....	74
Table 3.8: Rate of total organic carbon removal calculated in microcosm amended with 5 -20mM lactate.	75

CHAPTER 4

Table 4.1: Colour analyses of Kaolin 3 (Melbur Yellow HCP) after bioreduction in the presence of AQDS, NOM 1, NOM 2 or absence of electron shuttle	88
Table 4.2: Removal of Fe-bearing impurities in kaolin 2 (Remblend) using different iron reducing bacteria.	93
Table 4.3: Removal of Fe-bearing impurities in Kaolin 3 (Melbur Yellow HCP) using different electron shuttles in the presence of <i>S. putrefaciens</i> CIP8040.....	94
Table 4.4: Elemental composition of blank kaolin 2 (Remblend) using EDX analysis (quantitative analysis).these tables need to be simplified and corrected	97
Table 4.5: Elemental composition of biotreated Kaolin 2 (Remblend) using EDX analysis (quantitative analysis).....	98

CHAPTER 5

Table 5.1: Elemental composition of blank silica sand using EDX analysis.....	125
Table 5.2: Elemental composition of biotreated silica sand using EDX analysis	125

CHAPTER 6

Table 6.1: Certified standard reference values for standard 90, 70 and 60 provided by the suppliers.	135
Table 6.2: Preliminary assessment on the reliability and reproducibility of the ColorTouch analyser. The error represents the standard deviation from five replicate analyses.	136
Table 6.3: Colour analysis of Kaolin 4 (Melbur Yellow MGP) before and after bioreduction with <i>S. putrefaciens</i> CIP8040 at 30°C.....	143
Table 6.4: Colour values of Silica Sand (Oakamoor) before and after bioreduction with <i>S. putrefaciens</i> CIP8040 at 30°C.....	146
Table 6.5: Chemical composition (expressed as % oxides) and surface area for Kaolin 2 (Remblend) and Kaolin 3 (Melbur Yellow HCP) before and after biotreatment with <i>S. putrefaciens</i> CIP8040. Analyses carried out by Imerys Ltd.	147

CHAPTER 7

Table 7.1: Initial XRF (%) chemical data of various oxides and brightness index in chalk supplied by Omya Ltd.....	160
Table 7.2: Medium used for the culturing of <i>Desulfovibrio desulfuricans</i> ATCC27774 recommended by DSMZ.	161
Table 7.3: colour analysis of chalk (W41723) after bioreduction of ferric phase using <i>Shewanella putrefaciens</i> CIP8040.	165
Table 7.4: colour analysis of chalk (W41723) after 15 days bioleaching using <i>Pseudomonas mendocina</i>	167

Table 7.5: colour analysis after bioleaching of chalk (W41723) with <i>Desulfovibrio desulfuricans</i> at 30°C.....	168
---	-----

APPENDIX

APPENDIX 1: Data of Fe(II) measured in solution from the bioleaching of the different kaolin used in the experiments.

APPENDIX 2: Data of Fe(II) measured in solution from the bioleaching of the different silica sand used in the experiments.

APPENDIX 3: Data from both kaolin and silica sand bioreactor experiments.

APPENDIX 4: Data from bioleaching of carbonate mineral.

APPENDIX 5: Total organic carbon analysis data for kaolin and silica sand experiments.

APPENDIX 6: Preliminary bioreactor experiments result at room temperature for kaolin and silica sand including some images.

APPENDIX 7: Natural organic matter analysis and colour data supplied by industrial partners.

CHAPTER 1 : INTRODUCTION AND LITERATURE REVIEW

1.1: INTRODUCTION

Kaolin, and high grade carbonates (chalk) are important and valuable industrial raw materials widely used in paper, glass, ceramics, cosmetics, paint, porcelain, potteries, and rubber production. They are also used in waste treatment, agriculture, pigments, nanocomposites as a coating, and filler materials (Sengupta et al., 2008; Kahraman et al., 2005; Styriaková et al., 2003; Asmatulu, 2002; Psyrillos et al., 1999). The major principal glass products from the industrial use of silica sand include the colourless and coloured bottle containers, flat glass (windows, mirrors and vehicle glazing), light bulbs and fluorescent tubes, TV and computer screens and glass fibres that are used for insulation and reinforcement (British Geological Survey, 2009a; 2006a; Styriaková et al., 2003). High grade kaolin clays (China clays) are principally used as filler or coating pigment for paper making and as main material for making fine ceramics (British Geological Survey, 2009b; British Geological, 2006b). Pure forms of calcium carbonate are used as fillers and coating agents in plastics, paint and paper industries (British Geological Survey, 2006).

The quality and commercial value of these minerals largely depends on their overall purity, texture and colour properties such as brightness, whiteness, tint and opacity (Hosseini et al., 2007; British Geological Survey, 2006; Kahraman et al., 2005; Styriaková et al., 2003; Asmatulu, 2002; Lee et al., 2002; Manukyan and Gabrielyan, 1999; Psyrillos et al., 1999). Crystal size and shape of the mineral particle, and their bulk chemical composition, are among other properties of considerable importance in industrial application, in addition to their gloss, rheological and abrasion properties (Psyrillos et al., 1999). These minerals when mined are generally not pure, often associated with iron (hydr)oxide impurities usually in form of Fe^{3+} that are adsorbed on the mineral surface covering the entire mineral mass or admixed as a separate iron bearing phase. The impurities in silica sands and kaolin are generally in the form of haematite, magnetite, goethite, lepidocrocite, and/or ferrihydrite coating and binding strongly on the surface of individual grains or as discrete fine particles covering the entire clay mineral (Rusch et al., 2010; Styriakova et al., 2007). Calcium carbonates are particularly associated with ferrous mineral impurities, such as siderite

(FeCO₃); (Deer et al., 1999). The presence of such associated impurities remarkably lowers their industrial value and limits their area of application (Hosseini et al., 2007; Banza et al., 2006). For example the permissible limit of iron in glassmaking calcium carbonate is <0.036% Fe₂O₃ and in the glass-making sands not more than 0.07% of Fe₂O₃ for light engineering and medical glasses (Styriaková et al., 2007; British Geological Survey, 2006).

To attain high grade specification for industrial applications, there is growing need and requirement for the refining of these industrial mineral of which iron is the major impurity (Ryu et al., 1995). Therefore to achieve and maximise the required industrial quality and value specification of kaolin clay, silica sand and high grade carbonate, removal of associated iron impurities becomes absolutely imperative. The current conventional practice for the removal of iron impurities both as surface coating and as discrete fine form, involves physical and chemical methods such as froth flotation, magnetic separation, and selective flocculation. The chemical treatment mainly involves leaching with mineral acids and treatment with reductants such as Na-dithionite and Al-sulphate, hydrazine, sulphur dioxide and Al-powder, or sulphur dioxide and Zn-powder. (Mockovciaková et al., 2008; Styriakova et al., 2007; Ambikadevi and Lalithambika, 2000; Kostka et al., 1999b). However, these methods are known to have substantial technological, economic and environmental disadvantages (Ambikadevi and Lalithambika, 2000).

Because of the environmental disadvantages associated with the conventional physical and chemical refinement processes, recently, microbial leaching of iron has been receiving much attention as an alternative for refining Fe(III)-containing minerals. Microbial Fe(III) reduction has over the decades been established as an important process that catalyses the oxidation of organic matter coupled to Fe(III) reduction (Fredrickson et al., 2003; Lloyd, 2003; Lovley, 1997). Biogeochemical evidence exists to support the potential importance of many crystalline or amorphous Fe minerals as electron acceptors for Fe-reducing bacteria in soils and subsurface sediments (Jaisi et al., 2007b; Zachara et al., 1998; Lovley, 1997). Therefore, the ability to remove ferric iron impurities in kaolin, silica sand and carbonate through other means, such as application of metabolic activities of dissimilatory iron-reducing microorganisms and other fermentative organisms as the agent of iron bioleaching may potentially reduce cost, allow lower grade minerals to be recovered and hence improve the

efficiency of mineral processing (Lee et al., 2002). It is the purpose of this Thesis to investigate the phenomenon of microbial iron reduction in industrial minerals and materials.

1.2: OCCURRENCE, SUPPLY AND MARKET CONSUMPTION OF THE MINERALS

1.2.1: Kaolin

The St. Austell granite (Cornwall) and the Dartmoor granite in Devon (south-west of England) are the principal kaolin deposits accounting for 88% of England production. They are among the six major outcrops of Cornubian batholiths and form the largest and highest quality kaolin deposit in the world (Murray, 2007; Bristow and Scott, 1998; Psyrillos et al., 1998). The mineralogy of the granites is associated with quartz, feldspars, coarsely crystalline micas and other accessory minerals impurities (Psyrillos et al., 1999). The United Kingdom is ranked as the third world largest producer and exporter of kaolin clay with an annual production estimated at 1.36 to 3Mt which represent 10% of the world total output between 2001 and 2008 after the United States of America and Brazil (British Geological Survey, 2009b; Wilson, 2004; Wilson, 2003; Psyrillos et al., 1999). Kaolin has been Britain's most important mineral export after hydrocarbons and demand is mostly dominated by the paper industry (50%) and ceramic industry (30%) of the total annual sale. Imerys Minerals Ltd is the lead exporter with 88% of total production exported around the world with a major market in Europe (British Geological Survey, 2009b).

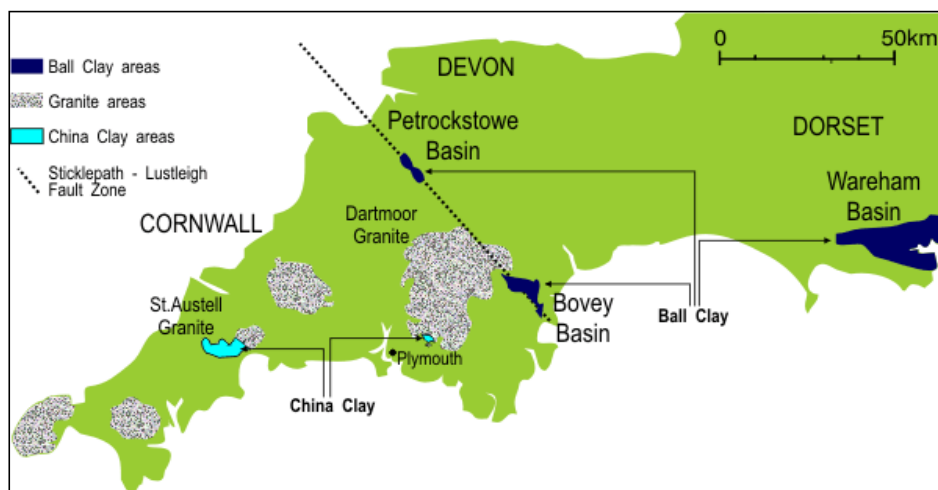


Figure 1.1: Granite outcrops and kaolin clay deposit of south-western England. Source: The ball clay heritage society (www.clayheritage.org/pages/whatisballclay.htm).

1.2.2 Silica sand

Sand and sandstone deposits are widely distributed across UK, but not all deposits possess the required physical and chemical properties to be characterised as a potential source of silica sand. Silica sand suitable for the manufacturing of colourless glasses is produced at only six locations in the UK. The silica sand of Pleistocene age in Cheshire and those of Lower Cretaceous age in eastern and southern England are considered the most important deposits, each accounting for around 40% of the total annual output (British Geological Survey, 2009a; British Geological Survey, 2006b). Silica sand production is relatively small with a total output of 5Mt in 2007 compared to construction sand (42Mt total output), with the glass industry as the major consumer. International export of silica is very small and mostly production is dominated by local consumption (5Mt per year). WBB Minerals Ltd, now Sibelco UK, is the largest and leading silica producer in the UK with an output of over 50% of total production (British Geological Survey, 2009a).

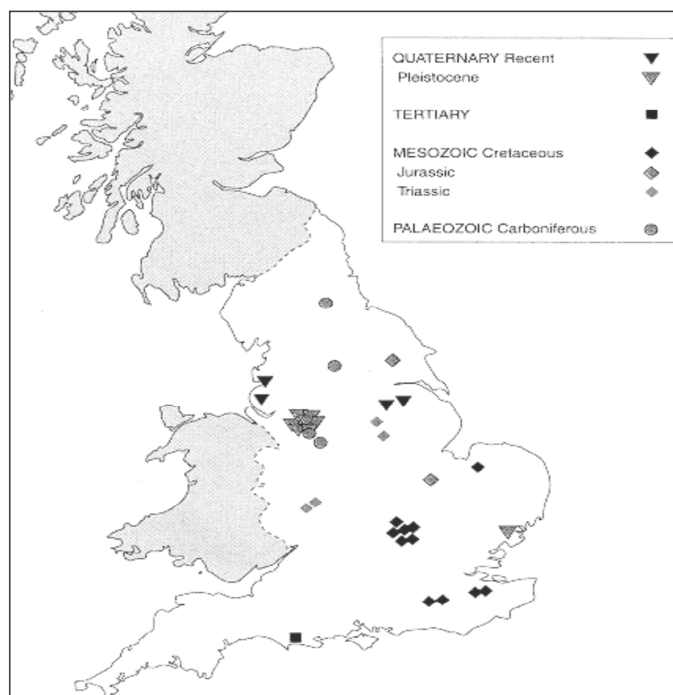


Figure 1.2: Locations of silica sand quarries in England, active in 1990, according to geological age of extracted deposit. Source (Department for Communities and Local Government., 1996).

Table 1.1: English production of silica sand in 2007 (British Geological Survey, 2009a).

Silica sand	Tonnes
Glass sand	
Flat glass	683,386
Colourless containers	582,391
Coloured containers	190,618
TOTAL: Glass sand	1,456,395
Foundry sand	400,544
Other industrial uses	942,732
Sand for Agricultural and leisure uses	324,828
Total production	3,124,499

1.2.3: Calcium carbonate (Chalk)

Chalk is a type of very fine-grained limestone and the demand for industrial purposes was estimated at 2.1Mt in 2004 alone. The United Kingdom was categorised as a modest exporter of chalk and limestone for industrial consumption with a total output of 9Mt, of which 23% was chalk and 77% limestone (British Geological Survey, 2006). The large proportion of chalk and limestone outputs is dominated by Derbyshire (British Geological Survey, 2006), and the Peak District National Park (British Geological Survey, 2006). Industrial chalk and limestone are widely distributed in the UK but many are not suitable for industrial application. The only important industrial deposits of chalk and limestone in UK are the Cretaceous-age Chalk and Carboniferous Limestone. However, the thick and extensive chalk deposits of Eastern and Southern England constitute an important and enormous source of limestone for cement and other industrial uses (British Geological Survey, 2006). OMYA Ltd is the global leading producer of calcium carbonate from the United Kingdom.

Table 1.2: England production of calcium carbonate (chalk) in 2004 (British Geological Survey, 2006).

Chalk	Thousand Tonnes
Constructional uses	705
Cement production	5,177
Industrial uses	2,114
Total production	7,997

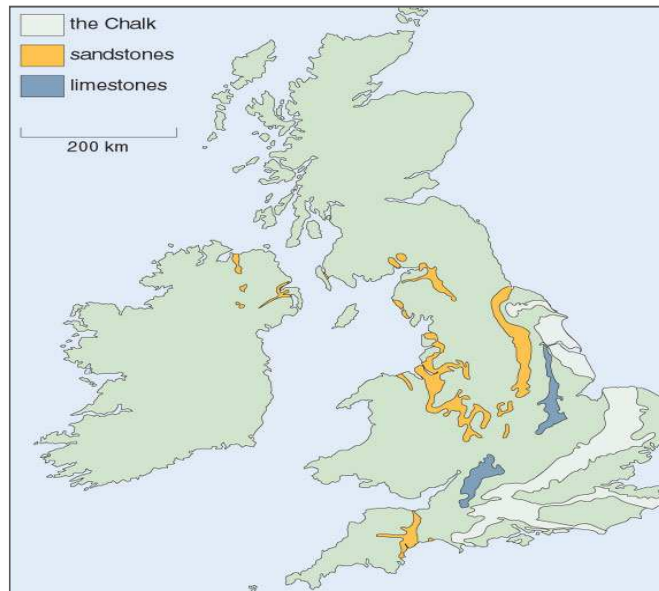


Figure 1.3: Distribution of principal industrial chalk resources in the United Kingdom. Source (online image access from (<http://openlearn.open.ac.uk/mod/oucontent/view.php?id=399847§ion=6>))

1.3: TRADE AND VALUES OF THE MINERALS

The industrial values of kaolin, silica sand and carbonate in terms of export and import is of considerable importance. It is necessary to consider the economic importance of these commodities in relation to their availability, trade values and consumption. Generally, individual industrial minerals have different range of application and also have considerable variation in terms of cost and monetary value (Manning, 1995). The value of industrial minerals is related to ways through which the minerals are mined and transported to the places they are needed. This also takes in to account the monetary value of the minerals including cost of transportation to consumer markets (Manning, 1995). Manning (1995) further categorised industrial minerals in to those with high place value and those with low place values. The industrial minerals with low intrinsic value and high transport cost (high place value commodities) are generally cheap, widely available and are relatively close to the places they are required. These minerals are not usually traded internationally and examples include sand, gravels and aggregates (Manning, 1995). On the other hand low place value minerals attract high monetary value and are traded internationally even though

the cost of transporting them is high. Low place value minerals command high monetary price and are produced from a fewer places; examples include kaolin and carbonates. Typical prices of kaolin, silica sand and chalk (per tonne) for different industrial applications are given in table 1.3.

Table 1.3: Prices (per tonne) of Kaolin, silica sand and chalk (Industrial Mineral, 2009).

Mineral	Price
Silica sand	
Foundry sand	£15.50 - 16.50
Glass sand	£15.00 - 17.00
Chalk	
Chalk, uncoated	£30 - 52
Coated fine grade	£80 - 103
Kaolin	
Filler, bulk	\$80 - 100
Paper coating grade	\$95 - 185

Similar prices from the total annual export and import statistics of these commodities in relation to the tonnage exported or imported between 2005 and 2009, and are given in Table 1.4 (Bide et al., 2010).

On the basis of the prices given in Table 1.3, it can be seen that the value of silica sand is generally low compared to the other two commodities. Removal of iron would increase grade so that a sand suitable for a foundry sand would become a glass sand, and the increase in value would be of the order of £1 per tonne. In contrast, improving the qualities of a kaolin so that a filler might be upgraded to a paper coating grade (and properties other than iron content would also need to change) would lead to an increase in value of as much as \$100 per tonne. Similarly, upgrading calcium carbonate to a coated fine grade (which involves additional processing as well as iron removal) could add £30 - £50 per tonne in value. The increase in value for kaolin is greatest, justifying the emphasis placed on kaolin in this thesis.

Table 1.4: United Kingdom summary of total annual exports and imports of silica sand, chalk and kaolin between 2005 -2009 with the total commodity prices based on the tonnage produced (Bide et al., 2010)

Commodity	2005	2006	2007	2008	2009	2005	2006	2007	2008	2009
						Price: £ Thousand				
Silica sand*										
Imports	127,992	190,813	61,454	48,112	79,629	8,453	9,234	8,516	8,045	8,076
Exports	174,236	388,440	222,581	156,451	115,746	4,586	6,402	6,393	4,614	4,794
Chalk										
Imports	3,675	4,249	5,689	5,447	3,878	384	315	450	716	627
Exports	43,846	36,918	34,594	126,594	30,890	1,994	1,670	2,082	4,510	1,870
Kaolin										
Imports	72,812	79,958	54,888	67,349	61,164	8,741	10,007	8,064	12,116	14,028
Exports	1,698,747	1,566,025	1,490,416	1,188,267	932,180					

Silica sand*= silica sand for glass making, moulding and other non-constructional uses

1.4: CURRENT CONVENTIONAL IRON LEACHING PROCESS

Impurities in industrial minerals like kaolin and silica sand include iron-bearing minerals and fine grained anatase (TiO_2). The removal of these colouring oxides is essential if high brightness saleable grade minerals are to be produced. A number of conventional physical and chemical means have been employed to improve or modify the quality and properties of various industrial minerals (Bloodworth et al., 1993; Prasad et al., 1991). Some of the techniques widely used are described below.

1.4.1: Froth flotation

This technique is used to remove dark iron-stained anatase and hydrated iron oxides which particularly discolour kaolin, and involves the use of a calcium carbonate carrier. Selective separation of iron-containing minerals is generally carried out in aqueous pulp at a controlled pH value. In this process, the dark iron-stained phase is selectively coated with a reagent which causes it to adhere to air bubbles sprayed into the slurry. The air bubble froth which contains the mineral impurities rises to the surface of the flotation cell and is skimmed off and discarded (Murray, 2007)

1.4.2: Selective flocculation

Selective flocculation is another process that can be used to reduce the percentage of iron-containing minerals and anatase. The process is normally applied to produce high brightness products of 90% or higher. Since its initial development, the selective flocculation process has been continually improved and is one of the current processes that is used extensively to produce high brightness products. This process is the reverse of flotation in that the dark iron-stained anatase is selectively flocculated so that it settles in a hydroseparator while the kaolin remains suspended in a dispersed condition (Murray, 2007; Prasad et al., 1991). The leaching process in this technique involves slurry acidification at a pH between 2.5 and 3, which solubilises some of the iron compounds that stain the mineral. Alum is sometimes used in combination with sulfuric acid to give a tighter floc. At the same time, a strong reducing agent, such as sodium dithionite, sulphur dioxide, sodium hypochlorite and/or sodium hydrosulfite, is added to the slurry to reduce ferric iron to ferrous iron, which then combines with sulfate to form a soluble iron sulfate, FeSO_4 . The high solubility of ferrous iron allows a small proportion of the hydrated iron oxides coating the minerals to be

removed in solution. The iron sulfate is removed by filtration during the process (Murray, 2007; Veglio et al., 1996; Bloodworth et al., 1993; Prasad et al., 1991).

1.4.3: Magnetic Separation

The magnetic separation technique generally involves the use of a powerful magnet having a field strength that ranges between 2 – 6 Tesla. The magnetic field is achieved by using liquid helium cooled superconducting coils, which results in considerable savings in electric power. During this process, the mineral impurities become magnetised when placed in a magnetic field. The process is based on the magnetic susceptibility of different species of the coloured mineral impurities such as hematite, mica and pyrite (Murray, 2007). These impurities are known to be feebly magnetic (lack magnetic strength), with a very low susceptibility. The magnetic minerals that are removed are dominantly hematite and yellowish iron-enriched anatase along with some magnetite, and biotite. Generally the mineral slurry is pumped through a highly compressed fine stainless steel wool matrix, which when energized separate the magnetic minerals and allows the non-magnetic mineral to pass through the matrix. Although the method has been successfully used with grades of kaolin that do not respond to conventional leaching technique, it was not cost effective (Murray, 2007; Prasad et al., 1991).

1.5: CHEMICAL AND STRUCTURAL COMPOSITION OF THE MINERALS

1.5.1: Mineral composition and structure of kaolinite

Commonly referred to as kaolin, especially in the context of industrial minerals, the mineral kaolinite is a member of a group of clays which characteristically have two layer 1:1 type of structure. Kaolinite has a structural formula $\text{Al}_2\text{Si}_2\text{O}_5(\text{OH})_4$ and the theoretical chemical composition is SiO_2 , 46.54%; Al_2O_3 , 39.50%; and H_2O , 13.96% (Murray, 2007). The basic structure of kaolinite is a layer of a single tetrahedral sheet (Si-O) and a single octahedral sheet (Al-O). The two sheets normally combine to form a unit in which the tip of silica tetrahedron forms a linkage with the octahedral sheet. In the structural unit, the apical oxygen of the silica tetrahedra point in the same direction. They are shared by a tetrahedral silicon and an aluminium in the octahedral sheet with hydroxyl that may be presence for charge balance (Murray, 2007; Deer et al., 1999). Iron is a major impurity element present in the silicate structure as substitute for octahedral aluminium in the kaolinite group. It may be

in oxide or oxyhydroxide forms, which have a fundamental effect on the refractory index and whiteness of the minerals (Mockovciaková et al., 2008; Reeves et al., 2006; Deer et al., 1999).

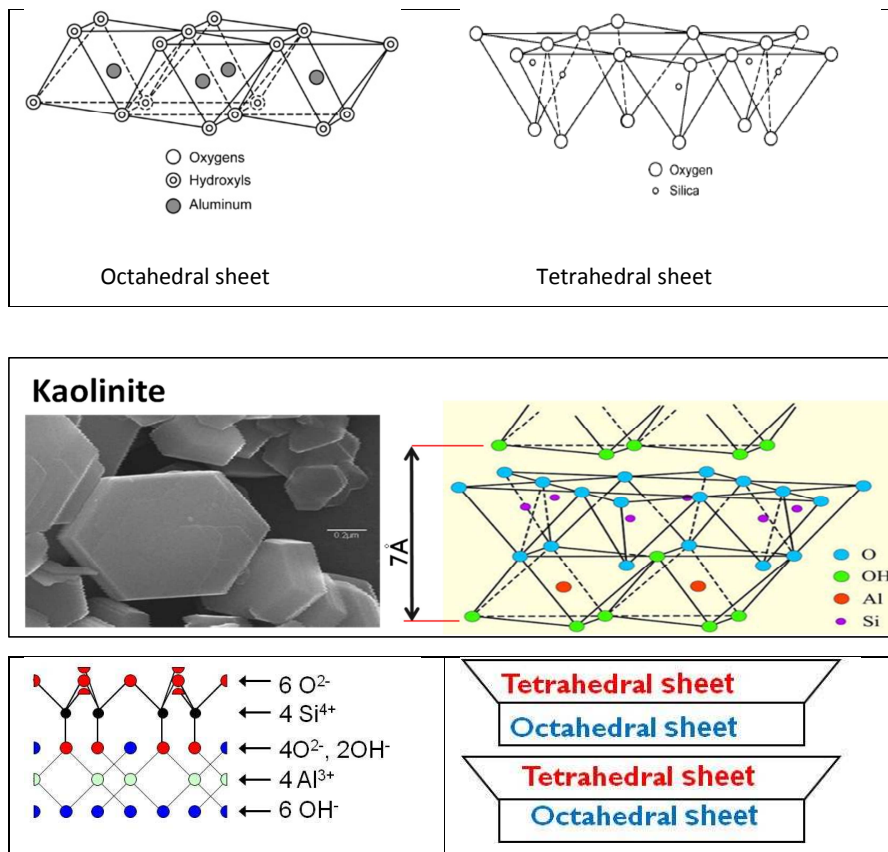


Figure 1.4: Diagrammatic sketch showing crystal structure of kaolinite mineral. The Al in the silicate structure may be substituted by Fe. Source (Dr. Claire Fialips lecture slides 2008)

1.5.2: Silica minerals and their chemical composition

Silica is the most abundant chemical component of the Earth's crust and is commonly found on the surface of the Earth as quartz or more rarely as the tridymite and cristobalite polymorphs. Chemically, silica constitutes nearly 59% of the total mass of the Earth's crust. The structural framework of the silica minerals is very simple, built from SiO_4 tetrahedra linked by each corner to another tetrahedron by oxygen atoms. The most common example of this structure is seen in quartz. Quartz is always pure silica (99.9%, SiO_2) with less than 0.2 percent of total impurities (Deer et al., 1999). Because silica and iron-oxides are ubiquitous

and often associated with one another in the soils and sediment, then naturally occurring quartz sands can be found to contain various iron-oxide impurities coating the silicate grains or sometimes the iron may be impregnated in silicate matrix (Rusch et al., 2010). Iron-oxides in quartz sand are mostly present in different impurity forms, in free impurity minerals, in impurity minerals joined to the quartz grains, or in impurities located inside the quartz grain, in iron-containing films coating the entire grain surface and sometimes in the structural impurities (Manukyan and Gabrielyan, 1999)

1.5.3: Calcium carbonate minerals and their chemical composition

Calcium carbonate (CaCO_3) is known to exist in different polymorphs, the most common of which are calcite, aragonite and vaterite. Carbonate also exists as dolomite ($\text{CaMg}(\text{CO}_3)_2$) with increasing magnesium in the structure. The essential unit structure of carbonate minerals is the $(\text{CO}_3)^{2-}$ ion. The structure of calcite is analogous to that of halite in which Na and Cl ion in the halite group are substituted by Ca and $(\text{CO}_3)^{2-}$ respectively (Deer et al., 1999). The unit cell of calcite contains 4CaCO_3 equivalent to the 4NaCl present in the cubic unit cell of the Halite group. The Ca in calcite is sometimes substituted by divalent ions such as Fe^{2+} leading to the formation of siderite (FeCO_3) as one of the major impurities which may affect the colour and refractory properties of the mineral (Deer et al., 1999).

1.6: THE IRON OXIDES AND OXYHYDROXIDE IMPURITIES

1.6.1: Iron oxy-hydroxide minerals

Iron is an abundant constituent in crystalline structure of many minerals, particularly clay minerals and the oxidation state of iron in the minerals may be ferric (Fe^{3+}) or ferrous (Fe^{2+}). The iron oxidation state generally determines and affects mineral physicochemical properties such as swelling, cation exchange capacity, surface area, surface acidity, organic matter interaction and redox properties, which may be of industrial importance (Jaisi et al., 2007c; Roden and Zachara, 1996).

Oxides and oxyhydroxides of iron are compounds which are widely spread in natural environments. They are ubiquitous components of various soils, sediments and subsurface sediments, with concentrations ranging from one to several hundred grams per kilogram (Cutting et al., 2009; Roden, 2004; Cornell and Schwertmann, 2003). Iron oxides are

reported to exist in various phases ranging from poorly crystalline amorphous phases such as ferrihydrite to well-crystallised phases like goethite and hematite. In addition, even a single Fe(III) mineral can exert various and different ranges of crystallinity, particle size, solubility and specific surface area. However, the poorly crystalline Fe(III) phases are known to be more susceptible to microbial attack than the more crystalline phases (Bonneville et al., 2009; Cutting et al., 2009; Luu and Ramsay, 2003; Roden and Zachara, 1996). Fe(III) is believed to be the most abundant electron acceptor in various soils and subsurface sediments. The importance and utilisation of many iron (III) oxides as electron acceptors for anaerobic respiration by various metal-reducing microorganisms in Fe-rich sediment has been well documented (Lovley et al., 2004; Nealson and Saffarini, 1994; Lovley, 1991). Much evidence gathered over the last decades has shown that these iron oxides and oxyhydroxides are present in various forms in clay and other Fe-containing minerals. The oxides and oxyhydroxides are notably present in clay minerals as hematite (red), ferrihydrite (red- brown), magnetite (black), maghemite (reddish-brown), goethite (yellow) and lepidocrocite (orange) among others (Reeves et al., 2006; Cornell and Schwertmann, 2003).

Table 1.5: Examples of oxides and oxyhydroxide irons in the environment, from Cornell and Schwertmann, (2003).

Oxides-hydroxides & Hydroxides	Oxides
Goethite α -FeOOH	Hematite α -Fe ₂ O ₃
Lepidocrocite γ -FeOOH	Magnetite Fe ₃ O ₄ (Fe ^{II} Fe ^{III} ₂ O ₄)
Akaganéite β -FeOOH	Maghemite γ -Fe ₂ O ₃
δ -FeOOH	β -Fe ₂ O ₃
Ferrihydrite Fe ₅ HO ₈ .4H ₂ O	ϵ -Fe ₂ O ₃
Feroxyhyte δ' -FeOOH	Wüstite FeO
High pressure FeOOH	
Bernalite Fe(OH) ₃	
Fe(OH) ₂	
Schwertmannite Fe ₁₆ O ₁₆ (OH) _y (SO ₄) _z . n H ₂ O	
Green Rust Fe _x ^{III} Fe _y ^{II} (OH) _{3x+2y-z} (A ⁻) _z ; A ⁻ = Cl ⁻ ; 1/2SO ₄ ²⁻	

1.6.2: Reduction of Fe(III) oxides in soils and sediments

Reduction of iron(III) oxides has been a very significant factor influencing the geochemistry of many anaerobic soils and sediments and recent studies have demonstrated that microbial activities are directly linked to reduction of various Fe(III) oxides (Luu and Ramsay, 2003; Lovley, 1991) resulting to the release of many metals in anaerobic environments (Kostka et al., 1999b). Reduction of metal plays a significant role in organic matter oxidation of many

sediments and the metabolism of metal-reducing bacteria in such sediments has been shown to greatly influence the mineralogy of many sedimentary environments (Nealson and Saffarini, 1994; Lovley, 1993). Crystalline and amorphous iron (III) oxides are characteristic components of many sedimentary environments (Roden and Zachara, 1996). However, the amorphous iron (III) oxides are the common form of Fe(III) oxides reduced in most anaerobic sediments (Roden and Zachara, 1996; Lovley, 1991) even though crystalline iron (III) oxides such as goethite and hematite are more abundant in various soils, minerals and sediments than the amorphous iron (III) oxide. This is largely because very small portions of iron are readily available for reduction in crystalline minerals due to constraints in accessing the crystalline form of Fe(III) oxides. Despite these constraints, a small reduction of iron(III) oxide can significantly affect the biogeochemistry of such soils, minerals and subsurface sediments (Roden and Zachara, 1996). Laboratory scale experiments using crystalline Fe(III) oxides in the presence of pure cultures have shown that goethite and hematite are also susceptible to bioreduction. It has also been reported that, even among the various crystalline iron oxide phases, the order of microbial iron reduction decreases in accordance with the sequence lepidocrocite > hematite > goethite (Munch and Ottow, 1983).

Several studies have been conducted to unravel factors that significantly control and regulate the rate and extent of Fe(III) oxide reduction. The susceptibility of metal oxide bioreduction of Fe(III) oxides as well as the rate and extent of bacterial reduction was shown to be fundamentally controlled by factors such as surface area, particle size, crystallinity and thermodynamic factors (Liu et al., 2001; Zachara et al., 1998; Postma and Jakobsen, 1996; Roden and Zachara, 1996; Lovley, 1991; Lovley, 1987). Roden (2003) and Fisher (1988) have shown that Fe(III) oxide heterogeneity may possibly play an important role in affecting the initial rate of bacterial reduction in many natural soils, iron mineral and sediments. Sorption of Fe(II) on the surface of oxide minerals or formation of soluble Fe(II) complexes have been reported to affect the microbial reduction of Fe(III) oxides (Urrutia et al., 1999).

Table 1.6: Lactate oxidation couple to the reduction of some iron oxide

Oxides and oxyhydroxide		
Ferrihydrite reduction		
$4\text{Fe}(\text{OH})_3 + \text{CH}_3\text{CHOHCOO}^- + 7\text{H}^+$	\longrightarrow	$4\text{Fe}^{2+} + \text{CH}_3\text{COO}^- + \text{HCO}_3^- + 10\text{H}_2\text{O}$
Goethite reduction		
$4\text{FeOOH} + \text{CH}_3\text{CHOHCOO}^- + 7\text{H}^+$	\longrightarrow	$4\text{Fe}^{2+} + \text{CH}_3\text{COO}^- + \text{HCO}_3^- + 6\text{H}_2\text{O}$
Hematite reduction		
$2\text{Fe}_2\text{O}_3 + \text{CH}_3\text{CHOHCOO}^- + 7\text{H}^+$	\longrightarrow	$4\text{Fe}^{2+} + \text{CH}_3\text{COO}^- + \text{HCO}_3^- + 4\text{H}_2\text{O}$
Magnetite reduction		
$2\text{Fe}_3\text{O}_4 + \text{CH}_3\text{CHOHCOO}^- + 11\text{H}^+$	\longrightarrow	$6\text{Fe}^{2+} + \text{CH}_3\text{COO}^- + \text{HCO}_3^- + 6\text{H}_2\text{O}$

1.7: BIOMINERALISATION OF IRON BY REDUCING MICROORGANISMS

1.7.1: Role of bacteria in biomineralisation of iron

Microbial iron reduction has been established as one of the main processes catalysing the biomineralisation of iron in several geological sediments resulting in the formation of iron minerals such as goethite and siderite (Zachara et al., 1998; Mortimer et al., 1997). This process plays a significant role in iron and organic matter mineralisation in natural environments (Roh et al., 2006). The bacterial biomineralisation of iron is a diverse and widespread process occurring in anaerobic sediments and aquatic environments. Fe(III) bioreduction forms one of the dominant electron accepting process in such environments because of the processes that involve iron cycling and iron remineralisation. Iron is described as a unique electron acceptor specifically because it can easily be reoxidised and deposited back in to sediments which provide a cycle for Fe(III) regeneration (Luu and Ramsay, 2003). Eventually, the regeneration and redistribution of Fe(III) in sediments and aquatic environments largely depends on the organic matter input. In the absence of organic matter Fe(III) may eventually continue to accumulate in the sediment with no or little continuation of the iron cycling (Lovley, 2001).

In natural environments, iron (III) oxides were illustrated in Figure 1.5, (Luu and Ramsay, 2003) to form a complex with some trace metal groups and phosphates which may subsequently settle in anoxic zones of a water or sedimentary environment. The iron-reducing bacteria in the anoxic zone can actively respire and couple the oxidation of organic carbon present to the reduction of Fe(III) oxides resulting to the production of soluble Fe(II)

with the release of any bound metals and phosphates. However, the majority of Fe(II) released during iron (III) bioreduction remains in a solid form (Luu and Ramsay, 2003; Lovley, 2001). The iron is described to precipitate as insoluble minerals such as siderite (FeCO_3), pyrite (FeS_2), magnetite (Fe_3O_4) and vivianite [$\text{Fe}_3(\text{PO}_4)_2$]. However, part of the iron may diffuse into the oxic zone of water or sediment and reoxidised insoluble Fe(III) oxides can then participate in the subsequent iron cycling.

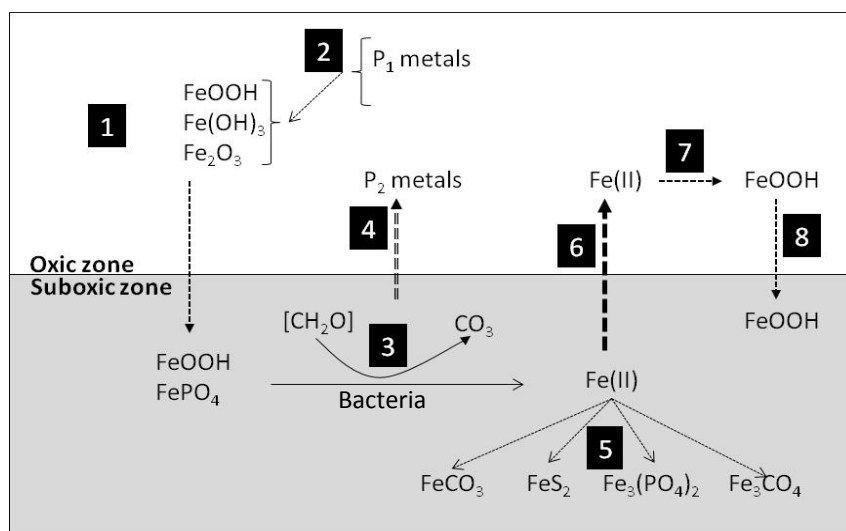


Figure 1.5: Iron cycling in natural environment. Source from Luu and Ramsay, (2003).

1.7.2: Diversity of dissimilatory iron-reducing bacteria in the environment

Dissimilatory iron reducers are a phylogenetically and metabolically diverse group of microorganisms that utilise metal oxides such as metals, metalloids and radionuclides as electron acceptors and couple their reduction to the oxidation of organic matter for energy and growth in many geochemical environments (Cummings et al., 2003; Lloyd, 2003; Lloyd et al., 2002; Zachara et al., 1998). They are also known to use various electron donors such as lactate, acetate, and formate and they can also ferment glucose to obtain energy. In addition some strains can oxidise short fatty acids to obtained energy (Lovley, 2001; Kostka et al., 1996). Iron-reducing bacteria catalyse the reduction of ferric iron to ferrous in soils and sediments (Zachara et al., 2002) and are also known to influence the fate of many organic (Lovley et al., 1989) and inorganic contaminants (Lovley and Lloyd, 2000). Studies

using iron-reducing bacteria are mostly carried out using pure cultures on soluble iron phases such as ferric citrate or Fe(III) oxides. Oxyhydroxide mineral such as ferrihydrite and goethite have also been used as the preferential source of Fe readily available for bioreduction. In addition, there are many investigations using phyllosilicate clay minerals that are associated with Fe oxides (Kostka et al., 2002; Thandrup, 2000)

Dissimilatory iron-reducing bacteria (DIRB) have been isolated from many anoxic sediments including the deep terrestrial subsurface. Some of the genera of DIRB identified include *Geobacter*, *Shewanella*, *Pelobacter*, *Geovibrio*, *Geospirillum*, *Ferimonas*, *Geothrix*, *Desulfuromusa* and *Desulfuromonas* amongst several others (Kieft et al., 1999). Members of the group *Shewanellae* and of the *Geobacteraceae* are among the most common iron-reducing bacteria available in pure cultures that are studied extensively and characterised in detail for their potential to conserve energy for growth from the reduction of Fe(III) mineral (Lovley, 2006; Lovley, 2000; Nealson and Saffarini, 1994). Organisms from both of these families are shown to catalyse and facilitate the reduction of clay bound Fe(III) in the presence of chelating agents and electron mediator that increase the bioavailability of Fe(III) in the clay mineral for reduction (Kostka et al., 1999a).

In particular, *Shewanella* generally consists of rod shaped, gram-negative, facultatively anaerobic bacteria, inhabiting the oxic-anoxic interface of sedimentary environments (Gao et al., 2006; Venkateswaran et al., 1999). Attention has been given to this group of iron reducers, because the strains have illustrated a great ability to respire and utilise various terminal electron acceptors such as Fe^{3+} , Mn^{4+} , Cr^{+6} and U^{+6} and oxygen, nitrate and sulphur, at circum-neutral pH. The bacteria of this genus have the potential to respire under aerobic and anaerobic conditions depending on the type of energy source present (Gebrehiwet and Krishnamurthy, 2007; Gao et al., 2006; Lloyd, 2003; Myers and Myers, 1997).

Although not all *Shewanella* strains are characterised, currently over 32 different species were isolated and recognised from various geological environments (Gao et al., 2006). Apart from iron reduction, few *Shewanella* strains are capable of degrading various pollutants such as chlorinated solvents (Petrovskis et al., 2004) and petroleum contaminants (Semple and Westlake, 1987). *Shewanella* are also reported to facilitate precipitation of metals

under suitable conditions (Lloyd et al., 2002; Fredrickson et al., 2001) and dehalogenation of halo-organic compounds (Kazumi et al., 1995; Picardal et al., 1995). They can also catalyse the mineralization of some aromatic compounds (Anderson et al., 1998) and participate in sequestration and remobilisation of trace elements like arsenic, cobalt, nickel and zinc (Cooper et al., 2000; Cummings et al., 1999). Some are known to also adapt and flourish under extreme conditions (Bozal et al., 2002; Kato et al., 1998). A summary of the conditions for growth required of some selected iron-reducing bacteria are given in Table 1.5.

Table 1.7: Summary of literature on some Iron reducing bacteria

Name	References	Type of bacteria	Temperature	Comments
<i>Geobacter lovleyi</i>	Sung <i>et al.</i> (2006)	strict anaerobe	30°C	Reduces ferric iron (ferric citrate); Derives energy from acetate oxidation coupled to polychloroethylenes dechlorination.
<i>Geobacter metallireducens</i>	Childers <i>et al.</i> (2002) Lovley <i>et al.</i> , (1993)	strict anaerobe	30°C	Reduces insoluble Fe(III) oxides; Synthesizes appropriate appendages to establish contact with insoluble Fe(III) oxides.
<i>Geothrix fermentans</i>	Bond and Lovley, (2005; Coates <i>et al.</i> , 1999)	strict anaerobe	30°C	Releases own electron shuttle in order to reduce Fe(III) oxides that it cannot directly reach.
<i>Geovibrio ferrireducens</i>	Caccavo <i>et al.</i> (1996a)	strict anaerobe	30°C	Grows in a defined medium with acetate as electron donor and ferric oxyhydroxide or elemental sulfur as sole electron acceptor.
<i>Rhodoferax ferrireducens</i> sp. nov.	Finneran <i>et al.</i> (2003)	facultative anaerobe/aerobe	4-30°C Optimum: 25°C	Oxidises acetate, reduces ferric iron. pH 7 is optimum. Can grow and reduce Fe(III) at temperatures as low as 4°C. Able to utilise an e ⁻ shuttle but does not reduce AQDS.
<i>Shewanella algae</i> BrY	Caccavo <i>et al.</i> (1997; 1996b; 1992); Turick <i>et al.</i> (2003; 2002); Cunningham <i>et al.</i> (2007)	facultative anaerobe/aerobe	28°C	Produces and uses melanin (extra cellular) as soluble electron shuttle for Fe(III) oxide reduction. Presence of melanin increases Fe(III) mineral reduction rates by x10. Can be resuscitated with a variety of electron acceptors. Cells adhere to amorphous Fe(III) oxides. Starved bacteria can survive for years but can be resuscitated.
<i>Shewanella livingstonensis</i> NF22	Bozal <i>et al.</i> (2002)	facultative anaerobe/aerobe	4-20°C Optimum: 15°C	Sodium ions not required. Can grow by dissimilatory Fe reduction or fermentation. Cells reduce nitrate to nitrite and grow anaerobically by reducing ferric compounds with lactate as e ⁻ donor.
<i>Shewanella oneidensis</i> MR-1	Venkateswaran <i>et al.</i> (1999); Kostka <i>et al.</i> (2002); Tang <i>et al.</i>	facultative anaerobe/aerobe	3-35°C Optimum: 22°C	Reduces Fe(III) oxide and oxyhydroxide minerals - amorphous materials reduced more quickly. Direct contact with the Fe-oxides is not required as <i>Shewanella</i> releases soluble quinones that can carry electrons from the cell surface to Fe(III) oxides. Reduction rate is much higher when AQDS is added to act as e ⁻ shuttle. Low

	(2007)			temperature growth possible but lag time of 100hrs and then 67hrs doubling time (at 3°C). At 22°C doubling time for cells is 40 min. The central metabolism of <i>S. oneidensis</i> is robust to changes in oxygen conditions.
<i>Shewanella pealeana</i> ANG-SQI	Leonardo <i>et al.</i> (1999)	facultative anaerobe/aerobe	4-30°C Optimum: 23-30°C	Marine bacteria. May be a producer of allelochemical or antibiotic which inhibits marine pathogens. Anaerobic reduction of Fe, Mn, NO ₃ , etc. Optimum growth at pH 6.5-7.5 in media containing 0.5M NaCl. Can grow in pH range 6-8 and in 0.125-0.75M NaCl.
<i>Shewanella putrefaciens</i> CL71	Semple and Westlake (1987)	facultative anaerobe/aerobe	22-25°C	Reduction of ferric iron, reduction of sulphite (to sulphide), reduction of thiosulphate (to sulphide). Characterisation of iron reducing <i>Alteromonas putrefaciens</i> strains isolated from crude oil field fluids.
<i>Shewanella loihica</i>	Roh <i>et al.</i> (2006); Gao <i>et al.</i> (2006)	facultative anaerobe/aerobe	0-42°C Optimum: 18°C	Psychrotolerant bacterium - capable of growing at 5°C or lower. Shows remarkable rates of growth at temperatures as low as 8°C and as high as 37°C. Able to reduce akaganeite to form well-formed single domain magnetite at 18-37°C. Can reduce Fe ³⁺ , Co ³⁺ , Cr ⁴⁺ , Mn ⁴⁺ and U ⁵⁺ over pH range of 7.0-8.9, a NaCl range of 0.05-5%. Aerobically grows well at pH 5.5-10.
<i>Shewanella putrefaciens</i> CIP8040 (ATCC8071)	O'Loughlin <i>et al.</i> (2007)	facultative anaerobe/aerobe	30°C	produces Fe(II) during dissimilatory Fe(III) reduction of 80 mM lepidocrocite with 75 mM formate as the electron donor; performs better than other <i>Shewanella</i> species: <i>S. p.</i> ANA-3, <i>S. oneidensis</i> MR-1, <i>S. saccharophila</i> , <i>S. alga</i> BrY, <i>S. loihica</i> PV-4, <i>S. amazonensis</i> , <i>S. baltica</i> and <i>S. denitrificans</i> .
<i>Shewanella putrefaciens</i> CN32	Fredrickson <i>et al.</i> (1998); Jaisi <i>et al.</i> (2008); O'Loughlin <i>et al.</i> (2007)	facultative anaerobe/aerobe	30°C	Cultured aerobically in tryptic soy broth; lactate (10 mM) as sole electron donor; reduces ferric iron in clay minerals; best results with AQDS additive; produces Fe(II) during dissimilatory Fe(III) reduction of 80 mM lepidocrocite with 75 mM formate as the electron donor; performs better than other <i>Shewanella</i> species: <i>S. p.</i> ANA-3, <i>S. oneidensis</i> MR-1, <i>S. saccharophila</i> , <i>S. alga</i> BrY, <i>S. loihica</i> PV-4, <i>S. amazonensis</i> , <i>S. baltica</i> and <i>S. denitrificans</i> .

1.8: MECHANISMS OF DISSIMILATORY IRON REDUCTION PROCESSES AND ROLE OF ELECTRON SHUTTLES

Dissimilatory iron (III) reduction is a process through which Fe(III) is used during bacterial respiration as an external electron acceptor, or is simply described as the process in which microorganisms transfer an electron to external solid Fe(III) and reduce it to Fe(II) for purposes other than iron assimilation (Lovley, 2001; Park and Kim, 2001). The unique difference between dissimilatory and assimilatory reduction is that in the dissimilatory reduction process, significant amounts of ferrous iron are accumulated outside bacterial cells during growth under a normal physiological conditions (Park and Kim, 2001). Microbial reduction and transformation of metals has recently been given much attention because the process when properly harnessed and utilised can play a vital role in the cycling of organic and inorganic compounds thereby offering a range of new biotechnological processes (Lloyd, 2003). During this process iron-reducing bacteria transform Fe(III) to Fe(II) on the surface of iron oxide particles in the mineral, which may cause changes in the mineral's surface reactivity resulting in alteration of the minerals ability to adsorb or release metals, nutrients and other organic compounds and causing a significant change on the mineral quality (Bose et al., 2009; Bonneville et al., 2004; Cummings et al., 1999).

It has been widely reported that iron-reducing bacteria must establish a means of contact or electron exchange across the solid Fe(III) substrate during iron reduction (Lovley et al., 1991). Therefore, for the Fe(III) mineral to serve as an electron acceptor an electron transport chain must be established between the iron (III) oxide particle and the bacterial cytoplasmic membrane (Park and Kim, 2001; Myers and Nealson, 1988). Various mechanisms through which iron-reducing bacteria facilitate electron transfer between the bacterial membrane and solid Fe(III) oxides surfaces have been proposed to include electron transfer via direct contact between the bacterial cell and the iron(III) oxide surface (Nevin and Lovley, 2000a), secretion of soluble chelating agents that facilitate and enhance Fe(III) solubility and bioavailability (Nevin and Lovley, 2002b; Lovley and Woodward, 1996), as well as electron transfer mediated via external electron shuttles such as quinones, humic material and flavins (Cutting et al., 2009; von Canstein et al., 2008; Newman and Kolter,

2000; Lovley et al., 1998) or sometimes electron transfer via extracellular pili “nanowires” (Gorby et al., 2006; Reguera et al., 2005; Childers et al., 2002)

1.8.1: Reduction via direct contact with insoluble iron (III) oxide

The way through which insoluble Fe(III) oxides are bioreduced by iron-reducing bacteria is of biogeochemical importance because this will provide a better understanding on the manner through which Fe(III) oxides in the soil and sediments are reduced biologically (Nevin and Lovley, 2000a). One of the mechanisms proposed through which some iron-reducing bacteria reduce Fe(III) minerals is by establishing direct contact with the surface of the iron (III) oxide mineral, unless electron shuttling compounds or Fe(III) chelators are added in to the system. Some experiments have supported and illustrated the need for a direct contact between iron-reducing organisms and Fe(III) oxide surface. The experiments directly involved physically separating iron-reducing microorganisms from the Fe(III) oxides using semi-permeable barriers, and no iron reduction was observed (Caccavo et al., 1992; Lovley et al., 1991).

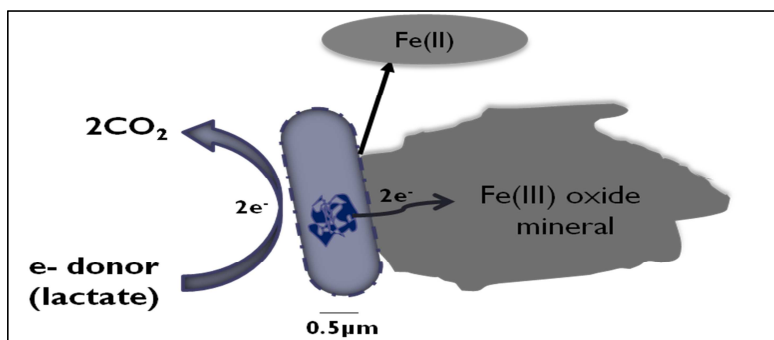


Figure 1.6: Mechanism of iron reduction via direct contact with the insoluble iron (III) oxide minerals.

Nevin and Lovley (2000a) have shown that *Geobacter metallireducens* must directly establish contact with iron (III) oxides before reduction to Fe(II) unless a soluble electron acceptor is supplemented in the growth medium. Further to this finding, *Geobacter metallireducens* and *Shewanella alga* BrY were shown to produce pili and flagella for attachment to iron (III) oxide surfaces and hence facilitated electron transfer (Reguera et al., 2005; Caccavo and Das, 2002; Childers et al., 2002; Das and Caccavo, 2001). Recently Gorby et al., (2006) reported that *Shewanella oneidensis* MR-1 can also produce pili-like

appendages in direct response to electron acceptor limitation. However, mutant strains with deficiency in genes for c-type cytochromes and the strains that lacked functional Type II secretion pathways produced nanowires that are poorly conductive.

1.8.2: Reduction of insoluble iron via an external electron shuttle

There is evidence that one of the mechanisms predominantly used by iron (III) reducing microorganisms for iron reduction involves the use of extracellular electron transfer mediators which shuttle electrons to solid iron (III) oxides (Luu and Ramsay, 2003). This mechanism generally alleviates the need for establishing contact between iron-reducing microorganisms with the surface of insoluble iron (III) oxide (Lloyd, 2003). In many sedimentary environments, humic substances are found naturally and were shown to have potential for serving as electron shuttles to Fe(III) oxides (Schröder et al., 2003; Lovley et al., 1998; Lovley et al., 1996). Humic substances contain quinone-like moieties that participated actively in redox cycling. Although the electron-accepting group(s) in humics are not yet identified or known, quinones are mostly used during abiotic electron transfer studies as humic analogs and are widely considered to be a very significant group of humic substances (Lovley et al., 1998). The compounds can function as terminal electron acceptors in their oxidised form, and after their reduction, the reduced hydroquinone moieties can then transfer electrons in the respiratory chain to Fe(III) oxide abiotically (Lloyd, 2003; Schröder et al., 2003).

A specific humic acid analog widely considered and used in many studies involving iron (III) oxide reduction is anthraquinone-2, 6-disulfonate (AQDS). Lovley et al. (1996) have shown that iron-reducing bacteria *Geobacter metallireducens* and *S. alga* are able to conserve energy to support growth by transferring electrons to AQDS and reducing it to anthrahydroquinone-2,6-disulfonate (AHDS). This could also mediate abiotic transfer of electron to Fe(III) oxides and reducing it to Fe(II) resulting in the subsequent oxidation of AHDS with the regeneration of AQDS. Several laboratory scale studies have demonstrated the role of AQDS in enhancing and accelerating the rate and extent of Fe(III) reduction in various iron(III)-containing minerals as well as several clays in comparison to experiments that had no or variable concentrations of electron shuttle (MacDonald et al., 2011; Cutting

et al., 2009; Jaisi et al., 2007b; Burgos et al., 2003; Nevin and Lovley, 2000b; Zachara et al., 1998)

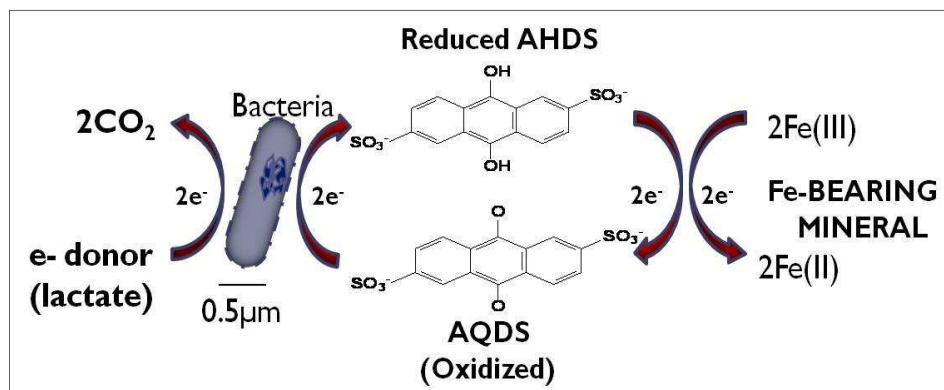


Figure 1.7: model for AQDS serving as an electron shuttle between iron (III)-reducing microorganisms and insoluble iron oxides

The third mechanism proposed for extracellular Fe(III) reduction is the potential for some iron-reducing microorganisms to secrete some soluble redox compounds that can also serve as electron transfer mediators during iron reduction in the absence of humics or AQDS (Lloyd, 2003; Schröder et al., 2003; Nevin and Lovley, 2002b; Newman and Kolter, 2000). *Geobacter fermentans* and *Shewanella alga* BrY were demonstrated to secrete diffusible electron transfer mediators that transport electrons to the Fe(III) oxide surface after being separated from the iron(III) oxide using a diffusible barrier. This shows that, in the absence of AQDS or humics, the microorganisms do not require any contact with the surface of Fe(III) oxides because of their potential to secrete electron mediators during active Fe(III) respiration (Nevin and Lovley, 2002b; Nevin and Lovley, 2002a). In addition, these authors also reported that *Shewanella oneidensis* and *G. fermentans* produce hydrophobic quinone-containing compounds that are yet to be identified. Similarly *S. alga* were also documented to secrete melanin that can serve as an extracellular electron mediator (Schröder et al., 2003; Turrick et al., 2002)

1.9: PREVIOUS STUDIES ON THE BIOLEACHING OF CLAY AND IRON CONTAINING MINERALS

Microbial bioreduction in various iron-containing minerals, particularly clays, is an important process that affects their general properties and iron biogeochemical cycling. Iron is one of the most abundant elements occurring in the structure of various clays and other industrial minerals. The ferric iron within the structure of many clay minerals like kaolin and those coating the surface of other industrial minerals like silica sand can be reduced chemically or biologically (Stucki, 2006; Dong et al., 2003; Gates et al., 1998; Kostka et al., 1996). However, the rate and extent of bioreduction of these minerals largely depends on the physicochemical properties of the mineral and is directly related to the oxidation state of the Fe within the mineral structures (Dong et al., 2003; Kostka et al., 1999b). While changes in the oxidation state of various iron-containing minerals can be caused by several abiotic chemical reactions, however, the role and importance of iron-reducing bacteria in altering iron oxidation state in various minerals has over the decades received much attention. The coexistence of iron-reducing bacteria along with iron-containing minerals, particularly clay minerals, in different geological environments has been fully described and the interaction between them has provided a better understanding of how the iron-reducing microorganisms significantly influence the mineralogical composition of several clays and other iron-containing minerals (Dong et al., 2003).

Until recently, the use of biological agents for refining of industrial minerals like kaolin, silica sand and carbonates has not attracted much attention. Most of the studies on bioreduction of structural Fe in clay minerals focused on minerals such as smectite (particularly nontronite), illite and chlorite (Jaisi et al., 2007a; Jaisi et al., 2007b; O'Reilly et al., 2006; Dong et al., 2003; Kostka et al., 1999b; Lee et al., 1999). For example, Dong et al. (2003) were able to reduce structural Fe(III) in illite and goethite by 25% in the presence of AQDS using the iron-reducing *Shewanella putrefaciens* CIP8040 strain. Similarly, bioreduction of structural iron in smectites was reported in which up to 15% of the total iron present was reduced within the first 4 hour of an experiment using *Shewanella putrefaciens* CIP8040, increasing to 25% and to 41% after 6 to 12 days (Kostka et al., 1996). Bacterial respiration on structural Fe(III) in nontronite was also reported (O'Reilly et al., 2006), where *Shewanella oneidensis* was the primary agent of Fe(III) reduction. These authors reported that the

bacteria mainly reduced Fe(III) in the aqueous phase of the system rather than Fe(III) within the crystalline structure of the mineral.

Previous studies on the microbial bioleaching of Fe to increase the refractoriness and industrial quality of kaolin (Hosseini et al., 2007; Cameselle et al., 2003; Lee et al., 2002; Styriakova and Styriak, 2000; Lee et al., 1999; de Mesquita et al., 1996) and silica sand have been reported (Styriakova et al., 2007; 2007; 2003), and have shown some potential for improving the quality of low grade minerals. However, development and optimisation of the bioleaching processes will be of biotechnological importance when fully harnessed. It is interesting to know that microbial refining of industrial kaolin and silica sand using pure cultures of iron-reducing bacteria has never been applied at full and pilot scale. However, small-scale laboratory studies for refining of kaolin were reported using two different strains of *Bacillus cereus* that anaerobically ferment glucose to obtain energy (Mockovciaková et al., 2008; Styriakova and Styriak, 2000). These bacteria initiate dissolution of kaolinite, resulting in the removal of 43% of free Fe present as oxyhydroxides and 15% of bound in mica (present as separate impurity in kaolin) after one month of bioleaching, and up to 53% after prolonging the bioleaching time (Styriakova and Styriak, 2000). Bioleaching of kaolin was also reported using the fungus *Aspergillus niger* that produced organic acids from the breakdown of sucrose (Hosseini et al., 2007; Cameselle et al., 2003; de Mesquita et al., 1996). The research used for the bioleaching process the spent medium or fermented acid solution (particularly oxalic acid) from sucrose breakdown during microbial growth. The reported increase in brightness ranged between 1.1 – 4.7% in different kaolin products (de Mesquita et al., 1996).

Related to our work is the experiment conducted at laboratory scale using iron-reducing bacteria by team of Korean scientists almost a decade ago that gives some promising results for possible bioleaching of industrial kaolin (Lee et al., 2002; Lee et al., 1999). These scientists were able to reduce the amount of iron impurities in low grade kaolin from 5.1 to 3.7 wt.% Fe₂O₃ by incubating the mineral in the presence of indigenous iron-reducing bacteria with maltose as a carbon source. In 70 hours of incubation, the brightness increased from 70.2 to 77.4%. They also showed that the type of carbon source (glucose > maltose > sucrose > galactose), and its concentration (1 to 5%), affect the rate of iron

leaching. This study demonstrated that iron-reducing micro-organisms can be used to leach iron-oxides from raw minerals and that the rate of bioleaching could be optimized by using an adequate carbon source. Recently, Guo et al. (2010) also reported the potential for increasing the quality of kaolin using dissimilatory iron-reducing bacteria. These researchers were able to bioreduce iron impurities in the kaolin from 0.88% to 0.48% with an increase in the whiteness index from 60.8% to 81.5% after 7 days of bioleaching treatment. However their studies have only used indigenous microbial communities within the samples and neither give details of the specific iron-reducing strains involved in the bio reduction process nor identified them because several competing species might have been present, and the bioleaching procedure had not been developed nor applied on a larger scale.

In a similar manner, experiments for the bio reduction of quartz sand are reported using *Bacillus cereus* and *Bacillus pumilus* cultures (Styriakova et al., 2007; 2007; 2003). Bio reduction with this bacterial strain decreased the Fe content in quartz by 60%. The rate of iron dissolution increased in the presence of 9,10-anthraquinone-2,6-disulphonic acid (Styriaková et al., 2007). Although no attention was given previously for the bioleaching of carbonates but studies on microbial dissolution of iron-containing minerals have been reported (Styriakova et al., 2007; Styriaková et al., 2007; O'Reilly et al., 2006; Maurice et al., 2001; Maurice et al., 2000; Kostka et al., 1999a). In addition, the iron acquisition potential for growth of aerobic *Pseudomonas mendocina* (Dhungana et al., 2007; Hersman et al., 2001; Hersman et al., 1996), will provide a prospect for the possible application of a microbial bioleaching process to carbonates.

1.10: AIM AND OBJECTIVES

The aim of this project reported in this Thesis was to develop and optimise microbiological processing methods to replace existing chemical refining techniques used for the processing of industrial minerals such as kaolin, silica sands and high grade carbonates (chalk) for the paper and glass industries. The new technology is based on the microbial leaching of iron impurities to a form readily removable by washing. The project also aimed to test the application of new bioleaching methods to carbonate minerals which currently cannot be processed through chemical means. It aimed to take initial small scale laboratory studies

through to larger scale bioreactor tests in order to outline the design of pilot production and to evaluate the quality, commercial and environmental benefits.

The main objectives of the study were to:

- Identify commercially available iron-reducing bacteria capable of leaching iron from three different mineral materials (kaolin, silica sand and chalk).
- Examine a range of conditions influencing bio-leaching processes by identifying the most suitable carbon source, temperature, and growth media.
- Optimisation of bioleaching conditions at small batch scale.
- Investigate the electron shuttling potential of natural organic matter (NOM) as an alternative to anthraquinone-2,6-disulfonate.
- Assessment of the quality of bioleached material with that of the initial raw material.
- To design and conduct large-scale (up to 4.5L) bioreactor experiments by putting in use the optimal conditions identified during small scale experiments.

CHAPTER 2 : MATERIALS AND METHODS

2.1: INTRODUCTION

This chapter gives a detailed description of various mineral samples used in this research and their suppliers. Procurement and revival of pure bacterial cultures as well as preparation of mineral material and bioreduction microcosms with their compositions are fully outlined. Chemical and analytical procedures conducted are also described in this chapter.

2.2: SAMPLE DESCRIPTION

Several samples of kaolin and silica were provided or were collected in this study. The samples were characterised for their physical, chemical and mineralogical properties by their suppliers.

2.2.1: Kaolin samples

About four different kaolin samples were used in this research. All the samples were provided by IMRYS Minerals Ltd. (Par Moor Center – Par – Cornwall; PL24 2SQ, UK). Descriptions of the samples are given below:

Kaolin 1: This is a fresh sample collected from a freshly exposed rock face in September 2007 by Dr. Claire Fialips and assisted by Dr. Asfaw Zegeye at Melbur Pit near St. Stephen, Cornwall, (Grid reference = SW 924 555). The samples were immediately gathered and placed in an anaerobic chamber with an oxygen consuming package (Anaero GenTM, Oxoid, Basingstoke UK.) and tightly sealed to maintain an anaerobic environment (Figure 2.1). AnaeroGen reacts very rapidly on contact with air to produce an atmosphere of <1% oxygen supplemented with carbon dioxide in less than 30 minutes. This provides an ideal condition for the survival of obligate anaerobic microorganisms. The sample was transported and kept in the same condition until required for use. This sample was obtained specifically for the isolation and identification of indigenous microorganisms.

Comment [1]:
David Manning 27/04/2011 18:53
Give grid reference – see me



Figure 2.1 : Picture showing sampling of freshly exposed rock of (a) kaolin 1 and (b) the anaerobic jar use to transport the sample under anoxic condition. (Photos from Asfaw Zegeye).

Kaolin 2: A dry kaolin sample was provided in April 2007 by IMERYS Minerals Ltd and labelled Remblend. The sample was sent along with colour and XRF data (Table 2.1). This sample was specifically provided to conduct small scale bioleaching experiments using various commercially available iron-reducing bacteria.

Kaolin 3: A kaolin sample labelled 'Melbur Yellow HCP, China Clay MIRO Sample' was provided in January 2009 by Imerys. The sample was a dark non-treated raw kaolin with high iron content. The sample was specifically provided in order to conduct and run a bioreactor experiment with commercially available iron-reducing bacteria particularly using *Shewanella putrefaciens* CIP8040. XRF and colour data for the sample was also provided (Table 2.1).

Kaolin 4: A chemically bleached kaolin labelled 'Melbur Yellow MGP Processed Sample for MIRO' was provided in May 2009 to also specifically conduct bioreactor experiments using *Shewanella putrefaciens* CIP8040. This sample was the same material as Kaolin 3 but has been chemically treated with sodium dithionite at Imerys Minerals Ltd. XRF and colour data of the sample was also provided (Table 2.1).

Table 2.1: Initial XRF, surface area, particle size and colour index data provided by Imerys Minerals Ltd. (kaolin) and WBB/Sibelco (silica sand) for the different mineral materials supplied for the experiments.

% Composition	Kaolin 2	Kaolin 3	Kaolin 4	Silica 2
SiO ₂ (%)	48.7	-	-	95.38
TiO ₂ (%)	0.08	-	-	0.086
Al ₂ O ₃ (%)	35.8	-	-	2.39
Fe ₂ O ₃ (%)	1.05	1.28	0.65	0.668
CaCO ₃ (%)	-	-	-	-
CaO (%)	0.06	-	-	0.01
MgO (%)	0.25	-	-	0.03
K ₂ O (%)	1.94	2.01	0.92	0.65
Na ₂ O (%)	0.07	-	-	<0.05
Mn ₃ O ₄ (%)	-	-	-	0.0098
LOI (%)	12.0	-	-	0.70
Surface area (m ² /g)	8.19	7.4	10.0	0.793
Brightness/ Violet (%)	76.1	68.1	82.9	-
Yellowness (%)	10.1	12.9	8.2	-
2 -10 µm (%)	-	20	4	-
1 - 2 µm (%)	-	35	47	-
0.75 – 1 µm (%)	-	24	32	-
<0.75 µm (%)	-	19	26	-

Comment [2]:

David Manning 27/04/2011 18:53
Make sure you use the same sample i/d as in the text! Also, in this table set it up so the decimal points are aligned – use the decimal point tab

... [1]

2.2.2: Silica sand samples

Three different silica sand samples were provided but only two of them were used in this research. All the samples were supplied by WBB/Sibelco UK, Whiston, Stoke-on-Trent ST10 20Z, UK. Descriptions of the samples are given below:

Comment [3]:

David Manning 27/04/2011 18:53
Give their address

Silica 1: A fresh sample collected from a freshly exposed silica surface in June 2007 by Dr. Claire Fialips at Moneystone Quarry – Oakamoor, (Grid reference = SK 042 461). The samples were immediately collected and placed in an anaerobic chamber with an oxygen consuming package (Anaero GenTM, Oxoid, Basingstoke UK.) and tightly sealed to maintain an anaerobic environment (Figure 2.2). The sample was transported and kept in the same condition until required for use. This sample was also obtained specifically for the isolation and identification of indigenous microorganisms.

Comment [4]:

David Manning 27/04/2011 18:53
Give grid reference

Silica 2: A purple-red silica sand sample in the form of rock from Moneystone Quarry – Oakamoor, (Grid reference = SK 042 461) was provided in April 2007 by WBB/Sibelco to conduct small scale bioleaching experiments using various commercially available iron-reducing bacteria (Figure 2.2). This sample was sent along with its colour and XRF data (Table 2.1). The rock sample was disaggregated into sand-grade powder for subsequent microcosm experiments.



Figure 2.2: Picture of Oakamoor quarry site used to sample silica sand 1 and silica sand 2. (Photo from Claire Fialips)

Silica 3: A third silica sand sample from the Leziate Beds (British et al., 2009a) was collected from King's Lynn - Grandcourt Quarry, (Grid reference = TF 679 168) in July 2008 following the announced closure of the Oakamoor Quarry in early 2008. The new sand was a yellow uncemented Cretaceous Lower Greensand (Figure 2.3). The sample is distinctly different from the Millstone Grit from Oakamoor Quarry (Silica 1 and Silica 2). However the King's Lynn silica sand is reported to respond well to acid leaching but does not respond well enough to dithionite bleaching to meet glass making requirements (personal discussion with the members of staff at the quarry site).

Comment [5]:

David Manning 27/04/2011 18:53
Can you give a reference to a description of these beds?

Comment [6]:

David Manning 27/04/2011 18:53
Insert grid reference



Figure 2.3: Picture of the sampling site for silica sand 3 (King's Lynn Quarry)

2.3: NATURAL ORGANIC MATTER

Two different natural organic matter (NOM) samples were received from Sibelco UK in order to test their electron shuttling potential and then compare them with commercially available synthetic AQDS to see if they could serve as a substitute to AQDS. The two NOMs were extracted at the same location from the lignitic kaolin ('Ball Blay') at Southacre Pit in the Bovey Basin, (Grid reference = SX 855 755). A brief extraction procedure of this samples is outlined below.

NOM 1: This sample was extracted by refluxing the organic matter in sodium hydroxide (NaOH) and then separated by centrifugation. This was then neutralised with sulphuric acid and evaporated to dryness after keeping for some weeks.

NOM 2: This sample was extracted the same way as NOM 1. The sample was found to contain a large amount of kaolinite after collecting the infrared spectrum of the sample. Therefore about 78g of the sample was redissolved in 1 liter of 2M NaOH, air excluded. This was filtered after centrifugation and the pH reduced to around 2 using HCl. The supernatant was a pale yellow, indicating the presence of fulvic acid. The sludgy precipitate was then separated by centrifugation and washed. The pH was finally adjusted to around 7.8.

However, most of the sludge dissolved and dispersed at around pH = 7.1 and this was filtered to remove particulate matter. The liquid phase was thereafter evaporated to dryness in a vacuum evaporator and finally oven dried at 40°C to complete the extraction process.

2.4: BIOREDUCTION CULTURES

2.4.1: Procurement of *Shewanella* pure cultures

An extensive literature review was conducted to identify suitable iron-reducing microorganisms based on their mode of culture (either obligate or facultative anaerobe), their availability as pure cultures from commercial suppliers, their ideal carbon source, their optimum condition and overall their efficiency in terms of rate and extent of iron reduction. Based on these conditions, six iron-reducing microorganisms from *Shewanella* strains were selected for this study. They include *Shewanella oneidensis* MR-1, *Shewanella loihica*, *Shewanella alga* BrY, *Shewanella putrefaciens* CN32, and *Shewanella putrefaciens* CIP8040. The cultures were purchased from NCIMB Ltd (Aberdeen, Scotland), DSMZ (Braunschweig, Germany) or LGC Standard (Teddington, Middlesex, UK).

2.4.2: Revival of purchased lyophilised *Shewanella* strains

Cultures were purchased in a freeze dried form packed in ampoules. To revive the frozen cultures, the ampoules were cut open at the tip after heating to red hot. About 0.5ml of tryptic soy broth (Fluka, Biochemica, Sigma-Aldrich, India) was aseptically dispensed into the ampoules containing lyophilized cells and mixed thoroughly. The ampoules were then aseptically emptied and inoculated into 100ml tryptic soy broth and incubated at 30°C for 48hours by continuous agitation. The cells were grown aerobically and cultures were harvested at late log-phase and washed with bacterial buffer solution (KH_2PO_4 : 3.0g L⁻¹, Na_2HPO_4 : 7.0g L⁻¹, NaCl : 4.0g L⁻¹, $\text{MgSO}_4 \cdot 7\text{H}_2\text{O}$: 0.2g L⁻¹) twice by centrifugation (10,000 x g at 25°C for 10min). The cells were re-suspended and stored in a sterile 20% glycerol buffer (100% glycerol, KH_2PO_4 : 3.0g L⁻¹, Na_2HPO_4 : 7.0g L⁻¹, NaCl : 4.0g L⁻¹, $\text{MgSO}_4 \cdot 7\text{H}_2\text{O}$: 0.2g L⁻¹) in a ratio of 50% glycerol : 50% bacterial buffer. The cells were frozen at a very low temperature for future use.

Comment [7]:

... [2]

2.4.3: Preparation of *Shewanella* inoculum

Frozen cells from a stock (20% glycerol) of *Shewanella* strain (depending on the ATTC reference strain used) were revived under aerobic conditions on tryptic soy agar (Fluka, Biochemica, Sigma-Aldrich, India). The cells were sub-cultured for a period of 48 hours twice. The colonies were aseptically scraped with a wire loop and used to prepare a cell suspension in tryptic soy broth (Fluka, Analytical, Sigma-Aldrich, India) with a target optical density of 0.55 ± 0.02 at $\lambda = 600\text{nm}$. About 10mL of the suspension was inoculated in 100mL of tryptic soy broth (Fluka, Analytical, Sigma-Aldrich, India) for the initial liquid pre-culture. Cells were grown overnight by continuous agitation at 300rpm and at 30°C .

Overnight cultures were harvested by centrifugation ($10,000 \times g$ at 25°C for 10min) and the cells were concentrated in 20mL TSB. However these cells were inoculated into a 1 litre conical flask containing 750ml of TSB to initiate the main culture by continuous agitation at 300rpm and at 30°C for 24hours to reach a stationary growth phase. These cells were finally harvested by centrifugation ($10,000 \times g$ at 25°C for 10min) and washed twice with sterile 0.9% NaCl by centrifugation at $10,000 \times g$ 25°C for 10 minutes. The cells were concentrated in 45 - 60mL sterile 0.9% NaCl to achieve a concentration of around $1.2 \pm 0.4 \times 10^8 \text{ cell mL}^{-1}$ in a 100mL serum bottle. Finally, the bottle was sealed with a thick butyl rubber cap. The cells were purged by bubbling oxygen-free N_2 gas for 30 – 40 minutes to make the environment completely anaerobic. These cells were finally used to inoculate the bioreduction cultures. A diagrammatic illustration of this procedure is shown in Figure 2.4.

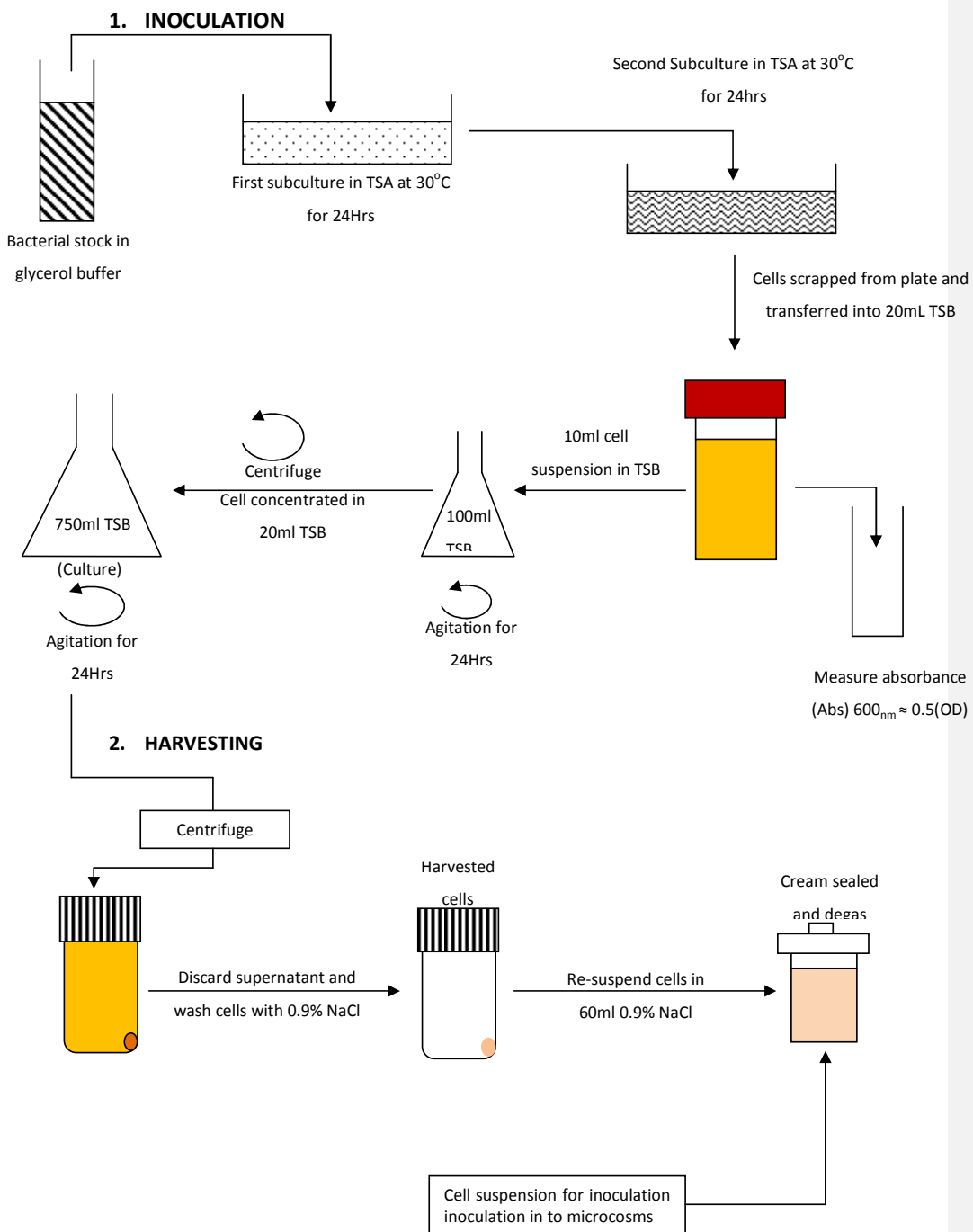


Figure 2.4: Diagrammatic illustration of bacterial culturing method.

2.4.4: Bacterial plate count using serial dilution

Bacterial plate counts were conducted from the harvested viable 60ml cell suspension using the serial dilution method in order to maintain the approximate concentration of 10^8 cells/ml. About 1ml of cell suspension was transferred and diluted in to 9ml of NaCl and thoroughly vortexed, representing a 10^{-1} dilution. 1ml from the 10^{-1} dilution was subsequently pipetted into a second test tube containing 9ml NaCl to give a dilution of 10^{-2} . The procedure was repeated for the remaining tube to give a dilution of 10^{-9} . Around 0.1ml from dilutions 10^{-7} , 10^{-8} , 10^{-9} was plated on solid tryptic soy agar (TSA) and incubated for growth at 30°C . Plates were checked after 24 hours and colonies observed were counted. The number of colony forming units (CFU) for each dilution plated was calculated using the formula in equation 1. A final concentration of $\approx 1.4 \times 10^8$ cells /ml was usually calculated from the plates counted.

$$\text{Number of CFU/mL} = \frac{\text{Colonies counted}}{\text{Volume plated (ml)} \times \text{Total dilution used}} \quad \dots\dots\dots (\text{Eqn 1})$$

2.4.5: Bioreduction cultures

Small scale bioreduction assays were conducted with kaolin and silica sand using a non-growth approach in an 80mL minimal medium (NaCl - 0.9% final). The culture medium contained 10g or 20g of kaolin, and/or 2.5g of silica sand samples with Fe(III) in the minerals as the electron acceptor and 10mM lactate (final) as the electron donor (unless otherwise specified). The media were sealed with a septum cap and sterilised at 121°C for 15min. 100 μm of AQDS (Anthraquinone-2,6,-disulfonate) sterilised by filtration (0.2 μm pore size millipore filter) was aseptically added in to the culture bottle using a sterile BD microlaneTM (0.5x16mm) syringe (Figure 2.5). The medium was then purged with oxygen-free N_2 to maintain anaerobic conditions. Working pH was adjusted and controlled at $\sim 7.1 - 7.3$. About 7mL ($1.2 \pm 0.4 \times 10^8$ cell mL^{-1}) of *Shewanella* cell suspension (unless otherwise specified) were aseptically added under sterile conditions and incubated at 30°C (unless otherwise specified) in the dark with continuous shaking at 60rpm. All samples were repeated in

triplicates or duplicate with a blank control that was cell-free or cell and electron donor-free, otherwise identical and similar to all other biotic samples.

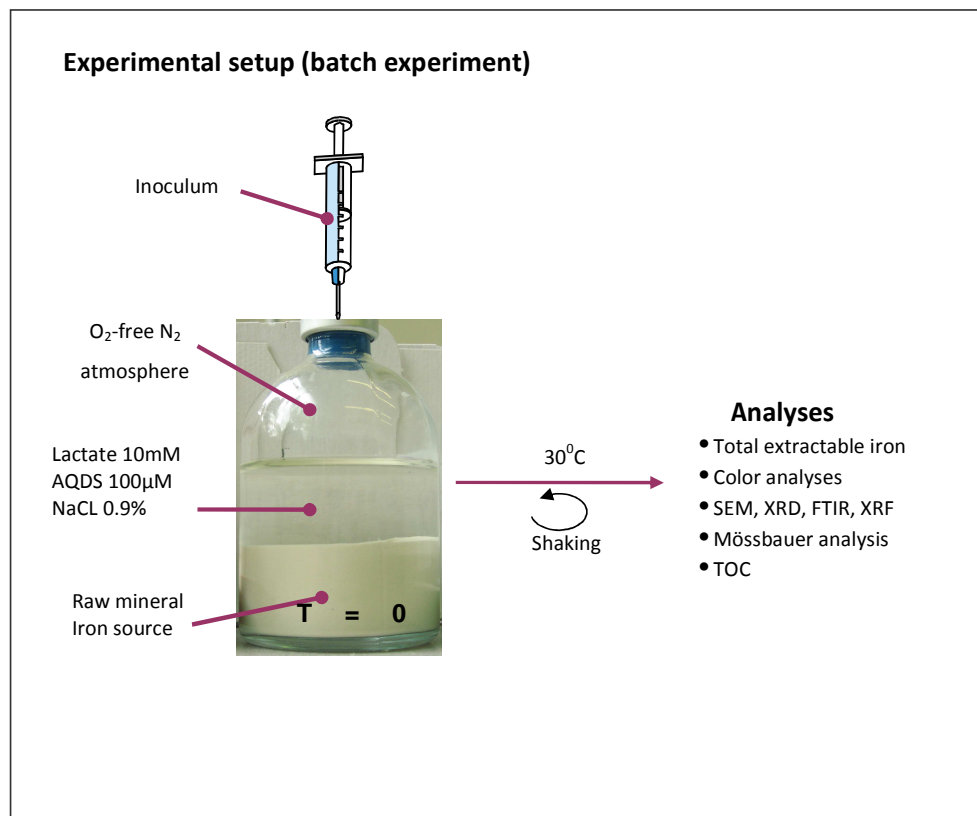


Figure 2.5: Illustration of experimental set up for the small scale bioleaching of kaolin and silica sand.

2.5: PREPARATION OF TITRATION SOLUTION

2.5.1: Fe(II) standard

The Fe(II) content leached from the mineral materials was determined and calculated by reference to calibration standard curve. A standard 0.1g L⁻¹ [Fe(II)] stock solution was prepared by initially adding 0.702g of Fe(NH₄)₂(SO₄)₂·6H₂O in to 2ml of concentrated H₂SO₄ until completely dissolved. The volume was made up to one litre with distilled water. The solution was stored at 4°C prior to any analysis.

2.5.2: 1, 10-Phenanthroline monohydrate

1,10-Phenanthroline monohydrate (ACROS Organics, New Jersey, USA) was used as the colorimetric indicator for determining the amount of Fe(II) leached in solution during bioreduction. Around 4.956g of phenanthroline was dissolved in 800ml of distilled water by stirring and heating the solution at a temperature between 35 - 40°C on a hot plate stirrer. A few drops of HCl were added to help for complete dissolution of crystals after which the volume was made up to 1 litre. This solution was kept in a dark bottle to prevent photo-oxidation and degradation of the compound.

Comment [8]:

David Manning 27/04/2011 18:53
Make sure this is spelled correctly

2.5.3: Glycine

A 0.5M glycine solution was also prepared as part of titration reagent. Glycine serves as a buffer in the titration solution and was prepared by dissolving 37.535g in 800ml of distilled water. The solution pH was adjusted to between 2.5 - 2.9 using HCl or NaOH after which it was made up to 1 litre.

2.5.4: Nitrilotriacetic acid (NTA)

0.1M solution of nitrilotriacetic acid (NTA) was prepared by dissolving 25.7g in to 800ml of distilled water and the pH was adjusted to 7. Nitriloacetic acid serves as a complexing agent in the titration solution and retards the reduction of $[\text{Fe}(\text{phen})_3]^{3+}$ in the system.

Comment [9]:

David Manning 27/04/2011 18:53
Is this a real word?

2.5.5: Preparation of titration mixture

Before calorimetric analysis of Fe(II) in bioleached samples, titration solution mixtures were always freshly prepared. The solution consists of a mixture of phenanthroline, glycine and nitrilotriacetic acid in a ratio of 5:5:1 respectively, and can be kept in a dark Duran bottle and used within 48 hours of preparation.

2.5.6: Measurement of standard calibration curve

A standard calibration curve with Fe(II) standard was calculated using a linear regression equation for every fresh stock of titration solution. This curve was used to work out the absolute concentration of Fe(II) leached in any bioleaching experiment. Different ranges and concentrations of Fe(II) standard were prepared from the initial 0.1g L^{-1} [Fe(II)] standard stock solution. A general example of the dilution procedure and titration method for calculating a standard calibration curve from an Fe(II) standard is shown in Table 2.2.

Table 2.2: Illustration of dilutions of Fe(II) standard solutions and absorbance values measured.

S/no.	Fe(II) stock (ml)	Fe(II) stock (μl)	H ₂ O (ml)	Titration solution(ml)	Fe ²⁺ equivalent (μg)	Abs _{510nm}
1	0	0	8	2	0	0.001
2	0.05	50	7.950	2	5	0.103
3	0.075	75	7.925	2	7.5	0.154
4	0.10	100	7.9	2	10	0.204
5	0.15	150	7.850	2	15	0.305
6	0.20	200	7.80	2	20	0.393

Comment [10]:

David Manning 27/04/2011 18:55
Make sure you are consistent and put figure and table captions after the figure or table, not before.

The unknown concentrations of Fe(II) leached from kaolin and silica sand are calculated from the known concentration of Fe(II) standard following the regression equation and are expressed in mmol L⁻¹ or (as is customary in the mineral industry) %Fe₂O₃ per gram of mineral material.

2.5.7: Analysis of HCl-extractable Fe(II) using the phenanthroline technique

The reduction of Fe(III) was measured as the production of Fe(II) in HCl extract using a modified 1,10-phenanthroline technique. At a selected time, 1mL of bioleached sample was taken from incubated microcosms with a sterile BD microlaneTM (0.5x16mm) syringe and added directly into a 10 mL tube containing 1mL of 2M HCl. This was allowed to stand for about 24hr before Fe(II) measurement and was finally filtered using a 0.2μm pore size Millipore filter into an empty 10mL tube. These extractions dissolved all the Fe(II) in the sample (both total Fe(II) and soluble Fe(II) fractions). However, the Fe(II) fractions in the HCl extract were determined using the modified 1,10-phenanthroline method described by Fadrus and Maly (1975). This method involves adding 1,10-phenanthroline titration solution to the HCl extract and determining the Fe(II) concentration by measuring the Fe(phen)₃²⁺ complex using UV-Visible spectroscopy at λ=510nm.

In general, about 2ml of 1,10-phenanthroline titration solution was added to a 10ml tube under red light followed by adding 0.5ml of HCl-Fe(II) extract. The volume was made up to 10ml by adding 7.5ml of water into the tube. This was then allowed to stand between 10 – 15 minutes under red light in a dark room in order to prevent photo-oxidation of phenanthroline. Optical density (absorbance) of the solutions was measured using UV-Vis spectroscopy at λ=510nm.

2.6: Soxhlet extraction of Natural Organic Matter

In order to further characterise composition of the NOMs, part of the NOM sample was purified using the soxhlet extraction method to remove free lipids that might be associated with the samples. The remaining bound compounds were then subjected to thermal pyrolysis. During extraction, about 1g of NOM sample was measured into cellulose thimbles and covered with cotton wool. Around 200ml of azeotropic mixture of dichloromethane (DCM) and methanol (MeOH) (93:7, v/v) was continuously recycled through the sample to extract the soluble component for a period of 24 hours. Small amounts of activated copper turnings were added into the solvent for free elemental sulphur removal. The bound compound in the cellulose thimbles were collected after soxhlet extraction for flash pyrolysis.

2.7: ANALYTICAL METHODS

2.7.1: Total Carbon Nitrogen and Hydrogen analysis

The natural organic matter samples (NOM 1 and NOM 2) were analysed to quantify their carbon, nitrogen and hydrogen contents. This was mainly carried out to characterize and find out the relative proportion of these major elements within the NOM samples. The samples were analysed at Advanced Chemical and Material Analysis (ACMA) Newcastle University, using a Carlo Erba 1180 Elemental Analyser controlled with CE Eager 200 software. The instrument was calibrated with an acetanilide organic analytical standard (Batch No. 131430 – certified and valid until 2012). The samples were weighed using a certified Mettler MX5 Microbalance. The precision value were 0.3% for solids and 0.5% for oils and liquids.

Comment [11]:

David Manning 27/04/2011 19:02
Be consistent with capital letters

2.7.2: Total Organic Carbon analysis

Liquid samples from the bioleach experiment were routinely sampled at a time interval and measured for dissolved organic carbon using a Shimadzu TOC- 5050A dissolved carbon analyser equipped with an AS1-5000A autosampler. Instrument calibration was conducted with low and high concentration carbon standards and water prior to analysis. For total carbon (TC) measurement, around 100µl of filtered (0.2µm pore size Millipore filter) sample was injected in to the sample port (directly connected to a furnace) using an auto-sampler, and heated to around 800°C. This converts the entire carbon content to carbon dioxide

which is carried in a stream of high purity air to an infrared detector that produces a signal directly proportional to the concentration of carbon dioxide.

For Inorganic carbon (IC) measurement, samples are auto - injected into the IC port which reacts with acidic quartz medium to produce carbon dioxide that is thereafter detected by the infrared detector as for TC. Subtracting the Inorganic Carbon (IC) value from the Total Carbon (TC) value gives the Total Organic Carbon (TOC).

2.7.3: Colour analysis using Colour Touch PC analyser

The optical properties (i.e., Whiteness, Brightness, Yellowness and **Lab** colour values) for the kaolin were measured before and after bioreduction using a Technidyne ColorTouch PC Spectrophotometer. The **Lab** system based on the colour value gives a perfect representation of the mineral colour properties, where **L** measures lightness/darkness, **a** measures red/green and **b** measures degree of yellow/blue shades. The ColorTouch analyser has three different apertures (27, 15, and 9.8mm). The model was equipped with a xenon flash lamp, holographic grating, scanning diode array, dual-beam ISO2469 optics and a built-in USB camera. The system conforms to ISO 2469, 2470, 2471 and 3681. Calibration of the system was conducted using certified paper standards (paper calibration kit supplied with brightness standard values 60, 70, 90 and a white fluorescence).

Comment [12]:

David Manning 27/04/2011 19:07
Is this all correct?

Before colour analysis, samples were first washed by centrifugation (10,000 x g at 25⁰C for 10min) using 2M HCl and then dried in an oven at a temperature of 110⁰C overnight. The sample was later pulverised and milled to a fine powder using an IKA A11 Basic Analytical mill (IKA-Werke, Stavfen, Germany) for 30 seconds. Roughly about 10g of the pulverised samples were pressed into pellets with an average size of 3.7cm diameter using a Technidyne Powder Press, by applying a force of ~50 pounds/square inch (50 psi) for 5-10 seconds as recommended in the protocol issued by Carisbrooke Instrument Service Ltd. Whiteness and **Lab** values were acquired using a D65 source and an illuminant D65/10⁰. ISO brightness was measured using a C source and an illuminant C/2⁰. Each pellet (sample) was automatically analysed 6 times by the machine to give the average colour values with standard deviation. To assess the performance and reliability of the ColorTouch PC machine, a number of standard samples provided by Imerys Minerals Ltd., WBB/Sibelco, and Omya

UK were analysed and the whiteness, ISO brightness and **Lab** values obtained agree with the values obtained by the industrial partners (APPENDIX 7.1).

2.7.4: X-ray Fluorescence spectrometry

X-ray fluorescence (XRF) is able to determine large a number of elements (up to 80) having different ranges of concentration. The technique is rapid and can quantify a number of trace and major elements in bulk geological samples including Na, Mg, Al, Si, P, K, Ca, Ti, Mn and Fe. The technique is mostly carried out using a wavelength dispersive system. Uniform homogenous sample preparation is paramount in XRF spectroscopy for accurate analysis. The most common procedure for XRF analysis is the fused glass disc method which involves fusion of sample with lithium borate flux, incorporating lanthanum oxide as absorber (Bain et al., 1996).

Comment [13]:

David Manning 27/04/2011 19:09
You don't need to say all this, as XRF is such a basic method

2.7.4.1: X-ray Fluorescence (kaolin samples)

X-ray fluorescence analysis of kaolin samples for determination of different oxides was conducted at Imerys in accordance to the principle given in British Standard 1902: Section 9.1:1987, *Analysis of alumino-silicate refractories by X-ray Fluorescence*. The procedure and method of oxide analysis in this technique involves chemical analysis by XRF using a standard lithium borate-lanthanum oxide fusion method in which sample was fused in a lithium borate glass bead as described in Norrish and Chappell (1967). About 0.1mg of dried homogenous fused sample was analysed using a Pananalytical Magic Pro XRF spectrometer equipped with a PW2540VRC automatic sample changer controlled by Panalytical SuperQ software run on a PC system. Prior to analysis, the analytical instrument was calibrated using commercially certified reference materials containing different ranges of oxides.

2.7.5: Infrared spectroscopy

Infrared spectroscopy is a rapid analytical technique that can be used to characterise clay minerals. Fourier transform and dispersive spectroscopy are the two most common infrared spectroscopy techniques used. In FTIR, the Fourier Transform Infrared Spectrometer may either be single or double beam. In single beam mode, the spectrum obtained from the sample is subtracted from background, while in double beam mode subtraction is carried out continuously from background (Russell and Fraser, 1996). The transmission (using KBr pellets) and diffuse reflectance (DR) modes are the most common methods widely used in FTIR spectroscopy. In transmission, the absorbance is directly proportional to the

concentration of the absorbing species present in the beam, and this is in accordance with the Beer-Lambert law (Russell and Fraser, 1996; Smith, 1996). The transmission method of analysis was chosen for sample analysis in this study.

2.7.5.1: Fourier Transform Infrared Spectroscopy

Kaolin, silica and natural organic matter samples were analysed by FTIR spectroscopy in transmission mode within the mid – infrared range region (400 to 4000cm⁻¹) using KBr pressed pellets. About 0.5 – 1% of sample concentration (1-2mg mineral material in 200mg KBr) was held in 99% FT-IR grade KBr using a manual hydraulic press system (SPECAC Ltd). The KBr/sample mixtures were loaded onto the hydraulic press plunger base in a compressor chamber and a load of 5 ton was gently applied for 5min and thereafter increased to 10 ton for another 10min to achieve a KBr pellet of approximately 13mm in diameter. All spectra were recorded at a resolution of 4cm⁻¹. A total of 100 scans were averaged for each sample or 32 scans for a quick spectrum acquisition. The prepared pellet was transferred onto a pellet holder which was then placed and attached to a special holder in Transmission E.S.P chamber. The instrument used was Nicolet AVATAR 360 FTIR ESP spectrometer equipped with OMNIC software for spectrum acquisition. Before spectrum acquisition, a pure KBr pellet was prepared and used as a background which was automatically subtracted from sample spectrum to give the ideal spectrum of the sample.

2.7.6: Electron Microscopy

Scanning electron microscopy (SEM) is a powerful technique that allows for observation as well as characterisation of various organic and inorganic materials and their surfaces at a micrometer (µm) and sub-micrometer scales (Goldstein et al., 1992). SEM is very important because it permits the analysis and examination of micro-structural characteristics of solid material at a very high resolution and at the same time at a very low magnification. One major advantage of this technique is the appearance of the image in three-dimensional orientation. SEM is used for examining the morphology of biological bodies and many heterogeneous materials such as clays, rocks, metals, polymers and ceramics. It may be used to also investigate and evaluate surface topography of solid materials (Goldstein et al., 1992). In addition, most scanning electron microscopes today are equipped with other analytical capabilities such as energy dispersive X-ray detection to give the elemental composition of a material. In this study, dry and wet samples were examined using different

analytical principles and SEM techniques to observe any interaction between microorganisms and mineral surface, or morphological alterations on the mineral surface.

2.7.6.1: Conventional Scanning Electron Microscopy

Batch reactor treated samples of silica sand and kaolin were analysed using conventional scanning electron microscopy to observe any interaction between microorganisms with the mineral surface. The mineral-cell suspension was initially fixed in 2% gluteraldehyde in Sorensens phosphate buffer (TAAB Laboratory Equipment, Aldermaston, Berks) overnight. This was then rinsed for about four different times by changing the Sorensens phosphate buffer. Samples were dehydrated successively using 25% ethanol, 50% ethanol, 75% ethanol (30 minutes) and 100% ethanol (2 x 1 hour). Final dehydration was carried out with carbon dioxide in a Baltec critical point dryer. The samples were mounted on an aluminium stub with Achesons silver dag, dried (Agar Scientific Stansted, Essex) overnight and finally coated with gold (standard 15nm) using a Polaron SEM Coating Unit. Samples were examined using a Stereoscan S40 Scanning Electron Microscope (housed in the Electron Microscopy Unit of the Medical School, Newcastle University) at an accelerating voltage of 8kV and around 6mm working distance.

2.7.6.2: Environmental scanning electron microscopy (ESEM)

Environmental Scanning Electron Microscopy of wet kaolin and silica samples was carried out using a Philips XL30 equipped with an Oxford instruments INCA 250 EDX analytical system that has elemental mapping capabilities, housed at the Electron Microscopy and Spectroscopy Centre (EMSC), Faculty of Engineering, University of Leeds. The samples were examined at a relatively low vacuum condition (around 10 Torr) in a water vapour atmosphere. The samples were run at a high resolution with an accelerating voltage of 3kV and a working distance of around 3mm.

2.7.6.3: Field Emission Gun – Scanning Electron Microscopy (FEG-SEM)

Dry kaolin and silica samples were also examined on the Field Emission Gun – Scanning Electron Microscope using very high resolution secondary electron imaging (SEI) at a high vacuum. Sample pre-treatment for the dry sample was carried out at Newcastle University. The samples were dried thoroughly, pre- mounted on aluminium stubs and kept in a desiccator before transport to the EMSC at the University of Leeds. The samples were immediately coated on arrival in Leeds using a high resolution sputter coater with a Pt/Pd

target to form a conducting layer all over the samples and between the Al stub and the sample (to prevent charging on exposure to the electron beam). The samples were scanned at an accelerating voltage of 3Kv and a working distance of around 3mm. The instrument used was a LEO1530 Gemini equipped with an Oxford Instruments INCA 350 EDX analytical system with a high resolution KE STEM detector.

2.7.7: X – Ray Diffraction

X-ray diffraction is a powerful, rapid and robust technique used to investigate the structure of materials at a molecular level and to identify unknown materials. It aids in investigating and understanding solid state science, chemical bonding and determining positions and arrangements of atoms and molecules in sub-microscopic assembly structures and crystals (Synder, 1999; Hukins, 1981). Identifying an unknown material using X-ray diffraction involves recording a reference X-ray pattern from various known materials. These are then compared with the X-ray pattern obtained from an unknown sample. The samples that coincide with any of the reference patterns are then mapped out and identified (Hukins, 1981). The technique is often employed and applied in material science, and in particular this method is used for identifying micro-crystals in powders. The powder X – ray diffraction method was used in this investigation.

2.7.7.1: X –ray diffraction analysis

X – ray (powder) diffraction measurements of the silica sand and kaolin samples before and after bioreduction were conducted at the School of Chemical Engineering and Advanced Materials, Newcastle University. Measurements were obtained with a PANalytical X'pert PRO MPD instrument using Cu K α radiation. The instrument is fitted with an X'Celerator detector and a secondary monochromator. The X'Celerator is an ultra-fast X-ray detector that uses Real Time Multiple Strip (RTMS), operating like an array of over a hundred detectors simultaneously collecting X-rays diffracted from a sample over a range of 2 θ angles. The X'Celerator is therefore able to give high quality diffraction patterns in approximately 1/100 of the time an older style diffractometer would require. The secondary monochromator eliminates fluorescent scattering from the specimen and so results in a better peak:background ratio for samples containing transition metal and rare earth elements.

In operation, a Cu anode was supplied with 40kV and a current of 40mA to generate Cu-K α radiation ($\lambda = 1.54439 \text{ \AA}$) or Cu-K α_1 ($\lambda = 1.54056 \text{ \AA}$). The data was acquired over a range of $2^\circ 2\theta - 70^\circ 2\theta$ with a nominal step size of $0.0034^\circ 2\theta$ and a nominal time per step of 99.70 seconds. Fixed anti-scatter and divergence slits of $1/4^\circ$ were used together with a beam mask of 0.38mm. All scans were carried out in continuous mode using the X'Celerator RTMS detector. Phase identification was carried out by means of X'Pert accompanying software program High Score Plus along with the ICDD Powder Diffraction File 2 database (1999) and the Crystallography Open Database (October 2010; www.crystallography.net).

2.7.8: Mössbauer spectroscopy

Mössbauer spectroscopy is a very powerful technique used to characterise the valency of iron in a sample, and has been used to investigate various iron oxide phases in soils. Iron oxide minerals are widespread and abundantly occur in the form of clay-sized particles. They include several oxides and oxyhydroxides. Mössbauer spectroscopy is often used in identifying the composition of these iron-containing compounds (Goodman, 1996).

2.7.8.1: Mössbauer spectroscopic analysis

Mössbauer spectra of silica and kaolin samples were obtained at 290K (17°C) in reflection mode and at 6.5K in transmission mode by Dr. Moustafa Abelmoula in the Laboratoire de Chimie Physique et Microbiologie pour l'Environnement (LCPME), University of Nancy, France. The spectra were obtained in accordance with the procedure described in Zegeye et al., (2007). In this procedure, the spectra were acquired using a constant acceleration Mössbauer spectrometer connected to a 512 multichannel analyser. Amplifier output and drive mechanism were manufactured by Hadler Electronics GmbH. The detector was equipped with NaI(Tl) scintillation counter. Spectra were maintained and acquired at room temperature (RT) using 50 mCi $^{57}\text{Co}/\text{Rh}$ matrix sources. Spectral calibration was conducted with 25- μm foil of $\alpha\text{-Fe}$ at room temperature. The spectra were fitted with Recoil (University of Ottawa, Canada) program using the Lorentzian or pseudo-Voigt method (Lagarec and Rancourt, 1997).

Similarly, a different kaolin material was analysed using Mossbauer spectroscopy by Dr. Ravi K. Kukkadapu at Pacific Northwest National Laboratory Richland, Washington, USA. These spectra were obtained both at 4.5K and at Room Temperature (RT) in accordance with the

Comment [14]:

David Manning 27/04/2011 19:56

Was there a monochromator on the source, so that it was CuK α_1 that was used?

Comment [15]:

David Manning 27/04/2011 19:55

Do you mean milliseconds?

procedure described in (Fredrickson et al., 2003; Zachara et al., 2002). The procedure involves initial preparation and storage of sample in an anaerobic atmosphere. The room temperature (RT) spectra were collected using ~50 mCi (1.85MBq) $^{57}\text{Co}/\text{Rh}$ single line thin source. The 4.5K spectra were obtained using a top-loading Janis exchange-gas cryostat with source drive. The Mössbauer bench (MB-500; WissEL, Germany) was equipped with a dual Mössbauer drive system. The velocity transducer (MVT-1000; WissEL) was operated in a constant acceleration mode ($23\text{Hz} \pm 10\text{mm/s}$). Data acquisition was conducted on 1024 channels and then folded to 512 channels to give a zero-velocity corresponding to the center shift (CS or δ) of a metallic-Fe foil at room temperature. Spectral calibration was conducted with 20 μm thick α -Fe foil (Amersham, England) placed in the same position as the sample to reduce error caused by changes in geometry. An Ar-Kr proportional counter was used for recording transmitted radiation. The Recoil Program (University of Ottawa, Canada) was used to evaluate unfolded spectra using a Voigt-based hyperfine parameter distribution method (Rancourt and Ping, 1991).

2.7.9: Pyrolysis - Gas Chromatography – Mass Spectroscopy

Pyrolysis-GC-MS analysis of NOM samples were performed on a CDS Pyroprobe 1000 via a CDS1500 valved interface (320°C) connected to a Hewlett-Packard 6890GC split injector (320°C) and linked to a Hewlett-Packard 5973MSD (electron voltage 70eV, emission current 35uA, source temperature 230°C, quadrupole temperature 150°C, multiplier voltage 2200V, interface temperature 320°C). The acquisition was controlled by a HP kayak xa chemstation in full scan mode (50-650amu).

Approximately 1mg of both the soxhlet extracted and non-soxhlet extracted natural organic matter was weighed into a quartz tube and covered with glass wool at both end. The tube was then placed into a pyroprobe platinum heating coil and then sealed into the valved interface. The run was then started with the sample being pyrolysed at 735°C for 10 seconds with the split open. At the same time the GC temperature programme and data acquisition commenced. Separation was performed on a fused silica capillary column (60m x 0.25mm i.d.) coated with 0.25 μm 5% phenyl methyl silicone (HP-5MS). Initially the GC was held at 40°C for 1 minute and then temperature programmed from 40°C-325°C at 5°C min and held at final temperature for 30 minutes, total 90 minutes, with helium as the carrier gas

(constant flow 1ml/min, initial pressure of 110kPa, split at 30 mls/min). Each acquired data run was stored on DVD for later data processing, integration and printing.

2.8: BIOREACTOR EXPERIMENTS

2.8.1. Design of bioreactor

Two separate 4.5 litre bioreactors were designed and constructed to up-scale Fe bioleaching from kaolin and silica sand. The reactors were designed to consist of an air-inlet and air-outlet for continuous circulation of nitrogen into the system to maintain permanent anaerobic conditions. Also in the upper part of the reactor was a sampling and injection port for daily sampling and injection of pure cultures of bacteria during bioleaching. The reactor was equipped with a stirrer blade to provide a continuous mixing and to keep the solution in proper suspension (Figure 2.7). The reactor was also equipped with pH and Eh probes to monitor changes in the solution chemistry during the bioreduction process. There was an external temperature probe to monitor if the temperature was within the range required for the growth of microorganisms in the reactor. The pH and Eh probes were linked to a desktop PC via a EL005 EnviroMon data Logger connected to a EL071 voltage and current converter (PICO Technology Ltd., Cambridgeshire, UK) for data acquisition. This allowed the electrical signal between the probes to be monitored in real time. For temperature data acquisition, external temperature probes were connected to EL005 EnviroMon data Logger via a EL041 4-channel thermocouple converter (PICO Technology Ltd., Cambridgeshire, UK).

2.8.2: Reactor bioreduction experiments

Bioleaching experiments were conducted with kaolin and silica sand in 4.5L bioreactors using *Shewanella putrefaciens* CIP8040. Around 300g of unsterile kaolin or 140g of unsterile silica sand (unless otherwise specified) were weighed and added in to the reactor. About 3L of 0.9% NaCl (sterilised at 121°C) was added to the reactor. A final concentration of 10mM lactate, serving as electron donor and 100µm of AQDS (anthraquinone-2,6-disulfonate) which serves as electron shuttle, were loaded into the reactor after filter sterilisation using a 0.2µm pore size millipore filter. The pH in the solution was then finally adjusted to around 7.2. The reactor lid was placed back and tightly screwed to ensure air tightness. pH, Eh and temperature probes were placed in their appropriate holes and screwed tightly. The reactor

medium was finally purged with oxygen-free nitrogen to make the environment anaerobic prior to cell injection. About 120mL of *Shewanella putrefaciens* CIP8040 cell suspension were prepared and aseptically added to the reactor. Daily sampling of bioleach slurry material was conducted for Fe(II) measurements. A blank control bioreactor that was cell-free was also set up and identical with the cell-treated reactor.

Real time data for Eh, pH and temperature were recorded for each bioreactor using PicoLog software on a desktop PC. Data output were recorded every second with pH and Eh probe output measured and recorded in Volt (V) over time, while temperatures were measured and recorded in degree Celsius ($^{\circ}\text{C}$) against time

Comment [16]:

David Manning 27/04/2011 20:05
Do you mean the liquid or the solid?

GENERAL REACTOR DESIGN

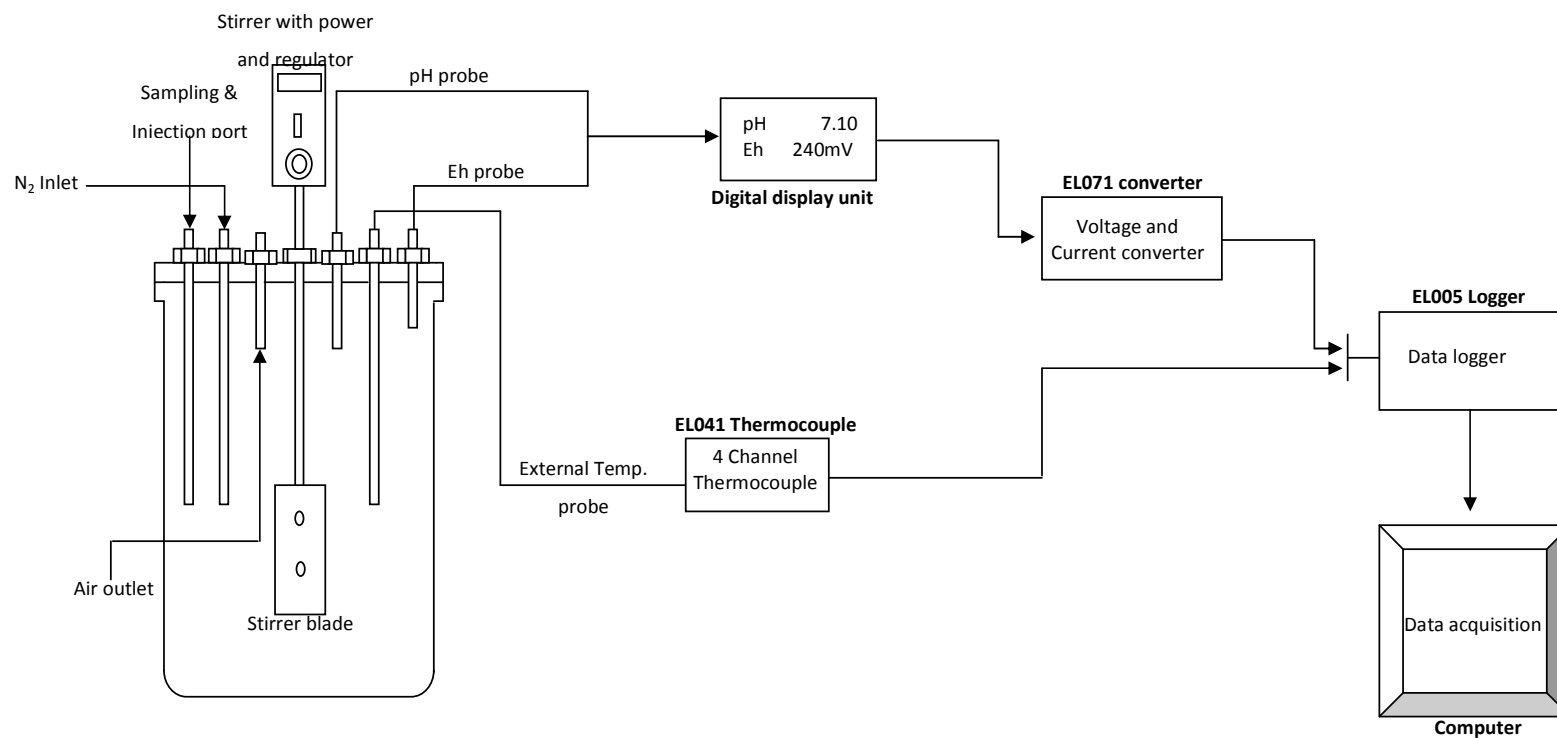


Figure 2.6: General illustration of the 4.5 litre batch bioreactor designed for the up-scaling of bioleaching experiment.

CHAPTER 3 : BIOREDUCTION OF KAOLIN PART I: OPTIMISATION AND MECHANISM OF REACTION

3.1: INTRODUCTION

Kaolin is a hydrous aluminium silicate ($\text{Al}_2\text{Si}_2\text{O}_5(\text{OH})_2$) clay mineral with average diameter of typically $<5\mu\text{m}$ for finely crystalline kaolin, and up to $100\mu\text{m}$ or more for the coarsely crystalline vermiform aggregate (Deer et al., 1999; Psyrillos et al., 1999). Kaolin is an important member of the kaolinite group with a wide and diverse range of industrial applications. It has a simple structure consisting of one tetrahedral silica sheet linked through oxygen to an octahedral alumina layer. The mineral is largely used as a raw material in paper coating, plastic, ceramics, cosmetics, paints, porcelain, potteries and brick manufacturing (Qinyan et al., 2009; Deer et al., 1999). Similarly, this mineral is also used in waste treatment, agriculture, pigments, nanocomposite coatings, acid base regulators and filler materials. The quality and commercial value of kaolin largely depend on its percentage purity, texture and colour properties such as degree of whiteness, brightness, **Lab** colour values, tint and opacity. The mineral when mined is rarely pure, containing some certain Fe-bearing impurities and other traces of various ions such as Ti, Cr, Mg and K that impart colour as contaminant and lower the mineral colour properties (Hosseini et al., 2007; Chandrasekhar and Ramaswamy, 2006; Asmatulu, 2002; Lee et al., 2002; Deer et al., 1999; Psyrillos et al., 1999).

The major impurities within this mineral are usually iron oxides (mainly Fe(III)-oxide) present in the form of oxides or oxyhydroxides adsorbed on the mineral surface covering the entire mineral mass, or admixed as a separate iron bearing phase such as hematite (red), magnetite (black), goethite (brownish yellow), lepidocrocite (orange), and ferrihydrite (brown red). Sometimes iron impurities in kaolin are present as either part of the kaolinite structure or within other minerals such as mica and anatase. The presence of these impurities lowers their industrial value (Styriakova et al., 2007; Chandrasekhar and Ramaswamy, 2006; Asmatulu, 2002). Moreover, a concentration of Fe(III) as low as 0.4% Fe(III) is sufficient enough to impart a remarkable colour change on the mineral surface (Styriakova et al., 2007). Hence, removal of these impurities becomes absolutely imperative

Comment [DM17]: This is not true for all kaolins.

in order to maximise a kaolin's industrial and market value. At present, chemical and physical treatments are the current refining methods widely used and employed by the mineral industries for removing iron impurities in kaolinite to achieve a desired value. But these processes are quite expensive (generating wastes), more energy consuming, have complex operating conditions and are environmentally unfriendly (Hosseini et al., 2007; Styriakova et al., 2007; Lee et al., 2002).

This chapter describes work designed to exploit and harness the dissimilatory iron reduction pathway for the bioreduction of kaolin-bound Fe(III) to improve the mineral's quality and industrial value. The chapter will examine the efficiency of Fe(III) removal using different iron-reducing bacterial strains and assess the extent of quality improvement. Moreover the chapter will investigate the rate of Fe(III) reduction kinetics as a function of electron donor concentration, biomass concentration, temperature and solid to liquid ratios under non growth conditions. The efficiency of natural organic matter (NOM) will also be investigated as a substitute for AQDS in enhancing the kinetics of Fe(III) reduction. AQDS is an electron transfer mediator designed to functionally behave in similar manner to natural organic matter for transferring electron to external electron acceptors (Royer et al., 2002). The compound contains a quinone group that is known to be present in the humic substance and plays a significant role in enhancing bioreduction of various redox sensitive metals including Fe(III), by serving as mediator between metals and microorganisms, thereby alleviating requirement for contact (Gu et al., 2005; Zachara et al., 1998).

3.2: METHODOLOGY

Small-scale microcosm experiments were conducted with Fe(III) in kaolin as the sole electron acceptor and lactate as the electron donor in the presence of a pure culture of *Shewanella* cells. Anthraquinone 2-,6-disulfonate (AQDS) was used to enhance electron shuttling in the system. All experiments were performed in triplicate (unless otherwise specified). The reduction of Fe(III) from kaolin was measured (as described in sub-section 2.5.7 of Chapter 2) as the production of Fe(II) in HCl extracts using modified phenanthroline techniques (Fadrus and Maly, 1975). Absorbance was measured using UV-vis-spectrophotometry at 510nm. Liquid samples from bioleaching experiments were analysed

for dissolved organic carbon using a Shimadzu TOC- 5050A carbon analyser equipped with an AS1-5000A autosampler.

To assess any improvement in mineral quality after bioleaching, both initial and bioleached minerals were analysed for colour properties (L^* , a^* , b^* , ISO Brightness, Whiteness and Yellowness) after mild acid washing with 2M HCl using a Technidyne ColorTouch PC Spectrophotometer. To observe changes in the mineralogy after bioleaching, X-ray (powder) diffraction measurements were obtained with a Philips X'pert PRO XRD system from 2° to 70° 2θ $\text{CuK}\alpha$, at 0.0334° 2θ per step and 99.70 seconds per step. Similarly, FTIR analyses of bioleached and initial minerals were measured and obtained in transmission mode using KBr pressed pellets (1-2mg mineral in 200mg KBr) in the mid-infrared range ($400 - 4000\text{cm}^{-1}$) using an AVATAR 360 FTIR ESP spectrometer.

Mössbauer spectroscopy was conducted at 290K (17°C) in reflexion mode and at 6.5K in transmission mode by Dr. Moustafa Abelmoula in the Laboratoire de Chimie Physique et Microbiologie pour l'Environnement (LCPME), University of Nancy, France. Some kaolin samples were also analysed using transmission Mössbauer spectroscopy at 4.5K and also at room temperature (TR) by Dr. Ravi K. Kukkadapu from Pacific Northwest National Laboratory, Richland USA. Scanning electron microscopy was conducted at the Electron Microscopy Unit of Medical School Newcastle University and at University of Leeds.

3.3 RESULTS

3.3.1: Selection of the most suitable iron reducing bacteria.

Microcosm studies for the bioreduction of kaolin Fe(III) were conducted with five selected iron-reducing bacteria under non growth conditions (as described in sub-section 2.4.5) to select the most suitable iron reducing bacteria that will effectively improve the quality of kaolin after bioleaching. Kaolin 2 (a dry kaolin labelled 'Remblend') was used in this experiment. In all of the selected bacteria investigated here, the rate of microbial reduction of Fe(III) in the mineral was observed to be fast in the first day and gradually decrease with time. The rate and extent of Fe(III) reduction were variable for the different *Shewanella* strains. However, the product concentration of Fe(II) in solution with *S. putrefaciens*

CIP8040 was observed to be 1.46mmol L^{-1} within 5 days (Figure 3.1). About 1.41mmol L^{-1} of Fe(II) was measured after leaching with *S. algae* BrY and 1.40mmol L^{-1} with *S. putrefaciens* CN32 within 5 days of incubation. Similarly Fe(III) reduction was also observed with *S. oneidensis* and the Fe(II) leached was measure to be 0.966mmol L^{-1} after 5 day of incubation. *S. loihica* was however observed to be the slowest and least efficient in bio-reduction with only 0.002mmol L^{-1} of Fe(II) leached in the solution within 5 days.

Therefore all the selected bacteria were able to reduce iron and increase its solubility in kaolin with the exception of *S. loihica*. The reduction of Fe(III) is always accompanied by changes in the colouration of supernatant from complete transparent suspension to an orange colour due to reduction of AQDS to AHDS. Statistical analysis of the results indicate that all the four tested bacteria are significantly better than *S. loihica* (t-tests, $P=0.000$). Similarly, *S. algae*, and *S. putrefaciens* CIP8040 are all significantly better than *S. oneidensis* (t-test, $p<0.013$). There is no significant difference between *S. algae*, *S. putrefaciens* CN32 and *S. putrefaciens* CIP8040 (t-tests, $p>0.175$).

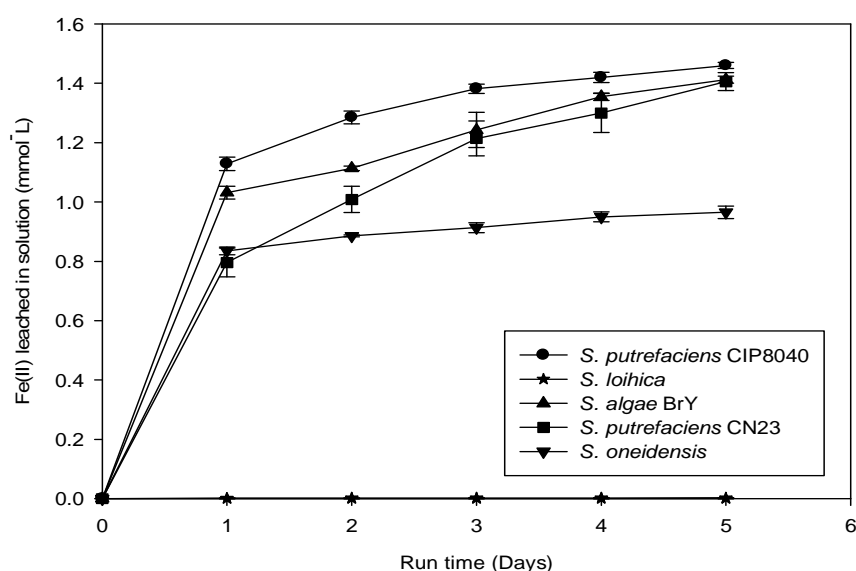


Figure 3.1 Line plots showing extractable Fe(II) concentration from 20g kaolin 2 (Remblend) as a function of time obtained to compare different iron-reducing *Shewanella* strains in the presence of 10mM lactate and 100 μ M AQDS at 20°C.

To assess improvement of the colour property after bioleaching with different iron reducers, colour index values were measured after terminating the experiment. The optical properties of the raw and bioleached kaolin were determined and results are shown in Figure 3.2. Although the amount of Fe(II) measured in solution is relatively low, a substantial improvement in the optical properties of biotreated mineral was achieved. Treatment with *Shewanella putrefaciens* CIP8040 was found to improve substantially the whiteness by 10.1% and ISO brightness by 3.6% with a decrease in the yellowness of 3.7%. *Shewanella putrefaciens* CN32 and *Shewanella algae* BrY were found both to have improved the whiteness by approximately about 7.4% and brightness by approximately 2.3%, while the yellow value decreased by about 3%. However, treatment with *S. oneidensis* MR1 improves the whiteness by 6.19%, brightness by 2.25% and yellowness decreases by about 2.4%.

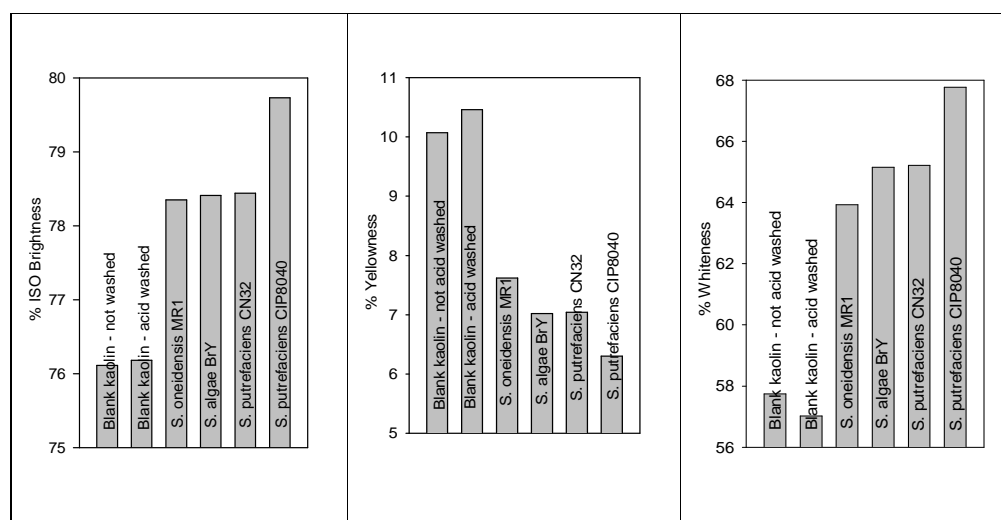


Figure 3.2: Bar chart showing the optical property of raw and bio-treated kaolin (A) % ISO Brightness (B) % Yellowness (C) % Whiteness using different iron-reducing *Shewanella* strains for 5 days at 20°C.

The optical properties of the raw blank kaolin after washing with 2M HCl were not significantly different from that of unwashed blank kaolin. Differences of 0.72% in whiteness, 0.09% brightness and 0.39% were measured between them. This suggests that biotreatment did increase the solubility of iron in kaolin and thereby made it easier to remove. The result is in agreement with the work carried out by Lee *et al* (2002), although the microbial culture they used was the indigenous community from fresh kaolin and was not identified nor specified. Although all the iron reducers used here show a good

performance in improving the colour property of kaolin, *S. putrefaciens* CIP8040 was found to improve the whiteness, brightness and decreases the yellowness better than the other iron reducers in addition to being better in leaching more Fe(II). For this reason *S. putrefaciens* CIP8040 was selected for subsequent experiments in this study.

3.3.2: Effect of temperature on the bioreduction of Fe(III) in kaolin

In order to have an optimisation of the bioleaching condition in this study, the effect of temperature on Fe(III) bioreduction in kaolin 2 (Remblend) was investigated using *Shewanella putrefaciens* CIP8040 (Figure 3.3). The temperature response of this iron reducer was monitored for the bioleaching of iron over different periods of time. The rate of Fe(III) reduction at 30°C was observed to be high and faster than when an elevated temperature of 36°C was used. At 30°C the amount of iron(II) measured in solution was 2.1mmol L⁻¹ on day 5 followed by a very slow increase with Fe(II) in solution of around 2.3mmol L⁻¹ after extending the bioleaching period to day 12. However, at 20°C the Fe(II) leached was 1.4mmol L⁻¹ on day 5, less than what was observed at 30°C. The lowest reduction efficiency was observed when bioreduction was monitored at 36°C with Fe(II) measured in solution of around 1.3 mmol L⁻¹. Although bioleaching occurs at 20°C and at 36°C, the highest rate was obtained at 30°C. The results have shown that temperature can have a major impact on bioleaching and at the same time can substantially affect the rate of iron reduction and dissolution in the mineral. Similarly the response of *S. putrefaciens* CIP8040 to bioleaching at different temperatures may equally result in different rates of iron reduction.

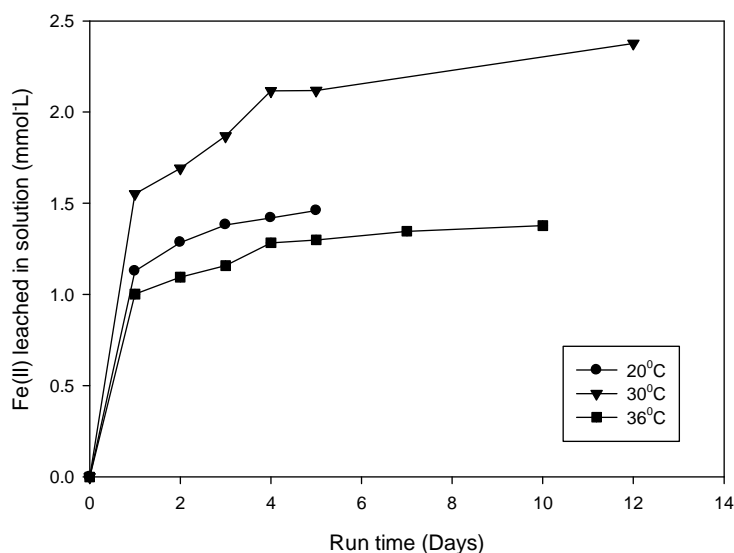


Figure 3.3: Line plots showing extractable Fe(II) concentration at different temperature using *S. putrefaciens* CIP8040.

3.3.3: Effect of solid/liquid ratio on bioreduction of Fe(III) in kaolin

Parallel experiments were carried out to evaluate and assess the impact of mineral/liquid ratio on the rate and extent of bioreduction of Fe(III) in kaolin 2 (Remblend) over time by using *S. putrefaciens* CIP8040 and *S. putrefaciens* CN32 cells. Two different mineral mass (10g and 20g) to liquid (80ml) ratios were used. All the experiments were incubated at 30°C with the injection of 7ml of suspended bacterial cells (1.2×10^8 CFU/mL). Analyses of colour property were conducted to observe any changes after bioreduction. This experiment shows different patterns of behaviour of the rate and extent of reduction by these two different iron reducers. It was generally observed that within the first 3 days the initial rate of Fe(III) reduction in 20g/80mL slurry is higher and so rapid that it exceeds and is double the rate when 10g/80ml slurry was used, irrespective of the type of bacterial strain present (Figure 3.4). We therefore assumed that since there is more solid in 20g/80ml slurries then more bio-reducible Fe(III) is expected in the system for these bacteria to reduce.

However, the rate of iron reduction was higher and more rapid on the first day with *S. putrefaciens* CIP8040 when 20g/80ml slurry was used, with 1.002mmol L^{-1} of Fe(II) measured in solution, and this continued to increase with time. On the other hand the rate of reduction in 20g/80ml slurry using *S. putrefaciens* CN32 (0.730mmol L^{-1}) was lower than what was measured with *S. putrefaciens* CIP 8040. Interestingly, similar trends in the rate of reduction were observed between these two iron reducers when 10g/80ml slurry was used. In contrast, by extending the bioleaching time, *S. Putrefaciens* CN32 was able to leach more Fe(II) in solution than *S. putrefaciens* CIP8040 in both different ratios. The amount of Fe(II) measured using *S. putrefaciens* CN32 within 10 days was about 1.56mmol L^{-1} for 20g/80ml slurry and around 0.861 mmol L^{-1} when 10g/80ml was used. But the extent of reduction was lower when *S. putrefaciens* CIP8040 for 20g/80ml slurry (about 1.378 mmol L^{-1}) and 10g/80ml (about 0.73mmol L^{-1}) when compared with the similar ratios using *S. putrefaciens* CN32. This shows that the extent of Fe(III) reduction with *S. putrefaciens* CIP8040 cells tends to flatten off after day 5 in both 10g/80ml slurry and 20g/80ml slurry but continuously increases over time with *S. putrefaciens* CN32.

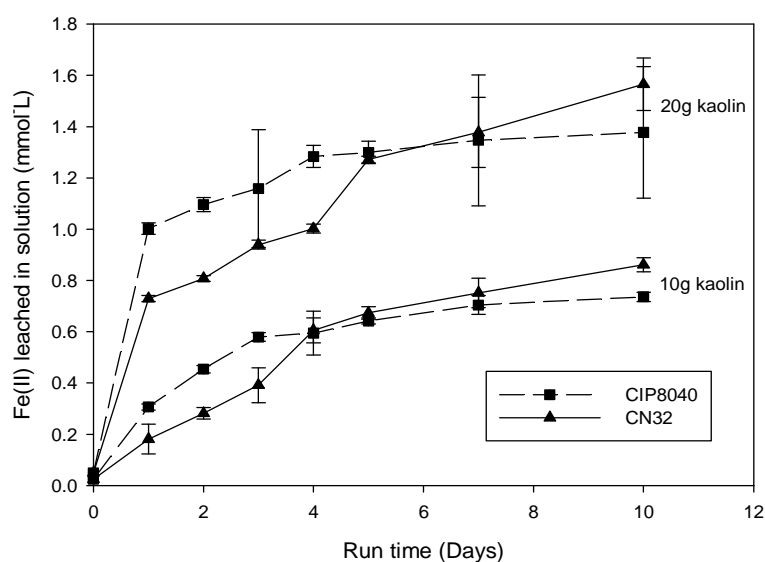


Figure 3.4: Bioreduction of kaolin bound-Fe(III) by *S. putrefaciens* CN32 and *S. putrefaciens* CIP8040 using 10g or 20g mineral mass in 80ml of solution. Experiments were run at 30°C .

Samples were taken and analysed for colour properties on day 5, day 7 and day 10 to monitor changes over time. There was remarkable improvement of the colour properties within the first 5 days of the experiment in all the amendments. However, extending the incubation period to day 7 shows a slight increase in brightness and whiteness and a decrease in yellowness in all the experiments. However this was not so when 10g/80ml was leached with *S. putrefaciens* CIP8040 (Figure 3.5). Further extension to 10 days shows no increase but rather a slight decrease in the colour index. Moreover, these two different strains were observed to behave differently. It was observed that with *S. putrefaciens* CIP8040, the whiteness, brightness and yellowness slightly improved more when 20g/80ml kaolin mineral was leached but less when 10g/80ml was leached. For example bioleaching of 20g/80ml slurry with *S. putrefaciens* CIP8040 increases the whiteness by 9.16%, brightness by 3.4% and yellowness decreases by 3.63% in comparison to whiteness increasing by 7.93%, brightness by 2.45% and yellowness decreasing by 3.25% when leached with *S. putrefaciens* CN32 within 7 days. In contrast, whiteness, brightness and yellowness improved more when 10g/80ml kaolin slurry was leached with *S. putrefaciens* CN32 over time but less when 20g/80ml slurry was leached (Figure 3.5). For example, whiteness increased by 9.79%, brightness by 3.1% and yellowness decreased by 3.75% in comparison to increases in whiteness of 8.95 %, brightness 2.8% and a yellowness decrease of 3.52% when leached with *S. putrefaciens* CIP8040 within 7 days.

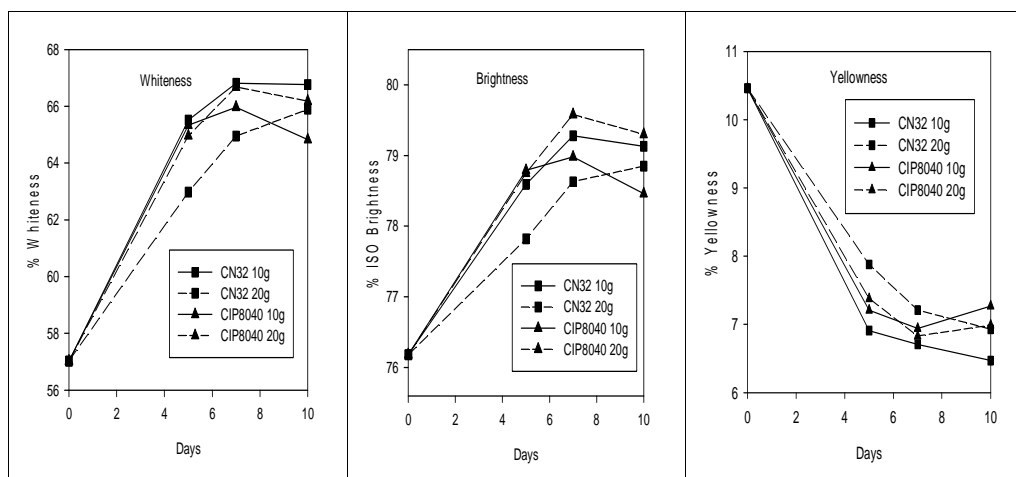


Figure 3.5: Colour analyses of kaolin after bioreduction with *S. putrefaciens* CN32 and *S. putrefaciens* CIP8040 using 10g or 20g at 30°C.

3.3.4: Effect of cell/solid ratio on Fe(III) bioreduction

Experiments were run with 10g and 20g kaolin 2 for the same amount of liquid (80ml/ microcosm) using different volumes of injected suspension of *S. putrefaciens* CIP8040 to evaluate the impact of cell/solid ratio on the bioreduction process. It was observed that within the first 10 days of bioleaching, the amount of bacterial cell injected in the system does not have a major impact on the rate and extent of bioleaching when less kaolin mass (10g) was used (Figure 3.6). Contrary to this, when 20g kaolin was leached, the cell/solid ratio does affect the rate and extent of bioleaching. The rate and extent of Fe(III) reduction were variable for 20g clay mineral. For example the extent of bioreduction of 20g mineral clay using 7ml cell suspension within 10 days was found to be the highest (1.728mmol/L) and lowest when 2ml cell suspension was used (0.229mmol/L). But irrespective of the amount of cells used, no substantial difference was observed when 10g of clay was leached. With 20g kaolin/7 ml cell suspension, the extent of reduction by ten days was almost doubled of what it was with 10g kaolin/7ml cell. Similar correlation was observed by comparing 20g kaolin/4ml cell with 10g kaolin/4ml cell suspension.

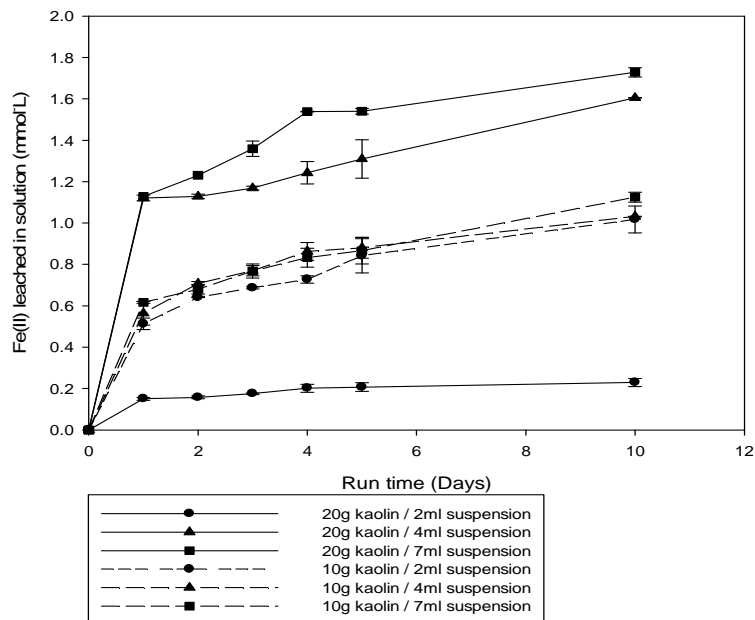


Figure 3.6: Bioreduction of Fe(III) from 10g and 20g kaolin using different injection of *S. putrefaciens* CIP8040 cell suspension ($1.2 \pm 0.4 \times 10^8$ CFU/mL) at 30°C.

Samples were obtained at the termination of the experiment for monitoring colour changes. The optical property results from biotreated and blank kaolin (Table 3.1) show that using 20g kaolin/4mL cell suspension has effectively improved % ISO brightness from 73.98% to 79.02% and % whiteness from 54.31% to 65.80%. Interestingly, there was reasonable agreement between % brightness (65.86%) and % whiteness (78.42%) results obtained when 10g kaolin was leached with 4ml cell suspension compared with that obtained when 20g kaolin was leached with 7ml cell suspension (Table 3.1). Furthermore, bioleaching 20g of kaolin with fewer cells (2ml cell suspensions) seems to have less impact on the % whiteness (57.10%) and % brightness (75.60%) when compared with the blank. Similarly with more cells in the system and less mineral (10g kaolin/7ml cell suspension), the ratio was observed to have less impact on the colour where the brightness increases to only 76.78% and whiteness to 63.32% (Table 3.1). Apart from whiteness and brightness values, Table 3.1 also gives the *Lab* value of the bioleached and blank mineral. The result shows improvement in both a^* and b^* values in most of the biotreated sample which are attributed to the removal of iron oxide from the mineral. A combined factor of higher L^* value (93.17) and more negative a^* value (-0.40) in 20g kaolin/4m cell suspension further indicates reasons for its recorded high % brightness of (79.02).

It is interesting to note that the degrees of brightness and whiteness of kaolin directly depend on the overall effect of the ***Lab*** value. The term L^* measures degree of lightness and darkness and varies from 100 for a clear perfect white to 0 for absolute black. However, a^* measures the red/green colour. The more positive the a^* value the greater the degree of its reddishness and the more negative the greater the greenishness. Yellow/blue is indicated by b^* and the more positive the more yellowishness and the more negative the more blueishness. Iron bearing minerals greatly influences the brightness and L index by decreasing their values (Chandrasekhar and Ramaswamy, 2006; Chandrasekhar and Ramaswamy, 2002).

Table 3.1: Colour analyses of kaolin after bioreduction with different injection of *S. putrefaciens* CIP8040 on day 5.

Sample	L*	A*	B*	% Whiteness	% Brightness
Blank Kaolin	91.81	-0.08	5.56	54.31	73.98
10g kaolin/2ml cell suspensions	92.86	-0.41	3.53	66.30	78.63
10g kaolin/4ml cell suspensions	92.78	-0.41	3.58	65.86	78.42
10g kaolin/7ml cell suspensions	92.14	-0.35	3.80	63.32	76.78
20g kaolin/2ml cell suspensions	92.40	-0.23	5.27	57.10	75.60
20g kaolin/4ml cell suspensions	93.17	-0.40	3.80	65.80	79.02
20g kaolin/7ml cell suspensions	93.00	-0.39	3.73	65.73	78.77

3.3.5: Effect of different concentrations of electron donor.

An experiment using reduced lactate concentrations (0.1, 0.3, 0.7 and 1mM) for the bioreduction of 20g kaolin 2 in the absence of AQDS was carried out to observe how varying electron donor concentration will influence rate and extent of Fe(III) reduction by adding 3ml of *S. putrefaciens* CIP 8040 cell suspensions in the system. The effect of different lactate concentrations was clearly evident from the initial rate and extent of Fe(III) reduction in kaolin followed by a lag phase after about 18 – 24 hours (Figure 3.7). It was observed that the rate and extent of Fe(III) reduction increases with increasing lactate concentration in the system. For example the bioreduction with 1mM lactate was faster with Fe(II) in solution increasing from 0.142mmol L⁻¹ within the first 2hrs to about 0.373 mmol L⁻¹ after 34hrs. But the bioreduction was much slower when 0.1mM lactate was used with Fe(II) in solution increasing from 0.0345mmol L⁻¹ within the first 2hrs to only about 0.032mmol L⁻¹ after 34hrs. As anticipated, increasing Fe(III) reduction is usually accompanied by a decrease in the lactate concentration. We therefore assumed lactate was mostly depleted within the first 24 hours, and this is the reason why reduction ceases. This experiment was in agreement with experiments conducted by Fredrickson et al., (2003) on reduction of hydrous ferric oxide (HFO) using *Shewanella putrefaciens* CN32 where rate and extent of Fe(II) production after HFO bioreduction increased with increasing lactate concentration.

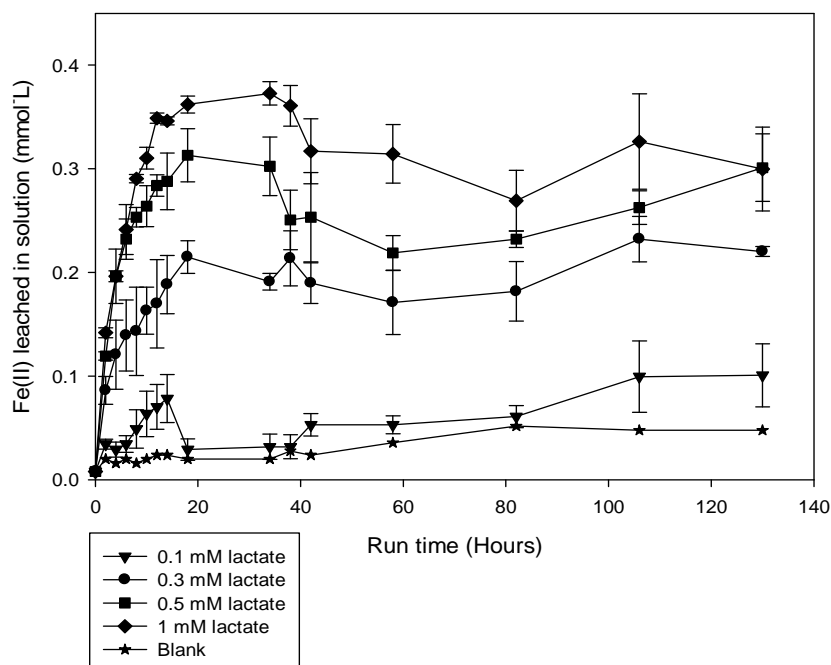


Figure 3.7: Bioreduction of 20g Kaolin under varying lactate concentrations (0.1 – 1mM) in the absence of electron shuttling system. Experiment was conducted at 30°C.

3.3.6: Effect of microcosm re-amendment on Fe(III) bioreduction

Experiments were conducted and monitored to assess the effect (a) of cell and kaolin re-inoculation and (b) re-injection of another electron donor (acetate) other than the initial electron donor (lactate) added for Fe(III) bioreduction. Four different sets of microcosm experiments were designed (triplicate each) in the absence of an electron shuttling system (AQDS). In the beginning of the experiment, all the different sets of microcosms were treated with the same composition (0.5mM lactate, 3mls of *S. putrefaciens* CIP 8040 cell suspension per microcosm, no AQDS) and monitored for aqueous Fe(II) production. After 192 hours, microcosms were re-amended by adding kaolin in one set, acetate in another set, and fresh *S. putrefaciens* CIP8040 cells were injected in a third set. However one of the sets was kept unamended since the start of the experiments, and there was also an experimental blank that has no lactate or cells added since the start of the experiment (Figure 3.8).

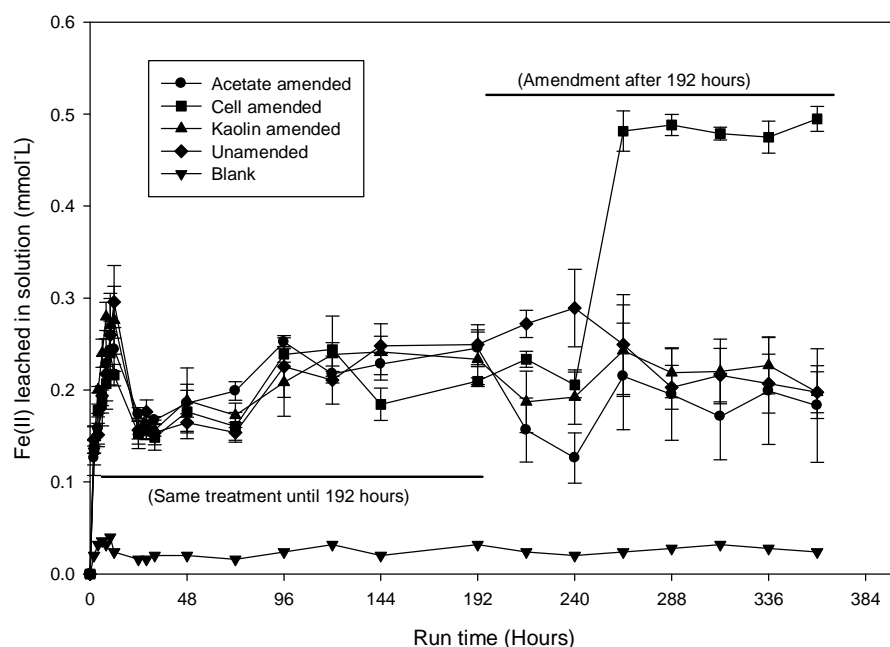


Figure 3.8: Bioreduction of 10g Kaolin 2 amended with acetate, kaolin and fresh cells at 192 hours with one of the treatment left unamended since the start of experiment. Experiment was run under 30°C using *S. putrefaciens* CIP8040.

A similar trend and pattern in the rate and extent of bioreduction at the beginning of the experiment was observed (Figure 3.8). This was obvious because all treatments were treated with the same composition during the first 192 hours of bioreduction. For all the treatments there was an increase in the extent of Fe(III) reduction within the first 24hr of incubation with approximately around 0.27mmol L^{-1} of Fe(II) determined. But all the systems showed a cessation in Fe(III) reduction after 24hrs, with no sample showing any increase in Fe(II) after the first 16hrs. However when microcosms were amended on day 8 (192 hours), resumption of Fe(III) bioreduction and a rapid change in reduction rate was noticed in microcosms re-inoculated with fresh *Shewanella* cell suspension. Fe(II) in solution increased to around 0.48mmol L^{-1} just within 24hrs of cell re-inoculation. It was observed in microcosms amended with cell suspension that when metabolically active cells were added to the initial old cultures in which Fe(III) bioreduction had previously ceased, resumption of Fe(III) bioreduction was observed and almost doubled. This suggests that cessation of Fe(III) bioreduction may not necessarily be due to exhaustion of bioavailable Fe(III) in the mineral

but may be attributed to some changes in the microbial cell physiology or alteration in the chemistry of the solution. This work is consisted with the work conducted by Jaisi et al., (2007b).

Table 3.2: Colour analyses of biotreated kaolin re-amended with acetate, *S. putrefaciens* CIP8040 cells and kaolin after 192 hours.

Amendments	L*	A*	B*	% Whiteness	% Brightness
Acetate amendment	92.77	-0.48	4.51	61.55	77.25
Cell amendment	92.12	-0.41	4.31	60.86	76.10
Kaolin amendment	92.60	-0.47	4.63	60.56	76.74
Not amendment	92.89	-0.45	4.57	61.46	77.33
Blank (Acid wash)	92.69	-0.41	4.74	58.29	76.77
Initial kaolin	92.78	-0.16	5.86	55.32	75.62

Even though the amount of Fe(II) measured was not high (Figure 3.8), an improvement in the % whiteness was observed in all the various amendments (Table 3.2). For example there was increase in the % whiteness after bioreduction from 55.32% to 61.55% in microcosms amended with acetate at the end of the experiment and to 61.45% in the microcosms not amended since the beginning of experiment. Similarly, ISO brightness increases from 75.62% to 77.25% in microcosms amended with acetate. Surprisingly, % brightness in microcosms amended with cell re-inoculation was lower (76.10%).

3.3.7: Influence of electron donor concentration and re-inoculation of cells for Fe(III) bioreduction in kaolin.

To examine the combined effect of different concentration of electron donor (lactate) and re-inoculation of microbial cell on Fe(III) bioreduction of kaolin, different microcosms containing different concentrations of lactate (5 , 10, 15 and 20mM) were prepared and monitored for about 18 days. Injection of 4ml cell suspension and re-inoculation of fresh *S. putrefaciens* CIP8040 were carried out at periodic intervals. The initial rate was observed to be rapid and almost similar in the first day of reduction with approximately around 0.6mmol L⁻¹ of Fe(II) measured in all the different lactate amendments (Figure 3.9).

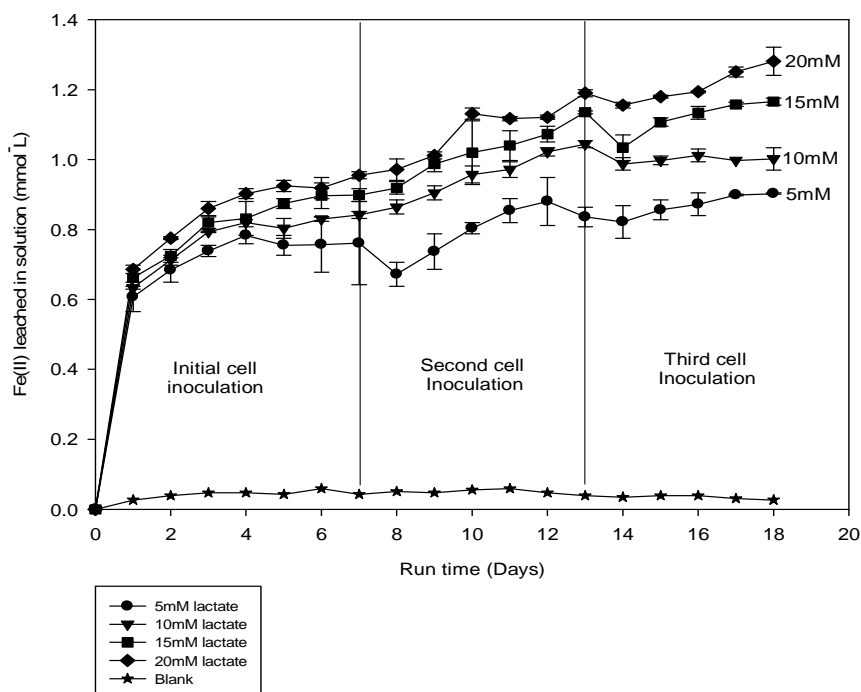


Figure 3.9: Bioreduction of kaolin under different concentration of electron donor (5–20mM) and multiple inoculations of *S. putrefaciens* CIP8040 at 30°C. Error bars represent standard error for three replicates

However, these gradually increase at a slower rate between day 2 and 18 with no apparent lag phase. The rate and extent of Fe(III) reduction were observed to be variable for the different lactate amendments at the end of the experiment. For example, the extent of bioreduction with 20mM lactate after 18 days was the highest with 1.28 mmol L^{-1} of Fe(II) measured in solution while lowest was observed in 5mM lactate with 0.90 mmol L^{-1} of Fe(II) measured. Bioreduction was observed to be slower even after fresh cells of *S. putrefaciens* CIP8040 were re-inoculated on day 5 and 13. But this was in contrast with the previous result (Figure 3.8) where after injecting fresh cells rapid bioreduction resumes. However it may suggest that with low concentration of electron donor the rate of bioreduction is slower and the bioreducible Fe(III) within the kaolin clay structure was not at all exhausted going by the stoichiometry of 1:4 ratio of lactate consumed to Fe(II) produce (see section 3.4 for the equation). Similarly with high concentration of lactate a high rate of bioreduction was observed within the first day of incubation. Possibly at high concentration the bacteria

were able to reduce a greater part of the Fe(III) in the clay mineral within the first day making the bioavailable Fe(III) very limited. These data also illustrated that multiple inoculation of cells has no effect on the rate but only prolongs the extent of bioreduction better than single inoculation.

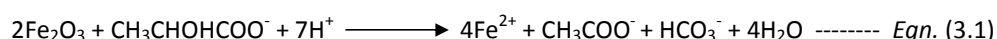
Improvement in % whiteness from 56.23% to approximately 63% was observed in all the microcosms amended with different concentrations of lactate (Table 3.3), except for microcosms amended with 5mM lactate with % whiteness increasing to 62.42%. ISO brightness increases very slightly from 75% to approximately 77% for all the amendments but to approximately 76% in the 5mM amended microcosm.

Table 3.3: Colour analyses of biotreated kaolin using different concentration of electron donor and re-injection of *S. putrefaciens* CIP8040 at different interval.

Concentrations	L*	A*	B*	% Whiteness	% Brightness
20mM Lactate	92.25	-0.42	3.73	63.91	77.13
15mM Lactate	92.03	-0.40	3.72	63.41	76.64
10mM Lactate	92.18	-0.36	3.87	63.10	76.81
5mM Lactate	91.85	-0.34	3.84	62.42	76.08
Initial	92.39	-0.22	5.45	56.23	75.27

3.4: STOICHIOMETRY AND MASS BALANCE OF MINERAL FE(III) RESPIRATION

Kinetic studies of mineral Fe(III) reduction and the stoichiometry for lactate oxidation during bioreduction were calculated. For better understanding of stoichiometry, the intention was to measure lactate and acetate in the microcosm after bioreduction in the system. However, due to some limitations during the course of the studies this was not achieved. Therefore only dissolved total organic carbon (TOC) was analysed and the TOC equivalent of lactate calculated and used. The overall reaction for the bioreduction of Fe(III) in the presence of lactate can be expressed as follows:



From the stoichiometry of equation 3.1, every 1 mole of lactate gives 1 mole of acetate and 1 mole of bicarbonate, and so expressing the equation in TOC (total organic carbon) terms, every 3 moles of TOC gives 2 moles of TOC and 1 mole of TIC (total inorganic carbon).

3.4.1: Total organic carbon analyses.

To quantify how much organic carbon was depleted in the system after bioreduction, samples were taken at the termination of experiment in microcosms containing 0.1mM, 0.3mM, 0.5mM and 1mM lactate for total organic carbon determination. Prior to these analyses, different standards of lactate and acetate solutions were prepared and analysed for total carbon, total organic carbon and inorganic carbon contents (Table 3.4 and Table 3.5.)

Table 3.4: Analyses of organic and inorganic carbon from different standard solutions of lactate

Lactate standard	Inorganic Carbon		Total organic carbon		Lactate equivalent of TOC (mM)
	IC (mg/l)	IC (mM)	TOC (mg/l)	TOC (mM)	
0.1 mM	0.901	0.08	4.34	0.36	0.12
0.2 mM	1.002	0.08	7.49	0.62	0.21
0.3 mM	1.079	0.09	11.29	0.94	0.31
0.5 mM	1.436	0.12	18.53	1.54	0.51
0.7 mM	1.126	0.09	25.36	2.11	0.70
1.0 mM	1.024	0.09	36.83	3.07	1.02

Table 3.5: Analyses of organic and inorganic carbon from different standard solutions of lactate and acetate

Standard	Inorganic Carbon		Total organic carbon		Lactate/acetate equivalent of TOC (mM)
	IC (mg/L)	IC (mM)	TOC (mg/L)	TOC (mM)	
1 mM Acetate	1.386	0.12	26.62	2.22	1.11
1 mM Lactate	1.014	0.08	37.23	3.10	1.03
0.5 mM Lactate/0.5 mM Acetate	1.060	0.09	31.50	2.63	0.53
1 mM Lactate/1 mM Acetate	1.613	0.13	61.12	5.09	1.02

The total organic carbon content in the system after bioreduction for 130 hours shows more organic carbon than was added in the beginning of the experiment (Table 3.6). This general increase of TOC observed in all the microcosms was attributed to carbon from bacterial biomass injected in to the system. It will be interesting to understand that approximately around 4 - 5mM or 15 – 20mg/L increase in the total organic carbon measured in the system

was contributed by bacterial biomass when compared with standard solutions of lactate analysed. Although the inorganic carbon measured was low (Table 3.6), it does shows an increase in inorganic carbon (bicarbonate) in microcosms with more lactate.

Table 3.6: Total organic carbon data in microcosm after 130 hours under varying lactate concentration.

Microcosm (lactate)	Inorganic Carbon		Total organic carbon		TOC equivalent of lactate (mM)
	IC (mg/l)	IC (mM)	TOC (mg/l)	TOC (mM)	
0.1 mM	1.735	0.14	20.84	1.74	0.58
0.3 mM	1.190	0.10	32.26	2.69	0.90
0.5 mM	2.156	0.18	37.67	3.14	1.05
1.0 mM	2.467	0.21	54.65	4.55	1.52
Blank (1.0mM)	0.704	0.06	38.72	3.23	1.08

3.4.2: Stoichiometry of lactate oxidation couple to Fe(III) reduction in kaolin

To define and understand lactate oxidation coupled to Fe(III) reduction in kaolin, samples were taken on day 2, 5, 10, 13 and 18 and analysed for TOC in each experiment where microcosms were treated with 5mM, 10mM, 15mM and 20mM lactate (Figure 3.9). The TOC equivalent of lactate were plotted against absolute amount of Fe(II) leached on those respective days (Figure 3.10) to assess changes in TOC equivalent of lactate against changes in Fe(II) leached in the system.

The Fe(II) concentration was observed to increase over time while the TOC equivalent of lactate decreases in all the microcosms containing different concentrations of carbon source. The TOC measured on day 2 was around 6.03mmol L^{-1} in microcosms to which 5mM lactate was added, but this gradually depleted to 5.19mmol L^{-1} over the period of bioreduction (Figure 3.10). Similarly, the Fe(II) was observed to simultaneously increase from 0.68mmol L^{-1} on day 2 to around 0.90mmol L^{-1} at the end of the experiment in the same microcosm to which 5mM lactate was added. It was observed that the amount of lactate taken up by *S. Putrefaciens* CIP8040 cells in all the microcosm was twice than that oxidised for Fe(II) production going by the stoichiometry as illustrated in equation 3.1 above. But the ratio of Fe(II) production to organic carbon consumption was fairly close to that expected (4:1 ratio) for lactate oxidation couple to Fe(III) reduction (Figure 3.10).

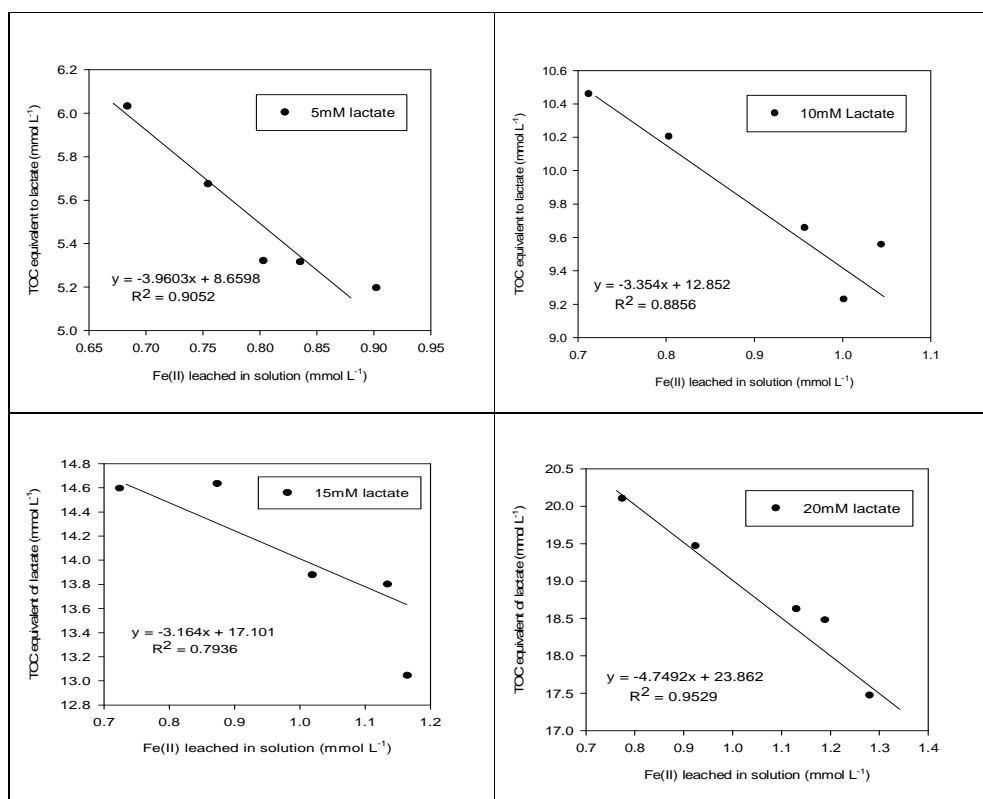


Figure 3.10: Correlation between TOC measured over time and Fe(II) leached after bioreduction of kaolin in experiment added with 5, 10, 15 and 20mM lactate. Equations and coefficients of regression (r^2) values determined from linear regression analysis are given from each lactate concentration.

The increase in TOC higher than the actual concentration of lactate initially added from the start of the experiment observed was attributed to bacterial biomass added in to the system and it has a more pronounced effect in microcosms with less concentration of lactate (such as observed in microcosms containing 5mM lactate). Also the TOC in microcosms containing 20mM lactate was 20.09mmol L⁻¹ in the first 2 days of experiment and decreased to 17.47mmol L⁻¹ after 18 days of incubation. Fe(II) was also observed to increase from 0.78mmol L⁻¹ on day 2 to 1.28mmol L⁻¹ at the termination of the experiment (Figure 3. 10). There was a positive stoichiometry correlation in all the experiment with a positive regression coefficient for carbon oxidation couple to Fe(III) reduction with $r^2 = 0.91, 0.89, 0.79$ and 0.95 in experiments added with 5, 10, 15 and 20mM lactate respectively. It was however noticed that the organic carbon oxidation couple to Fe(III) reduction in microcosms

added with 20Mm lactate was more than what was observed in microcosms added with 5mM lactate. This further confirms that the rate of Fe(III) reduction is control by concentration of lactate added in the system.

3.5: BACTERIAL FE(III) REDUCTION KINETICS IN KAOLIN

3.5.1: Rates of reaction

The effects of different lactate concentration on kaolin bioreduction as illustrated in Figure 3.7 show an increase in the rate of Fe(III) reduction with increase in lactate concentration within the first 18hour of the commencement of experiment. This indicates that an increase in lactate concentration is the primary cause for increase in rate of reduction. Thus this relationship was further investigated to see if the increase observed obeys first order rate law kinetics. In the first order rate law, increase in rate is proportional to concentration of reactant and is given by the equation below:

$$r = d[\text{Fe(II)}]/dt = -k[\text{Fe(II)}] \text{----- Eqn (3.2)}$$

To determine whether a reaction follows first order kinetics a semi-log plot of Fe(II) concentration against time was used as shown in equation 3.3 and was expected to give a straight line graph with slope $-k$, where k is the rate of reaction.

$$\ln[\text{Fe(II)}] = \ln[\text{Fe(II)}]_0 - k t \text{----- Eqn (3.3)}$$

Hence a plot of natural log of Fe(II) against time for each individual lactate concentration was analysed and a straight line graph with a negative slope was obtained (Figure 3.11). Similarly a plot of rate against concentration was also explored to further reveal the reaction kinetic order in our system and is reported in 3.5.2.

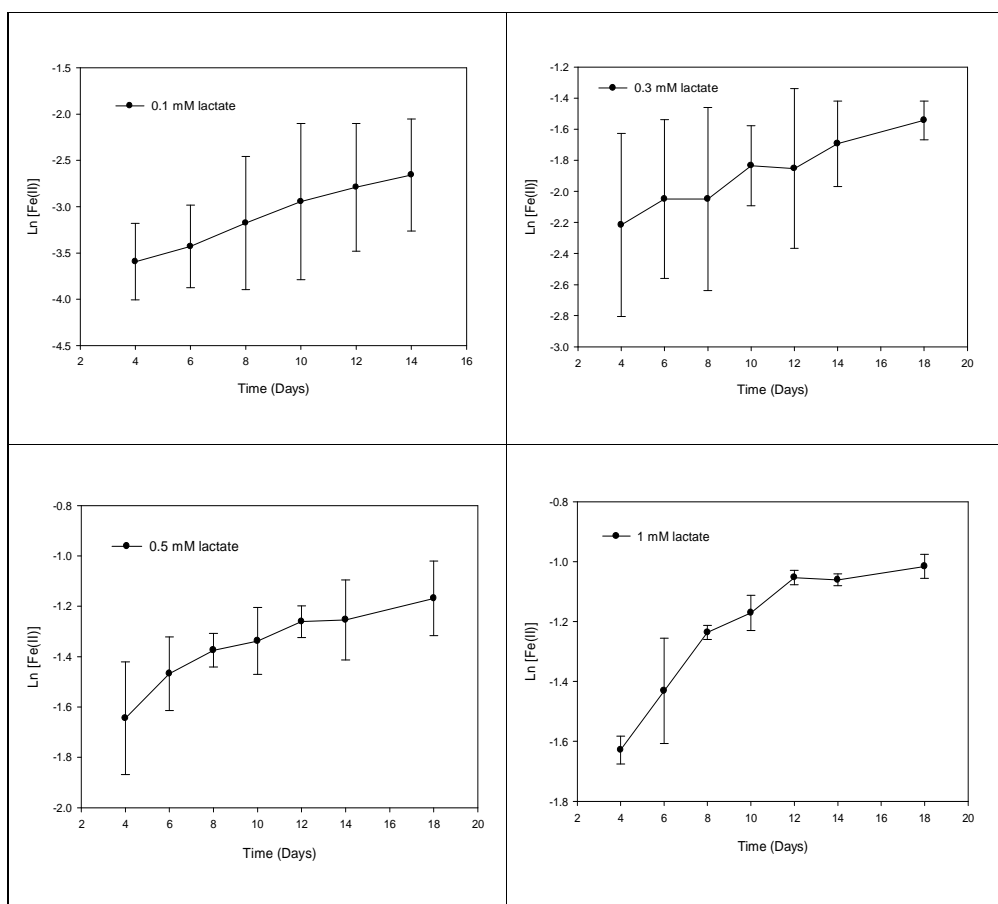


Figure 3.11: Semi-log plot of Fe(II) concentration against time for different concentration of lactate (0.1 – 1mM) predicting reaction kinetic order of Fe(III) reduction in kaolin.

The results obtained show first order kinetics for all the different lactate concentrations after plotting natural log of Fe(II) produce against time. The rate plot of Fe(II) concentration over time resulted in very strong linear relationships with $r^2 = 0.98, 0.96, 0.88$ and 0.82 for lactate concentrations of 0.1, 0.3, 0.5 and 1mM respectively (Figure 3.11). The equations and coefficients of regression (r^2) determined are not shown on the graph. The accumulation of Fe(II) observed in these experiments was attributed to the first order consumption of lactate and could be well described by a rate law equivalent to equation 3.2. The rates of reduction of Fe(III) over time determined in each individual treatment are given in Table 3.7.

Comment [DM18]: Give the rates that you determined in a table.

Table 3.7: Rate of Fe(III) reduction determined in microcosms amended with 0.1 – 1mM lactate.

Rate of reduction of Fe(III) over time (Mm/Hour)				
Time (Hours)	0.1mM lactate	0.3mM lactate	0.5mM lactate	1mM lactate
2	0.0173	0.0431	0.0597	0.0710
4	0.0073	0.0302	0.0491	0.0491
6	0.0058	0.0232	0.0387	0.0402
8	0.0061	0.0179	0.0317	0.0363
10	0.0064	0.0163	0.0264	0.0310
12	0.0059	0.0142	0.0237	0.0291
14	0.0056	0.0135	0.0206	0.0247
18	0.0016	0.0119	0.0174	0.0201

Similarly, in the experiment conducted with high concentration of lactate (5 – 20mM lactate), bioreduction of Fe(III) was also accompanied by lactate consumption (determined from TOC equivalent of lactate). A very strong correlation (approximate $r^2= 0.9$) of lactate removal over time was observed, demonstrating a linear consumption of organic carbon over time in the system (Figure 3.12).

Comment [DM19]: The sentence I deleted didn't have a clear meaning. You should calculate the rate of TOC removal – or does this come later? If so, say so.

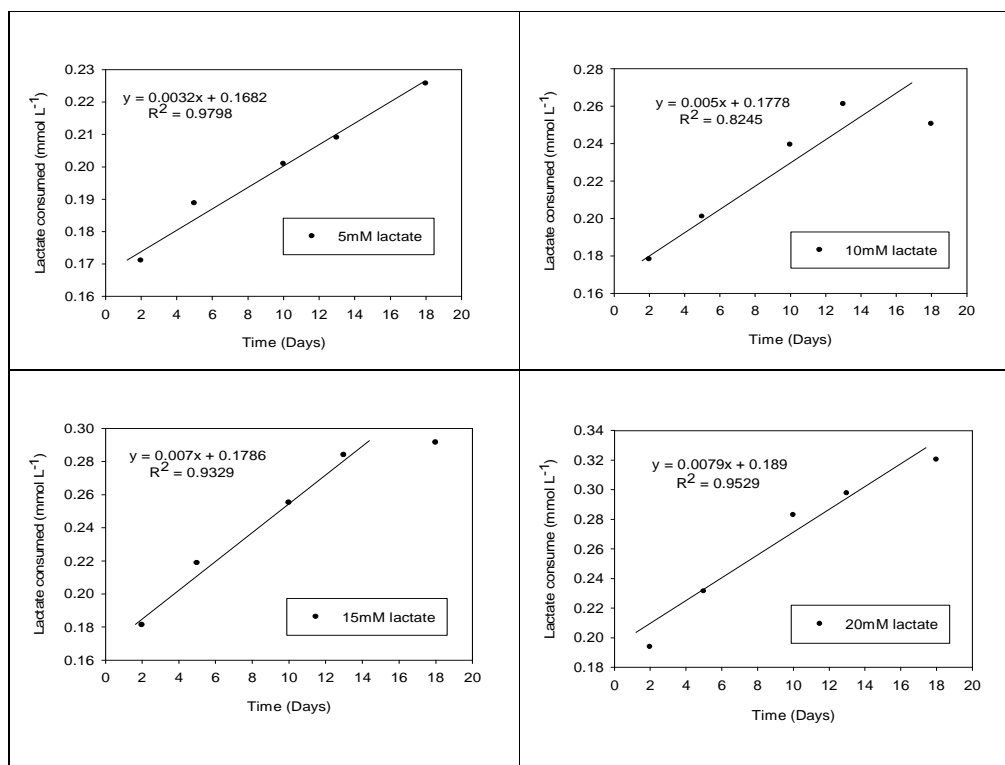


Figure 3.12: TOC equivalent of lactate depleted over time during bioreduction of kaolin under varying concentration of lactate. Equations and coefficients of regression (r^2) values determined from linear regression analysis are given for each lactate concentration.

The rate of TOC removal in the system was observed to be faster within the first 2 days of the experiment in all the different amendments (5 – 20mM lactate) and it continued to progress slowly over time. The rates of total organic carbon removal calculated from Figure 3.12 above are given in Table 3.8.

Table 3.8: Rate of total organic carbon removal calculated in microcosm amended with 5 -20mM lactate.

Rate of TOC removal overtime (Mm/day)				
Time (Day)	5mM lactate	10mM lactate	15mM lactate	20mM lactate
2	0.0855	0.0891	0.0906	0.0969
5	0.0378	0.0402	0.0437	0.0462
10	0.0201	0.0239	0.0255	0.0283
13	0.0161	0.0201	0.0218	0.0229
18	0.0125	0.0139	0.0162	0.0178

3.5.2: Integrated rate order kinetics for Fe(III) reduction in kaolin.

Moreover, an integrated rate law was used to further confirm that the reaction showed first order kinetics where instantaneous rate of production of Fe(II) over time was plotted against different concentrations of lactate (Atkins and De Paula, 2010). Plotting the rate of Fe(II) against concentrations from Figure 3.13 results in a good linear increase of Fe(II) over time with a perfect correlation where $r^2 = 0.99$ when only 0.1, 0.3 and 0.5mM lactate concentration point were considered (Figure 3.13). With 1mM lactate, the kinetics of Fe(III) reduction appeared to shift from first-order with respect to lactate concentration to nearly zero order (Figure 3.14). On this basis, it was assumed that possibly equilibrium or saturation point was reached where the reaction no longer proceeded.

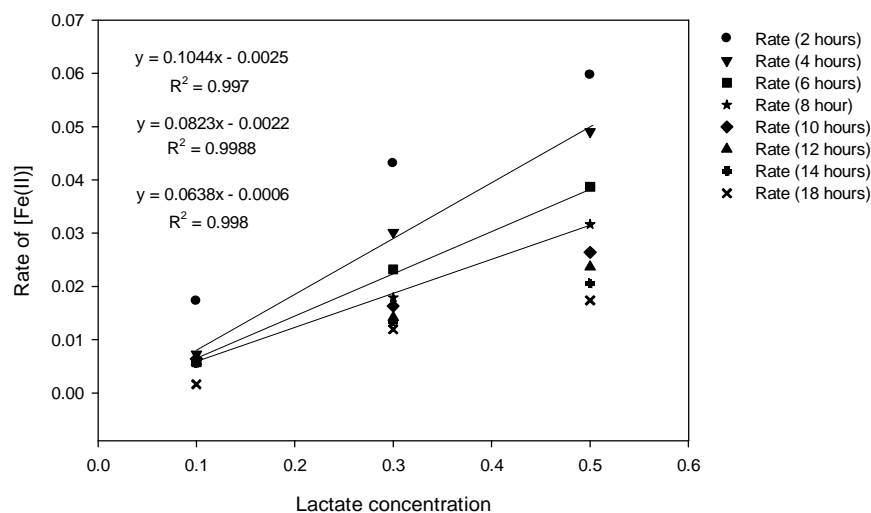


Figure 3.13: Plot of rate of Fe(III) reduction overtime against concentrations of lactate (0.1 -0.5) showing first order rates and linear increase of Fe(II) production between 2 to 18 hours. Equations and coefficients of regression (r^2) values determined from linear regression analysis are given for 4, 6 and 8 hours.

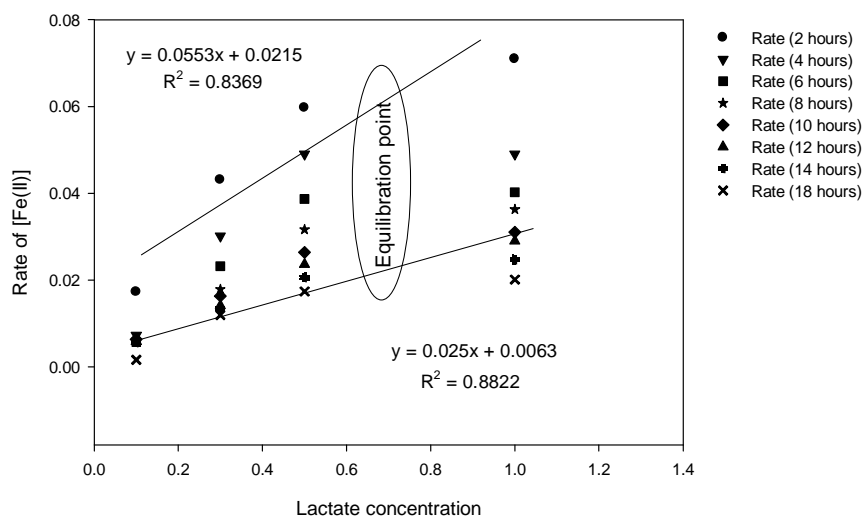


Figure 3.14: Plot of rate of Fe(III) reduction over time against concentrations of lactate (0.1 -1mM) linear increase of Fe(II) production and possible saturation point. Equations and coefficients of regression (r^2) values determined from linear regression analysis are given for 4 and 12 hour.

3.5.3: Rate of Fe(II) production and substrate consumption using Michaelis-Menten kinetics

The effect of different lactate concentrations on the initial rate of Fe(III) bioreduction in kaolin (Figure 3.7) was further investigated using Michaelis-Menten kinetics (Atkins and De Paula, 2010). The approach involves monitoring the rate (v) of product formation from substrate (S) in the presence of enzyme (E) (Atkins and De Paula, 2010). One of the principle of this approach was that for any given enzyme (*S. putrefaciens* CIP8040) and substrate concentration (lactate), the rate of product formation (Fe(II) in solution) is proportional to initial concentration of substrate (lactate). Hence the rate of product formation according to the Michaelis-Menten mechanism is given by:

$$v = k [ES] \text{ -----Eqn (3.4)}$$

Where: v = Rate

k = Michaelis-Menten constant

E = Enzyme (*S. putrefaciens* CIP8040 cells)

S = Substrate (lactate)

By plotting rate of reaction obtained from the slope of Fe(II) leached against individual lactate concentrations, it was observed that the rate of formation of Fe(II) increases as substrate concentration increases (Figure 3.15). Furthermore, as the reaction proceeds, the system starts to become saturated with increasing substrate (lactate) concentration around 0.5mM lactate. However the rate of Fe(II) production reaches a maximum value (v_{\max}) of 0.018mmol h⁻¹ after which the *Shewanella* cells no longer catalyse the reaction.

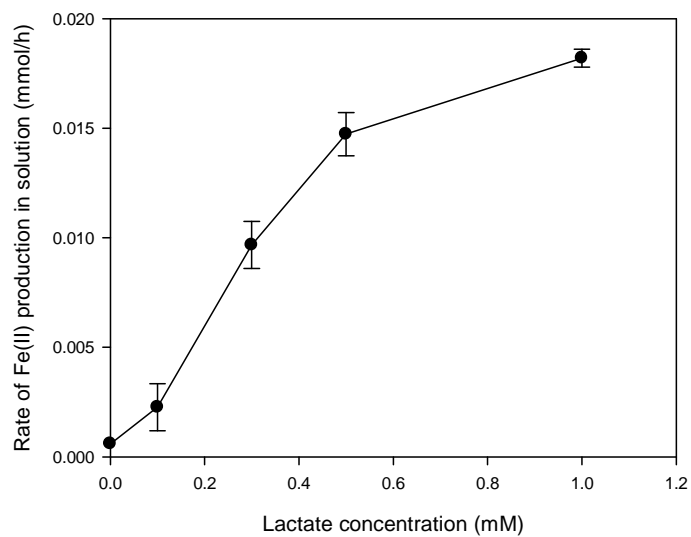


Figure 3.15: Plot of rate of Fe(II) production overtime against concentrations of lactate (0.1 -1mM) using Michaelis-Menten kinetic.

3. 6: DISCUSSION

This chapter presents studies on the application of the dissimilatory microbial reduction pathway for the removal of iron impurities to improve the quality and value of industrial kaolin through testing different iron reducing *Shewanella* strains for the selection of the bacterial culture that can best bioleach Fe(III) from kaolin. The study exploits documented evidence that many iron-respiring bacteria are capable of anaerobically utilising insoluble Fe(III) and other metals as the sole electron acceptor in the presence of organic acids as the electron donor (Lloyd, 2003; Lovley, 2001) for the reduction of Fe(III) in kaolin to Fe(II) which is more soluble and leachable (Lee et al., 2002). However for Fe(III) reduction to serve as a terminal electron-accepting process anaerobic conditions must be provided with no or limited oxygen present (Lovley, 2001).

In the batch scale microcosms, almost all the 5 different *Shewanella* strains tested were significantly able to couple oxidation of lactate to the reduction of Fe(III) in the kaolin with the exception of *S. loihica*, with substantial differences in the rate and extent of Fe(III) reduction. The bioreduction of Fe(III) increases rapidly within the first day of incubation by all the different strains with the *S. putrefaciens* CIP8040 showing the greatest rate and extent of Fe(III) reduction in the system. These observations are inconsistent with the work on potential for green rust formation from bioreduction of lepidocrocite (γ -FeOOH) in the presence of formate, where different rate and extent of Fe(II) production were reported with different *Shewanella* strains (O'Loughlin et al., 2007). Colour analysis conducted after bioleaching further confirms that *S. putrefaciens* CIP8040 improves both whiteness and brightness more than other strains, even though *S. putrefaciens* CN32 and *S. algae* BrY are quite effective. Similarly, treatment with *S. putrefaciens* CIP8040 has substantially removed more Fe(III) from the initial Fe-bearing impurities present in kaolin than the other iron reducers.

The temperature dependence of the rate of Fe(III) reduction using *S. putrefaciens* CIP8040 in the range of 20 – 36°C shows that temperature affects the rate of Fe(III) reduction. Although Fe(II) was observed to be leached at both low and at elevated temperatures during bioreduction, significant variation in Fe(III) reduction due to the temperature response

resulted in different rates and extent of bioleaching. *S. putrefaciens* CIP8040 was documented to optimally perform at 30°C (O'Loughlin et al., 2007), thus temperature was determined to be paramount in enhancing the rate and extent mineral bioreduction.

Furthermore, slurry density (solid to liquid ratio) was found to affect the rate of Fe(III) bioleaching in kaolin. Maintaining constant volume of liquid with varying mass of mineral can result in different rates for the kaolin bioleaching process. Deploying more mineral in the slurry tends to produce increased bioleaching rate and extent, irrespective of *Shewanella* strain used. However, deploying a smaller mineral mass using the same volume of liquid with constant biomass (8.4×10^8 cells mL⁻¹) could reduce the rate and extent of the bioleaching process. Similarly, cell density to mineral ratio is another factor that was observed to influence the effectiveness of the bioleaching process. The rate of Fe(II) production increases substantially when more mineral mass (20g) was leached in the presence of high bacterial biomass (8.4×10^8 cells mL⁻¹). Retardation in the rate of Fe(III) bioreduction occurred with reduction of cell density from 8.4×10^8 cells mL⁻¹ to 2.4×10^8 cells mL⁻¹ for the same mineral mass. This finding is in agreement with the work of O'Loughlin (2008), where an increase in cell numbers substantially affects the rate of Fe(II) production during reduction of 80mM lepidocrocite in the presence of AQDS and *S. putrefaciens* CN32. In his work, he observed that production of Fe(II) after lepidocrocite reduction substantially increases with increase in cell number from 1×10^9 cells mL⁻¹ to 3×10^9 cells mL⁻¹ with no further increase when biomass was increased to 1×10^{10} cells mL⁻¹ for the same lepidocrocite concentration. Contrary to this, reducing the mass of mineral by half (10g) has no substantial effect on the rate and extent of Fe(II) production irrespective of how much bacterial biomass was present.

The fact the bacterial cell density, mineral mass ratio and slurry density were varied in our experiments means that the surface area available for the mineral-bacterial interaction also changed. This may explain the variation observed in the rate of Fe(III) reduction when different mineral mass was used against different cell ratio. Some factors are known to affect rate of Fe(III) reduction which include differences in the mineral surface area, morphology, and particle sizes (Roden and Zachara, 1996). Similarly adsorption of Fe(II) on the mineral and bacterial surface during bioreduction affects the rate and extent of

Comment [DM20]: Reference?

reduction (Bose et al., 2009; Zachara et al., 1998; Roden and Zachara, 1996). Hence these combined factors may explain differences observed in the rate of reduction in our system. In general effective bioleaching process is a function of using appropriate biomass number with a specific mineral mass.

Following the initial and more rapid reduction period in some microcosms, a decline in microbial reduction rate was noticed and this could be correlated with the crystallinity and solubility of different iron phases present in the mineral (although we are not sure of the type of iron phases present in the mineral). Different Iron hydroxide phases are generally known to have different solubility and hence Fe(III) reduction is substantially more in poorly crystalline phases like ferrihydrite than highly crystalline phases such as goethite and hematite. The solubility of these iron phases decreases from ferrihydrite to goethite and then to hematite (Cutting et al., 2009; Hansel et al., 2004). Another reason for the observed decline in the rate of reduction suggests the possibility of Fe(II) accumulation and adsorption on Fe(III) oxide surface or formation of surface coating iron phases that may hinder further microbial Fe(III) reduction in the mineral due to interaction between soluble Fe(II) and Fe(III) mineral surfaces (Hyacinthe et al., 2008; Roden and Zachara, 1996).

Results obtained from experiments with variable lactate concentration demonstrated that using different lactate concentration can have a profound influence on the rate and extent of Fe(III) reduction in kaolin by *S. putrefaciens* CIP8040. The rate of reduction of Fe(III) however increased with an increase in the concentration of lactate most particularly at a lower concentration (between 0.1 – 1mM) within the first 18 hours. The relative amount of Fe(II) production varies with the different concentration of lactate in the system. This further confirms the work of (Fredrickson et al., 2003), where variation in electron donor significantly influences the rate of hydrous ferric oxides (HFO) bioreduction. Thus it clearly shows that the rate of Fe(III) reduction in kaolin directly depends on the concentration of lactate and is usually accompanied by a decrease in the lactate concentration with time. However at a higher concentration of lactate (5 – 20mM) the reduction was faster and more Fe(II) is produced within the first day with variability in the extent of Fe(III) reduction throughout the period of incubation and no apparent lag phase.

In one of the experiments where all microcosms (containing 0.5mM lactate) were treated with the same composition and mid-way from the start of the experiment then re-amended, these microcosms were observed to show no changes after going through a period of lag phase except in experiment injected with fresh *Shewanella* cells. This indicates that addition of metabolically active fresh cells may change the system energetics and thus initiate renewed Fe(III) bioreduction in the mineral. This result further supported the observation made by Jaisi et al. (2007b) where after reinjection of fresh cells resulted in resumption of bioreduction. The prolonged lag phase could be due to sorption of Fe(II) on the surface of the bacteria or changes in the system's chemistry which may partially inhibit bacterial activities.

Resumption of Fe(III) bioreduction in microcosms treated with high concentration of lactate (5 – 20mM lactate) after multiple inoculation of fresh *Shewanella* cells was very slow. This is possible because Fe(II) production was very fast and rapid in the first day due to the excess concentration of electron donor in all the microcosms. This suggests that the large amount of Fe(II) accumulated in the first day may possibly be coated onto the mineral surface and so inhibits accelerated Fe(III) bioreduction in the mineral even after injecting fresh *Shewanella* cells in the system, as observed when low concentrations of lactate were used. Fe(III) reduction activities may be partially compromised through blockage of the electron transfer chain when Fe(II) is sorbed onto mineral surfaces, thereby limiting the reactive surface (Jaisi et al., 2007b). Another reason for non-resumption of bioreduction may be attributed to exhaustion of high proportions of Fe(III) within the first day of reduction making the bioavailable Fe(III) very limited. Considering that our system is nutrient-limited (a non-growth system), the effects caused through inhibition of bacterial activity may be more severe under this condition, because the cells may have limited ability to remove the possible sorbed Fe(II) by actively growing and reproducing cultures (Jaisi et al., 2007b). However, under growth conditions or in a natural environment some cells may exhibit a repair mechanism or cell surface recovery that may help alleviate the Fe(II) sorption constrain or blocking effect through cell reproduction.

The lactate-driven bioreduction of Fe(III) in equation 3.1 shows that *Shewanella* cells couple the reduction of Fe(III) in kaolin to the oxidation of lactate. According to the stoichiometry,

Comment [DM21]: This is a very awkward sentence

for every 1 mol of lactate oxidized, 4 mol of Fe(II) is produced (lactate:Fe(II) produced = 1:4) and in turn 1 mol of acetate is produced in a 1:1 ratio of lactate to acetate. As acetate was not determined, only TOC analysis was conducted and TOC equivalent of lactate left was used to determine the stoichiometry following Fe(III) reduction in kaolin. The concentration of lactate consumed as determined from the amount of Fe(II) measured reasonably followed the expected molar ratio in the stoichiometry equation with little variability. This work also supported previous studies that showed that *Shewanella* strains couple reduction of goethite in the presence of lactate (Zachara et al., 1998; Roden and Zachara, 1996). However, it was observed that the amount of lactate taken up by *S. Putrefaciens* CIP8040 cells in all the microcosm was almost similar to that oxidised for Fe(II) production with only a slight deviation). This slight deviation from stoichiometry between Fe(II) produced and TOC equivalent of lactate measured in the kaolin indicates that Fe(II) may possibly be retained in the solid phase of the mineral (Hansel et al., 2004).

The approximately first-order consumption of lactate for the microbial reduction of Fe(III) to Fe(II) in the mineral was also demonstrated by this study. The pattern of accumulation of Fe(II) over time was attributed to first order consumption of lactate in the experiments. The increase in the absolute amount of Fe(II) increase linearly over time due to the increase in concentration of electron donor until a saturation point is reached at around 0.1mM lactate where the high concentration has no further effect on the rate of reduction. The reduction rate then appeared to shift from first-order with respect to lactate concentration to nearly zero order. Therefore the kinetic model presented here shows saturation of Fe(II) production kinetics with increasing lactate concentration, and it obeys first order rate kinetics. This further confirms the model presented by Bonneville et al. (2006) of a kinetic model for reduction of Fe(III) colloids by *S. putrefaciens* where increases in reduction kinetic were monitored with respect to increasing cell density. In the model they observed that saturation of microbial Fe(III) reduction increases with increase in cell density. Therefore the initial Fe(III) reduction rate for kaolin in our system increases linearly with increasing concentrations of electron donor present. The rate of Fe(III) reduction in our system was also supported by interpretation based on Michaelis-Menten enzyme kinetics where the rate of Fe(II) formation directly depends on the concentration of electron donor and *Shewanella* cell present.

In terms of colour properties, the brightness and whiteness of biotreated kaolin remarkably improved after bio-reduction compared to blank and initial kaolin. The optical properties of the raw blank kaolin after washing with 2M HCl were not significantly different from those of unwashed blank kaolin. This suggests that biotreatment did increase the solubility of iron in kaolin, thereby making it easier to remove and improve the colour index. Treatment with *S. putrefaciens* CIP8040 has substantially increased the % whiteness and brightness with decrease in yellowness, in comparison better than the remaining iron-reducing microorganisms tested. However, it was noticed that further extension of bio-leaching period has little impact on the colour properties. Effective improvement in brightness and whiteness was achieved when 20g kaolin/4ml cell suspension was used. Although high cell density with more or less mineral mass was found to also substantially improve the colour index, when lower cell densities are employed with high mineral mass no improvement was achieved compared to the initial kaolin colour index. Multiple re-inoculation of a cell suspension does not seem to have a major impact on the colour index when compared with microcosms with single inoculation, even though resumption of Fe(III) reduction was apparently observed.

CHAPTER 4 : BIOREDUCTION OF KAOLIN PART II: PROPERTIES OF SOLID PRODUCTS

4.1: INTRODUCTION

In this research, Chapter 3 and Chapter 4 both deal with bioreduction of kaolin material for batch scale microcosm experiment. As described and reported earlier, Chapter 3 generally deals with optimisation and mechanisms of reaction during Fe(III) bioreduction in the solution. On the other hand, this Chapter (Chapter 4) follows up with a description on the properties of solid product after bioleaching of kaolin from Chapter 3 in order to assess any changes in the mineralogy of biotreated mineral material. In addition, this chapter also reports and describes experiments conducted to test the efficiency of natural organic matter (NOM) as a potential substitute for AQDS in enhancing Fe(III) reduction kinetics. It also describes experiments designed to assess the relative importance of biogenic and abiotic factors on the bioreduction of Fe(III) in kaolin material. A summary of the experimental design and methodology used in this section are reported in Chapter 3 (see section 3.2).

4.2: RESULTS

4.2.1: Bioreduction of kaolin-bound Fe(III) in the presence of AQDS, NOM or absence of electron shuttle

Experiments were set up to investigate and assess the influence of presence or absence of electron shuttling compound (AQDS) on the rate and extent of Fe(III) bioreduction in kaolin. However, two different natural organic matter types (NOM 1 and NOM 2) supplied by Sibelco Ltd (one of the major partners in this project) were also tested in this experiment to assess their electron shuttling efficiency and to see if they could serve as substitute to AQDS (expensive and not readily available in large commercial quantities from any known supplier in UK) in enhancing the bioleaching process using *Shewanella putrefaciens* CIP8040 at 30°C. Prior to using NOM 1 AND NOM 2, these compounds were characterised to understand their compositions and results are shown in Appendix 7.2 and 7.3.

In this experiment around 0.66g L^{-1} (same mass as that of AQDS) of the first natural organic matter received (NOM 1) was used as replacement to AQDS. Three different sets of experiment were prepared with Kaolin 4 (Melbur Yellow MGP, a chemically bleached kaolin), two of which received added AQDS or NOM 1 while the last one was set up without NOM 1 or AQDS. A blank experiment contained neither *Shewanella* cells nor electron shuttle. Increase in the Fe(III) reduction rate was observed in all the experiments within the first day of bioleaching with an increase in the AQDS treated experiment after 3 days. The rate and extent of Fe(III) reduction was higher in the presence of AQDS; around 0.7mmol L^{-1} of Fe(II) was measured at the end of the experiment (Figure 4.1). The reduction rate in experiments with NOM 1 was faster than for the experiment without an electron shuttle but the extent was almost similar at the end with approximately 0.6mmol L^{-1} of Fe(II) in each. This suggests that NOM 1 could enhance electron shuttling by increasing the rate of Fe(III) reduction compared to when no electron shuttle was in the system but overall was less effective than the synthetic AQDS.

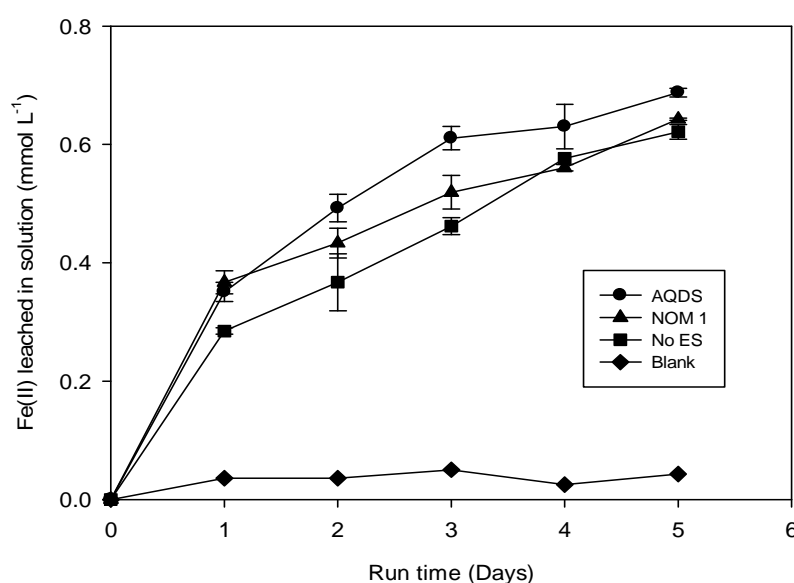


Figure 4.1: Comparison of rate and extent of microbial Fe(III) reduction from Kaolin 4 in the presence of either AQDS, NOM 1 or absence of electron shuttle at 30°C using 20g kaolin mineral.

Another set of experiments was designed to test the two different NOM (NOM 1 and NOM 2) as a replacement to AQDS and also to compare their electron shuttling potential in enhancing rate and extent of Fe(III) reduction with AQDS and without an electron shuttle using kaolin 3 (Melbur Yellow HCP, a non treated, unbleached kaolin) at 30°C using *S. putrefaciens* CIP8040. The result in Figure 4.2 shows the rate and extent of Fe(III) reduction after 5 days, both in the presence of AQDS, NOM 1, NOM 2 and in the absence of electron shuttle. In all cases, different and variable rates and extent of Fe(III) reduction were observed. The rate of reduction and the amount of Fe(II) leached in the first day with AQDS (0.8mmol L^{-1}) was higher and two times faster than the rate and absolute amount of Fe(II) observed with NOM 1 (app. 0.4mmol L^{-1}). The rate of reduction when AQDS was used is also faster than in the presence of NOM 2 and faster than in the absence of electron shuttle with approximately 0.6mmol L^{-1} and 0.5mmol L^{-1} of Fe(II) respectively on the first day. Contrary to the experiment with kaolin 4, it was observed that replacing AQDS with NOM 1 to leach Fe(II) from Kaolin 4 has less effect on the bioleaching rate when compared with the experiment carried out without an electron shuttle. On the other hand the rate and extent of bioleaching with NOM 2 was higher when compared to experiments conducted without electron shuttle.

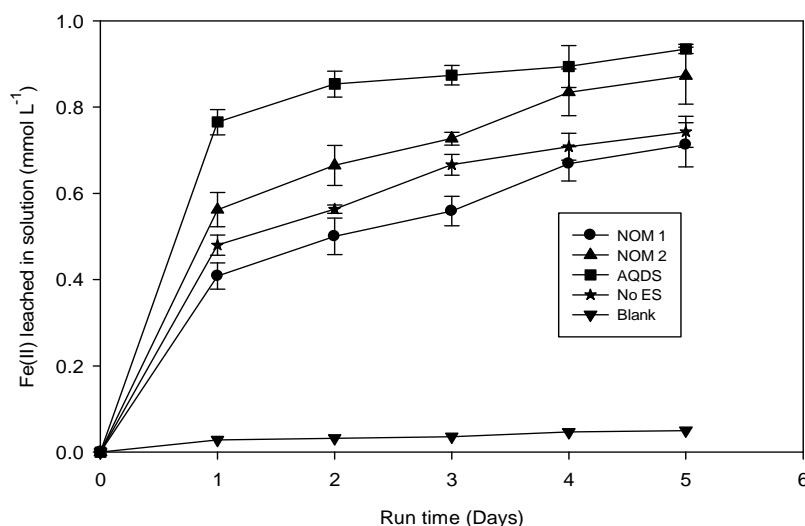


Figure 4.2: Comparison of rate and extent of microbial Fe(III) reduction from Kaolin 3 in the presence of either AQDS, NOM 1, NOM 2 or absence of electron shuttle at 30°C using 10g kaolin mineral.

Colour analysis was conducted to monitor changes after bioreduction of kaolin 3 (Melbur Yellow HCP). The % brightness, whiteness and lab values measured are given on Table 4.1. Improvement in % whiteness from initially 35.57% to 43.84% and % brightness from 67.88% to 69.53% was observed in microcosms leached in the presence of AQDS. Although the amount of Fe(II) leached in microcosms treated with NOM 2 was higher than when NOM 1 was used, % whiteness and brightness improved more in microcosms containing NOM 1. Whiteness increases from 35.57% to 39.92% and to 37.15% in NOM 1 and NOM 2 treated microcosms respectively (Table 4.1). It was noticed that % brightness in NOM 2 microcosms decreased to 66.22% below the initial brightness value of 67.88%. Similarly, both whiteness and brightness in the blank microcosm falls below the average value of the initial raw kaolin.

Table 4.1: Colour analyses of Kaolin 3 (Melbur Yellow HCP) after bioreduction in the presence of AQDS, NOM 1, NOM 2 or absence of electron shuttle.

SAMPLE	L*	a*	b*	% Brightness	% Whiteness
NOM 1	90.17	0.35	7.75	68.08	39.92
MON 2	89.33	0.59	7.90	66.22	37.15
AQDS	90.56	0.29	7.13	69.53	43.84
No ES	90.49	0.39	7.76	68.71	40.73
Blank	90.13	0.96	9.71	65.85	30.62
Initial	90.80	0.87	9.03	67.88	35.57

4.2.2: Bioreduction of kaolin Fe(III): relative importance of biogenic and abiotic factors

Experiments were conducted with two different kaolin minerals to investigate if the Fe(III) reduction observed was biogenic (mainly from inoculated cell suspension and/or from activities of indigenous microorganisms present in the kaolin) or is abiotic due to some chemical reactions in the system. In this investigation, Kaolin 3 (Melbur Yellow HCP, a non treated, unbleached kaolin) and Kaolin 4 (Melbur Yellow MGP, a chemically bleached kaolin) were used. For each kaolin, three different amendments were prepared; one of these was a sterile kaolin with cells added, then a sterile kaolin without cells and the last amendment was unsterile kaolin without cells. In the course of this experiment, Fe(III) reduction from kaolin was monitored for 10 days at 30°C using 7ml of *S. putrefaciens* CIP8040 cell suspension.

A faster rate of Fe(III) reduction was observed in amendments inoculated with *Shewanella* cells in both bleached and unbleached kaolin with more Fe(II) measured in the unbleached example. Around 1.4mmol L^{-1} of Fe(II) was determined in unbleached kaolin 3 on the first day, almost three times higher than what was measured in bleached Kaolin 4 (0.5mmol L^{-1}). This difference continue to increase by extending the bioleaching time to 10 days (Figure 4.3 and Figure 4.4). In contrast, evidence of Fe(III) reduction were not detected in all the uninoculated bottles containing both sterile and unsterile kaolin minerals with no added cells. It is therefore apparent that the Increase in Fe(II) with time reflects the progress of bioreduction by the *S. putrefaciens* CIP8040 employed and addition of a cell suspension in the system generally stimulates reduction of kaolin-bound Fe(III) because control cultures shows no reduction of kaolin-bound Fe(III) to Fe(II). Therefore it was concluded that the absence of extractable Fe(II) in samples with no cells confirms that Fe(III) reduction under the conditions employed here is mainly biogenic from the cells added and is not abiotic.

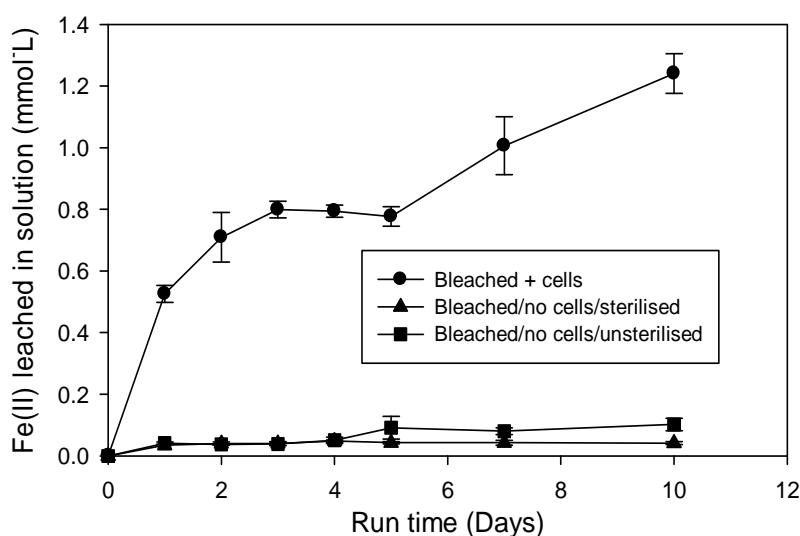


Figure 4.3: Rate and extent Fe(III) bioreduction from Kaolin 4 (Melbur Yellow MGP, a bleached kaolin) as a function of microbial cell suspension added. The experiment was run at 30°C .

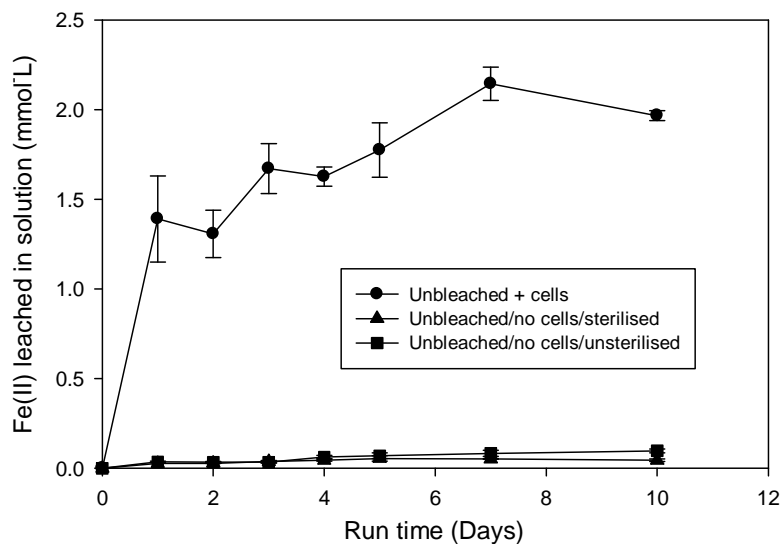


Figure 4.4: Rate and extent Fe(III) bioreduction from Kaolin 3 (Melbur Yellow HCP, an unbleached kaolin) as a function of microbial cell suspension added. The experiment was run at 30°C.

To monitor improvement after biotreatment samples were analysed for colour properties. In bleached kaolin, ISO brightness improves from 74.27% to 78% while the whiteness increases from 53.77% to 64%.65 in bottles that were inoculated with cell suspension. However little increase in the brightness and whiteness were noticeable in both sterile and unsterile controls without cells (Figure 4.5).

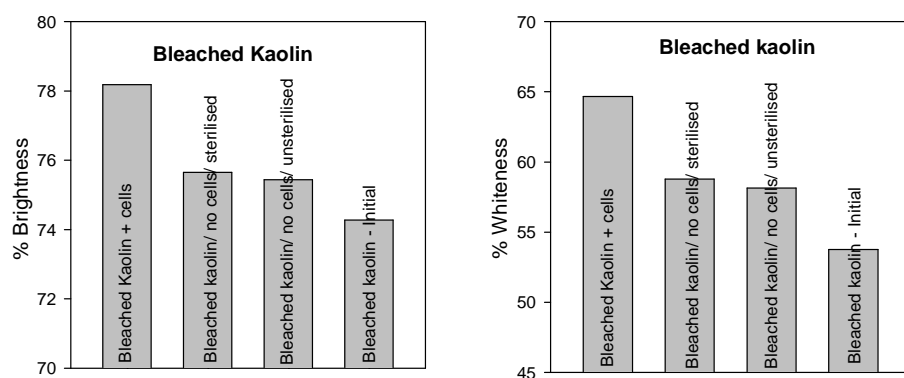


Figure 4.5: Colour analysis of biotreated Kaolin 4 (Melbur Yellow MGP, a bleached kaolin) after 10 days incubation using *Shewanella putrefaciens* CIP8040.

Increases in ISO brightness from 68.35% to 70.35% and whiteness from 38.90% to 44.99% were achieved in unbleached kaolin for the treatments that were inoculated with *Shewanella* cell suspension (Figure 4.6). In contrast, there was a decrease in both ISO brightness and whiteness in sterile and unsterile controls without cells below the initial kaolin value. For example in unsterile unbleached kaolin without cells, the % whiteness decreased to 30.23% from 38.90% while brightness decreased to 65.83% from 68.35%. Also in the sterile unbleached control without cells, the % whiteness decreased by 18.81% while brightness decreased by 5.79%. This observation was peculiar to Kaolin 3 (Melbur Yellow HCP, a non treated, unbleached kaolin) and suggests possible adsorption of AQDS (which is a humic acid analogue) or other additive on the surface of kaolin thereby decreasing the whiteness and brightness of the mineral.

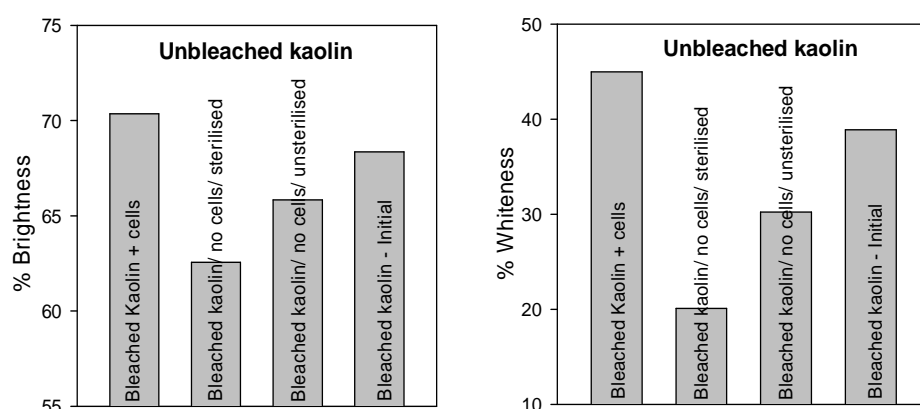


Figure 4.6: Colour analysis of biotreated Kaolin 3 (Melbur Yellow HCP, an unbleached kaolin) after 10 days incubation using *Shewanella putrefaciens* CIP8040.

4.2.3: Investigation and assessment of possible AQDS Sorption on the surface of Kaolin 3

A simple preliminary microcosm experiments were carried out to investigate possible adsorption of AQDS on the surface of kaolin 3. The idea was to understand if the decrease in the brightness and whiteness noticed in Kaolin 3 (Melbur Yellow HCP) that were not injected with *Shewanella* cells was as a result of AQDS sorption on the surface of kaolin. Two different set of experiment were prepared and each set contains 4 different treatments. The first set of the experiment was injected with same volume of lactate and AQDS, while the second set was injected with the same volume of lactate only but no AQDS. The four

different amendments in each set were prepared to contain different mass of the kaolin material (5g, 10g, 20g, and 40g) in the same volume of solution (80ml). The bottles were incubated untouched for 5 days. The colour properties were measured at the end of experiment to see if there will be any variation in the colour properties between these bottles. The microcosm compositions were identical to all the other previous microcosm experiments but no cells were injected in to the system.

The results obtained shows increase in whiteness and brightness in the systems even though cells were not added. Therefore sorption of this substrate on the mineral surface could not be evidently verified. We assumed that AQDS and lactate may have been likely utilised by indigenous microbial community resulting to mobilisation and reduction of Fe(III) in the system. It was noticed that the brightness and whiteness decrease when mineral mass increases (Figure 4.7). For example, in the microcosm containing both AQDS and lactate the brightness was 65.34% when 5g of kaolin was added. The brightness was observed to decreases down to 61.91% in the microcosm amended with 40g of the kaolin material. Similarly the whiteness was observed to be 29.40% when in the presence of 5g kaolin and then decrease to 19.75% when the mass was increased to 40g. Similar patterns were observed with microcosms containing only lactate.

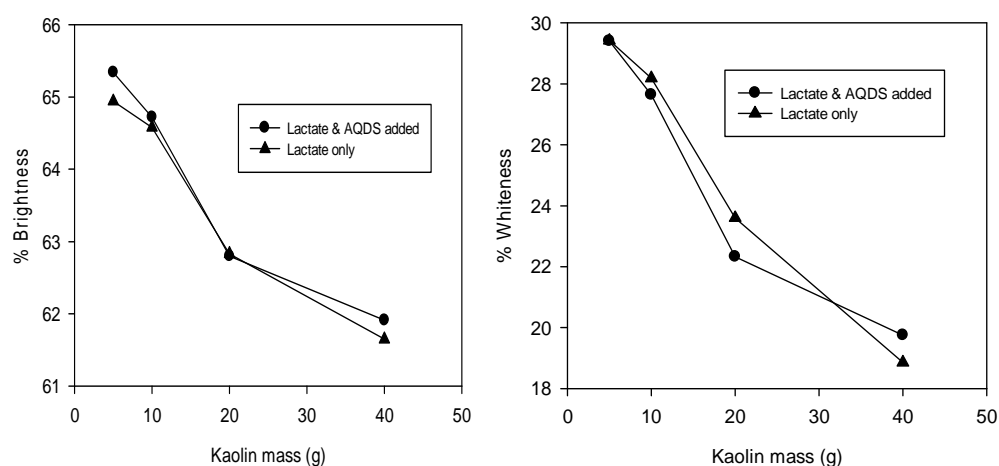


Figure 4.7: Investigation of adsorption of AQDS and lactate on different surface area of Kaolin 3 (Melbur Yellow HCP, an unbleached kaolin).

4.3: PERCENTAGE REMOVAL OF FE- BEARING IMPURITIES FROM INITIAL KAOLIN

The experiment conducted for selection of the most suitable iron reducing bacteria in Chapter 3 (Figure 3.1) and that for the comparison of different electron shuttling systems (Figure 3.18) were used to express percentage removal of bioavailable Fe_2O_3 from the initial total Fe-bearing impurities present in the mineral in relation to Fe_2O_3 determined from XRF analyses, and to determine how efficient each treatment was. Details of the calculations are given in appendix 7.3. The percentage bioavailable Fe_2O_3 removed using *S. putrefaciens* CIP8040 was approximately around 47mg per 100g of kaolin equivalent to 4.44% of total Fe-bearing impurities present in Kaolin 2 (Remblend) after 5 days of incubation. Approximately around 45mg per 100g of kaolin equivalent to 4.3% of iron impurities present was similar removed by both *S. putrefaciens* CN32 and *S. algae* BrY (Table 4.2). Treatment with *S. loihica* was the least efficient with only 0.01% Fe_2O_3 removed. Therefore treatment with *S. putrefaciens* CIP8040 has substantially removed more bioavailable Fe_2O_3 than the other iron reducers.

Table 4.2: Removal of Fe-bearing impurities in kaolin 2 (Remblend) using different iron reducing bacteria.

Fe(III) reducing bacteria	Mineral mass (g)	Fe(II) mmol/L	% Fe_2O_3 (g/gram of kaolin)	% Fe_2O_3 (mg/g of kaolin)	Fe-impurities removal (%)
<i>S. putrefaciens</i> CIP8040	20	1.460	0.047	46.6	4.44
<i>S. putrefaciens</i> CN32	20	1.406	0.045	44.9	4.28
<i>S. algae</i> BrY	20	1.413	0.045	45.1	4.30
<i>S. oneidensis</i>	20	0.965	0.031	30.8	2.94
<i>S. loihica</i>	20	0.002	7.8E-05	0.08	0.01

Comment [DM22]: Are these % values calculated from Fe concentrations? What was the original Fe_2O_3 content?

Results obtained from experiments using different electron shuttles in enhancing the removal of Fe_2O_3 in Kaolin 3 shows that addition of AQDS better enhances removal of Fe with approximately 60mg per 100g of bioavailable Fe_2O_3 removed (around 5% of Fe-bearing impurities present in the mineral). The natural organic matter (NOM 2) also shows greater effect on Fe removal than NOM 1, with around 55.7mg of bioavailable Fe_2O_3 per 100g of mineral, which is equivalent to 4.4% of the original Fe impurities. A reasonable improvement was also observed in the treatment added with no electron shuttle (Table 4.3).

Table 4.3: Removal of Fe-bearing impurities in Kaolin 3 (Melbur Yellow HCP) using different electron shuttles in the presence of *S. putrefaciens* CIP8040.

Electron shuttle	Mineral mass (g)	Fe(II) mmol/L	% Fe ₂ O ₃ (g/gram of kaolin)	% Fe ₂ O ₃ (mg/g of kaolin)	Fe- bearing impurities removal (%)
NOM 1	10	0.713	0.046	45.5	3.6
NOM 2	10	0.873	0.056	55.7	4.4
AQDS	10	0.935	0.060	59.7	4.7
No. ES	10	0.742	0.047	47.4	3.7

4.4: EFFECT OF BIOREDUCTION ON THE MINERALOGY AND TEXTURE OF KAOLIN.

To investigate any biogenic alteration of kaolin after bioreduction, mineralogical analyses were carried out using XRD, FTIR, SEM, EDX and Mössbauer spectroscopy. The mineral material yielded a preferred orientation of kaolin pattern with all peaks clearly resolved. The interpretation of the XRD pattern shows that the mineral was composed mainly of highly crystalline kaolinite but also contains some illite which is an accessory mineral found in both the biotreated and blank kaolin material. The peaks at approximately $2\theta = 12, 17, 20-22, 25, 27, 35-37^\circ$ confirms kaolinite while those at $2\theta = 8, 17, 30$ and 45 correspond to illite (Figure 4.8). The XRD patterns obtained following treatment with *S. putrefaciens* CIP8040 appear to be unaltered with peak similarity before and after the treatment. This may be due to the mineral being highly crystalline; Fe(III)-bearing crystalline phases are more resistant to bacterial reduction and therefore longer incubation may be required to cause dissolution compared to poorly crystalline minerals (Cutting et al., 2009).

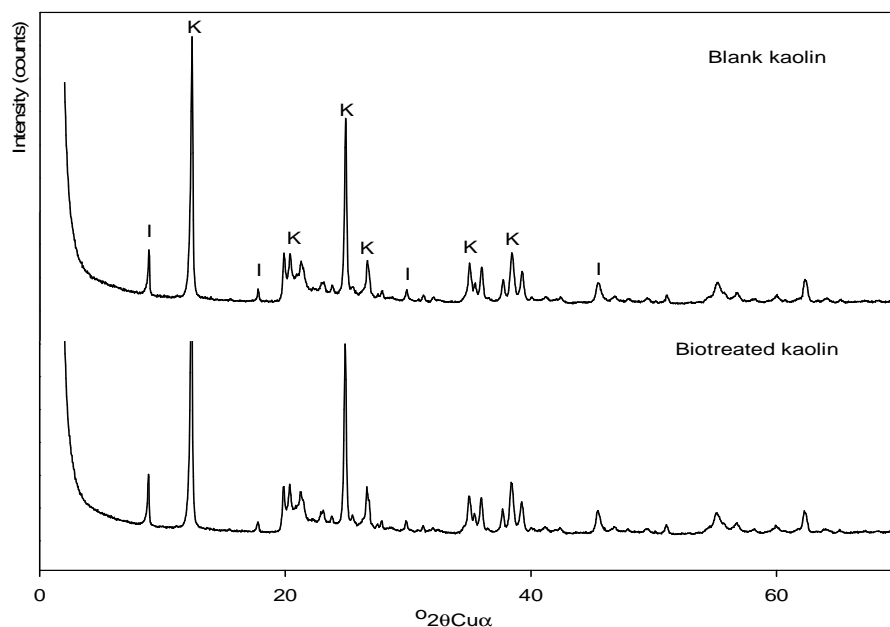


Figure 4.8: XRD pattern of Kaolin 2 (Remblend) before and after bioreduction using *S. putrefaciens* CIP8040 at 30°C.

FTIR was used in this study mainly in the mid-infrared region ($4000-400\text{cm}^{-1}$) to characterise various OH- groups via hydroxyl bond vibration. The FTIR spectra reveal a highly defined and well crystalline kaolinite but illite is barely seen suggesting that it may be in a very low quantity (Figure 4.9). Within the mid infrared region, the band near 3620cm^{-1} was due to internal OH-stretching while the band near 3700cm^{-1} was a result of internal surface OH-stretching vibrations; these bands are characteristics of kaolin group. The OH deformation band at 938cm^{-1} and 916cm^{-1} are due to inner OH groups and inner surface OH respectively. Bands observed near 750cm^{-1} and 800cm^{-1} are used to characterise well crystalline kaolinite. In addition the ratio of hydroxyl vibration bands around 3700cm^{-1} and 915cm^{-1} are also useful in assessing the crystallinity of kaolinite, and confirm that the kaolin was highly crystalline (Russell and Fraser, 1996).

The weak region near 3600cm^{-1} and 880cm^{-1} were demonstrated to be due to OH stretching and bending vibrations of $\text{AlFe}^{3+}\text{OH}$ which occur as a result of Fe^{3+} substitution with Al within the octahedral structure of kaolin. However no alteration or deformation was observed by FTIR after biotreatment at the small shoulder band near 3600cm^{-1} which was associated with AlFe-O-H stretching vibration in kaolinite in comparison with an untreated sample. This indicates that the bioleaching does not probably have much impact on the structural Fe(III) impregnated within the structure of kaolin but possibly only the iron oxides on the kaolinite surface were bio-reduced by the bacteria.

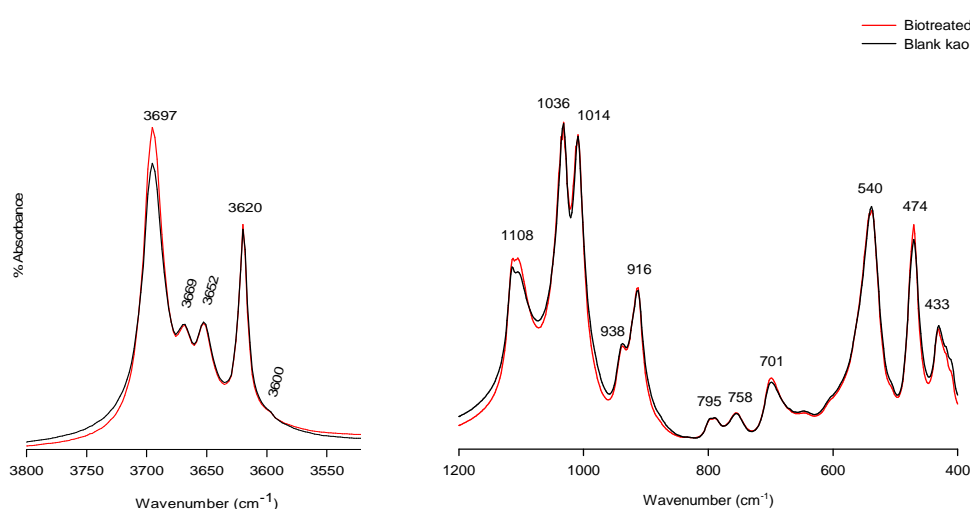


Figure 4.9: FTIR spectra of Kaolin 2 (Remblend) before and after bioreduction using *S. putrefaciens* CIP8040 at 30°C .

The scanning electron micrograph (Figure 4.10) shows untreated kaolinite particles in stack form with varying sizes that are morphologically arranged in face to face pattern. The image further reveals a very well formed kaolinite containing large crystals with clear hexagonal outline. Some rough and rolled edge kaolinite particles were also observed. However, scanning electron microscopy showed some partial destruction and disintegration in the morphology of the biotreated mineral (Figure 4.10). The texture of the kaolinite particles was observed to be different from the blank and seems to be more angular after biotreatment and partially altered at the edges.

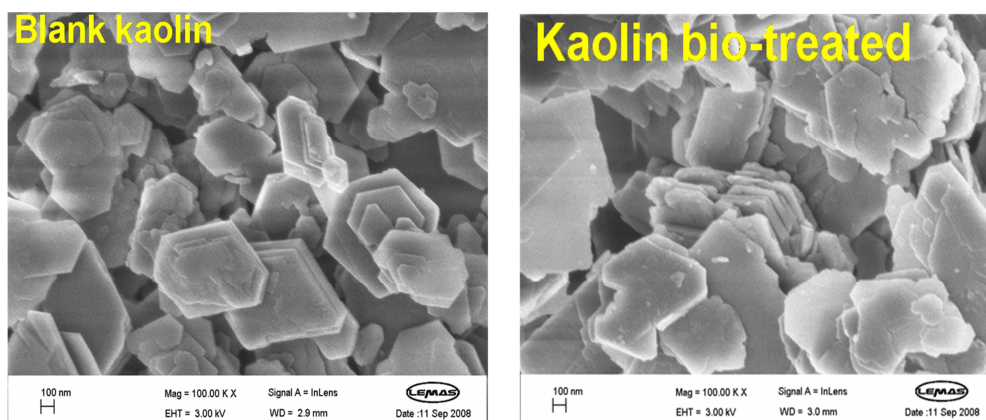


Figure 4.10: Scanning electron micrographs showing the morphology of Kaolin 2 (Remblend) before and after bioreduction using *S. putrefaciens* CIP8040 at 30°C.

The SEM facility was equipped with EDX (energy dispersive X-ray spectroscopy) capability for semi-quantitative analysis. Some differences were observed in the composition of kaolin after biotreatment with *S. putrefaciens* CIP8040 (Table 4.4 and Table 4.5). The percentage atomic content of Fe was 0.39% in the blank sample and decreased to 0.21% in the biotreated kaolin sample. Similarly the approximate concentration of Fe decreases to 0.35% from 0.65% after bioleaching. Slight decreases in Al and K are also observed after bioreduction. Therefore bioreduction has some effect on elemental composition of the mineral.

Comment [DM23]: Does this match the change deduced from XRF data or from solution data?

Table 4.4: Elemental composition of blank kaolin 2 (Remblend) using EDX analysis (quantitative analysis).these tables need to be simplified and corrected

Element	Weight percent	Atomic percent
O	58	71
Al	17	12
Si	20	14
K	1	1
Fe	1	0.4
Total	100.00	

Table 4.5: Elemental composition of biotreated Kaolin 2 (Remblend) using EDX analysis (quantitative analysis).

Element	Weight percent	Atomic percent
O	60	72
Al	17	12
Si	20	14
K	1	0.7
Fe	0.6	0.2
Total	100.00	

Characterisation of different Fe phases in kaolin 3 (from Figure 4.11) was conducted using transmission Mössbauer spectroscopy at 4.5K and also at room temperature (TR) for both treated (bioreduced with AQDS) and blank kaolin samples. These samples were analysed by Dr. Ravi K. Kukkadapu from Pacific Northwest National Laboratory, Richland USA. Because of the small particle size nature of different Fe(III) phases, Mössbauer measurement at liquid nitrogen temperature (4.5K) was employed here and the results confirm the presence of doublet Fe(III) and Fe(II) in their octahedral coordination as expected for other Fe-oxide phases (Figure 4.11). The room temperature (RT) Mossbauer measurements similarly confirmed the presence of well resolved doublets of Fe(III) and Fe(II) with some mixture of small particle oxides (Figure 4.12). All the spectra obtained at RT and 4.5K were well resolved and are reasonably fitted with paramagnetic quadrupole doublets for different Fe phases.

The 4.5K spectrum of the blank kaolin shows that 55% of Fe was in the form of Fe(III) either as Fe-oxide (41%) or Fe(III) doublet (14%) with the remaining 45% in the form of Fe(II) doublet. The percentage of Fe(III) decreases to 45% with Fe-oxide calculated to be (22%) and Fe (III) doublet (23%) while Fe(II) was calculated to increase to 55% after bioreduction (Figure 4.11). The increase in Fe(III) doublet after bioreduction with *S. putrefaciens* CIP8040 may probably be due to Fe-oxide coating on the surface of the mineral such as goethite resulting from the formation of a biogenic iron mineral.

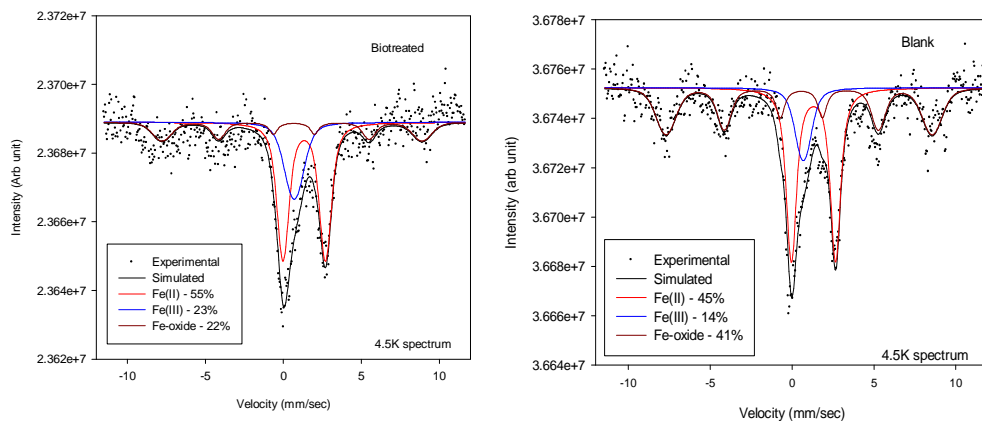


Figure 4.11: Mössbauer spectra (4.5K) of biotreated and blank Kaolin 3 (Melbur Yellow HCP) in the presence of AQDS using *S. putrefaciens* CIP8040 at 30°C.

The Mössbauer spectrum of the blank kaolin at room temperature also indicates that the majority (66%) of Fe was in the form of Fe(III), consisting of small particle oxides (48%) and Fe(III) inner doublet (18%) with the remaining 34% constituting Fe(II) outer doublet. The ratio of Fe(II) increase to 50% after bioreduction with a major decrease of small particle oxide to 21% (Figure 4.12)

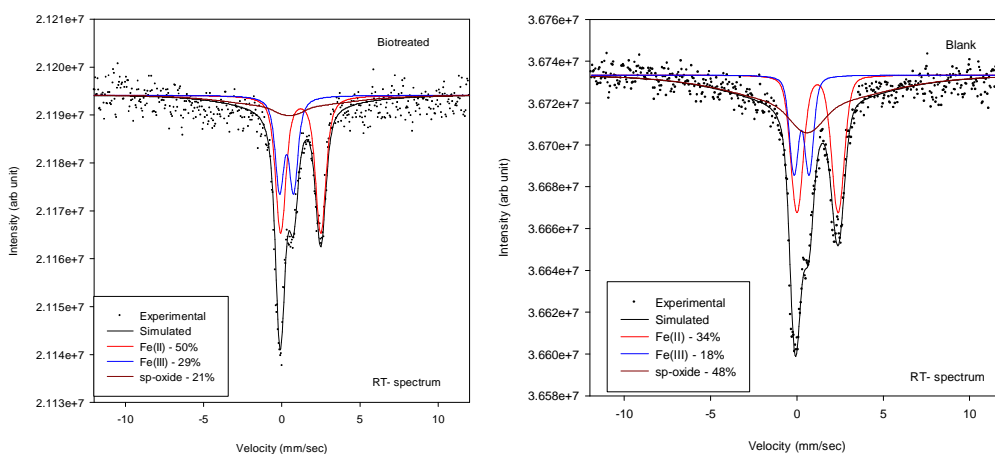


Figure 4.12: Room Temperature (RT) Mossbauer spectra of biotreated and blank Kaolin 3 (Melbur Yellow HCP) in the presence of AQDS using *S. putrefaciens* CIP8040 at 30°C.

Kaolin 2 (a dry kaolin labelled Remblend) was also subjected to Mossbauer spectroscopy in **reflexion** mode (290K) and transmission mode (6.9K). The samples were analysed by Dr. Moustafa Abdelmoula of LCPME, University of Nancy, France. The analyses conducted in reflection mode confirm two doublet characteristics of Fe^{3+} and Fe^{2+} in their octahedral coordination (Figure 4.13). The first doublet was assigned to Fe(II) and corresponds to the ferrous state of Fe while the second doublet was assigned to Fe(III) which corresponds to the ferric state of Fe. However the $\text{Fe}^{2+}(\text{VI})$ doublet was observed to increase in intensity after bioreduction with *S. putrefaciens* CIP8040 when compared with the blank. Similarly an increase in the intensity of the Fe^{3+} doublet was also observed after bioreduction but less pronounced than the increase in the Fe^{2+} doublet. It is considered probable that substantial amounts of Fe^{2+} formed after bioreduction are adsorbed on the kaolinite surface.

Comment [DM24]: Is this correct?

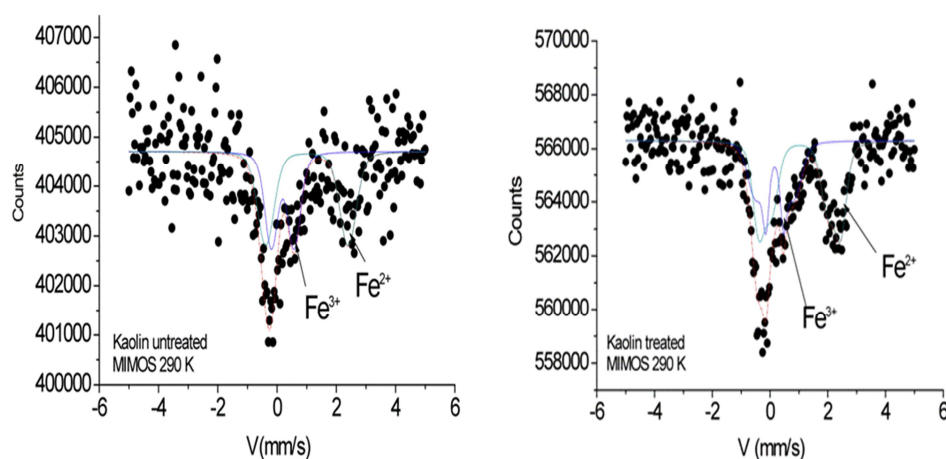


Figure 4.13: Mössbauer spectra (290K) of Kaolin 2 (Remblend) before and after bioreduction using *S. putrefaciens* CIP8040 at 30°C in reflection mode.

A transmission mode Mössbauer analysis conducted at 6.5K (Figure 4.14) also confirms two doublet characteristics of Fe^{3+} and Fe^{2+} . However in this mode, the relative intensity of the Fe(II) outer doublet was observed to be much less pronounced than the Fe(III) inner doublet in the sample treated with *S. putrefaciens* CIP8040

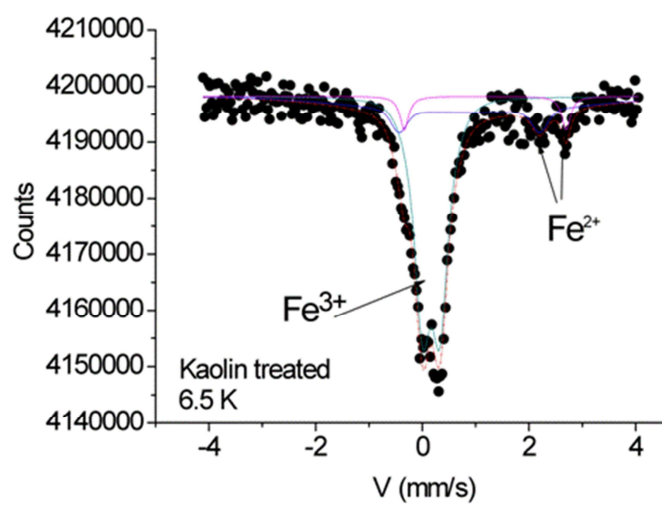


Figure 4.14: Mössbauer spectra (6.5K) of Kaolin 2 (Remblend) after bioreduction using *S. putrefaciens* CIP8040 at 30°C in transmission mode.

4.5: DISCUSSION

This section investigates and assesses the influence of different electron shuttling compounds on the initial rate and extent of Fe(III) reduction in kaolin. Previous research shows that the presence of humics and other extracellular quinones can rapidly increase the rate of reduction of Fe(III) oxides and other insoluble metal oxides (Cutting et al., 2009; Lloyd, 2003). At the same time they enhance microbial respiration and electron delivery to several Fe(III) oxides (Zachara et al., 1998). The effect of electron shuttling has been demonstrated using AQDS (anthraquinone-2, 6-disulfonate, a humic acid analogue) for the enhancement of the rate of Fe(III) reduction by different iron-reducing *Shewanella* spp (Royer et al., 2002). In our research, addition of AQDS also enhances and accelerated the initial rate of reduction. The enhancement in the rate of reduction was largely due to the electron shuttling potential of AQDS which alleviates the requirements for establishing direct contact between the iron-reducing organisms and the mineral surface (Lloyd, 2003). This enhancement in the rate and extent was due to diffusion of AQDS/AH₂DS into the pore space of the mineral, which facilitates electron acceptance (Jaisi et al., 2007b).

Similarly, natural organic matter was recently shown to mediate and enhance rates of Fe(III) reduction through the electron shuttling mechanism (Royer et al., 2002). Natural organic matter (NOM), or humic acids, are reported to be redox sensitive for their potential to reduce redox sensitive metals including Fe(III), Cr(VI), Mn(IV) etc. (Gu and Chen, 2003). Electron shuttling mechanisms of NOM behave in a manner similar to AQDS with quinone moieties being involved in the electron transfer. In addition also to serving as electron shuttles, humics are known to stimulate bioreduction by complexing with Fe(III) thereby making it more readily and easily accessible to the iron-reducing microorganisms. Besides, humics may also complex with Fe(II) and limit its adsorption on to the mineral and microbe surfaces hence providing adequate “free surface” for Fe(III) bioreduction (Kappler et al., 2004). The result of this study further demonstrated that both NOM 1 and NOM 2 can promote electron shuttling as well as enhancing and stimulating Fe(III) bioreduction using *Shewanella putrefaciens* CIP8040. Although NOM 2 was observed to be more efficient than NOM 1 this may be attributed to their chemical composition. Elemental analyses of these compounds shows NOM 1 to mainly constitute sulphur and only 1.3% of carbon. NOM 2

Comment [DM25]: This cannot be correct!

contains 0.6wt% of nitrogen, 19.1wt% of carbon, and 0.77wt% of hydrogen. This may explain the tendency for NOM 1 to have less effect on the rate of bioreduction of kaolin 2.

Bioreduction was also observed in an experiment that has not been amended with an electron shuttle. This indicates that *Shewanella putrefaciens* CIP8040 is capable of bioreducing Fe(III) within the mineral in the absence of any electron shuttle. Earlier studies suggest that some iron-respiring *Shewanella* spp can switch to and utilize the enzymatic reduction pathway for the reduction of Fe(III) in the absence of quinones through secretion of soluble electron shuttling compounds such as flavin mononucleotides and riboflavin or some small quinone-containing extracellular compounds (Cutting et al., 2009; Lloyd, 2003). Alternatively in the presence of insoluble Fe(III) minerals some iron reducers are capable of generating appendages or flagella that promote movement and attachment onto the mineral surface via direct contact. In addition some research shows that the rate and extent of Fe mineral reduction directly depends upon contact between microorganisms and the mineral surface (Kostka et al., 1999a). Therefore the reduction observed in the absence of any electron shuttles might suggest one of the surface-based mechanisms mentioned.

The absence of extractable Fe(II) in samples without *Shewanella* cells confirms that the bioreduction observed in these studies was mainly from the cultures of *Shewanella* strains added and not from the activities of indigenous microorganisms or chemical reaction. This is because no Fe(II) was detected in the uninoculated microcosms containing both sterile and unsterile kaolin 3 and kaolin 4, or in the blank sets in every experiment conducted. The result further shows that there was no existence of any inherent Fe(III) reducing microorganisms in the kaolin mineral. However the presence of inherent indigenous microorganisms could not be completely ruled out but a longer incubation period may possibly be required for them to properly grow. In addition our system is nutrient-limited and therefore nutrient supplements may be required for them to be detected. Therefore the bioreduction seen is biologically performed from the addition of pure cultures of *Shewanella*.

Sorption of AQDS and lactate was not tentative on the surface of kaolin 3 in experiments without added *Shewanella* cells, but we suggests possible utilisation of AQDS and lactate by indigenous microbial community resulting to mobilisation and reduction of Fe(III) thereby increasing its colour properties. Adsorption of these compounds tends to be more at a very high kaolin surface area. Although fredrickson et al. (2003) reported sorption of lactate on hydrous ferric oxides (HFO). In their studies they observed that around 50% of lactate in their systems strongly adsorb to HFO at pH 7 which exactly is our control pH. However, AQDS is known to be a humic acid analogue and several studies for controlling water quality suggested that humic acid could be transferred from liquid phase to solid phase by adsorption. Moreover humic acids are known to affect metal ion sorption and desorption in the environment, and in addition they can be adsorbed onto the surface of several minerals including kaolin (Qinyan et al., 2009). Sorption of these substrates may not be completely ruled out but more experiment to determine their sorption isotherm may be required. It is reported that sorption on kaolin particles is a function of solution pH, ionic strength and solid to liquid ratio, and the surface acidity of the clay particle. We therefore assumed that the reduction in colour properties of kaolin 3 observed may possibly be due to AQDS and lactate sorption. Therefore AQDS and lactate adsorption on the mineral may have reverse effect on the colour properties especially when no cells are added.

Like in Chapter 3, brightness and whiteness effectively improved better when kaolin was bioleached in the presence of AQDS. Bioleaching with NOM 1 and NOM 2 also showed improvement in whiteness and brightness when compared with the blank and initial kaolin material. Treatment in the presence of AQDS also substantially removed more Fe₂O₃ from the initial Fe-bearing impurities present in kaolin 3 more than in the presence of NOM1 or NOM2 as well as in the absence of an electron shuttle.

Assessment of the mineralogical transformation after bioreduction using X-ray diffraction analysis of powdered samples confirmed the typical diffraction pattern of kaolinite. The ordering patterns of the kaolin structure obtained before and after bioleaching further confirm the crystallinity of the mineral. No difference was evidently seen that could be due to bacterial destruction or transformation between the biotreated and blank sample. However the diffraction patterns also provide evidence of illite in both samples. The

Comment [DM26]: We saw this in Psyrillos et al's Clay Minerals paper

presence of this associated ancillary mineral observed within the kaolinite was also reported by (Psyrillos et al., 1999). The mid infrared spectrum obtained by FTIR further reveals the crystallinity of the kaolin material. It seems that the bioleaching process did not have a major impact within the mineral structure after bioreduction because the OH absorption bands characterising the AlFeOH group between 3600cm^{-1} and 880cm^{-1} are not affected after bioleaching. However, partial destruction of the hexagonal platey morphology of the mineral was confirmed by SEM after bioreduction. The bulk mineralogical composition as determined by EDX reveals a decrease in the Fe content of kaolin after bioreduction and therefore the bioleaching did affect the main elemental composition of the mineral. It is considered that the structural Fe within the mineral framework is not likely to be attacked during bioleaching but probably iron oxides on the mineral surface are being bioreduced.

Increases in the Fe(II) doublet and Fe(III) doublet were demonstrated by Mossbauer spectroscopy obtained both at RT and 4.5K and in transmission (6.5K) and reflection (290K) mode after bioreduction of kaolin 3 and kaolin 2 respectively. But a substantial decrease in the percentage of small particle oxides was apparent after bioreduction of kaolin 3. Although we are not sure of the different iron phases in our mineral, we assume that poorly crystalline phases are more susceptible to bioreduction than highly crystalline phases (Cutting et al., 2009; Hansel et al., 2004). The reduction of small particle oxides may cause Fe(II) sorption which may possibly be retained in the solid phase of the mineral surface (Hansel et al., 2004). The retention of Fe(II) in the solid phase of kaolin may promote mineral transformation in our system to more crystalline Fe(III) oxides. This may explain the increase in the Fe(III) doublet noticed after bioreduction. Similarly production of excess biogenic Fe(II) may promote transformation of poorly crystalline iron oxides to ferrous-containing crystalline phases such as magnetite (Zachara et al., 2002), and this may also explain the increase in the Fe(II) doublet after bioreduction. This result agrees with other work conducted on biomineralisation of poorly crystalline Fe(III) oxides using iron reducing bacteria (Zachara et al., 2002). Using Mössbauer spectroscopy, these authors demonstrated possible transformation of poorly crystalline Fe(III) oxide by iron-reducing bacteria to crystalline phases such as hematite, goethite and lepidocrocite, and ferrous-containing crystalline phases such as magnetite.

In conclusion, Chapter 3 and Chapter 4 have highlighted that iron reducing bacteria are capable of coupling oxidation of lactate for the reduction of Fe(III) in kaolin with *S. putrefaciens* CIP8040 identified to be the most effective strain. The presence of anthraquinone-2,6-disulphonate serving as an electron shuttle enhances the reduction kinetics, but natural organic matter could still serve as substitute. Bioleaching has no major impact on the structural Fe within the kaolin, but possibly iron oxides on the mineral surface are bioreduced.

CHAPTER 5 4: BIOLEACHING OF SILICA SAND USING BATCH MICROCOSM

54.1: INTRODUCTION

Silica ~~sand~~ is one of the most ~~widely occurring and~~ abundant ~~mineral chemical components~~ of ~~the~~ the surface of the ~~E~~earth and ~~is~~ commonly found in nature as sand or quartz together with other silica minerals like tridymite and cristobalite. These three principal crystalline forms of silica polymorphs have ~~a general denoted with a the~~ formula SiO_2 . Moreover, quartz is one of the most abundant silica minerals and forms the major parts of many igneous, metamorphic and sedimentary rocks. The chemical compositions of silica sands ~~that are composed mainly of~~ quartz constitute ~~of~~ almost 100% SiO_2 but they show some small amounts of other oxides ~~(present~~ as inclusions of other minerals) such as Fe_2O_3 , Al_2O_3 , TiO_2 , K_2O , Na_2O and MnO_2 . Structurally the mineral quartz is built from SiO_4 tetrahedra linked ~~in their by each~~ corner to another tetrahedron through oxygen (Deer et al., 1999). Silica sand is ~~also~~ one of the most versatile industrial minerals with wide range of applications particularly in the glass making industry (Styriakova et al., 2007).

~~I~~For example, the major principal glass products from the industrial application of silica sand include the colourless and coloured bottle containers, flat glass, light bulbs and fluorescent tubes, TV and computer screens and glass fibres that are used for insulation and reinforcement (British et al., 2009a). ~~I~~Perhaps industrial application of silica sand can be limited by the presence of ~~a~~ heavy metal content particularly iron (Banza et al., 2006) and for glass manufacturing, silica sand must contain a very low amount of iron (Zhao et al., 2007). The permissible Fe_2O_3 content in glasses ~~sands~~ of different grades should not ~~contain~~ ~~be~~ more than 0.05% for house-hold glasses, 0.012-0.02% in clear glasses, 0.025-0.035% in crystal glasses, 0.07% in light engineering and medical glasses and 0.09-0.20% in sheet glasses (Styriaková et al., 2010). ~~The p~~Presence of ~~these~~ iron generally affects the transparency of glasses, stains ceramic products, impairs transmission in optic fibers and also lowers ~~the~~ melting point of refractory materials (Mowla et al., 2008). The associated ~~irons~~ impurities can be found as iron hydroxides coating the entire quartz mineral grain, and are reported to bind strongly on the surface of quartzsilica in various surfaces of sand thereby make it rusty in appearance (Rusch et al., 2010; Zhao et al., 2007). ~~I~~However, these

Comment [DM27]: Do you mean Fe_2O_3 in the glass or in the sand?

iron ~~oxy~~-hydroxide coatings are generally characterised as the minerals ferrihydrite, hematite, goethite and lepidocrocite, with the iron content in the various oxide phases usually ranging between 0.074 and 44.2mg Fe per gram of sand in various soils and sediment (Rusch et al., 2010).

~~Although~~ substantial efforts have been ~~constantly~~ committed to the problem of removing iron contamination~~nt~~ using chemical and physical methods for iron removal from silica sands. The methods conventionally employed include gravity and magnetic separation techniques, attrition, floatation, ultrasonic-assisted oxalic acid treatment, method and acids or alkaline leaching techniques (Du et al., 2011; Mowla et al., 2008; Bain et al., 1996). Chemical methods s that requires leaching with organic or inorganic acids such as sulphuric and hydrochloric acids ~~which~~ are generally cost ineffective and the resulting effluents after leaching are environmentally unfriendly. Similarly the use of inorganic acids may further contaminate the mineral with SO_4^{2-} and Cl^- after ~~bio~~leaching (Du et al., 2011). However a combination of various techniques may be imperative required, depending on mineral type, size and form for optmaximisation of iron removal efficiency.

In a similar way to Chapter 3, kaolin chapter, this chapter presents work that was ~~was also~~ designed to exploit and harness the dissimilatory iron reduction pathway for the bioreduction of silica-bound Fe(III) to improve theits quality and industrial value of silica sand. The chapter will ~~however~~ as before examine efficiency of Fe(III) removal using different iron-reducing bacterial strains and assess the quality improvement. Moreover the chapter will investigate the rate and extent of Fe(III) reduction kinetics as a function of electron donor concentration, and biomass concentration to solid ratios under non-growth conditions. The efficiency of natural organic matter (NOM) will also be investigated as a substitute for AQDS in enhancing the kinetics of Fe(III) reduction in silica sand.

54.2: METHODOLOGY

Small scale microcosm experiments were conducted with Fe(III) in silica sand as the sole electron acceptor and lactate as the electron donor in the presence of ~~pure cultures~~ of *Shewanella* cells. Anthraquinone 2,6 disulfonate was used to enhance electron shuttling in

the system. All experiments were performed in triplicate (unless otherwise specified). The reduction of Fe(III) from silica sand was measured (as described in sub-section 2.5.7 of material and method) as the production of Fe(II) in HCl extracts using modified pPhenanthroline techniques (Fadrus and Maly, 1975). Absorbance was measured using UV-vis-spectrophotometry at 510nm. Liquid samples from bioleaching experiment were analysed for dissolved organic carbon using a Shimadzu TOC- 5050A dissolved carbon analyser equipped with an AS1-5000A autosampler.

To assess any changes and improvement in mineralogy after bioleaching ~~processes~~, X-ray (powder) diffraction measurements were obtained with a Philips X'pert PRO XRD system recording from 2° to 70° 2θ CuK α , at 0.0334° 2θ per step and 99.70 seconds per step. Similarly, FTIR ~~analyses-spectra~~ of bioleached and initial minerals were measured and obtained in transmission mode using KBr pressed pellets (1-2mg mineral in 200mg KBr) in the mid-infrared range ($400 - 4000\text{cm}^{-1}$) on an AVATAR 360 FTIR ESP spectrometer. Mössbauer spectroscopy was conducted at 300K in transmission mode at University of Nancy, France. Scanning electron microscopy was ~~also~~ conducted at University of Leeds to observe changes in the morphology of the mineral.

54.3: RESULTS

54.3.1: Selection of the most suitable iron reducing bacteria

Similar to the experiments with kaolin ~~experiments~~, ~~a~~ microcosm studies for the bioreduction of silica Fe(III) were conducted using four selected iron-reducing bacteria under non-growth conditions. It was ~~intendaimed~~ to examine the dissimilatory Fe(III) reduction potential of the different *Shewanella* species s and to select the most suitable iron-reducing bacteria that will effectively improve the quality of silica after bioleaching.

~~Sample~~ However, Silica 2 (a sand obtained from Oakamoor Quarry) was used in this experiment for the bioleaching process. From the result obtained, nearly all the *Shewanella* species s examined showed some significant Fe(III) reduction in the mineral over time with the exception of *S. loihica*. Considerable variation in the rate of Fe(II) production was observed among the *Shewanella* species with *S. algae* leaching iron at the fastest rate and greatest ~~str~~ extent after 5 days. ~~But~~ *S. oneidensis* and *S. putrefaciens* CIP8040 were observed

Comment [DM28]: Explain what this sample is

to exhibiting almost similar pattern in the rate and extent of Fe(III) reduction. It was also observed that the rate of reduction with *S. oneidensis* and *S. putrefaciens* CIP8040 flattens off after the initial rate on day one but with *S. algae* it gradually continues gradually with *S. algae* until around day 5 before it flattens off. The rate of Fe(II) production observed for *S. algae* on day 5 was 0.44mmol L^{-1} and 0.37mmol L^{-1} for *S. oneidensis* but 0.35mmol L^{-1} for *S. putrefaciens* CIP8040 (Figure 54.1). *S. loihica* was the least efficient iron reducer with Fe(II) production as low as 0.02mmol L^{-1} after 5 days of incubation.

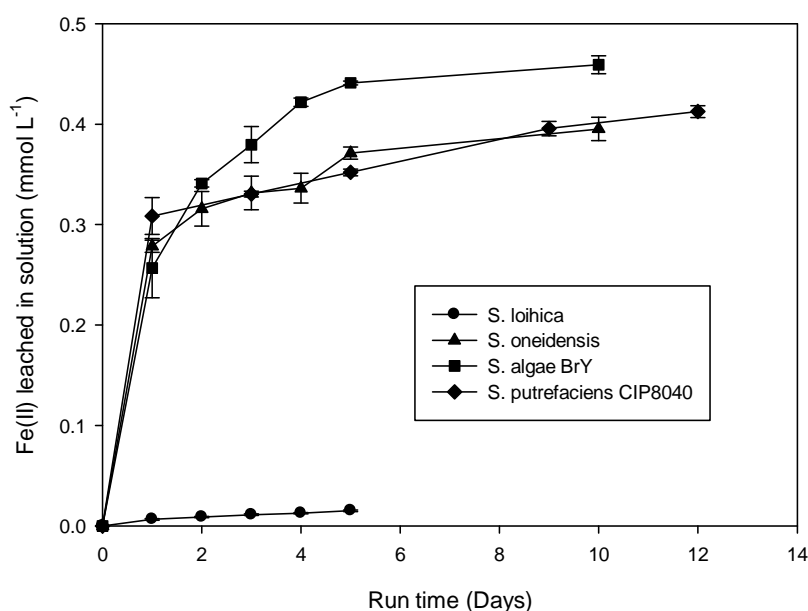


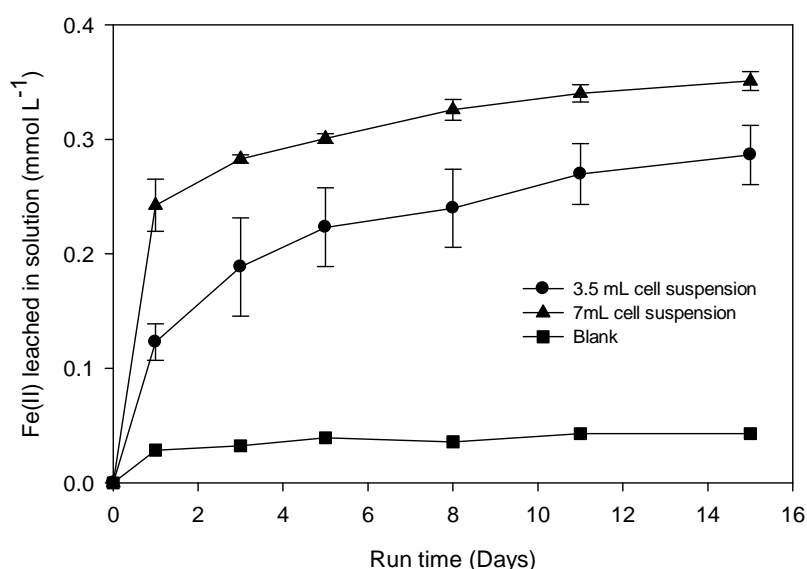
Figure 5.14: Line plot showing extractable Fe(II) concentration from 2.5g Silica Sand 2 as a function of time to compare different iron-reducing *Shewanella* strains in the presence of 10mM lactate and 100μm AQDS at 20°C

54.3.2: Effect of cell density on the rate and extent of Fe(III) reduction.

The impact of cell density on the bioleaching process was evaluated using 2.5g of sample Silica Sand 3 (a sand obtained from King's Lynn Quarry) containing the same amount of liquid (80ml) but with injection of different amount of *Shewanella putrefaciens* CIP8040 cell suspensions ($1.2 \pm 0.4 \times 10^8$ CFU/mL). It was generally observed that cell density does affect the rate and extent of bioleaching. The rate of bioleaching with 7ml cell suspension was observed to be faster and doubled the rate observed when 3.5mL cell suspension was used.

Comment [DM29]: Are all your samples labelled in a systematic way?

For example the amount of Fe(II) measured on day one was 0.24mmol L⁻¹ when 7ml suspension was used but only 0.12mmol L⁻¹ when half of the cell suspension was injected in to the system (Figure 54.2). This was followed by gradual increase by extending the period of bioreduction with 0.35mmol L⁻¹ in microcosms with 7ml cell suspension and 0.28mmol L⁻¹ in microcosms added with 3.5ml cell suspension.



-Figure 5.2: Bioreduction of Fe(III) from 2.5 g Silica Sand 3 using different injection of *S. putrefaciens* CIP8040 cell suspension ($1.2 \pm 0.4 \times 10^8$ CFU/mL) at 30°C. Error bars represent standard error for three replicates.

54.3.3: Effect of electron shuttling system on the initial rate and extent of Fe(III) reduction

Experiments ~~were~~ conducted to evaluate ~~the~~ effect of presence ~~or~~ absence of electron shuttling compound (AQDS) for the bioleaching of ~~S~~silica ~~S~~sand 3. The experiment was conducted using 2.4g of silica sand with the injection of 4ml of *S. putrefaciens* CIP8040 cell suspension. Addition of AQDS was found to have very little effect on the initial rate of Fe(II) production compared to microcosms that had~~s~~ not been ~~added-with~~~~received~~ AQDS (Figure 54.3). Extending the reduction period resulted ~~into~~ a linear increase in Fe(II) concentration over ~~time~~ ~~time~~ with Fe(II) production rate increasing from 0.098mmol L⁻¹ on first day to around 0.224mmol L⁻¹ after 15 days and a little higher than when no AQDS was present (0.186mmol L⁻¹). These results were in contrast with the results demonstrated in the kaolin

experiment where AQDS generally stimulates the rate of Fe(III) reduction to a larger extent compared to experiments without an electron shuttles in them. It was known that AQDS enhances the rate and extent of microbial reduction of Fe(III) in various oxides and many clay minerals by alleviating the need for direct contact between mineral and microbes (Jaisi et al., 2007b). This enhancement was attributed to AQDS/AH₂DS diffusion in to the micropore space of the clay minerals because of the clay's permeability. Because silica sand is less permeable and we therefore assumed that AQDS/AH₂DS will have limited permeability access by permeability to pores within the to the entire mineral por mineral grains. e and t This generally slower-reduced the rate of Fe(III) reduction in the silica minerals that was observed, especially in the presence of fewer-least concentrated *Shewanella* cell suspensions (4ml cell suspension).

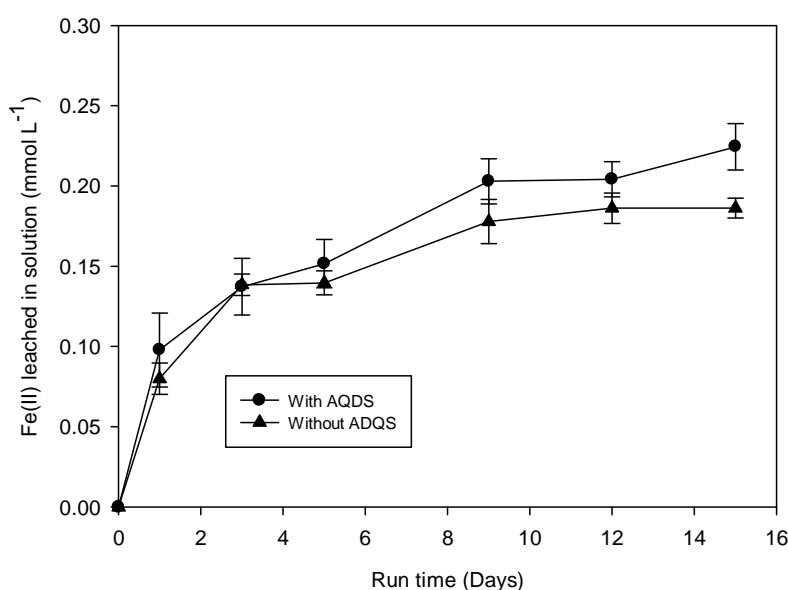


Figure 5.34: Rate and extent of microbial reduction of Fe(III) using Silica Sand 3 in the presence and absence of AQDS at 30°C with the injection of 4ml of *S. putrefaciens* CIP8040 cell suspension at 1.2×10^8 CFU/mL.

Parallel experiments were conducted in the presence of AQDS and NOM 2 to further access and investigate the impact of electron delivery potential of AQDS and NOM2 on the rate and extent of silica sand bioreduction with using different cell density. It was observed that the rate of Fe(II) production on the first day substantially increased in the presence of AQDS

when ~~higher~~ cell suspension (7ml cell suspension) was used but ~~lower~~ ~~decreased~~ in the presence of NOM2. However, in the presence of fewer cells (3.5ml cell suspension), the bioreduction rate was lower when AQDS was added as electron shuttles compared to when NOM 2 was present. Although the rate and extent of Fe(III) reduction were variable in the different amendments ~~but~~ a consistent linear increase in the extent was observed in microcosms ~~added~~ ~~treated~~ with ~~a~~ 7ml cell suspension in the presence of NOM 2 within 15 days of incubation (Figure 54.4). The amount of Fe(II) leached in the system was 0.35mmol L⁻¹ in the presence of AQDS when high cell number was added but around 0.38mmol L⁻¹ in the presence of NOM 2. In general, a combined factor of high cell numbers in the presence of AQDS was observed to effectively improve the rate of Fe(III) reduction in silica sand within the first 5 days more than using fewer cell numbers. Similarly NOM 2 improves the extent of bioleaching in the presence of high cell numbers in comparison to when few *Shewanella* cells are present. This further confirms that addition of higher cell numbers is necessary and required ~~to~~ for the enhancement of rate and extent of bioleaching in the presence of electron shuttle. ~~This contrasts with~~ ~~unlike~~ observations for ~~ed in~~ kaolin which is a clay mineral with a fine grain size that permit the soluble electron shuttles to easily ~~enter by~~ ~~diffuse~~ ~~in~~.

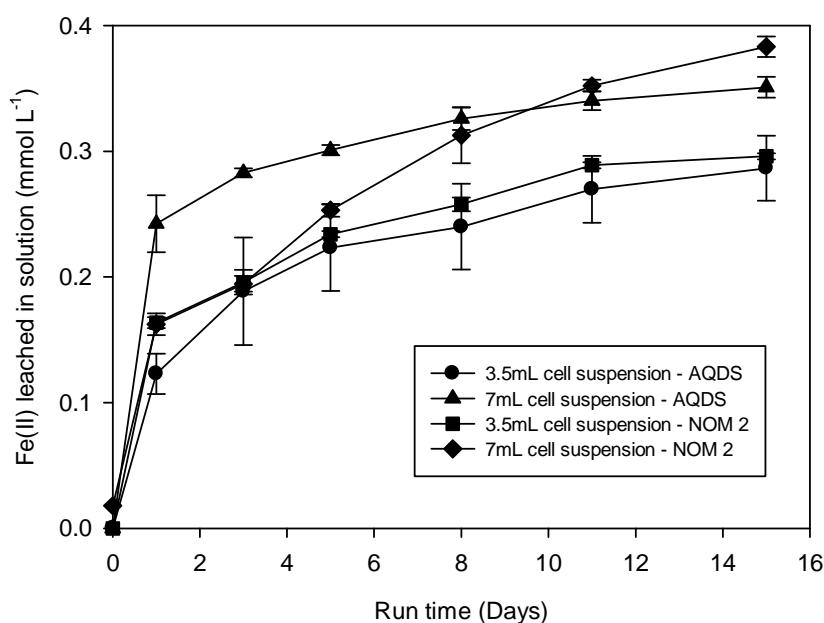


Figure 5.44: Impact of electron potential of AQDS and NOM 2 on the Fe(III) reduction rate of Silica Sand 2 with variable injection of *S. putrefaciens* CIP8040 at 30°C.

5.4.3.4: Bioreduction of silica sand bound Fe(III) in the presence of AQDS, NOM or absence of electron shuttle.

Experiments were conducted to assess the two different NOM (NOM 1 and NOM 2) as replacement for AQDS, and to also compare their electron shuttling potential in enhancing rate and extent of Fe(III) reduction with AQDS, and without an electron shuttle, using silica sand 3 at 30°C with the addition of 4ml *S. putrefaciens* CIP8040 cell suspension. The results in Figure 5.4.5 show the rate and extent of Fe(III) reduction after 15 days, both in the presence of AQDS, NOM 1, NOM 2 and in the absence of electron shuttle. In all cases, similar rates of Fe(III) reduction were observed on the first day in all the experiments except in experiment added one with no electron shuttle in it. The extent of reduction and the amount of Fe(II) leached in the experiment with NOM 1 and NOM 2 was similar with each measuring $0.204 \text{ mmol L}^{-1}$ and $0.208 \text{ mmol L}^{-1}$ respectively. A slightly better bioleaching extent was observed with AQDS. The improvement on the rate and extent of Fe(III) in silica sand 3 in the presence of electron shuttles (AQDS, NOM 1 and NOM 2) was not substantial when compared to the experiment run without electron shuttle added (Figure 5.4.5).

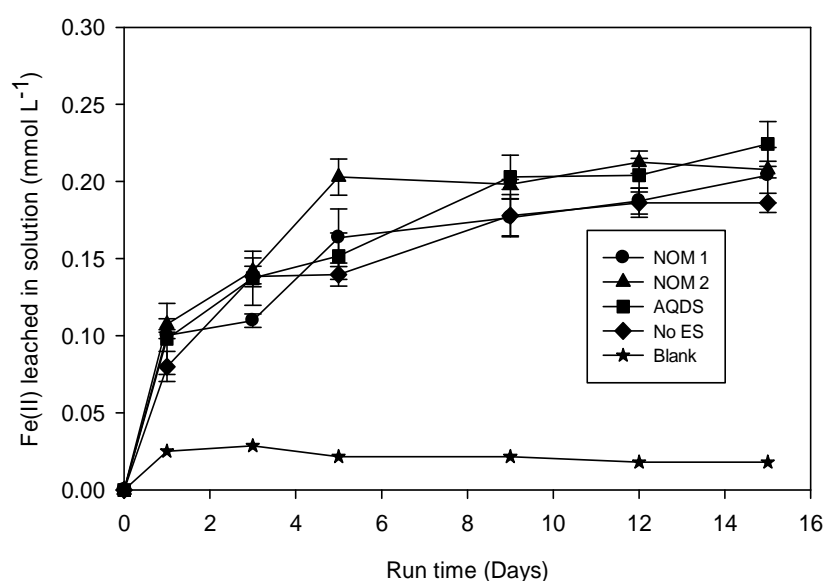


Figure 5.54: Comparison of rate and extent of microbial Fe(III) reduction from Silica Sand 3 in the presence of either AQDS, NOM 1, NOM 2 or absence of electron shuttle at 30°C with the injection of 4ml cell suspension of *S. putrefaciens* CIP8040.

54.3.4: Effect of electron donor concentration and re-inoculation of cells for Fe(III) reduction in silica sand

~~Possible c~~Complementary effects of different concentrations of electron donor (lactate) and re-inoculation of microbial cell at different time intervals for Fe(III) bioreduction in ~~S~~silica Sand 3 were examined. Microcosms containing different concentrations of lactate (1~~M~~mM, 5~~M~~mM, 10mM and 15mM) were prepared and monitored for 28 days (672 hours). Initial injection of 4ml *S. putrefaciens* cell suspension was made followed by subsequent re-inoculation of 3ml cell suspension at different intervals. A combined plots for the bioleaching of silica sand using different lactate concentrations ~~is~~are shown on Figure 54.6, ~~however-and~~ individual plots for each concentration ~~to apparently to~~ show the effect of different cell re-injection at various points for each individual lactate concentration used are ~~given in~~shown on Figure 54.7.

Formatted: Font: Italic

~~Fe~~The reduction was observed to ~~immediately~~commence immediately after initial inoculation without any apparent lag phase in all the different microcosms. Even though the reduction rate was ~~however~~slower ~~but~~ a nearly similar rate of Fe(II) production was apparent ~~foramong~~ the different concentrations of lactate within the first 24 hours, with more Fe(II) leached in the microcosms ~~added-treated~~ with a high concentration of electron donor. However, the results obtained clearly shows variability in the extent of Fe(II) production for the different concentrations of lactate at the termination of the experiment, with 0.35mmol L⁻¹ and 0.32mmol L⁻¹ of Fe(II) determined in microcosms ~~treatedadded~~ with 10mM and 15mM lactate respectively (Figure 54.6).

Similarly, total organic matter was determined at different intervals in the ~~various~~ experiments where microcosms were treated with 1mM, 5mM, 10mM and 15mM lactate. Production of Fe(II) is expected to be accompanied by organic carbon consumption but an increase in TOC overtime was ~~however~~ observed. ~~This which~~ was generally attributed to cells being injected in the system at periodic intervals ~~period~~. ~~However these~~ data are shown in Appendix 5.1.

Comment [DM30]: Say which appendix

Formatted: Font: 12 pt

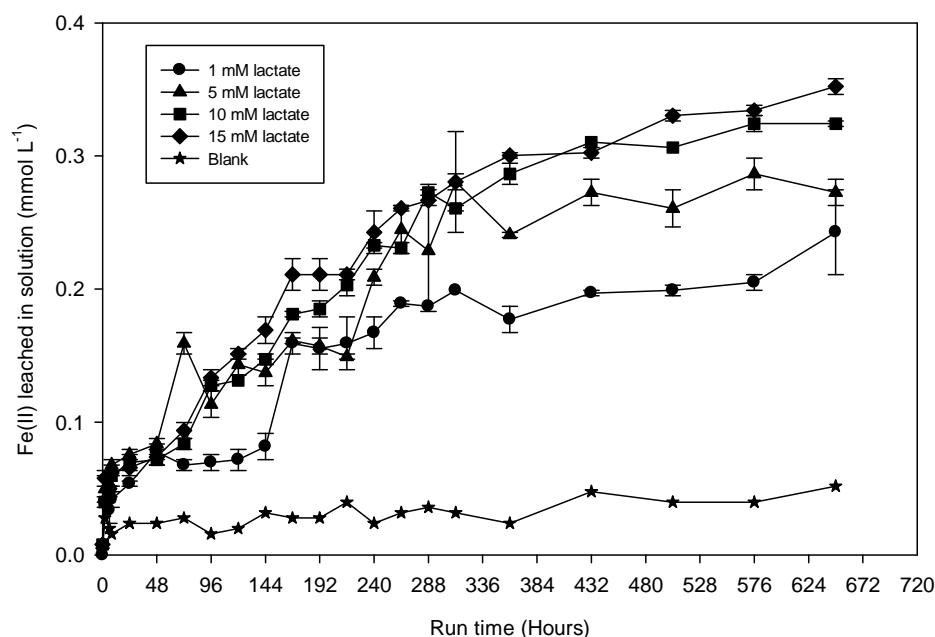
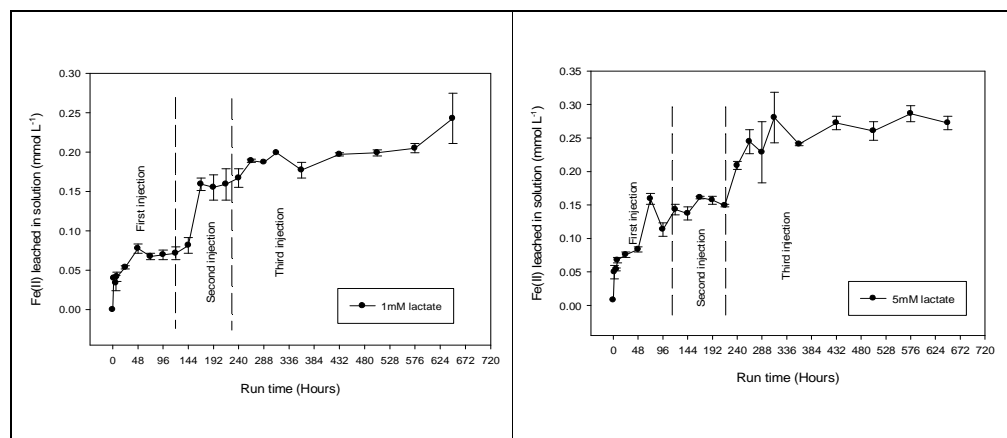


Figure 5.64: Bioreduction of Silica Sand 3 under different concentration of electron donor (1 – 15mM lactate) and multiple inoculations of *S. putrefaciens* CIP8040 at 30°C. Error bars represent standard error for three replicates.

However, from the various concentration range of electron donor concentration used, it was noticed that bioreduction tends to cease faster more quickly and reaches a lag phase after the initial reduction rate in the microcosms added with low concentration of lactate. For example, after the initial reduction rate in the microcosms treated added with 1mM lactate, cessation of bioreduction was apparent within the first 24 hours and a lag period was attained. In contrast, but the rate of bioreduction progresses slowly in the microcosms treated added with 5, 10 and 15mM lactate (Figure 54.7). After second injection of metabolically active *Shewanella* cells, a rapid increase in the rate of reduction resumes in the microcosm treated added with a low concentration of lactate (1mM lactate). Hence the rate of Fe(II) production increases with Fe(II) measured from 0.07mmol L⁻¹ after 120hr (5 days) to 0.16 after 216hrs (9 days). A rapid increase was not noticed, but a steady and slow

increase in the rate of Fe(II) production was ~~only~~ apparent only in those microcosms containing high concentrations of lactate after second re-inoculation. For example, Fe(II) increases from 0.15mmol L⁻¹ to 0.21mmol L⁻¹ in the microcosm containing 15mM lactate after second injection of fresh *Shewanella* cells. These observations established and further confirmed the result obtained with kaolin where bioreduction resumes when fresh cells were added after cessation was observed in microcosms added with 0.5mM but progresses slowly with no rapid resumption in microcosms amended with high concentration (5, 10 15 and 20mM) of lactate even after re-inoculated with fresh *Shewanella* cells.

The results obtained also suggests that the cessation of Fe(III) bioreduction observed in microcosms added with 1mM lactate may not be due to exhaustion of bioavailable Fe(III) in the silica sand but to changes in the cell physiology or alteration in the solution chemistry. The cessation may also be attributed to the inhibition effect of sorption or surface precipitation of Fe(II) on the cell surface, and hence was the reason behind resumption of bioreduction after injection of fresh cells. (Jaisi et al., 2007b).



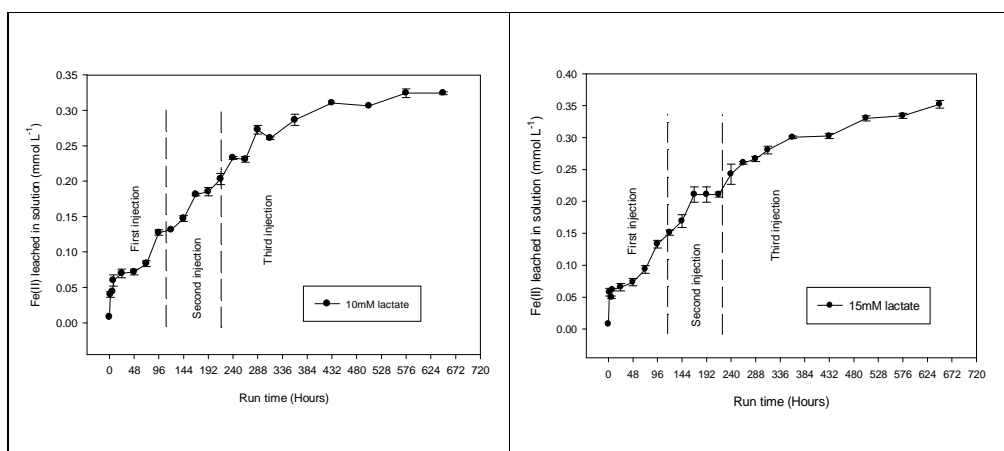


Figure 5.74: Individual plots for the bioreduction of Silica Sand 3 under different concentration of electron donor (1 – 15mM lactate) showing different inoculations time of *S. putrefaciens* CIP8040 at 30°C. Error bars represent standard error for three replicates.

In addition the steady and slow bioreduction observed in the microcosms with high concentrations of lactate suggests that, possibly at high cell concentration number the bacteria were able to initially reduce greater part of the Fe(III) in the silica sand within the initial hours, making the bioavailable Fe(III) very limited. Furthermore the results led to the observation and assumption that in the presence of more excess electron donor the *Shewanella* cells can remain partially active and can kinetically drive the reaction after the initial rapid Fe(III) reduction, than in the presence of low concentration of electron donor the reason why cessation was not observed in microcosms added with high concentration of lactate but only in those with low concentration of lactate. In general, this experiment also indicated that multiple inoculation increases the total extent of bioreduction when compared to results obtained with a single inoculation.

54.3.4: Rate order reaction kinetics

The effect of high lactate concentration on the initial rate of Fe(III) reduction in silica was investigated (Figure 54.6 and Figure 54.7). Increase in the The reduction rate was observed to simultaneously increase in all the different lactate concentrations with no apparent variation in the rate of Fe(II) production. This suggests that at high concentration, lactate does not significantly affect the rate of Fe(III) reduction when compared to what was observed with in kaolin when in the presence of low concentration, was used and It therefore follows a zero order rate law. The kinetics were investigated using first order

Comment [DM31]: Is this correct?

Comment [DM32]: Did kaolin show this as well?

rate law where increase in the rate is proportional to concentration of reactant and is given by:

$$r = d[\text{Fe(II)}]/dt = -k[\text{Fe(II)}] \text{ -----Eqn (54.1)}$$

~~But in the~~ In Zero order kinetics, the rate of reaction is independent ~~of~~ the concentration of the reactant and therefore increases in the concentration of the reactant or one of the reacting species will not affect or increase the reaction rate, which ~~and~~ is given by:

$$r = d[\text{Fe(II)}]/dt = -k \text{ -----Eqn (54.2)}$$

Comment [DM33]: Ho do these two equations differ? Explain

These two equations differ because in first order rate law the rate of reaction is proportional to the concentration of reactant, and the concentrations of the reactants are raised to their first power. This shows that the rate of Fe(II) production is proportional to the concentration of reacting species present (lactate and Fe(III)oxide). The plot of the logarithm of [Fe(II)] versus time is a straight line with $k = -\text{slope of the line}$. However, the rate in zero order is independent of the concentration of the reacting species and the rate of reaction remains constant and never change. The plot of [Fe(II)] versus time is a straight line with $k = -\text{slope of the line}$.

To further show s that increase in concentration has no effect on the rate of reaction and possibly obeys zero order kinetics, a semi-log plot of Fe(II) concentration against time was plotted. ~~A~~ plot of natural log of Fe(II) against time was analysed and a straight line curve with negative slop was obtained with respect to individual lactate concentration with a good linear correlation trend (Figure 54.8). The good linear trend (with $r^2 = 0.87, 0.93$ and 0.93 in lactate concentration of 5, 10 and 15Mm respectively) shows ~~that individual~~ lactate concentration controls the rate of accumulation of Fe(II) production. No line was fitted in the microcosms added with 1mM lactate because of the change in Fe(II) on second injection of cell suspension. But increasing the concentration from 1mM to 5mM and to 15mM does not increase the rate and therefore follows a zero order reaction rate as described in equation 4.2.

Comment [DM34]: This doesn't make sense

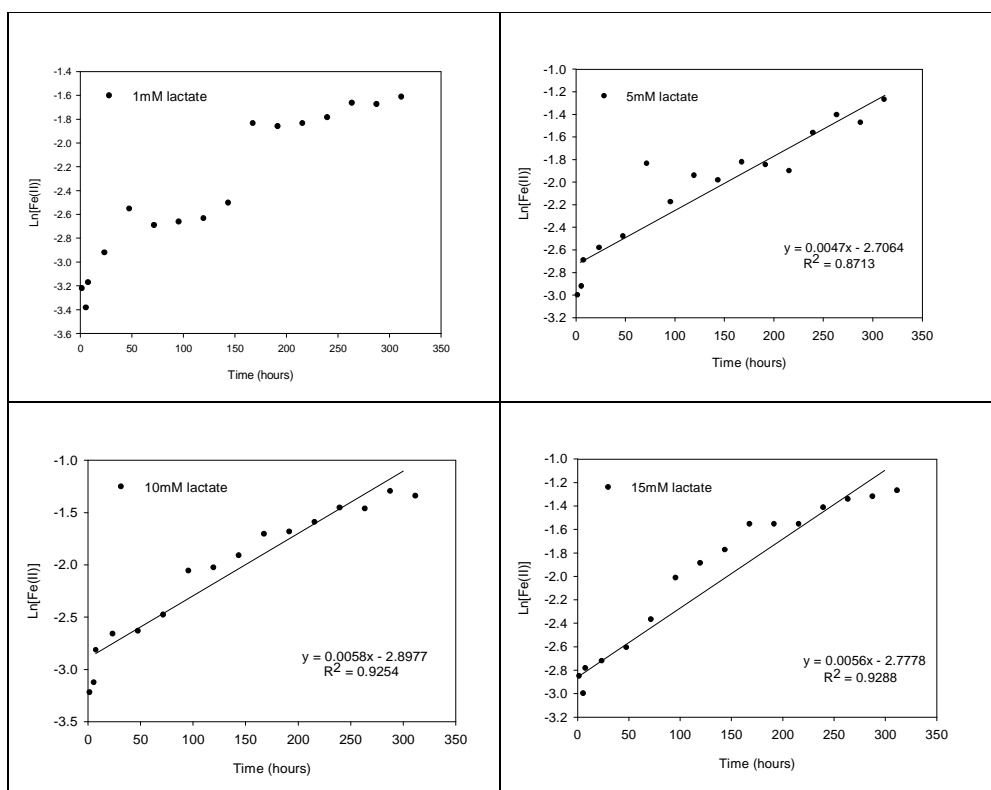


Figure 5.84: Semi-log plot of Fe(III) concentration against time for different concentration of lactate (1 – 15mM) predicting reaction kinetic order of Fe(II) production in silica sand. Equations and coefficient of regression (r^2) values determined from linear regression analysis are given for each lactate concentration.

54.3.5: Integrated rate order kinetics

For a first order kinetics, a plot of rates against concentration should yield a straight line curve with a negative slope. Therefore an integrated rate law was used to further investigate the reaction order where rate of Fe(II) production was plotted against the different concentration from (Figure 54.8). The results obtained shows a very weak correlation between rate and different concentrations with $r^2 = 0.42$ and 0.31 after the first 2 and 6 hours of the start of reaction. It was evidently observed that increasing lactate concentration in the system has no effect on rate of Fe(II) production (Figure 54.9). Therefore the rate observed may possibly depend on the concentration of lactate to some extent and appeared to shift to zero order with time. It was therefore assumed that equilibrium may have been reached at a concentration lower than 1mM lactate where the reaction no longer proceeds due to the exhaustion of one of the reacting species. Although

this could not be concluded because more replicate data point will be needed to help for proper interpretation of the result.

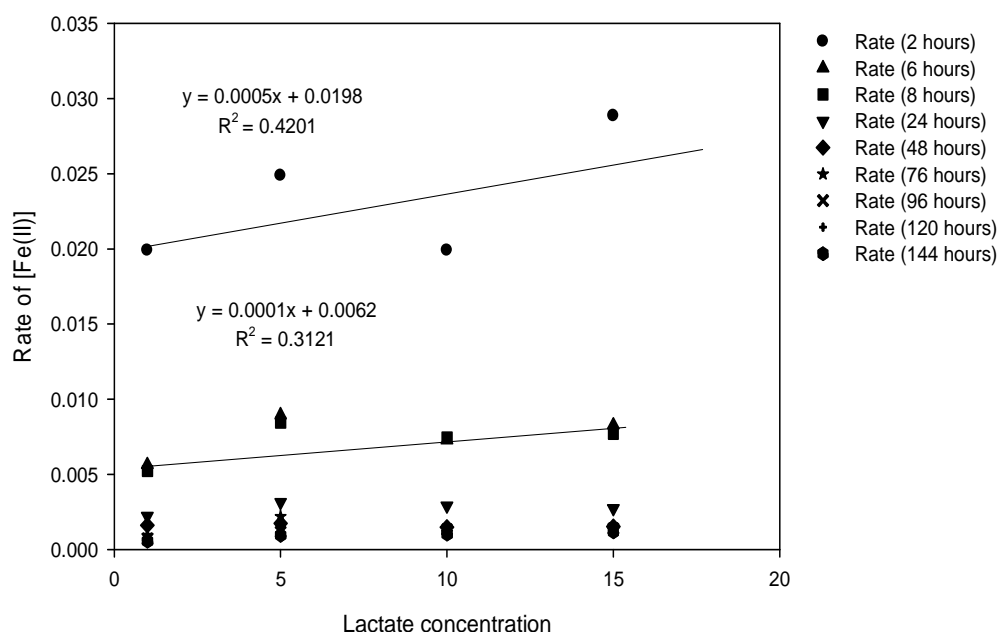


Figure 5.94: Plot of rate of reduction overtime against concentrations of lactate (1 – 15mM) showing zero order rate of Fe(II) production. Equations and coefficient of regression (r^2) values determined from linear regression analysis are given for 2 and 6 hour.

54.4: EFFECT OF BIOREDUCTION ON THE MINERALOGY OF SILICA SAND

Mineralogical analyses were carried out using XRD, FTIR, SEM-EDX and Mossbauer Mössbauer spectroscopy to observe any biogenic alteration of kaolin after bioreduction. However, the mineral yielded a more defined XRD pattern with all peaks clearly resolved. The XRD pattern shows that the silica mineral-sand is composed mainly of quartz with traces of kaolinite and feldspar (Figure 54.10). The XRD pattern of biotreated silica sand was almost identical to that ofwith untreated kaolin-silica sand after 15 days biotreatment with *Shewanella putrefaciens* CIP8040. This shows that the bioleaching of silica sand does not produce significant amounts of crystalline bi-products during bioreduction-process. But decrease in the intensity of kaolinite mineral was evident after bioreduction which may be attributed to bacterial dissolution of the kaolinite phase in the mineral.

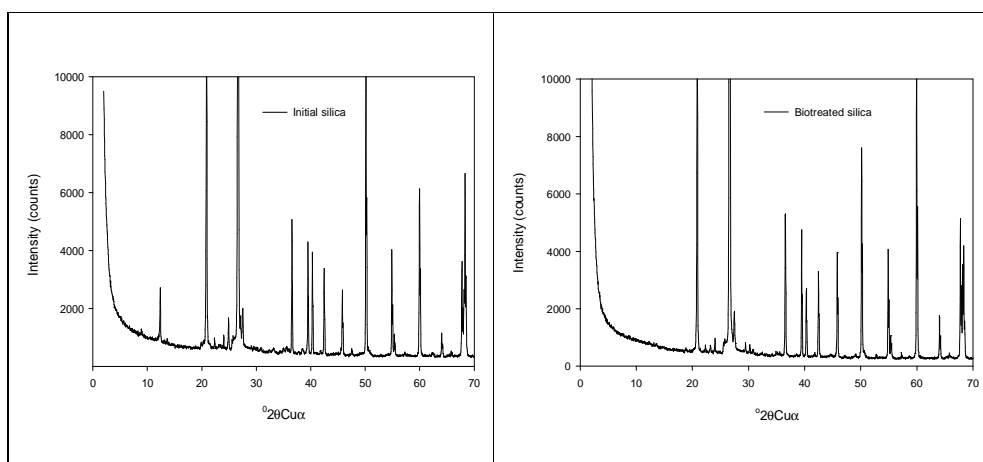


Figure 5.104: XRD pattern of silica sand 3 before and after bioreduction with *S. putrefaciens* CIP8040 at 30°C.

FTIR was used mainly within the ~~mid-MID~~ infrared region ($4000 - 400\text{cm}^{-1}$) to characterise the silica mineral. The spectra obtained show several sharp bands between 400cm^{-1} and 1200cm^{-1} which are a characteristic of silica minerals. No distinguishing differences were observed between biotreated and blank samples. However, the spectrum observed at approximately 460 , 800 and 1080cm^{-1} generally corresponds to quartz SiO_2 . The presence of surface silanol Si-OH groups, which characterise the quartz surface, are clearly resolved and identified by their spectral signature at a region between 3500 and 3700cm^{-1} in both acid washed and non- acid washed initial samples but were observed to decrease in intensity after bioreduction as well as in the blank microcosm (Figure 5.4.11). The wavenumbers of these two representative strong absorption bands of the silanol Si-OH group appeared at 3620 and 3695cm^{-1} .

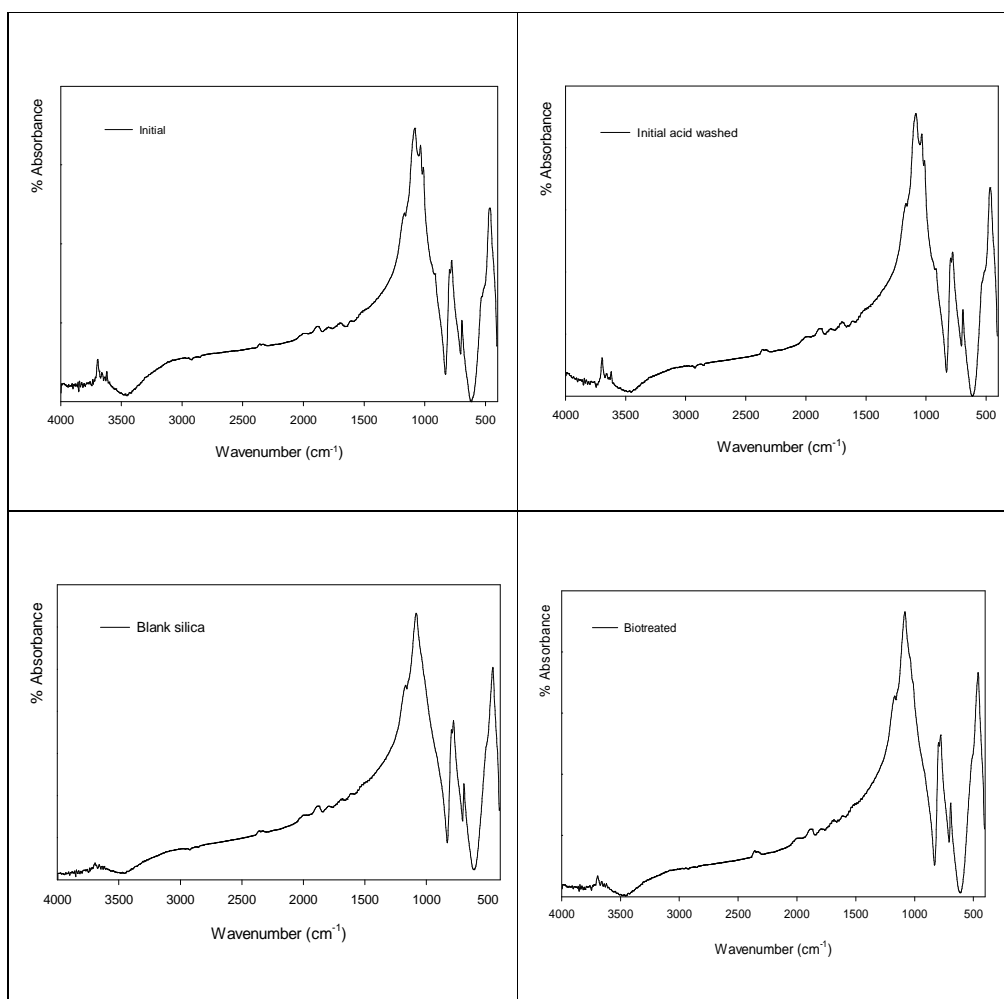


Figure 5.114: FTIR spectra of silica sand 3 after biotreatment with *S. putrefaciens* CIP8040 at 30°C.

The mineral-silica sand is mainly composed of quartz constituent due to the band observed at 800cm^{-1} and 781cm^{-1} . These doublet bands are generally useful for quartz characterisation, and an important feature that distinguishes it from other silica minerals such as tridymite and cristobalite (Russell and Fraser, 1996). The strong broad absorption bands observed at approximately $1090 - 1080\text{cm}^{-1}$ was attributed to asymmetric vibration of Si-O-Si while the absorption bands around 800cm^{-1} is associated with symmetric Si-O-Si stretching (Figure 54.12). A broad absorption band from 600 to 400cm^{-1} observed suggests a wide dispersal of vibrational states which is characteristic of an amorphous network (Popa et al., 2010).

Formatted: Font: 12 pt, Superscript

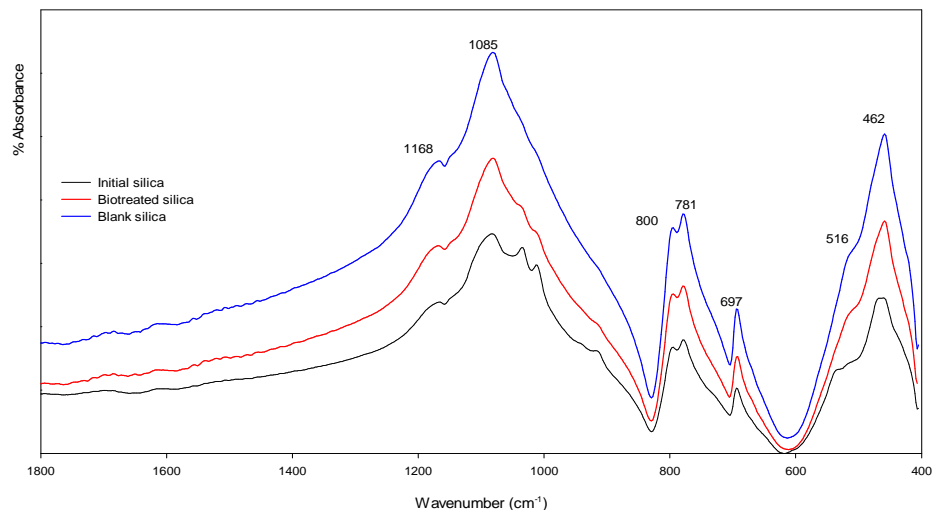


Figure 5.124: FTIR spectra of initial, blank and biotreated silica sand 3 using *S. putrefaciens* CIP8040 at 30°C.

Formatted: Font: 12 pt, Italic

The scanning electron micrograph of Silica sand 3 reveals that the quartz grains are angular to semi-rounded with smooth and weathered surfaces. The SEM micrographs observed before bioreduction with *S. putrefaciens* CIP8040 have shown some small particles partially covering the surface of the untreated quartz (Figure 5.13). But these particles are not seen after biotreatment suggesting that the particles covering the individual quartz grain are being removed by the bioleaching procedure (Figure 5.14).

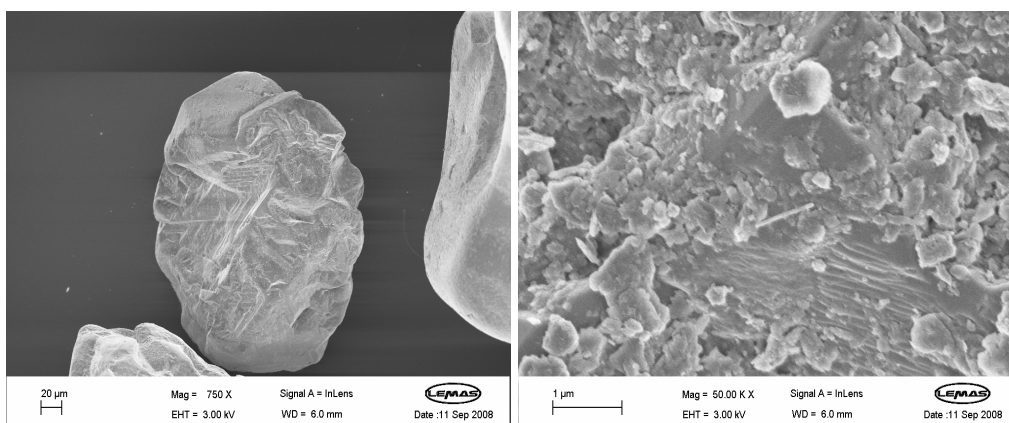


Figure 5.134: Scanning electron micrographs showing the morphology of silica sand 3 before bioreduction.

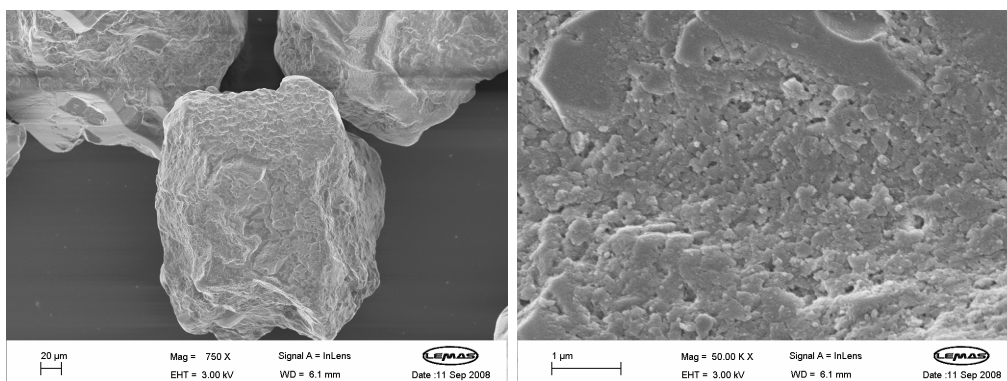


Figure 5.144: Scanning electron micrographs showing the morphology of S-silica Ssand 3 after bioreduction with S. putrefaciens CIP8040 at 30°C.

Formatted: Font: 12 pt, Italic

Like in kaolin, ~~T~~the SEM facility was used ~~here was also equipped with EDX (energy dispersive X-ray spectroscopy) capability for semi-quantitative elemental analysis~~ of the silica sand mineral. The elemental composition of both blank and biotreated samples are shown on Table 54.1 and Table 54.2. The analysis generally shows that the mineral is rich in silica; no other species were detected. ~~oxide with around 99.55% atomic composition.~~ However, ~~th~~Thee EDX analyses taken at the surface of the grains in the untreated sand gives a %Fe value of 0.45% but the % Fe at the surface of quartz grain in the biotreated sample was ~~not detected~~below detection. It was assumed that vast majority of the iron on the surface of the quartz ~~z~~s grains was bioleached, ~~and possibly t~~The remaining Fe on the mineral surface ~~isare~~ below the detection limit of the equipment, ~~or are-is~~ completely bioleached.

Table 5.14: Elemental composition of blank silica sand using EDX analysis

Element	Weight percent	Atomic percent
O	59.	72
Si	39.	27
Fe	1	0.5
Total	99	

Comment [DM35]: We need to discuss these tables

Table 5.24: Elemental composition of biotreated silica sand using EDX analysis

Element	Weight percent	Atomic percent
O	58	70
Si	41	29

Total	99
-------	----

Only untreated Ssand 3 was analysed using Mossbauer—Mössbauer spectroscopy in transmission mode because the sample was freshly received and prioritised by the industrial patters—arepartners—more interested in getting result from this mineral. However the result reveals only one doublet and singulet. The doublet has an isomer shift of $\delta = 0.18\text{mm/s}$ and a quadrupole split of $\Delta = 0.34\text{mm/s}$ with a relative abundance of 77.5% corresponding to Fe^{3+} in tetrahedral sites. The singulet has an isomer shift of $\delta = 0.3\text{mm/s}$ with a quadrupole split of $\Delta = 0\text{mm/s}$ having a relative abundance of 22.5% corresponding to Fe^{3+} in a nanophase (Figure 54.15). Assignment of this Fe^{2+} and Fe^{3+} state of iron phases was also reported by (Zegeye et al., 2007) in their work on microbial bioreduction of biogenic hydroxysulfate green rust (GR) using sulfate reducing bacteria. In their work, the starting material before bioreduction exhibit doublet D_1 and D_2 assigned to Fe^{2+} and Fe^{3+} respectively in GR and the doublet D_L assigned to paramagnetic Fe^{3+} in lepidocrocite.

Comment [DM36]: Can you give a reference in support of this observation?

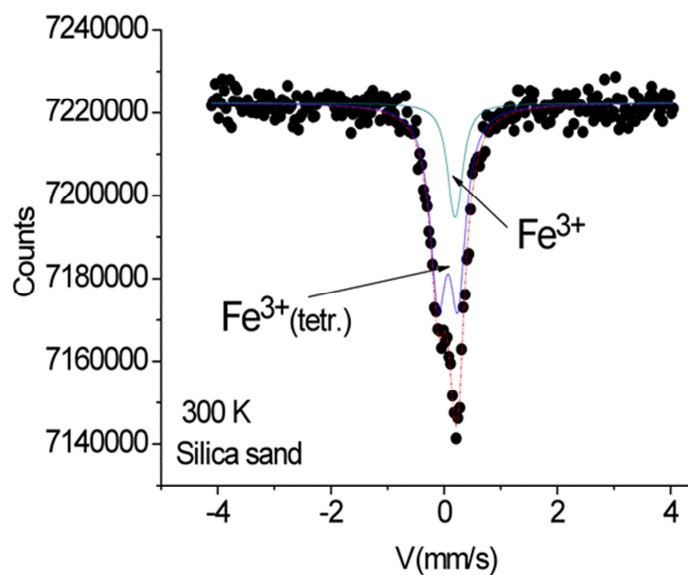


Figure 5.154: Mössbauer spectra of un-treated Ssand 3 in transmission mode.

54.5: DISCUSSION

Bioreduction in silica sand ~~and mineral~~ was tested with Fe(III)-reducing *Shewanella* species in the presence of lactate as the sole electron donor in the system and AQD serving as electron shuttling compound under non-growth ~~conditions using approach in~~ the same approach ~~to what was reported for in kaolin in Chapter 3~~. ~~Although the genus Shewanella isare severally~~ reported to consist of phylogenetically diverse groups of facultative anaerobes capable of reducing various ~~range of~~ electron acceptor ~~(metals)~~ through anaerobic respiration, ~~and~~ coupling this reduction to the oxidation of ~~several~~ organic acids in a dissimilatory manner (O'Loughlin et al., 2007; Lloyd, 2003; Nealson et al., 2002; Lovley et al., 1998). In this chapter therefore, potential for dissimilatory Fe(III) reduction in silica sand has been investigated using ~~series of~~ different *Shewanella* species.

All the *Shewanella* species examined here have been able to anaerobically respire and reduce Fe(III) within the silica sand, ~~thereby~~ coupling this reduction to the oxidation of lactate with the exception of *S. loihica* ~~such as observed with kaolin~~. Furthermore, *S. oneidensis* and *S. putrefaciens* CIP8040 results in similar rate and extent of Fe(III) reduction but variation in the extent of Fe(III) was evident with substantial reduction of Fe(III) using *S. algae* BrY. The strains *S. algae*, *S. Oneidensis* and *S. putrefaciens* CIP8040 have been reported to utilise lactate as the typical electron donor for anaerobic respiration of solid electron acceptors (Rosenbaum et al., 2011; Anton and Terry, 2007; Konishi et al., 2007). In our system *S. loihica* was not effective in coupling lactate oxidation to Fe(III) reduction in silica sand. ~~Although studies of~~ bioreduction of lepidocrocite and iron-monosulfide production show that *S. loihica* utilizes electron donors such as lactate and formate for anaerobic respiration (Nakamura et al., 2010; O'Loughlin et al., 2007). Therefore, the observed lack of Fe(II) production by *S. loihica* was likely not constrained by the carbon source (lactate), pH (7.1 – 7.5) or temperature (25 – 30°C) ~~of experimental conditions~~

employed in our system, as these parameters were within the reported- tolerable limits of this microorganism, suggesting that other limiting factors might be responsible.

Cell density was seen to effectively influence the bioleaching process, because substantial increases in the rate and extent of Fe(III) reduction ~~were~~ achieved in the presence of high numbers of cells (7ml cell suspension) within the period of bioleaching, ~~compared with and better than~~ when half of the cell number (3.5ml cell suspension) was used for the same mass of silica sand in the presence of the same concentration of electron shuttling compound. This was also supported by the observed in work on ferrihydrite reduction using *Geobacter sulfurreducens* where increase in biomass load was understood to substantially influence the rate and extent of bioreduction (MacDonald et al., 2011). Similarly, it further confirms the results obtained for kaolin (Chapter 3), section and work conducted by O'Loughlin, (2008) where increase in cell number improves the rate and extent of bioreduction. It is therefore clear that high bacterial cell suspension is required for an effective bioleaching of silica sand.

Anthraquinone-2, 6-disulphonate (AQDS) ~~was~~ known to enhance electron delivery to various oxides in many minerals (Jaisi et al., 2007b; Lovley et al., 1998), However, addition of AQDS in the presence of low *Shewanella* cells suspension was generally found to have no significant effect on the rate and extent of reduction when compared with the experiments that has not been added without AQDS. ~~It~~ Although it was observed that the presence of high numbers of cells substantially influences the initial rate of Fe(III) reduction. ~~In, however we assumed that in~~ the presence of fewer cells, the bioreduction process progresses slowly even when AQDS was added, ~~to promote electron delivery in the system. Hence these~~ steady and slow progression in Fe(II) production over time could results into and promote precipitation of ferrous minerals such as ~~like~~ siderite (FeCO_3) which may possibly inhibit the rate and extent of Fe(III) bioreduction. These ~~observation conclusions~~ was in agreement are supported by with the experiment work conducted on the role of biomass and electron shuttle for ferrihydrite reduction kinetics (MacDonald et al., 2011).

Furthermore, because silica sand is less permeable than kaolin mineral, ~~there may be limitations on~~ electron delivery ~~may have some limitation~~ in the molecule cycle between

Formatted: Font: 12 pt, Subscript

AQDS and AH₂QDS which could influence the initial rate and extent of Fe(III) reduction. ~~suggesting that the~~ The rate of transfer of AH₂QDS to silica sand may be slower and less than the rate of transfer of electrons from lactate to AQDS especially with the presence of few cells. Moreover, we also assume that the electron shuttle (AQDS) may have less or no effect on the bioleaching process, but *Shewanella* cells actively promote electron shuttling by direct contact or alternatively by other enzymatic reduction pathways because *Shewanella* ~~has been~~ were proposed to have potential for direct electron transfer to insoluble Fe(III) oxides (Cutting et al., 2009; Lloyd, 2003). This could support the reason as to why the presence of high cell concentrations greatly influences the initial rate and extent of Fe(III) reduction in the system ~~than in the presence of fewer *Shewanella* cell suspension.~~ Experiments comparing the effect of biomass addition ~~on~~ for Fe(III) reduction in the presence of AQDS or NOM 2 using different cell densities further reveal that a combination of AQDS with high biomass of *Shewanella* cells (7ml cell suspension) greatly influences and improves the rate of bioreduction. However, replacing AQDS with NOM 2 only affects the extent but has less impact on the initial rate of reduction in the presence of high cell number. ~~A, but~~ similar pattern in bioreduction rate and extent was observed for both AQDS and NOM 2 when a low concentration (3.5ml suspension) of *Shewanella* cells was employed.

This chapter also investigates the influence of electron shuttling potential of AQDS, NOM 1, and NOM 2 ~~and without electron shuttle~~ on bioreduction process. As mentioned in Chapter 3, kaolin section AQDS and natural organic matter are ~~severally~~ demonstrated to enhance and mediate microbial respiration and electron delivery to many Fe(III) oxides (Royer et al., 2002; Zachara et al., 1998). The results obtained for silica sand shows that all ~~the~~ three different electron shuttles ~~employed here~~ have similar effects on the bioreduction process and gave no difference to ~~including the~~ treatments that ~~was not added with any~~ lacked an electron shuttle. ~~Hence, this further reassert the suggestion~~ confirms that the bioreduction observed was mainly from the direct reduction activities of the *Shewanella* cells present in the system because all the different microcosms were added with same biomass concentration (4ml cell suspension).

In this research, varying lactate concentration influences the total extent of Fe(III) reduction. Similarly, a faster rate of reduction was initially observed in all the different amendments, ~~as like~~ seen in experiments with kaolin ~~material~~. Although lactate consumption is accompanied by microbial reduction of Fe(III) to Fe(II), ~~but~~ the pattern of accumulation of Fe(II) follows ~~a~~ zero order reaction kinetics with respect to ~~de~~crease in lactate concentration. However, Fe(III) reduction ceases after the first 48hr of incubation particularly in experiments ~~experiment added~~ with low concentration of lactate (1mM lactate), but continuously progresses at slower rate in ~~those~~ experiments containing high concentration of lactate (5, 10, 15mM lactate). The slow progression and cessation of Fe(III) reduction after the ~~first~~ initial injection of the cell suspension may partly be attributed to possible decline in cell viability or may be related to Fe(II) adsorption on cell surfaces, but is not limited by lactate concentration. Generally, Fe(II) sorption decreases cell activities and viability in a way that could limit the rate and extent of Fe(III) reduction (Urrutia et al., 1998). Similarly saturation on the surface of Fe(III) mineral with Fe(II) has been demonstrated in batch experiments as a dominant factor that promotes cessation of Fe(III) reduction by several iron-reducing bacteria ~~in batch experiments~~ (Roden and Zachara, 1996).

~~W~~Subsequently, when fresh cells were added after initial cessation, further bioreduction of Fe(III) in silica sand resumes immediately, most apparently in cultures containing low concentration of lactate (5mM lactate). Bioreduction ~~but~~ continues to ~~linearly~~ progresses linearly in cultures containing high concentration of lactate without a noticeable lag period. This result is consistent with previous investigations confirming that addition or multiple inoculation of fresh metabolically active cells results into resumption of Fe(III) bioreduction (Jaisi et al., 2007b; Urrutia et al., 1998).

~~Possible explanations for resumption of Fe(III) bioreduction are that, bioreducible Fe(III) surface sites were available but the initial cells were unable to have access to them due to Fe(II) sorption on their surface as well as occlusion by Fe(II) precipitates, or Fe(II) being transferred from Fe oxide surface to a clean cell surface thus revealing free oxide surface for further bioreduction (Urrutia et al., 1998).~~

Assessment of the mineralogy after bioreduction confirms a clear XRD pattern of typical crystalline quartz as the major mineral with some traces of kaolinite. According to the XRD

Comment [DM37]: This is an awkward sentence – rethink what you want to say.

pattern obtained the characteristic quartz peaks remain the same after biotreatment showing no significant changes in the mineral composition between biotreated and untreated silica sand, even though Fe(II) ~~is~~are measured in the solution. This shows that the crystallinity of quartz was not affected by the bioleaching process, and ~~hence~~ no other crystalline bi-products are evident. FTIR ~~spectra~~ obtained from mid-infrared region clearly display bands that ~~generally characterise the mineral to compose of mainly quartz sand~~confirm the predominance of quartz. The band displayed at 3500 and 3700cm⁻¹ which characterise the quartz surface are more intense in the initial untreated samples compared to biotreated ~~samples~~ and a blank sample that was not ~~added-treated~~ with cells. SEM observation reveals on the untreated silica particle surface some fine sub-particles of irregular shapes and sizes. Disappearance of these particles ~~covering the untreated quartz samples~~was evident after biotreatment with *Shewanella putrefaciens* CIP8040 suggesting bioreduction and transformation of surface Fe-oxides after bioreduction. The surface EDX analysis of quartz grains also confirms changes in bulk mineralogical composition with %Fe content decreasing or simply decreased ~~beyond~~below detection limit of the analytical technique after bioreduction ~~with Shewanella cells~~. Mössbauer spectroscopy on the untreated silica sand ~~as reveal by Mossbauer spectroscopy~~confirms the presence of ~~the~~ Fe³⁺ doublet ~~to be~~corresponding to a dominant iron phase having the relative abundance of 77.5%, and the remaining percentage constituted mainly of Fe³⁺ ~~in their~~ nanophases. This indicates that the silica mineral contains readily bioavailable iron phases ~~es amenablee~~ for bacterial reduction.

~~Conclusively~~In conclusion, this section demonstrates that some selected strains of iron-reducing *Shewanella* are capable of coupling lactate oxidation to the reduction of Fe(III) in silica sand. In addition, high concentrations of biomass ~~are in~~ necessary for effective bioleaching as ~~the~~ presence of AQDS does not have a major impact, especially in the presence of low concentrations of cell suspension. ~~This~~ suggests ~~ing~~ direct Fe(III) bioreduction by *Shewanella* cells. Bioleaching appears to have some impact on the surface of quartz grains with %Fe drastically decrease as confirmed by EDX ~~and apparent removal of surface oxide coatings~~.

CHAPTER 6 5: BIOLEACHING OF KAOLIN AND SILICA SAND USING 4.5L BATCH BIOREACTOR

65.1: INTRODUCTION

The quality and commercial value of kaolin and silica sand were shown to largely depend on their purity, texture and colour properties. The removal on a commercial scale of mineral impurities and iron oxide coating individual grains, which in effect lowers the colour index, requires complex procedures (Styriaková et al., 2010; Chandrasekhar and Ramaswamy,

Comment [DM38]: Is this right?

2002; Psyrillos et al., 1999; Prasad et al., 1991). Leaching of iron impurities by microbial actions could possibly offer an alternative to the conventional chemical processes when fully ~~harnessed-developed~~ (Lee et al., 2002). Microbial activities under anoxic conditions has ~~severally~~ been demonstrated to catalyse ferric iron (Fe^{3+}) reduction in clay minerals such as kaolin, and in other iron-bearing bulk minerals. This results ~~into~~ increased solubility of iron as ferrous iron (Fe^{2+}) and subsequently ~~leadsing~~ to removal of iron-oxides and oxyhydroxides from the mineral materials (Mockovciaková et al., 2008; O'Reilly et al., 2006; Lee et al., 2002).

Bacterial refinement of iron-bearing clay minerals using iron-reducing bacteria has never been applied at a pilot or full scale. ~~Until now, Because,~~ studies on microbial Fe(III) reduction were mostly conducted ~~ast~~ small scale laboratory work. The small scale laboratory work previously conducted gave promising results for the possible commercial bioleaching of kaolin. For successful commercial exploitation of small scale laboratory processes, ~~the need for~~ process optimisation ~~iwas~~ necessary to attain ~~an~~ effective full scale approach. Although the processing time scales observed at small scale were relatively long compared to conventional chemical leaching ~~thebut~~ improvement in the mineral quality is appreciable. ~~For e~~Example, studies carried out by Lee et al., (2002) successfully removed iron impurities in lower grade kaolin from 5.1 to around 3.7wt% Fe_2O_3 even though the bioleaching was conducted using unidentified indigenous microorganisms in the presence of maltose as a carbon source. Likewise, the microcosms study ~~conducted in our present research reported earlier in this thesis~~ demonstrated a promising outcome. It shows that iron-reducing microorganisms can be used to leach iron-oxides and oxyhydroxides from bulk ~~mineral~~ raw materials and the rate could be optimised when adequate and appropriate electron donor, biomass concentration, temperature and solid to liquid ratio are ~~asu~~plied.

This chapter presents work designed to up-scale bioleaching of kaolin and silica sand using 4.5L batch bioreactor experiments. ~~The section highlightedIt describes~~ experiments ~~conducted by supplementing the earlier optimaldesigned on the basis of results from the small scale microcosm study that identified~~ conditions ~~identified thate~~ effectively influenced Fe(III) reduction ~~during small scale microcosms study. Preliminary investigationPilot experiments using batch reactors were~~ conducted using kaolin and silica sand to assess how effectively the reactors ~~performedwork~~ prior to commencement of the main experiment

~~was reported~~. Optimal growth temperature, pH and redox potential were monitored continuously for changes in the solution chemistry ~~are documented~~. The chapter also assesses the reliability and reproducibility of the ColourTouch analyser used to measure colour improvement.

6.2: METHODOLOGY

~~BA~~ batch bioreactor experiments were conducted using kaolin and silica sand for the up-scaling of small microcosms experiments with continuous monitoring of pH, Eh and temperature ~~of~~ the system. The Fe(III) in kaolin and silica sand serves as the sole electron acceptor and lactate as the electron donor in the presence of a pure culture of *Shewanella putrefaciens* CIP8040. The experiments ~~were~~ monitored in a controlled temperature room held at 30°C. Anthraquinone-2,6-disulfonate was used to enhance electron shuttling in the system. As described in sub-section 2.5.7 of Chapter 2, ~~t~~ the reduction of Fe(III) from kaolin was measured ~~(as described in sub-section 2.5.7 of material and method)~~ as the production of Fe(II) in HCl extracts using modified pPhenanthroline techniques (Fadrus and Maly, 1975). Absorbance was measured using UV-vis-spectrophotometry at 510nm. Solid samples were examined using a Stereoscan S40 Scanning Electron Microscope (housed in the Electron Microscopy Unit of the Medical School at Newcastle University) at an accelerating voltage of 8kV and around 6mm working distance.

Comment [DM39]: Check the accelerating voltage.

~~Assessment of~~ improvement in mineral quality after bioleaching was also ~~assess~~ conducted. Both initial and bioleached kaolin and silica sand bulk minerals were analysed for colour properties (L*, a*, b*, ISO Brightness, Whiteness and Yellowness) using a Technidyne ColorTouch PC Spectrophotometer after mild acid washing with 2M HCl. To observe changes in the mineralogy after bioleaching, X-ray (powder) diffraction measurements were obtained ~~using~~ with a Philips X'pert PRO XRD system from 2° to 70° 2θCuKα, at 0.0334° 2θ per step and 99.70 seconds per step. Similarly, FTIR analyses of bioleached and initial minerals were measured and obtained in transmission mode using KBr pressed pellets (1-2mg mineral in 200mg KBr) in the mid-infrared range (400 – 4000cm⁻¹) on an AVATAR 360 FTIR ESP spectrometer. Determination of chemical composition of kaolin, expressed

as different oxides, was determined by Imerys Ltd conducted using a Pananalytical Magic Pro XRF spectrometer equipped with a PW2540VRC automatic sample changer.

6.3: RESULTS

6.3.1: Preliminary investigation and optimisation

6.3.1.1: ColourTouch analyser: Reliability and reproducibility

Preliminary investigation to assess the reliability and reproducibility of the ColourTouch analyser used in measuring colour properties was tested. Certified standard reference paper (Paper calibration kit N12415: for 90, 70 and 60 standard) provided by the suppliers should conform to the standard values in Table 5.1 after every calibration.

Comment [DM40]: Is it ColorTouch or ColourTouch?

Table 6.15: Certified standard reference values for standard 90, 70 and 60 provided by the suppliers.

Sample	L*	a*	b*	%Brightness
90 standard	97.734	0.01	2.10	91.49
70 standard	95.05	-0.48	10.06	76.05
60 standard	84.12	0.89	1.52	63.01

To assess the reliability and reproducibility of the Technidyne ColourTouch, certified standard reference paper (90, 70 and 60 standard) was analysed 5 separate times. Initial and biotreated Kaolin 3 (Melbur Yellow HCP) were analysed 5 times each for colour properties and L*a*b values. Averages from 5 different runs were obtained and standard deviations calculated. The test results (Table 6.2) show a very good agreement between the data obtained from standard reference paper in comparison with standard values provided by the suppliers. For example, % brightness measured by the colour analyser was 91.47% as against the 91.49% provided by the suppliers for the 90 standard reference paper. The difference between different runs was very low, with measured deviation ranging between 0.004 - 0.13% (Table 6.2). For better comparison between the replicate data analysed using ColorTouch analyser with accepted values, the accepted standard values from Table 6.1 are also given in Table 6.2.

Table 6.25: Preliminary assessment on the reliability and reproducibility of the CeolourTouch analyser. The error represents the standard deviation from five replicate analyses.

Accepted	L*	a*	b*	%Brightness	%Whiteness
90 standard	97.73	0.01	2.10	91.49	Not given
70 standard	95.05	-0.48	10.06	76.05	Not given
60 standard	84.12	0.89	1.52	63.01	Not given
Measured					
90 standard	97.73 ±0.008	-0.02 ±0.007	2.09 ±0.027	91.47 ±0.031	84.97 ±0.119
70 standard	95.42 ±0.005	-0.49 ±0.039	9.80 ±0.027	76.61 ±0.034	44.26 ±0.129
60 standard	84.31 ±0.015	0.84 ±0.038	1.33 ±0.010	63.57 ±0.030	58.02 ±0.040
Biotreated	90.96 ±0.020	0.27 ±0.005	7.54 ±0.013	69.91 ±0.055	42.94 ±0.117
Blank	90.43 ±0.004	0.92 ±0.008	9.72 ±0.008	66.39 ±0.015	31.36 ±0.025
Initial	90.89 ±0.008	0.79 ±0.005	9.11 ±0.007	67.98 ±0.024	35.40 ±0.049

Comment [DM41]: Give the accepted values as well, so the reader can compare them. So, combine Tables 1 and 2.

In addition, to further assess the reliability of the colour analyser, a number of standard reference mineral samples were provided by Imerys Ltd., WBB/Sibelco and Omya UK. The brightness, yellowness and L-a-b values obtained show a good agreement with those obtained by the industrial partners. The measured brightness difference ranges from 0.2% to 3.7% and 0.4% to 2.9% for the yellowness. The t-Test results are presented in Appendix 7.1.

Formatted: Font: 12 pt, Not Italic

6.3.1.2: Batch bioreactor experiment: Preliminary assessment

Prior to the batch reactor experiments, a preliminary experiment was conducted at room temperature to understand how best the reactor will perform using Kaolin 3 (Melbur Yellow HCP) and Silica Sand 3 (Oakamoor) in the presence of *Shewanella putrefaciens* CIP8040. In this experiment, around 500g of kaolin and 125g of silica sand were placed in separate reactors and the volume was completed to 4.5L containing a solution of 0.9% NaCl sterilized at 121°C. 10Mm lactate, and 100µm AQDS final concentrations sterilised by filtration (0.2µm pore size Millipore filter) were added in to the reactors. About 120mL ($1.2 \pm 0.4 \times 10^8$ cell mL⁻¹) late log-phase of *Shewanella putrefaciens* CIP8040 was aseptically added in to the reactor. The suspension was continuously stirred at ~40 rpm and flushed with oxygen-free nitrogen to maintain anaerobic conditions. Biotreated slurry suspensions were taken daily

for Fe(II) analysis and the results of these are shown in [Appendix 6.1](#). Some constraints were encountered during the preliminary investigation which include leakage at the reactor cap and high slurry density which affect the stirring process.

65.3.2: Batch bioreactor experiment with [Kaolin 2](#)

A batch bioreactor experiment was set up to up-scale bioleaching of [Kaolin 2](#) ([Remblend](#)) material using *Shewanella putrefaciens* CIP8040 at 30°C. To attain proper stirring and keep [the](#) kaolin slurry in suspension, 300g of kaolin was used, based on [the](#) observations made during [the](#) preliminary investigation. The reactors were then [completed-made up](#) to 4.5L with a solution of 0.9% NaCl, 10mM lactate [in the presence of and](#) 100µM AQDS. During 5 days of biotreatment, it was observed in the bioreactor [added-treated](#) with cell suspension that the Fe(II) removed was 0.27mmol L⁻¹ within the first day, and thereafter increases [ing](#)es to 0.52mmol L⁻¹ at the [termination-end](#) of the experiment (Figure [65.1](#)). Although the amount of Fe(II) leached was less than observed in the microcosms, [but](#) there was good correlation considering that less kaolin [mass](#) was used (300g) [compared with the microcosm experiments instead of](#) (562.5g [would be equivalent to the](#)) [when considering](#) 10g used in microcosm studies, or (1125g) [for in](#) the 20g [microcosms](#)). [Expressing the amount of iron released in the bioreactor to that removed in the microcosm experiment from Kaolin 2 \(Remblend\) in weight% \(Fe/Kg\) gives a very good correlation. In comparison, the amount of iron released in microcosm was 46.6mg of bioavailable Fe\(III\) per 100g of kaolin \(equivalent to 4.4% of the total Fe-bearing impurities initially present in the kaolin\). On the other hand, the amount of iron released during bioreactor experiment from the same Kaolin 2 material \(Remblend\) was 62.6mg of bioavailable Fe\(III\) per 100g of kaolin \(~5.9% of the total Fe-bearing mineral present\) which was even better than the amount of Fe released from microcosm experiments.](#) No evidence of bioleaching was observed in the blank bioreactor, further confirming that the bioleaching observed was mainly as a result of *Shewanella* cells injected into the system.

Comment [DM42]: Remind us what Kaolin 2 is.

Comment [DM43]:

Comment [DM44]: Is it worth calculating the release Fe/kg kaolin so that the microcosm and bioreactors can be compared?

Formatted: Font: 12 pt, Italic

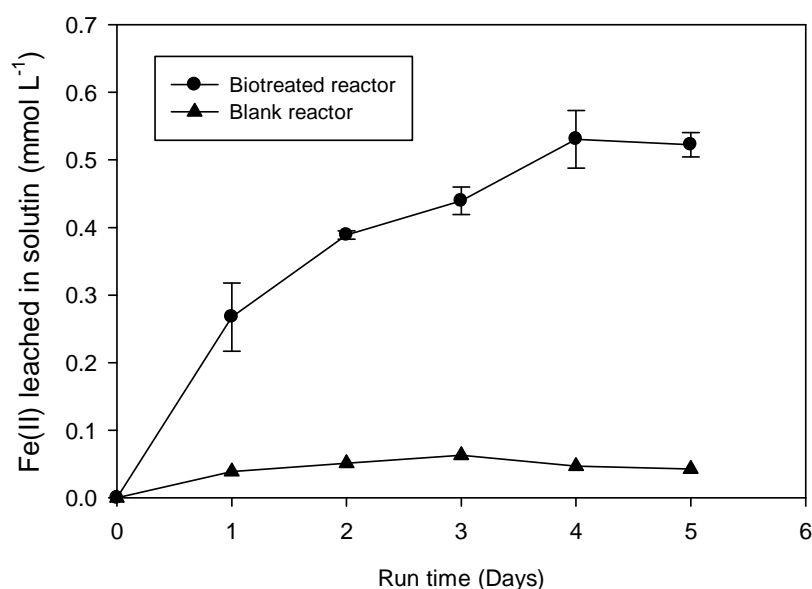


Figure 6.15: Bioleaching of Fe(III) in Kkaolin 2 (Remblend) using in a batch bioreactor experiment as function of time. Error bars represent standard error for two replicates.

To monitor changes in the solution chemistry, pH and the redox potential (Eh) during bioleaching were measured. The medium pH fluctuates between 7.5 to around 8 during in bioreduction and between 6.8 and 7.2 in the blank reactor. The Redox potential (Eh) of the initial solution before addition of *Shewanella* cells was around 400mV to 600mV on the digital display unit. This was observed to decrease to around -150mV and -240mV immediately after *Shewanella* cells were injected, indicating anaerobic environment conditions. Because the redox potential and pH measured using probes are recorded and converted to a voltage, and the data logger transformed the reading to the negative logarithm (Figure 6.5.2).

Formatted: Font: 12 pt, Not Italic

Formatted: Font: 12 pt, Not Italic

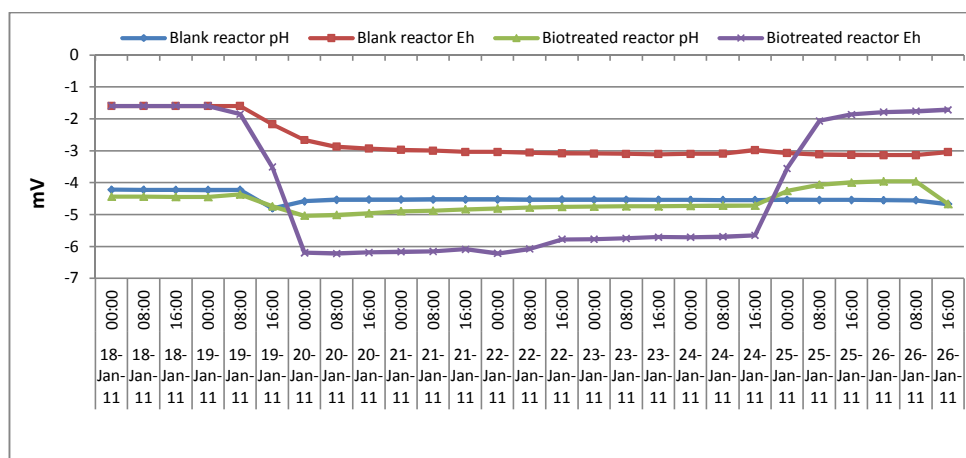


Figure 6.25: Time profile of pH and redox potential (Eh) in biotreated and blank reactor during bioleaching of Kaolin 2 (Remblend) using *Shewanella putrefaciens* CIP8040 from 19/Jan/2011 to 24/Jan/2011.

Comment [DM45]: Mark on this the dates of the start and end of the experiment

The optimum temperature range required for the growth of *Shewanella putrefaciens* CIP8040 as observed in the microcosm experiments was within the range of approximately 30°C. As a result of this and in order to achieve effective bioleaching process, the reactors were kept in a controlled temperature room where the temperature was regulated and controlled between 29 – 31°C throughout the bioleaching period (Figure 6.3).

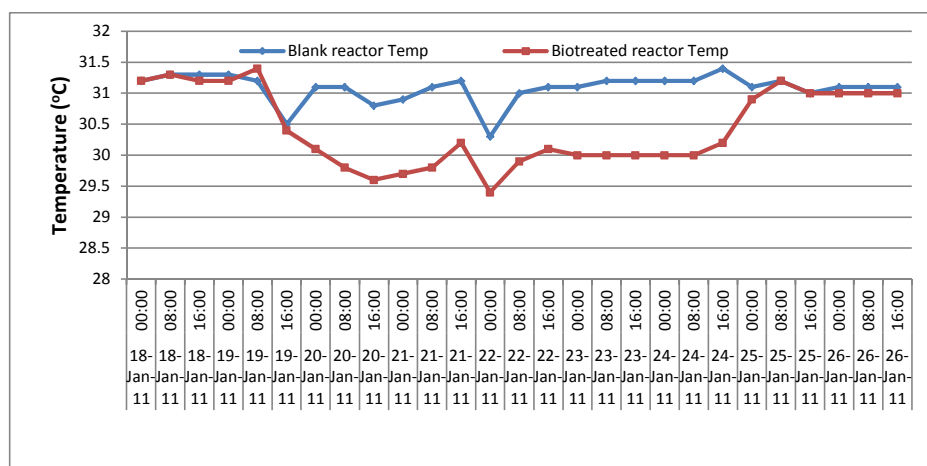


Figure 6.35: Time profile of temperature plot in biotreated and blank reactor during bioleaching of Kaolin 2 (Remblend) using *Shewanella putrefaciens* CIP8040 from 19/Jan/2011 to 24/Jan/2011.

As in the small scale microcosm study, to monitor improvement after biotreatment such as in small scale microcosm study, samples were analysed for colour properties. In the biotreated reactor, ISO brightness improved from 75.79% to 79.06% while the whiteness increased from 55.69% to 66.01%. Increases in the percentage brightness and whiteness were also observed in the blank reactor to around 77.89% and 61.00% respectively when compared with the blank initial sample (Figure 6.4).

Formatted: Font: 12 pt

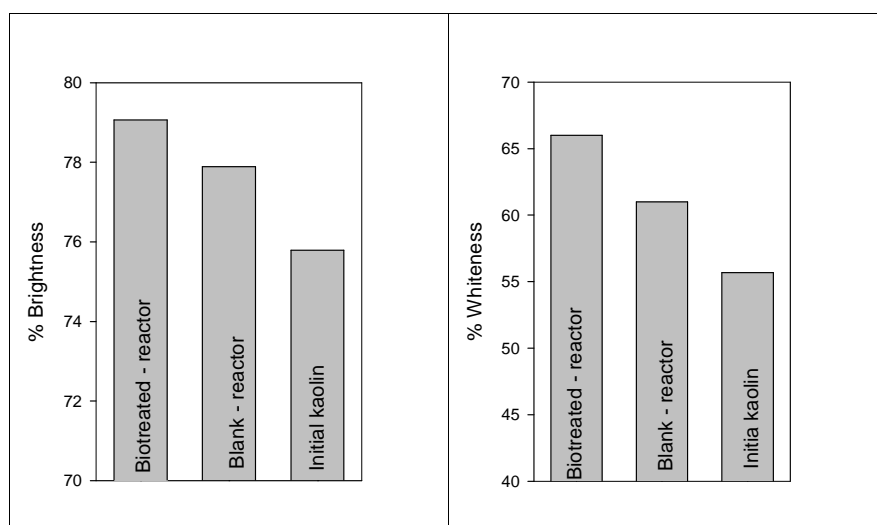


Figure 6.45: Colour analysis of Kaolin 2 (Remblend) before and after bioreduction with *S. putrefaciens* CIP8040 at 30°C.

6.3.3: Batch bioreactor experiment with Kaolin 3

A similar batch bioreactor experiment was conducted with Kaolin 3 (Melbur Yellow HCP) using *Shewanella putrefaciens* CIP8040, thereby extending the bioleaching period to 10 days. However, the biotreated reactor was further re-inoculated with 120ml of fresh *Shewanella putrefaciens* CIP8040 cell suspension on day 5. Prior to cell re-injection, samples were taken for colour analyses to monitor colour improvement on day 5 and after termination of the experiment. A rapid rate of Fe(III) reduction was observed with around 0.71mmol L⁻¹ of Fe(II) measured in the solution on day 1, and increasing to around 0.96mmol L⁻¹ on day 5. After addition of fresh *Shewanella* cell suspension on day 5, resumption of Fe(III) bioreduction was apparently not observed within the period of 10 days (Figure 6.5). The amount of Fe(III) removed was almost similar to what was observed

using the same kaolin material in [the](#) microcosms study, when [the](#) mass of kaolin used was [put taken](#) in-to consideration (as shown in Figure 3.20 of [kaolin chapterChapter 3](#)). The pH, Eh and temperature were monitored and regulated within the requirement of *Shewanella* cells and the results of these are shown in Appendix Z.

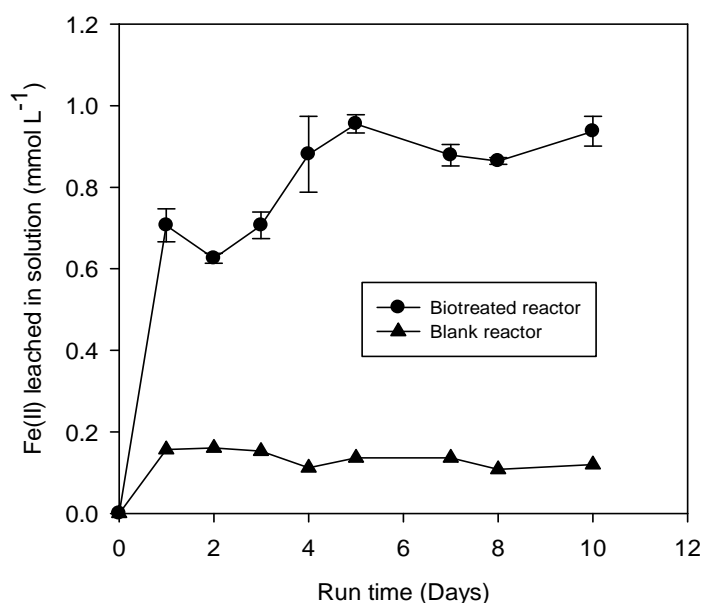


Figure 6.55: Bioleaching of Fe(III) in [Kkaolin 3](#) (Melbur Yellow HCP) [using in a](#) batch bioreactor experiment as function of time. Error bars represent standard error for two replicates.

[Suspension](#) samples were taken and [solids](#) analysed for colour properties on days 5 and 10 to monitor colour changes over time. In [the](#) bioreactor [treataded](#) with *Shewanella* cells, ISO brightness improves from 68.49% to 70.65% while whiteness increases from 37.70% to 43.06% on day 5. In contrast there was a colour decrease in the blank bioreactor below the initial value with whiteness decreased to 32.66% from 37.70%, while ISO brightness decreased to 67.15% from 68.49% on day 5 (Figure 65.6). This decrease in brightness and whiteness below the initial value in the untreated blank was also observed in microcosm study using the same [Kkaolin 3](#) material (Melbur Yellow [HCP](#)).

Comment [DM46]: Excellent!!!!

However, extending the bioleaching period to day 10 after cell re-injection shows an increase in brightness and whiteness in both biotreated and blank reactors even though no

resumption in Fe(II) reduction was apparent in the system. In the biotreated reactor, the ISO brightness further increased to 72.18% on day 10 from 70.65% measured on day 5 and whiteness further increased to 49.62% from 43.06% after day 10. Surprisingly, an increase in whiteness was observed after the initial colour decline below the initial value on day 5 in blank reactor from 32.66% to 41.20% and brightness from 67.15% measured on day 5 to 69.20% on day 10 (Figure 6.6).

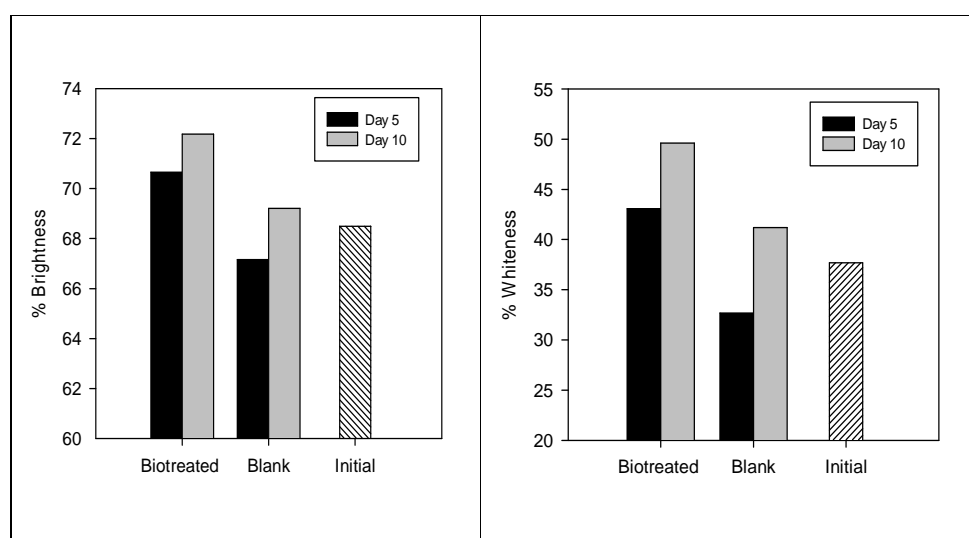


Figure 6.6: Colour analysis of Kaolin 3 (Melbur Yellow HCP) on day 5 and 10 before and after bio-reduction with *S. putrefaciens* CIP8040 at 30°C.

6.3.4: Batch bioreactor experiment with Kaolin 4

A third-round batch bioleaching experiment was conducted with Kaolin 4 (Melbur Yellow MGP) material using *Shewanella putrefaciens* CIP8040 at 30°C. Similarly, during 6 days of biotreatment, it was observed that the Fe(II) removed was 0.41mmol L⁻¹ within the first day and thereafter increases to 0.58mmol L⁻¹ at the termination of the experiment and no bio-reduction was apparent in the blank reactor (Figure 6.7). However, pH, Eh and temperature were monitored and regulated within the requirement of *Shewanella* cells (Appendix 3.7).

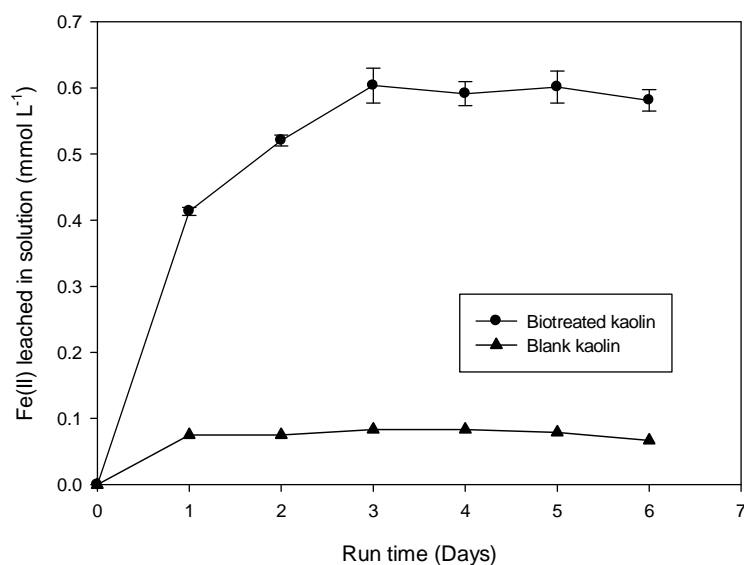


Figure 6.75: Bioleaching of Fe(III) in Kkaolin 4 (Melbur Yellow MGP) using batch bioreactor experiment as function of time. Error bars represent standard error for two replicates.

Solid samples were analysed at the termination of the experiment to monitor colour properties. The percentage whiteness, ISO brightness and lab values measured are given on Table 6.3. Improvement was observed in % ISO brightness from initially 75.79% to 77.61% and % whiteness from 55.69% to 63.89% was observed in biotreated reactor. It was noticed that % brightness and whiteness in the blank reactor also increases to 76.38% and 62.40% (Table 6.1).

Table 6.35: Colour analysis of Kkaolin 4 (Melbur Yellow MGP) before and after bioreduction with *S. putrefaciens* CIP8040 at 30°C.

Sample	L*	a*	b*	%Brightness	%Whiteness
Biotreated kaolin	93.82	-0.02	4.05	77.61	63.89
Blank kaolin	92.76	0.12	4.32	76.38	62.40
Initial Kaolin	92.82	-0.19	5.8	75.79	55.69

6.4: Bioleaching of silica sand

A batch bioreactor experiment was designed to up-scale bioleaching of Silica Sand 3 (Oakamoor) ~~material~~ using *Shewanella putrefaciens* CIP8040 at 30°C. Around 140g of Silica Sand 3 was used in 4.5L of bioleaching medium. The result obtained shows rapid increase of Fe(II) production with around 0.40mmol L⁻¹ measured on day 3. Fe(III) bioleaching was observed to seized ~~cease~~ after 4 days of incubation and continue ~~then~~ decline to around 0.22mmol L⁻¹ after 10 days (Figure 6.8). Production of Fe(II) was more in the bioreactor experiment when compared with the amount of Fe(II) leached in the microcosm study. In addition the rate of iron production was high with more Fe(II) leached within the first few days ~~than lower rate and longer extent of bioleaching observed~~ compared with the in microcosm study. The blank experiment shows no evidence of reduction when compared with the biotreated reactor. The pH evolution, redox potential and temperature during the bioleaching process are shown in Appendix 3.8.

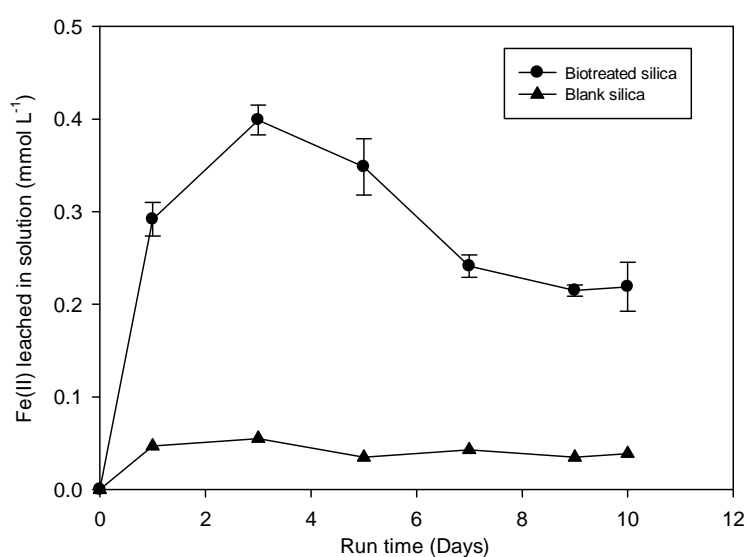


Figure 6.8: Bioleaching of Fe(III) in 140g Silica Sand (Oakamoor) using batch bioreactor experiment as function of time. Error bars represent standard error for two replicates.

A second batch bioreactor experiment was carried out using 70g of Silica Sand 3 (Oakamoor). This was aimed at achieving proper stirring, because silica sand could not be

kept in suspension and therefore tends to settle at the bottom of the bioreactor due to its density. Although less mineral mass was used in this experiment ~~but~~ the amount of Fe(II) leached was almost the same ~~as~~ when 140g of silica was employed. The bioleaching process removed 0.29 mmol L^{-1} of Fe(II) on day 1 and this increased to 0.51 mmol L^{-1} after day 4. Decline in Fe(II) production was evident after day 4 (Figure 6.9.9). The drop in ferrous iron concentration observed in both experiments may suggest formation and precipitation of secondary mineralisation products such as siderite. ~~Similarly, the plots of pH evolution,~~ redox potential and temperature during the bioleaching process are shown in Appendix 3.9.

Comment [DM47]: Is there any evidence for this? We could check quickly using TG-DSC-QMS

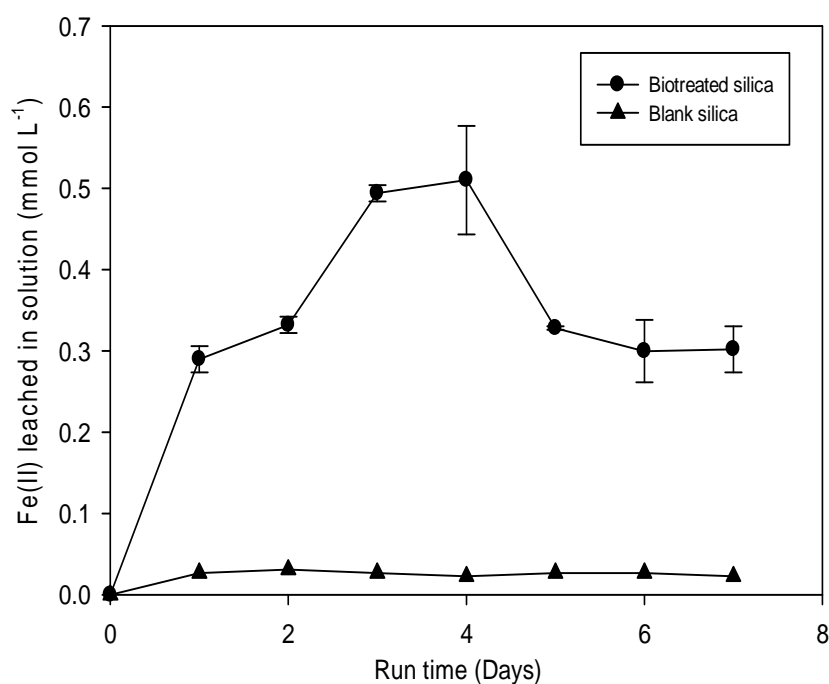


Figure 6.9.9: Bioleaching of Fe(III) in 70g silica sand and 3 (Oakamoor) using in a batch bioreactor experiment as function of time. Error bars represent standard error for two replicates.

The biotreated silica sand visually ~~appear~~ looks different to that from the blank treatment and initial material. ~~This prompted the curiosity to measure~~ Consequently, the optical properties ~~were measured in an attempt to quantify the observed difference, although this is not normally done and the ColorTouch is not designed for use with such a coarse~~

~~material~~ ~~so as to have an idea on colour values~~. Improvement in the colour index was observed. ~~Improvement, with an increase~~ in whiteness ~~values~~ from initial -148.68% to -96.52% ~~was observed~~ in the first bioreactor experiment (containing 140g silica sand). The colour value a_L which indicate reddishness, ~~was also observed to improve from 5.93 to 4.37~~ ~~(t-The more positive the a value the greater the reddishness of the material)~~. Improvement of colour properties ~~iesy~~ was similarly evident in the second bioreactor experiment in comparison to initial silica sand (Table 65.4).

Table 6.45: Colour values of Silica Sand (Oakamoor) before and after bioreduction with *S. putrefaciens* CIP8040 at 30°C.

Sample	L*	a*	b*	% Brightness	% Whiteness
Biotreated silica (140g)	43.80	4.37	13.43	9.21	-96.52
Blank silica (140g)	41.43	4.94	14.65	7.68	-112.36
Biotreated silica (70g)	42.18	4.28	13.67	8.33	-102.59
Blank silica (70g)	35.02	6.03	14.58	5.06	-129.21
Initial silica	44.51	5.93	20.47	7.57	-148.68

65.5: EFFECT OF BIOREDUCTION ON THE MINERALOGY

The chemical ~~assay composition~~ and surface area properties of ~~K~~kaolin 2 (Remblend) and ~~K~~kaolin 3 (Melbur Yellow HCP) before and after biotreatment, ~~as determined by Imerys Ltd~~, are given in Table 5.5. The % Fe_2O_3 in Remblend decreased ~~d~~ from 1.085% to 1.025% after biotreatment, ~~while TiO_2 decreases by 0.005%~~. This decrease in Fe_2O_3 ~~has resulted is~~ ~~associated with-in~~ an increase in brightness ~~of by~~ 3.3%. Similarly, The % Fe_2O_3 content in Melbur Yellow HCP decreased ~~ds~~ by 0.11% after biotreatment, ~~and also -while- TiO_2~~ decreased ~~ds~~ by 0.02% ~~(TiO_2 can act as a pigment; no change was observed in the TiO_2 content for Remblend)~~. ~~Theis~~ slight decrease in Fe content ~~also-is associated with an~~ improvement ~~ins~~ the brightness of the mineral by 3.7% after bioleaching. Other impurities present in the mineral are also reported (Table 65.5).

Comment [DM48]: The change in TiO_2 is not relevant.

Formatted: Font: 12 pt, Subscript

Formatted: Font: 12 pt, Subscript

Formatted: Font: 12 pt, Subscript

Table 6.55: Chemical ~~assay composition (expressed as of different% oxides) concentration and surface area for in K~~kaolin 2 (Remblend) and ~~K~~kaolin 3 (Melbur Yellow HCP) before and after biotreatment with *S. putrefaciens* CIP8040. Analyses carried out by Imerys Ltd.

Elements (wt.%)	Remblend			Melbur Yellow HCP		
	Biotreated	Blank	Initial	Biotreated	Blank	Initial
SiO ₂	47.49	47.54	47.66	47.84	47.97	48.18
TiO ₂	0.083	0.081	0.087	0.090	0.089	0.106
Al ₂ O ₃	36.61	36.66	36.69	36.11	36.04	36.04
Fe ₂ O ₃	1.025	1.083	1.085	1.262	1.354	1.371
CaO	0.014	0.016	0.039	0.013	0.011	0.054
MgO	0.265	0.266	0.285	0.276	0.278	0.302
K ₂ O	2.002	2.005	2.021	2.224	2.235	2.297
Na ₂ O	0.199	0.161	0.030	0.244	0.235	0.072
L.O.I.	12.18	12.06	11.96	11.83	11.68	11.47
Surface Area (m ² g ⁻¹)	IS*	7.60	7.94	IS*	7.02	8.21

IS* = Insufficient sample

The chemical ~~assay and mineralogy of the impurities in composition of S~~silica ~~S~~sand 3 (King's Lynn) using XRF (carried out by Sibelco Ltd) ~~shows that major part of the iron impurities is in the form of Fe₂O₃ and some portion of it is in the form of~~ is given in Table 5.6TiO₂. A ~~d~~Decrease of Fe₂O₃ by 0.06% was achieved after bioreducing 140g of the silica sand. The biotreatment of 70g silica sand decreases the Fe₂O₃ content by 0.07% (Table 65.6). This indicates that parts of the Fe present in the silica sand is free and are leachable.

Table 65.6: Chemical assay of different oxides concentration in Silica Sand 3 (King's Lynn) before and after biotreatment with *S. putrefaciens* CIP8040. Analysis carried out by Sibelco Ltd.

Elements (wt.%)	Biotreated (140g)	Blank (140g)	Biotreated (70g)	Blank (70g)	Initial
SiO ₂	98.07	98.14	98.27	98.04	98.10
TiO ₂	0.027	0.023	0.028	0.024	0.027

Al ₂ O ₃	0.88	0.83	0.79	0.85	0.82
Fe ₂ O ₃	0.106	0.118	0.093	0.121	0.165
CaO	0.01	0.01	0.01	0.01	0.04
MgO	<0.03	<0.03	<0.03	<0.03	<0.03
K ₂ O	0.61	0.58	0.54	0.59	0.51
Na ₂ O	<0.05	<0.05	0.06	0.05	<0.05
LOI	0.23	0.24	0.18	0.27	0.27

Conventional scanning electron microscopy images of Kaolin 3 (Melbur Yellow HCP) had show some larger and smaller individual kaolinite grains with rough edges (Figure 65.10). The micrograph also reveals some crystalline kaolin with pseudo hexagonal platelets in both biotreated and blank sample. Some of the clay particles are below 10µm size. More deformed and smaller size kaolinite particles are presented in the biotreated kaolinite (Figure 65.10). Stacks of kaolinite are also observed in both blank and biotreated samples. No EDX spectrum was obtained to show the changes in elemental composition.

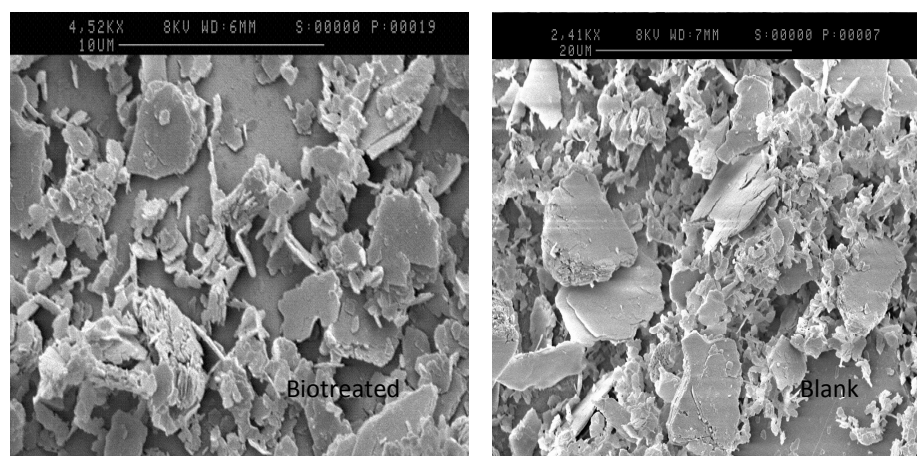


Figure 6.105: Scanning electron micrograph showing the morphology of Kaolin 3 (Melbur Yellow HCP) before and after bioreduction using *S. putrefaciens* CIP8040.

Scanning electron micrographs of biotreated (Figure 65.11) and blank (Figure 65.12) silica sand obtained with conventional scanning electron microscope show the presence of some large and spherical-rounded particles of quartz, which are the sand grains. Some grains are

angular with weathered and smooth surfaces while others are semi-rounded. The image at high magnification reveals some microcracks and spongy surfaces in the biotreated sample.

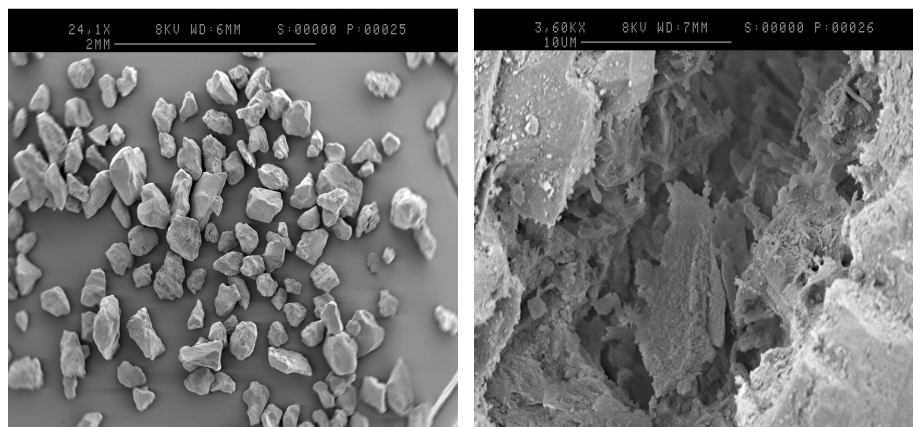


Figure 6.115: Scanning electron micrograph showing the morphology of Silica Ssand 3 (Oakamoor) after bioreduction using *S. putrefaciens* CIP8040.

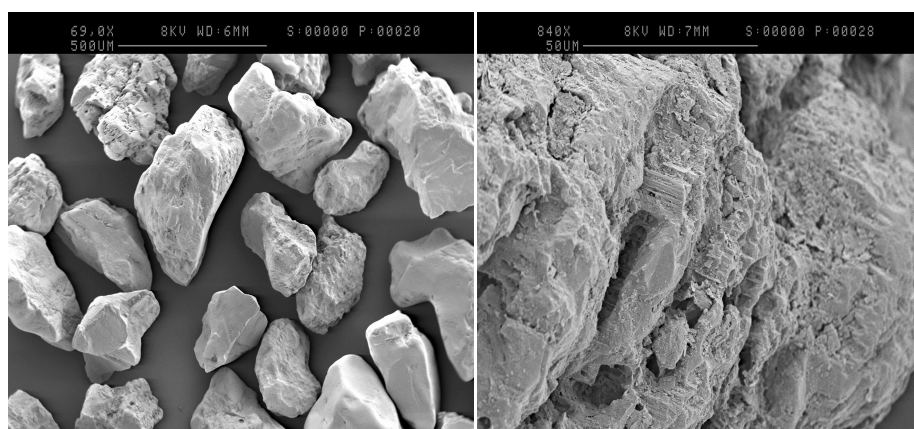


Figure 6.125: Scanning electron micrograph showing the morphology of blank Silica Ssand 3 (Oakamoor).

An X-ray diffraction analysis was conducted ~~to to give an overall picture of~~investigate any changes in the mineralogy in the kaolin. Figure 65.13 represents the XRD powder pattern of Kkaolin 3 (Melbur Yellow HCP). Kaolinite is the major mineral and clearly shows evidence of preferred orientation. Other ~~ancillary mineral~~ impurities are illite, quartz and muscovite which are present in very low amounts in ~~both~~ bioleached, blank and untreated samples.

Mineralogically, samples before and after treatment ~~remain identical~~ show no detectable change. Treatment with *Shewanella putrefaciens* CIP8040 does not have any major impact on the kaolinite crystallinity after bioreduction and new crystalline phases are not formed.

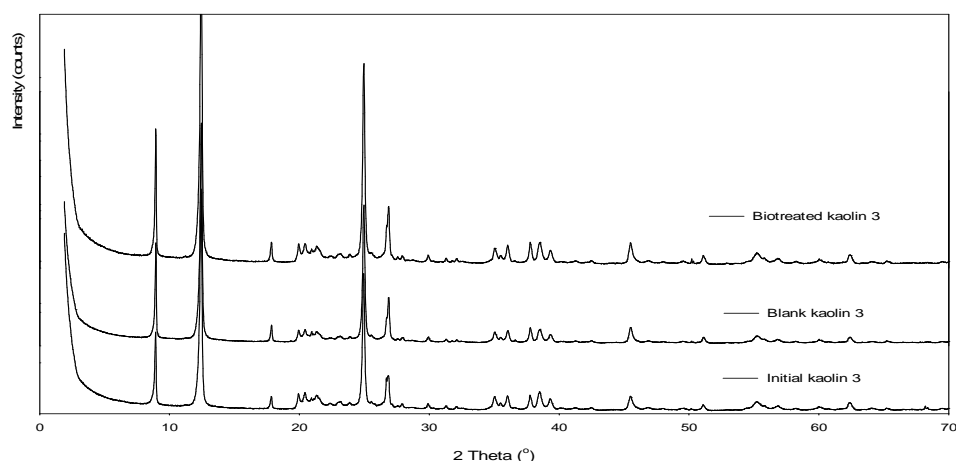


Figure 6.135: XRD pattern of Kaolin 3 (Melbur Yellow HCP) before and after batch bioreactor experiment using *S. putrefaciens* CIP8040.

The XRD pattern of ~~K~~kaolin 4 (Melbur Yellow MGP) exhibited similar kaolinite crystallinity before and after biotreatment. Kaolinite is the major mineral with traces of Illite, muscovite, and quartz as ancillary minerals. The samples are also identical before and after treatment with *Shewanella Putrefaciens* CIP8040 (Figure 65.14).

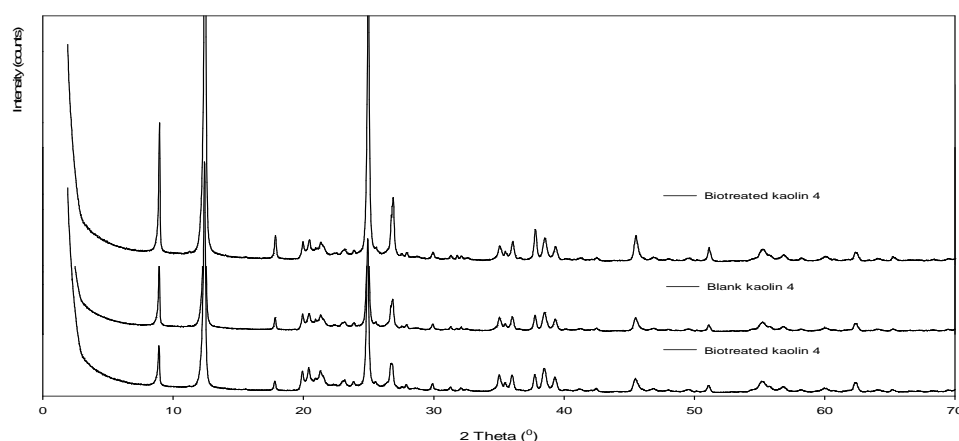


Figure 6.14: XRD pattern of Kaolin 4 (Melbur Yellow MGP) before and after batch bioreactor experiment using *S. putrefaciens* CIP8040.

The XRD pattern obtained before and after batch bioreactor experiments shows that the silica sand is composed mainly of quartz and feldspar (Figure 6.15). The XRD pattern of both biotreated, blank and initial silica sand were almost identical after biotreatment with *Shewanella putrefaciens* CIP8040. This was similar to what was observed during small scale bio-reduction. Similarly no crystalline bi-product was produced during bio-reduction.

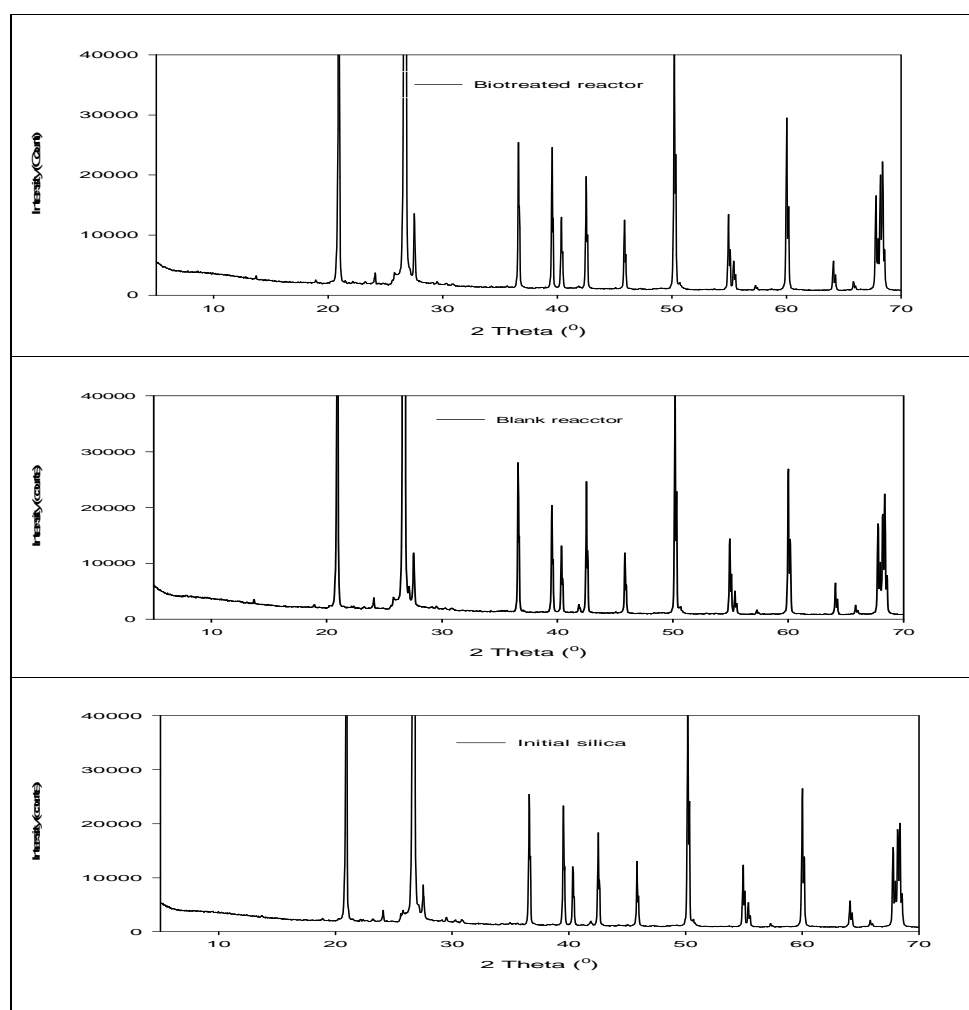


Figure 6.15: XRD pattern of Silica Sand 3 (King's Lynn) before and after batch bioreactor experiment using *S. putrefaciens* CIP8040.

Fourier transformed infrared (FTIR) spectroscopic analyses of Kaolin 3 (Melbur Yellow HCP) and Silica Sand 3 (Oakamoor) were performed in the mid infrared region (4000 – 400 cm⁻¹).

This enables characterisation of various functional groups in the minerals and identifying possible changes within the structure. The spectrum obtained displays a well crystalline and highly defined kaolinite (Figure 6.16). The kaolinite absorption bands of the treated and untreated kaolin spectra are all highly intense and sharp. The vibration band observed near $750 - 800\text{cm}^{-1}$ is useful in characterising crystalline kaolinite. Evidence of kaolinite crystallinity was further confirmed with respect to the H_2O vibrations in the range $4000 - 3000\text{cm}^{-1}$ region largely due to the presence of strong and sharp absorption bands at 3630 and 3698cm^{-1} , alongside other sharp but less intense bands at 3660cm^{-1} . The distance of OH group to the oxygen of neighbour groups determines the frequency of these bands (Granizo et al., 2000).

The spectra also reveal various inner OH deformation bands at 938cm^{-1} and 916cm^{-1} which are mainly due to inner OH groups and inner surface OH respectively (Russell and Fraser, 1996). The FTIR spectra before and after bioleaching with *Shewanella putrefaciens* CIP8040 are nearly identical and remain almost the same. Structural deformation or disappearance of bands was not observed by FTIR at the OH stretching and bending vibration of $\text{AlFe}^{3+}\text{OH}$ which occur due to Fe^{3+} substitution with Al within the kaolinite octahedral structure (Figure 6.16). This indicates that bioleaching does not remove Fe(III) from the structure of the kaolinite.

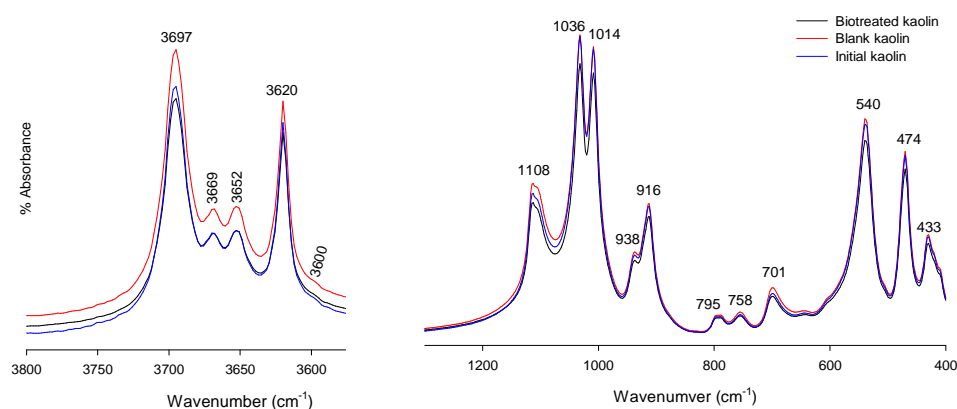


Figure 6.16: FTIR spectra of Kaolin 3 (Melbur Yellow HCP) before and after batch bioreactor experiment in the presence of *Shewanella putrefaciens* CIP8040.

For the silica sand sample, several characteristic sharp bands of silica mineral were observed between 400cm^{-1} and 1200cm^{-1} after FTIR analysis. Spectral peaks that generally correspond to quartz are displayed at a region between 460 , 800 and 1080cm^{-1} . The doublet band at 800cm^{-1} and 781cm^{-1} which are important bands used to characterise quartz are also observed. The spectra also present absorption bands at region around $1090 - 1080\text{cm}^{-1}$ which are assigned to asymmetric vibration of Si-O-Si. Similarly, a symmetric Si-O-Si band stretching was observed at 800cm^{-1} . However, no major change in the spectrum for Silica Sand 3 was obviously observed after biotreatment with *Shewanella putrefaciens* CIP8040 (Figure 6.17). This suggests that there is no evidence of any effect on the quartz structure, not the structural iron.

Comment [DM49]: No-one is suggesting that there is structural iron in quartz.

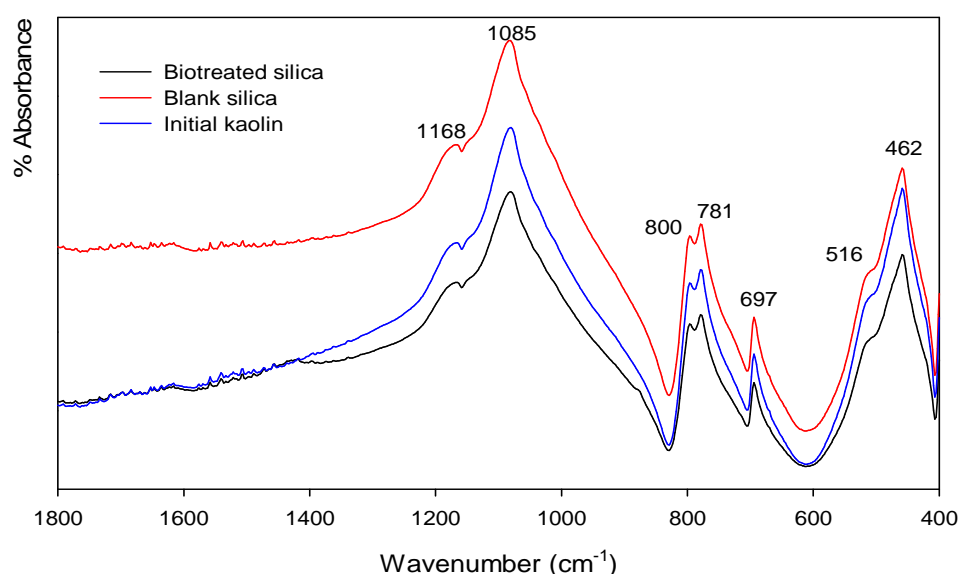


Figure 6.17: FTIR spectra of Silica Sand 3 (Oakamoor) before and after batch bioreactor experiment in the presence of *Shewanella putrefaciens* CIP8040.

6.6: DISCUSSION

This chapter presents a study conducted for large scale laboratory bacterial refinement of kaolin and silica sand using a closed system batch bioreactor. In each experiment, ~~t~~The bioreactor's content and composition were designed and held to mimic small-scale microcosm conditions. This is because the small-scale study shows promising results, at the same time demonstrating that iron-leaching for commercial benefit using iron-reducing bacteria is possible and may be optimised. The iron—reducing strain *Shewanella putrefaciens* CIP8040 ~~earlier~~ observed earlier to ~~respond to treatments better~~perform best at a ~~at~~ small-scale was used in this study to harness its iron respiring potential for anaerobic utilization of insoluble Fe(III) in silica sand and kaolin at a ~~more~~ larger scale. The bacterium is capable of respiring and utilising a variety of oxidised compounds including Fe(III) as electron acceptor in the absence of oxygen (Park and Kim, 2001).

In this study, the bioreactor was observed to be capable of supporting Fe(III) reduction in both kaolin and silica sand. ~~Because~~ *Shewanella putrefaciens* CIP8040 ~~has~~ve been able to anaerobically couple reduction of Fe(III) to the oxidation of lactate at a large scale ~~experiment~~ in the presence of anthraquinone-2,6-disulphonate (AQDS). AQDS as ~~earlier~~ mentioned earlier serves the role of enhancing electron delivery to various oxides in many minerals (Lovley et al., 1998). A substantial amount of Fe(II) was leached in all ~~the~~ three different kaolin samples, even though (compared with the microcosm experiments) proportionately less mineral mass was used. More Fe(III) ~~was~~are leached in Melbur Yellow HCP (Kkaolin 3) on the first day compared to the amount of Fe(III) removed in Remblend (Kaolin 2). However the amount of reduced Fe(II) was observed to gradually accumulate over time. Resumption of Fe(III) bioreduction was not apparent in the experiment conducted with Kkaolin 3 (Melbur Yellow HCP) ~~where following reinjection of a fresh~~ *Shewanella* cell suspension ~~were re-injected~~ on day 5, and this may suggest coating of Fe(II)

onto the mineral surface ~~that and so~~ inhibits further Fe(III) reduction even after injection of fresh *Shewanella* cells (Jaisi et al., 2007b).

The pH of the solutions remained ~~ed fairly~~ consistent at around 7.5 – 8 throughout the experiments in the biotreated reactor suggesting low accumulation of organic acids ~~like acetate~~. Furthermore, ~~a~~ reducing ~~ed~~ environment that supports iron-reducing bacteria was immediately attained ~~ed following after~~ injection ~~on of~~ *Shewanella* cells. The E_h continued to decrease to around -150 and -240 mV, indicating an anaerobic environment where active Fe(III) reduction performed better (Lee et al., 2002). Fe(II) was not detected in the control reactor confirming that reduction observed was mainly due to *Shewanella* cells added. The pH and E_h in the control reactor almost remained the same throughout the experiment with no apparent change in the solution chemistry.

Similarly, *Shewanella putrefaciens* CIP8040 was able to couple oxidation of lactate to the reduction of Fe(III) in experiments with silica sand. The rate of microbial reduction of Fe(III) was fast in the first 3 days after which a decline in Fe(II) accumulation over time was clearly apparent. Although different mineral masses of silica sand (70g and 140g) ~~were as~~ used in the same volume of solution, ~~but~~ nearly the same amount of Fe(II) was removed after bioleaching. The drop in Fe(II) concentration observed after initial accumulation may suggest possible formation and precipitation of ferrous minerals such as siderite (FeCO_3) which may inhibit rate of Fe(III) reduction (MacDonald et al., 2011). ~~A r~~Reducing environment that supported Fe(III)-reduction was also observed after injecting *Shewanella* cells. However the pH was observed to increase to around 8.2 and 8.5 from the initially adjusted 7.2.

Improvement in the whiteness and brightness of kaolin was achieved after bioreduction with *Shewanella putrefaciens* CIP8040 ~~if or~~ all the three different kaolin samples ~~used~~ when compared to blank and initial kaolin values. The improvement in the whiteness and brightness was almost in agreement with what was obtained in the small scale microcosms. However, re-injection of *Shewanella* cells on day 5 after initial cell injection further increased the brightness and whiteness of Kkaolin 3 (Melbur Yellow HCP). Biotreatment with *S. putrefaciens* CIP8040 also increased the optical values of silica sand when compared

Formatted: Font: 12 pt, Not Superscript/ Subscript

Formatted: Font: 12 pt, Not Italic

to the initial silica sand ~~value~~ with a substantial decrease in the redness (a value) of the bulk mineral ~~(- Because the initial silica sand hadve more positive values for a and b indicating redness and yellowness). But biotreatment with *Shewanella putrefaciens* CIP8040 brought down the two values where decreased the values of a decreases from 5.93 to 4.37 and b to decrease 13.3 from 20.47. The decrease in the a value (redness) is attributed to the removal of free iron oxides on the mineral surface, possibly together with other titaniferrous material mineral (Chandrasekhar and Ramaswamy, 2002).~~

Reliability and reproducibility of the ColourTouch analyser ~~tested~~ shows a very good agreement between the results obtained from analysing the certified reference standard in comparison to the supplied values. Similarly, test results also show a very good agreement between analyses we conducted with those performed by the industrial partners. Further more the results obtained are highly reproducible with a very small standard deviation. This suggests that the ColourTouch analyser is analytically reliable.

Assessment of the mineralogical changes after bio-reduction of Kkaolin 3 (Melbur Yellow HCP) and Kkaolin 4 (Melbur Yellow MGP) using X-ray diffraction confirms a clear ~~and preferred orientation of kaolinite pattern, with preferred orientation.~~ The ordering pattern reveals the crystallinity in the different kaolin samples material. Biotreatment does not appear to have a major impact on the kaolinite structure as no transformation was evidently seen between biotreated and blank samples in both Kkaolin 3 and Kkaolin 4. FTIR spectra obtained within the mid-infrared region displays bands that confirms the predominance of quartz. Likewise the FTIR spectrum obtained from Kkaolin 3 further reveals the crystallinity of the kaolin material. The OH adsorption bands characterising the AlFeOH group between 3600cm^{-1} and 880cm^{-1} are not affected after biotreatment. Conventional SEM analyses of Kkaolin 3 reveals more deformed and smaller pseudo hexagonal platelets with rough edges in the biotreated sample.

For the silica sand, FTIR spectra obtained within the mid infrared region displays bands that confirms the predominance of quartz. Similarly, typical crystalline quartz was also confirmed as the major mineral in silica sand by the XRD pattern obtained. The quartz peaks remain the same after biotreatment revealing no major changes in the mineral composition

Formatted: Font: 12 pt, Highlight

Comment [DM50]: Do you mean to say this here?

Formatted: Font: 12 pt, Superscript

Formatted: Font: 12 pt, Superscript

Comment [DM51]: Do you mean to say this here?

between biotreated and blank silica sand. Some large and spherical particles of quartz ~~were~~ also revealed by SEM with some microcracks and spongy surfaces in the biotreated samples.

~~The~~ chemical ~~analysis~~ by X-ray fluorescence (XRF) reveals some decrease in the % of Fe_2O_3 in both silica sand and kaolin (Remblend and Melbur Yellow HCP) after biotreatment with *Shewanella putrefaciens* SIP8040. Even though, the amount of Fe_2O_3 removed was low ~~but~~ an improvement in optical properties was achieved. In addition, the biotreatment did not alter the main elemental composition in the minerals. The Al_2O_3 and SiO_2 was found to be 36 and 48wt% respectively in the kaolin, while the SiO_2 content in silica sand remain around 98wt% before and after biotreatment. It is generally considered, as observed in microcosm study, that the structural Fe within the mineral framework is not likely to be attacked during bioleaching. ~~In-but the case of silica sand it is probable that~~ iron oxides on the mineral surface are being bio-reduced.

In conclusion, refinement of iron bearing minerals for commercial benefit should be considered is possible, given that scaling up to batch reactor experiments gave similar results to the microcosm experiments. ~~because~~ The strain *Shewanella putrefaciens* CIP8040 was capable of coupling oxidation of lactate for the reduction of Fe(III) in kaolin and silica sand at a larger scale. Although the amounts of Fe(III) removed ~~were~~ low, ~~but~~ improvement in the brightness and whiteness in kaolin as well as decrease in redness in silica sand ~~were~~ appreciable. Bioleaching does not have a major impact on the structural Fe within the minerals but possibility iron oxides on the mineral surface are bio-reduced. This was similar to what was observed earlier ~~observed~~ in the small scale microcosm study.

Formatted: Font: 12 pt, Subscript

CHAPTER 7 : BIOLEACHING OF CALCIUM CARBONATE (CHALK)

7.1: INTRODUCTION

Carbonate minerals are generally a group of industrial minerals characterised to essentially have $(\text{CO}_3)^{2-}$ ions in their structural unit. Carbonates exist in a variety of forms but the most common ~~polymorphs of calcium carbonate~~ are calcite (CaCO_3) and dolomite ($\text{CaMg}(\text{CO}_3)_2$). Calcite (CaCO_3) is a common rock-forming mineral in sedimentary environments and it is the principal constituent of all limestone including chalk. ~~But~~ chalk is a type of limestone characterised to have ~~a~~ very fine-grained particles (Deer et al., 1999). Calcium carbonate is an important mineral with ~~a vast~~ wide industrial applications. The mineral is primarily used as ~~a~~ raw material in cement manufacturing, ~~paints,~~ ceramics and glass making. Pure forms are used as fillers and coating agents in the plastics, paints and paper industries. The industrial values of calcium carbonate in higher specification applications is are mainly attributed to their high chemical purity (~~typically consisting~~ $>97\%$ CaCO_3) and whiteness. Yet, varying degree of impurities in the form of iron, clays and sand materials are often associated with most calcium carbonate minerals (British Geological Survey, 2006).

Formatted: Font: 12 pt, Subscript

Formatted: Font: 12 pt, Subscript

Formatted: Font: 12 pt, Subscript

Comment [DM52]: What is this reference?

The greater part of Fe-impurities associated with calcium carbonate are mostly presented in the form of siderite (FeCO_3) and Mn and Mg carbonate also occur. The structure of siderite is similar to that of calcite but with calcium being substituted by Fe^{2+} . Calcium substitution for Fe^{2+} is limited to between 10-15% CaCO_3 (Deer et al., 1999). Moreover, it is the amount of impurities present such as iron that dictates the overall industrial importance of the mineral.

rather than the absolute calcium carbonate content present in the mineral. For example, the amount of iron in glassmaking calcium carbonate should contain <0.036% Fe₂O₃ (British Geological Survey, 2006).

~~T~~However there ~~is~~are currently a growing need and concern for testing a new application for the removal of iron bearing impurities in carbonate minerals which currently cannot be processed economically through conventional chemical methods. Therefore, new bio-refinement technology has become ~~absolutely imperative~~attractive as an option in order to maximise carbonate industrial value. Moreover, for the bioleaching of iron in carbonate materials, approaches other than dissimilatory Fe-reduction would have to be employed, because iron-bearing impurities in carbonate (chalk) ~~are~~were mostly ferrous (Fe²⁺) and could not be bioleached by iron reducing bacteria. For that reason, the work reported here contrasts with that reported for kaolin and silica sand. Experiments have been carried out in whichusing aerobic *Pseudomonas mendocina* (known to chelate Fe in mineral materials) and *Desulfovibrio desulfuricans* (a sulfate-reducing bacterium known to precipitate FeS) were tested for the bioleaching of iron in calcium carbonate (chalk).

In this study, growth tests in a synthetic medium were conducted to monitor the growth of aerobic *Pseudomonas mendocina* as the primary agent of chalk bioleaching. *Pseudomonas mendocina* was shown to be capable of obtaining iron from Fe(hydr)oxide mineral phases for the purpose of assimilation (Hersman et al, 2001; Maurice et al, 2000). The organism acquires Fe by secreting a siderophore which is an extracellular ligand that has a very high Fe-affinity. This facilitates ~~the~~ mineral dissolution through formation of a siderophore-Fe(hydr)oxide complex (Hersman et al, 2001). In addition, *Desulfovibrio desulfuricans*, a sulphate-reducing bacterium, has also been tested for its ability to mediate FeS formation in the presence of dissolved or solid iron (Antonio et al., 2000). This was meant to examine the possibility of precipitating Fe from the carbonate mineral phase as iron sulphide. However, some fraction of Fe in the carbonate mineral (~10%) is known to be ferric. Hence, dissimilatory Fe(III)-reduction approach was also used to see if reduction of this fraction could be achieved.

7.2: METHODOLOGY

Small scale microcosm experiments for the bioleaching of carbonate wereas conducted using both aerobic and anaerobic bacteria. Details of the methodology employed are described below.

7.2.1: Carbonate sample:

A carbonate (chalk) sample labelled W41723 was provided by OMYA UK Ltd in April 2007 to conduct a small scale bioleaching experiment. The sample was send along with colour and percentage-XRF data (Table 7.1).

Table 7.1: Initial XRF (%) chemical data of various oxides and brightness index in chalk supplied by Omya Ltd.

SiO ₂	TiO ₂	AlO ₃	Fe ₂ O ₃	CaCO ₃	CaO	MgO	K ₂ O	Na ₂ O	Mn ₃ O ₄	LiO	Brightness/Violet
1.4	-	0.11	0.11	97.7	-	0.30	-	-	-	-	84.4

7.2.2: Selection of commercially available bacteria for the bioleaching of carbonate

Apart from the various iron reducing-bacteria earlier mentioned in Cchapter 2, two other commercially available bacteria were tested for the bioleaching of carbonate (chalk). This is because the greater portion of the iron -phase-in carbonate was mostly ferrous (reduce Fe²⁺ form). The bacteria used in these experiments are:

7.2.2.1: Desulfovibrio desulfuricans

A sulfur₋-reducing bacteria, *Desulfovibrio desulfuricans* ATCC27774 was tested for the bioleaching of Fe from carbonate (chalk). The bacteria can have the ability to produce FeS₂ from different Fe-bearing minerals. The bacterium also grow in the presence of oxygen (Lobo et al., 2007; Antonio et al., 2000). Bacterial cultures were obtained from DSMZ (Braunschweig, Germany)

7.2.2.2: *Pseudomonas mendocina*

Selection of *Pseudomonas mendocina* was considered because the bacterium was known to produce siderophores which areis capable of chelating iron and facilitating mineral dissolution, thereby increasing iron solubility for the purpose of assimilation. This bacterium have been tested for growth in batch culture containing various insoluble Fe-bearing minerals such as hematite, goethite and ferrihydrite (Hersman et al., 2001; Hersman et al.,

Formatted: Font: 12 pt

Comment [DM53]: Do you mean FeS or FeS₂?

Formatted: Font: 12 pt, Subscript

1996). The bacterium was capable of utilising these Fe-bearing minerals as a sole source of Fe for growth. *Pseudomonas mendocina* ~~was~~ an obligate aerobic bacterium and can optimally be cultured on nutrient agar under aerobic condition. It was obtained from NICIMB Ltd (Aberdeen, Scotland).

7.2.3: Microcosm experiment using *Desulfovibrio desulfuricans*

Small-scale bioleaching experiments were conducted using *Desulfovibrio* desulfuricans for the bioleaching of chalk. Anaerobic microcosms were prepared using solution A and C (Table 7.2). Solution A was first boiled for a few minutes, then cooled to room temperature under a nitrogen atmosphere. Solution C was added to solution A and pH adjusted to 7.8 with NaOH under N₂ gas. Around 10g of chalk (providing the source of Fe in the system) were measured and transferred in-to 100mL serum bottles. A measured volume of mixed solution (80mL) was transferred in-to the serum bottles while gassing with oxygen-nitrogen-free nitrogen-oxygen. Lactate (10mM final) was added as carbon source. The bottles were immediately sealed with a septum cap and autoclaved at 121°C for 15 min. About 5mL of *Desulfovibrio desulfuricans* suspension ($0.9 \pm 0.2 \times 10^8$ CFU/mL) cultured overnight on solid agar containing medium described above was injected and the flasks flushed with oxygen-free nitrogen for 30min to maintain anaerobic conditions. The bottles were incubated at 30°C for FeS formation.

Comment [DM54]: Check the spelling all the way through. Until now it has been 'desulfurican'.

Comment [DM55]: Do you mean oxygen free nitrogen?

Table 7.2: Medium used for the culturing of *Desulfovibrio desulfuricans* ATCC27774 recommended by DSMZ.

Solution A	
K ₂ HPO ₄	0.5g
NH ₄ Cl	1g
Na ₂ SO ₄	1g
CaCl ₂ x 2H ₂ O	0.1g
MgSO ₄ x 7H ₂ O	2.g
DL-Na-lactate	1g
Yeast extract	1g
Distilled water	980mL
Solution B	
FeSO ₄ x 7H ₂ O	0.5g
Distilled water	10mL
Solution C	
Na-thioglycolate	0.1g
Ascorbic acid	0.1g
Distilled water	10mL

7.2.4: Bioleaching experiment using *Pseudomonas mendocina*

Small scale bioleaching experiments were conducted using aerobic *Pseudomonas mendocina*. In this experiment, bacterial growth was used as a means of monitoring Fe dissolution in the carbonate mineral. Therefore a growth test in a synthetic medium was carried out in a 250ml Erlenmeyer flask containing 10g of chalk-sample and 100mL of Fe-deficiency medium (FeDM): g/Litre 0.5 of K₂HPO₄; 1 of NH₄Cl; 0.2 of MgSO₄·7H₂O; 0.05 of CaCl₂; 5 of ~~s~~Succinic acid and 0.125ml of trace element solution (0.025g of MnSO₄·H₂O; 0.0325g of CoSO₄·7H₂O; 0.0115g of CuSO₄; 0.0165g of ZnSO₄ and 0.012g of MoO₃ in 500mL of distilled, deionised water). These method was adapted after a procedure carried out by Dhungana et al., (2007), Hersman et al., (2001) and Maurice et al., (2000). The bioleaching medium was ~~then~~-sterilised at 121°C for 15min. The ~~f~~lask was finally inoculated with 6mL overnight growth of early ~~lag~~-phase of *Pseudomonas mendocina* suspension (having an optical density of 0.2 at 600nm). The flask was later incubated at 30°C by agitation. The experiment was monitored aerobically and absorbance was periodically measured at 600nm for 15 days.

Comment [DM56]: Log or lag?

7.2.5: Microcosms experiments with Iron reducing bacteria

Because some fraction of the carbonate mineral (~10%) is known to be ferric (Fe³⁺ form), the~~refere~~ dissimilatory Fe(III)-reduction approach was also used to see if reduction of this fraction could be achieved. A small scale bioreduction assay was conducted using ~~a~~ non-growth approach in an 80mL minimal medium (NaCl - 0.9% final). The culture medium contains 10g and/or 20g of carbonate (chalk) with 10mM lactate (final) as the electron donor. The media were sealed with a septum cap and sterilised at 121°C for 15 min. 100µm of AQDS (~~a~~Anthraquinone-2,6,-disulfonate) and 3mM of NTA (~~n~~Nitrilotriacetic acid) sterilised by filtration (0.2µm pore size millipore filter) were aseptically added ~~in~~-to the culture bottle using a sterile BD microlane™ (0.5x16mm) syringe. The medium was then purged with oxygen-free N₂ to maintain anaerobic conditions. About 7mL (1.2 ± 0.4 x 10⁸ cell mL⁻¹) of *Shewanella* cells suspension were aseptically added under sterile conditions and incubated in the dark with continuous shaking at 60rpm. A blank control that was cell-free otherwise is identical and similar to the biotic sample.

Formatted: Font: 12 pt, Italic

7.2.6: Mineralogical assessment

Assessment of improvement in mineral quality after bioleaching was also conducted. Both initial and bioleached carbonate (chalk) minerals were analysed for colour property (L^* , a^* , b^* , ISO brightness and whiteness) using a Technidyne ColorTouch PC Spectrophotometer after repeated washing with deionised waters. To observe changes in the mineralogy after bioleaching, X-ray (powder) diffraction measurements were obtained with a Philips X'pert PRO XRD system from 2° to 70° 2θ $\text{CuK}\alpha$, at 0.0334° 2θ per step and 99.70 seconds per step. Similarly, FTIR analyses of bioleached and initial minerals were measured and obtained in transmission mode using KBr pressed pellets (1-2mg mineral in 200mg KBr) in the mid-infrared range ($400 - 4000\text{cm}^{-1}$) on an AVATAR 360 FTIR ESP spectrometer.

7.3: RESULTS

7.3.1: Batch scale microcosm studies using iron-reducing bacteria

Two series of experiments were conducted for the bioreduction of ferric (Fe^{3+}) fraction of chalk (*Omya product* W41723) mineral. *Shewanella loihica* and *Shewanella putrefaciens* CIP8040 were selected to examine their potential for dissimilatory iron reduction of the ferric iron phase present in chalk mineral.

Comment [DM57]: Is this right?

In the first experiment *Shewanella loihica* was tested for iron bioleaching in the presence of AQDS (anthraquinone-2,6-disulfonate) for electron delivery enhancement and NTA (nitrilotriacetic acid) which stimulates Fe(III) reduction. NTA is a synthetic complexing compound that serves as an Fe(III) chelator and stimulate iron reduction. It has potential to influence bacterial iron reduction by solubilisation of both Fe^{3+} from insoluble Fe(III) phases and biogenic Fe^{2+} (Zachara et al., 1998; Lovley and Woodward, 1996). In this study, three different amended microcosms were prepared. One of the amendments contains NTA, while the other set contains AQDS only, and the last one contains both NTA and AQDS.

The result using *S. loihica* shows a very small proportion of Fe(III) reduction when compared to the blank experiment that has both NTA and AQDS with no bacteria added into it. Around 0.09mmol L^{-1} of Fe(II) was measured in all the different amendments after 5 days incubation (Figure 7.1). Therefore a little degree of bioreduction of Fe(III) was achieved using *Shewanella loihica* even though AQDS and NTA were supplemented in to the system.

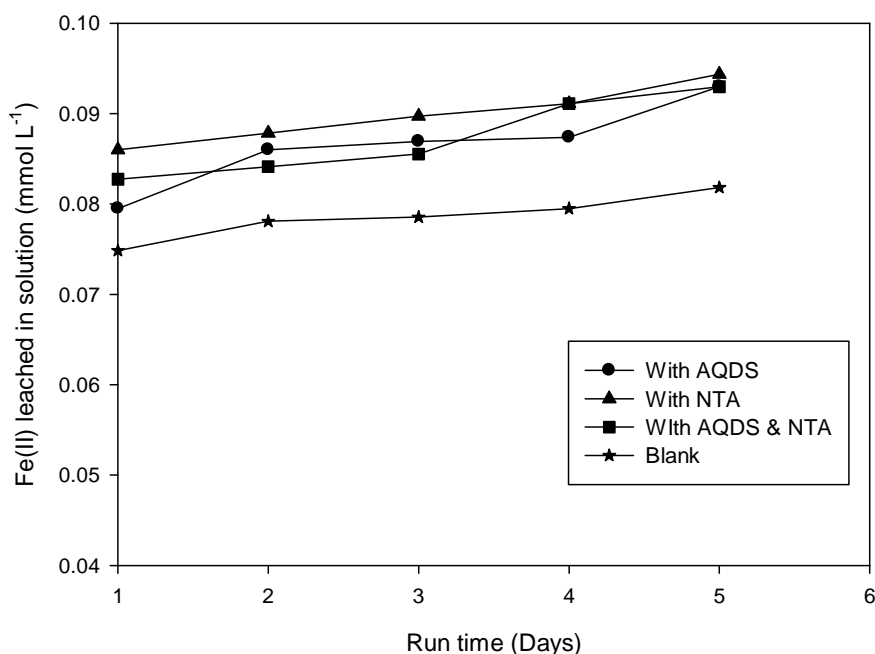


Figure 7.1: Production of Fe(II) from chalk (W41723) at 20°C using *Shewanella loihica* suspension in the presence of ADQS and/or NTA.

A second set of experiments was conducted using *Shewanella putrefaciens* CIP8040 in the presence of AQDS. Two different mineral masses (10 and 20g) in 80ml of liquid were used. A greater portion of Fe(III) was observed to be bioleached when *Shewanella putrefaciens* CIP8040 was used. Even though the amount of Fe(III) leached was low, but the rate of Fe(III) reduction was high when 20g of chalk was used, with 0.13 mmol L⁻¹ of Fe(II) measured on first day and increases to 0.25 mmol L⁻¹ on day 5. The amount of Fe(II) measured on day 1 for 10g chalk microcosms was 0.08 mmol L⁻¹ with an apparent lag phase observed around day 3 (Figure 7.2).

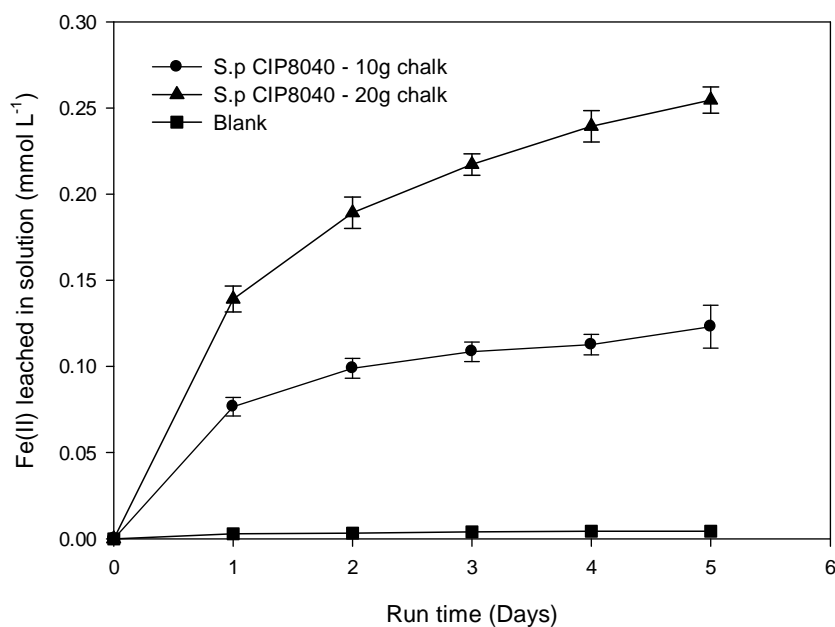


Figure 7.2: Production of Fe(II) from 10 and 20g chalk (W41723) at 30°C using *Shewanella putrefaciens* CIP8040 suspension in the presence of ADQS

Colour analysis of chalk conducted after 5 days bioleaching with *Shewanella putrefaciens* CIP8040 did not show any improvement even though a portion of Fe(III) was leached but rather shows a decrease below the initial chalk value. ISO brightness was observed to decrease by approximately 1.52% in both microcosms containing 10g and 20g chalk, while whiteness decreasedd by 2% in microcosms containing 20g and by 2.63% in those containing 10g of chalk (Table 7.3)

Table 7.3: colour analysis of chalk (W41723) after bioreduction of ferric phase using *Shewanella putrefaciens* CIP8040.

Samples	L*	a*	b*	% Whiteness	% ISO Brightness
Biotreated chalk - 10g	94.56	0.37	3.56	70.40	82.21
Biotreated chalk - 20g	94.57	0.42	3.45	70.94	82.35
Initial chalk	95.00	0.43	3.26	73.09	83.73

7.3.2: Bioleaching of chalk using *Pseudomonas mendocina*

An experiment to promote chalk dissolution and the subsequent Fe uptake for assimilation was conducted using *Pseudomonas mendocina*. In this experiment, monitoring of *Pseudomonas mendocina* growth by measuring optical density was used as an indirect means of assessing chalk bioleaching. Figure 7.3 show the image of the experiment conducted to monitor *Pseudomonas mendocina* growth curve at absorbance of 600nm. It was difficult to measure the optical density properly in the presence of calcium carbonate. However, evidence of bacterial growth from the culture flask over time was visually observed due to increase in turbidity. We are not sure if *Pseudomonas mendocina* was able to promote chalk dissolution and utilize iron present in the chalk.

Comment [DM58]: Check the formatting here so you don't have a big gap in a line.



Figure 7.3: Bioleaching of chalk (W41723) using aerobic *Pseudomonas mendocina*. Experiment was run at 30°C for 15 days.

Formatted: Not Hidden

Colour properties were measured at the termination of the experiment. The result obtained shows no any improvement in the colour values. A slight colour decrease below the initial value was observed. The whiteness decreases by almost 1% and brightness remains almost the same after bioleaching using *Pseudomonas mendocina* (Table 7.4).

Table 7.4: colour analysis of chalk (W41723) after 15 days bioleaching using *Pseudomonas mendocina*.

Samples	L*	a*	b*	% Whiteness	% ISO Brightnes
Biotreated chalk	94.07	0.32	3.43	72.27	83.56
Initial chalk	95.00	0.43	3.26	73.09	83.73

7.3.3: Bioleaching of chalk using *desulfovibrio desulfuricans*

An experiment was also conducted in an attempt to identify a better approach to bioleach iron impurities in carbonate (chalk) by precipitating Fe in the form of FeS. In this experiment, *Desulfovibrio desulfuricans*, a sulfur-reducing bacteria (SRB), was used as bioleaching agent in chalk. Microcosms were prepared and injected with 5mL of *Desulfovibrio desulfuricans* suspension ($0.9 \pm 0.2 \times 10^8$ CFU/mL). After SRB cells injection, the chalk suspension was observed to immediately turn to light grey as a result of the dark colouration of SRB cells (Figure 7.4). During 15 days incubation period, the colour of the suspension was observed to become darker with time. The change in colouration observed shows that Fe in carbonate was being precipitated as a dark FeS phase by *Desulfovibrio desulfuricans* (Figure 7.4). However attempts were made to separate the chalk from the darker phase through slow sedimentation and sequential centrifugation but all were unsuccessful.

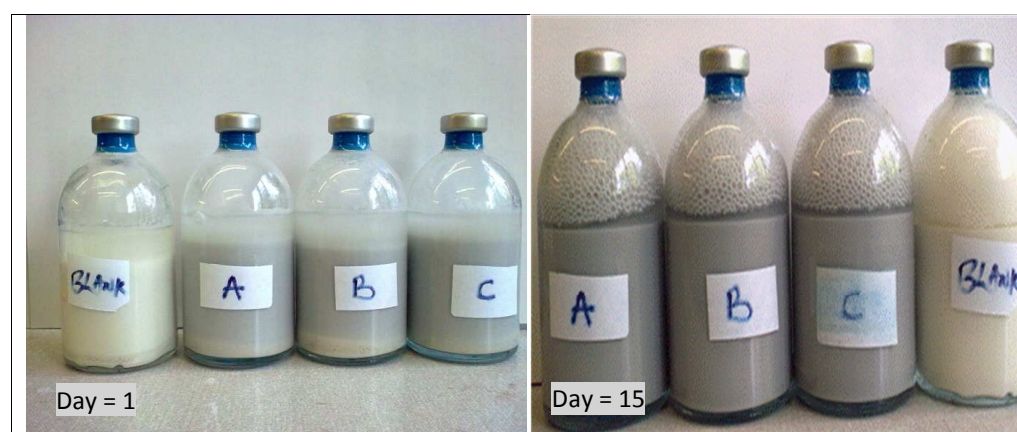


Figure 7.4: Picture of chalk (W41723) on day 1 and day 15 during bioleaching with sulfur-reducing *Desulfovibrio desulfuricans* at 30°C.

Colour analyses were conducted after sequential centrifugation to monitor the colour properties. The colour properties after vigorous washing gave a very poor result with whiteness decreasing to 64.81% from initial 73.09% while brightness decreases to 80.16% from 83.73% (Table 7.5).

Table 7.5: colour analysis after bioleaching of chalk (W41723) with *Desulfovibrio desulfuricans* at 30°C.

Samples	L*	a*	b*	% Whiteness	% ISO Brightness
Biotreated chalk	94.26	0.60	4.62	64.81	80.16
Initial chalk	95.00	0.43	3.26	73.09	83.73

7.4: EFFECT OF BIOLEACHING ON THE MINERALOGY

Mineralogical analyses were carried out to characterise the chalk mineral using FTIR in the range of 400 – 4000 cm⁻¹. In addition, powder X-ray diffraction was employed to assess any mineralogical alteration further investigate the crystal structure present in the chalk before and after bioleaching with *P. mendocina* and *D. desulfuricans* to assess any mineralogical alteration. The FTIR used within the mid infrared region (4000 – 400 cm⁻¹) indicates the presence of pure calcite structure as the main primary mineral within the chalk (Figure 7.5). Calcites are easily identified by their spectral bands appearing at 1428 cm⁻¹, 878 cm⁻¹ and 714 cm⁻¹ (Russell and Fraser, 1996). The IR absorption band near 712 cm⁻¹ was due to symmetric CO₃ deformation while absorption band near 876 cm⁻¹ was assigned to asymmetric CO₃ deformation. However, the symmetric CO₃ stretching vibration gives rise to a very strong band at region near 1435 cm⁻¹ (Gunasekaran et al., 2006). No apparent changes or deformation was observed after bioleaching with *P. mendocina* and *D. desulfuricans* in comparison to the blank sample (Figure 7.5).

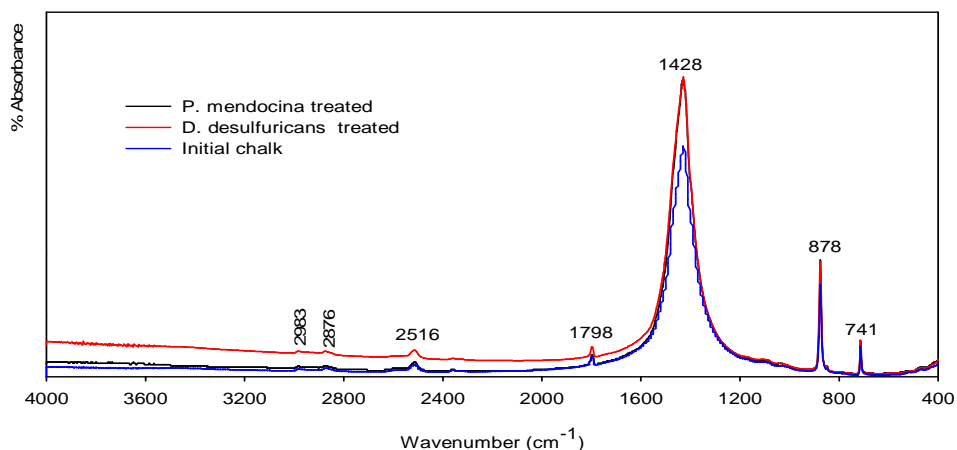


Figure 7.5: FTIR spectra of chalk (W41723) after biotreatment with *P. mendocina* and *D. desulfuricans*.

The powder XRD diffraction pattern obtained shows a typical ~~XRD~~ pattern for pure calcite mineral with clear and sharp peaks. The biotreated sample remains unchanged with peaks similar to that of the blank sample after bioleaching. Moreover, no other crystalline by-product was observed after bioleaching with *P. mendocina* (Figure 7.6)

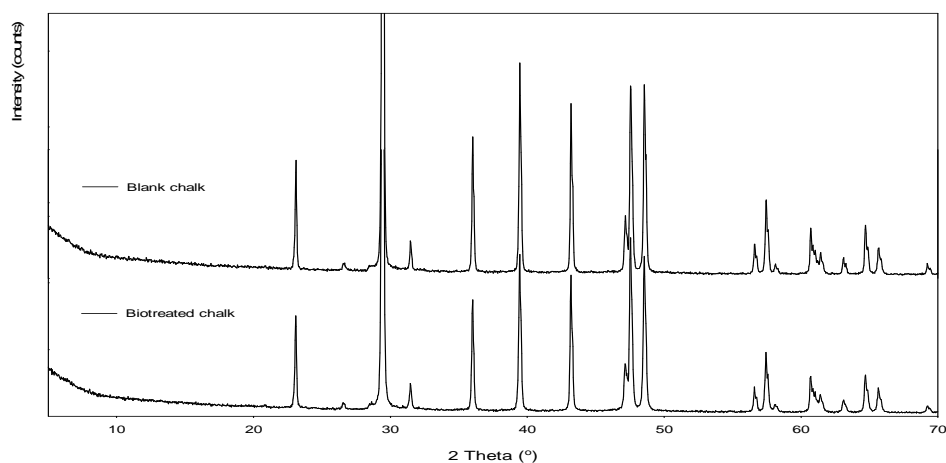


Figure 7.6: XRD pattern of chalk (W41723) before and after bioleaching with *Pseudomonas mendocina*.

Comment [DM59]: Do you have any results for the mineralogy of the desulfovibrio experiments?

7.5: EFFECT OF BIOLEACHING PROCESS ON THE MINERAL TYPE

It is useful to examine and compare the response of the three different minerals used (kaolin, silica sand and carbonate) to assess how best the bioleaching process affects iron removal in each mineral. Results of the experiments conducted in the presence of *Shewanella putrefaciens* CIP8040 from those microcosms designed to select the best iron reducing bacteria for each mineral were compared. It was observed that the rate of reduction and the amount of Fe(II) measured when kaolin was used is almost three times faster than in the presence of silica sand or carbonate (chalk) with 1.13mmol L^{-1} of Fe(II) measured on the first day. Only small portion of iron was removed, with approximately 0.14mmol L^{-1} of Fe(II) determined (Figure 7.8). Statistical analysis of the results show that the biotreatment significantly removed more iron from kaolin than removed from silica sand and carbonate (t-tests, $P < 0.018$). There is no significant difference in the amount of Fe(II) leached between silica sand and carbonate (t-test, $P = 0.121$).

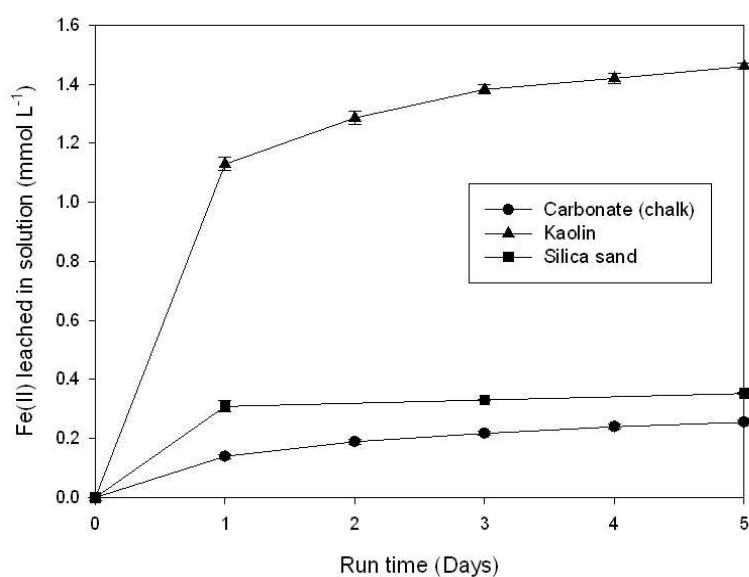


Figure 7.7: Amount of Fe(II) removed in aqueous solution (80mL) between kaolin (20g), silica sand (2.5g) and carbonate (20g) leached in the presence of *S. putrefaciens* CIP8040.

A different result was obtained when comparing the iron removed from these different minerals in terms of %Fe₂O₃ per 100g of mineral material (as is customary in the mineral industry). In this case, more iron is removed per gram of the mineral for silica sand than for the kaolin and carbonate. Around 78.8mg of bio-reducible Fe₂O₃ per 100g of silica sand was removed compared to 36mg of bio-reducible Fe₂O₃ leached from kaolin on day 1. Only 4.4mg of the Fe(III) fraction per 100g in carbonate (chalk) was leached.

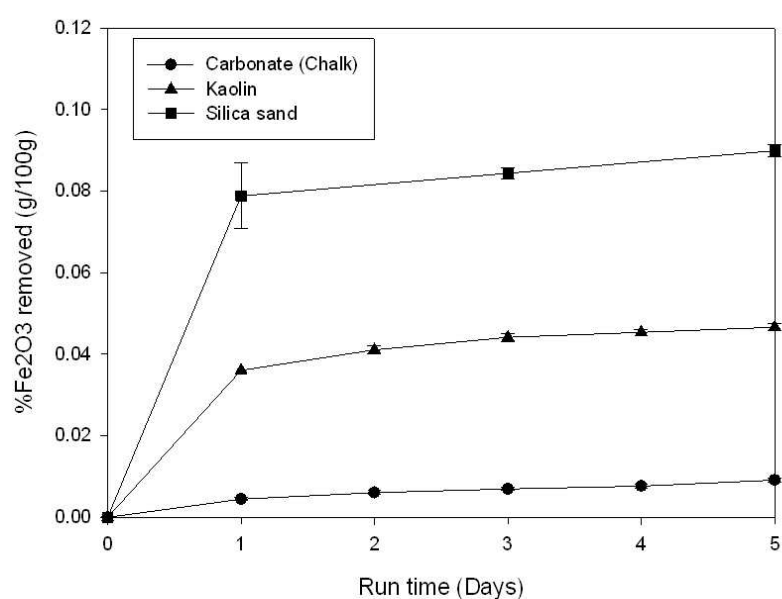


Figure 7.8: Amount of Fe₂O₃ removed in gram per 100g of kaolin, silica sand and carbonate in the presence of *S. putrefaciens* CIP8040.

7.6: DISCUSSION:

Although ~~chalk~~calcite (including chalk) is a relatively pure carbonate bulk material, in which calcite is dominant, but ferrous iron is one of the major Fe-impurities associated with it (Gunasekaran et al., 2006). Therefore, compared with kaolin and silica sand, entirely different bioleaching approaches ~~would have to be~~ required. For this reason, several bioleaching methods involving the use of both aerobic and anaerobic bacteria were employed ~~for to investigate~~ Fe removal in chalk. Bioreduction of the ferric (Fe^{3+}) fraction was achieved using *S. putrefaciens* C18040 on both 10g and 20g chalk. Even though the ferric fraction present in carbonate mineral was quite small, but *S. putrefaciens* was able to utilise ~~the~~ Fe(III) portion in the carbonate mineral as the terminal electron acceptor by couple oxidation of lactate to the Fe(III) reduction. AQDS ~~supplied~~ may also play a role in enhancing the rate of bioreduction observed with *S. putrefaciens* by alleviating requirements for establishing contact with the mineral surface. The amount of Fe(II) measured was low but a substantial difference in the rate was observed when two different masses of chalk was used. Slurry density was therefore found to have an effect on the rate of reduction of Fe(III) fraction of chalk because the Fe(II) measured in 20g chalk was more than Fe(II) measured in 10g. The change in slurry density may perhaps change the surface area for mineral bacterial interaction and this may explain the variation in the rate observed when different mass was used.

~~On the order~~In contrast, ~~hand~~ bioleaching using *S. loihica* was not effective in coupling respiration on lactate to the reduction of Fe(III) fraction of chalk even though the organism is known to conserve energy to support growth by coupling oxidation of various organic acids for the reduction of Fe(III) oxides (Nakamura et al., 2010; O'Loughlin et al., 2007). Addition of NTA, known to chelate and solubilise Fe(III), and AQDS, which enhances electron shuttling, was less effective when Fe(III) was leached in the presence of *S. loihica*. Contrary to this, reduction was observed when *Shewanella putrefaciens* CIP8040 was used in the presence of AQDS. Studies have shown that NTA does solubilise several other cations including iron in ~~several~~ sediments (Lovley and Woodward, 1996). This may suggest that Fe(III) was possibly solubilised by ~~n~~Nitrilotriacetic acid (NTA) and readily available to accept electrons but *S. loihica* was ~~therefore~~ not capable of coupling its reduction in chalk due to

other limiting factors. It is important to note that all necessary conditions such as pH, temperature and carbon source known from the literature to favour respiration of *S. loihica* were adequately supplied in these experiments. This similar observation was made in Chapter 3 and Chapter 5 where *Shewanella loihica* was unable to couple Fe(III) reduction in comparison to other iron-reducing *Shewanella* strains.

A progressive and substantial growth of *Pseudomonas mendocina* in the presence of chalk was observed from the optical density measurements. Although this was the only means used to indirectly assess Fe bioleaching in the system. The growth of *Pseudomonas mendocina* in iron deficiency medium (FeDM) indicates that a sufficient amount of Fe was released from carbonate (chalk) into the medium to support the bacterial metabolism. However no estimate of Fe concentration leached was made, but the optical density measured determines bacterial growth and does reveal that iron has been liberated. This bacterium was documented to be an obligate aerobe that is unable to utilise Fe as an electron acceptor, but Fe acquisition is only for metabolic requirement (Hersman et al., 2001). In addition to this, *Pseudomonas mendocina* was reported to have potential to sense and detect iron deficient environments and then produce a low-molecular-weight Fe-chelating siderophores that solubilised and transport Fe into cells from solid Fe-bearing phases and sediments. Siderophores facilitate Fe-mineral dissolution for their potential to have strong binding affinity to Fe (Dhungana et al., 2007; Dhungana and Crumbliss, 2005). Growth of *Pseudomonas mendocina* in iron deficiency medium (FeDM) was also reported by Maurice et al., (2000) in their experiment where goethite was supplied as a source of Fe in the system. Similar observations were also reported by Dhungana et al., (2007) where *S. mendocina* was reported to facilitate ferrihydrite dissolution in iron deficiency medium and utilised Fe liberated for assimilation and metabolic needs.

The sulfate-reducing bacteria *Desulfovibrio desulfuricans* was able to leach Fe in the carbonate (chalk), but the Fe-leached Fe immediately precipitated as a different iron phase given a characteristic grey colouration to the chalk. This may suggest biologically-mediated FeS production by the action of *Desulfovibrio desulfuricans*. The organism is known to grow in the presence of low or excess FeSO₄ thereby producing a black or brownish

precipitate (Antonio et al., 2000). Spectroscopic analysis by Antonio et al., (2000) of precipitate in the same similar studies on extracellular iron-sulphur precipitates from the growth of *Desulfovibrio desulfuricans* by Antonio et al., (2000) shows that the characteristic black precipitate produced by *Desulfovibrio desulfuricans* was largely due to the formation of an iron-sulfur phase with 6 nearest S neighbours distributed about a central Fe at an average distance of 2.24(1)Å.

In terms of colour improvement, the optical values of the chalk after biotreatment were not impressive-improved, with decreases in colour properties below the initial value after treatment using iron reducers, *Pseudomonas mendocina* and *Desulfovibrio desulfuricans*. Although Fe(II) was measured after treatment with *S. putrefaciens* CIP8040, but no improvement was achieved in the whiteness and brightness. We assume that, probably there was formation of other iron-mineral phases after bioleaching that in turn decreased the colour values. Also because carbonates (chalk) cannot be acid washed with HCl, but only water was used for the washing (unlike kaolin and silica), and the iron-content leached may not be completely leached removed after by washing.

In addition, whiteness and brightness slightly goes down or remain the same after bioleaching with *Pseudomonas mendocina*. Consequently Fe leaching was not quantitatively measured but was only assessed indirectly from bacterial growth. But several microorganisms including *Pseudomonas mendocina* were reported to only require Fe in the range of micromolar concentration to support growth (Hersman et al., 2001). This may possibly explain the reason as to why not much increased in whiteness and brightness was observed after bioleaching, because the bacteria requires only small amounts of Fe for growth. Treatment with *Desulfovibrio desulfuricans* gave a very poor brightness and whiteness values below the initial value after bioleaching. This was largely due to the black FeS phase produced by *Desulfovibrio desulfuricans* that may require a special separation technique from the treated chalk phase.

FTIR spectra obtained within the mid-infrared region (4000 – 400 cm⁻¹) to assess mineralogical changes shows bands that confirms a pure calcite mineral. No differences were seen after FTIR examination that could be due to bacterial transformation or

destruction ~~between-comparing~~ chalk biotreated with *P. mendocina* and ~~s~~Sulphate reducing *Desulfovibrio desulfuricans* ~~in-comparison-to-the~~with a blank sample ~~after-FTIR-examination~~. Similarly, the XRD ~~pattern-diffractograms~~ further reveals a pure calcite with ~~a~~ peaks similar~~rrity~~ ~~between-for~~ treated and untreated chalk ~~sample~~. However no formation of any crystalline by-product was ~~spotted-observed~~ after biotreatment ~~with~~ *Pseudomonas mendocina*.

In conclusion, this section shows that ~~the~~ sulphate--reducing bacterium *Desulfovibrio desulfuricans* is capable of precipitating Fe in chalk as ~~a~~ dark FeS phase but a technique is required to separate the FeS phase from the chalk ~~phase~~. Similarly, aerobic *Pseudomonas mendocina* can support growth by utilising Fe present in chalk, but the Fe uptake by this bacterium has no major impact on the colour properties considering that the Fe concentration required by this organism to support growth is ~~within-a-rangeof the order~~ of micromolar concentrations. Moreover, the Fe(III) fraction in chalk can be bio-reduced ~~using~~ ~~the~~by dissimilatory iron reduction approach, but because the iron ~~bearing~~ present in chalk was mostly ferrous ~~the~~ bio-leaching was unable to improve the colour properties.

CHAPTER 8 : GENERAL DISCUSSION

Kaolin, silica sand and high grade carbonate are industrial minerals used extensively in the production of paper, ceramics, paint, glass products, cement, chalks, cosmetics, potteries, fillers and coating agents, among many applications (Kahraman et al., 2005; Deer et al., 1999). The industrial application and commercial value of these minerals could be enhanced by improving their purity, texture and colour properties such as whiteness, brightness, opacity and tint. These properties are primary and crucial for their wider industrial and commercial applications. But presence of metals such as iron is a major factor affecting and limiting their industrial application and uses. The greater the Fe-impurity contents in the mineral, the lesser the area of its industrial application (Mowla et al., 2008; Banza et al., 2006; Psyrillos et al., 1999). The whiteness and brightness index are largely dependent on the overall effect of *Lab* values. The values of *a* and *b* can be directly correlated to “free” and “structural” iron in the minerals respectively (Chandrasekhar and Ramaswamy, 2006). The “free” iron is more easily attacked by bacteria than the structural one because of its low solubility (Chandrasekhar and Ramaswamy, 2006). Removal of these impurities from Fe(III)-bearing minerals like kaolin and silica sand using conventional methods is reported to be quite expensive and environmentally unfriendly due to the waste generated (Hosseini et al., 2007; Styriakova et al., 2007; Lee et al., 2002).

The work presented in this thesis describes the application of dissimilatory reduction mechanisms as an alternative for improving industrial value of kaolin, silica sand and to a lesser extent calcium carbonate (chalk). This is because several studies have demonstrated that dissimilatory iron-reducing bacteria, like *Shewanella* strains, can use insoluble Fe(III) oxide minerals as a terminal electron acceptor for energy conservation and growth which in the process transformed Fe(III) to Fe(II) at the surface of iron oxide particles. This facilitates an industrial mineral's ability to release metals which can have a profound impact on the

mineral or environmental quality (Bose et al., 2009; Lee et al., 2002). In addition to this, an entirely different bioleaching approach was employed for chalk because Fe-impurities associated with carbonate are mostly present in the form of siderite (FeCO_3). The studies generally involved initial optimisation of bioleaching processes using a small scale microcosm approach where Fe(III) removal efficiency was evaluated through examining the bioreduction potential of some selected commercially available iron reducing *Shewanella* strains. The effect of temperature, cell density, slurry density, electron donor concentration, multiple cell inoculation were investigated, and an assessment was made of the impact of anthraquinone-2,6-disulphonate (AQDS) and natural organic matter (NOM - as a possible substitute to AQDS) in enhancing the rate of electron transfer between iron reducers and Fe(III) oxides in the mineral. Of interest in this study is that the outcome of small scale laboratory studies was tested on a pilot scale using 4.5L batch bioreactors with the aim of understanding and outlining procedures for larger scale pilot production for commercial and environmental benefit.

8.1: Optimisation of bioleaching process using small scale microcosm

For industrial application all the five selected iron-reducing bacteria (*Shewanella putrefaciens* CIP8040, *Shewanella putrefaciens* CN32, *Shewanella oneidensis*, *Shewanella algae* BRY and *Shewanella loihica*) are potential candidates for bioleaching of Fe(III), with the exception of *S. loihica*, through coupling oxidation of lactate to the reduction of Fe(III) in kaolin and silica sand. However, there were significant differences between these strains with respect to the rate and extent of Fe(III) reduction. The maximum removal of Fe(III) in kaolin (Chapter 3 and 4) is achieved using *Shewanella putrefaciens* CIP8040 leading to the removal of ~46.6mg of bioreducible Fe_2O_3 per 100g of kaolin 2 (Remblend) after 5 days of bioleaching (in comparison to Fe_2O_3 determined by XRF analysis). This is equivalent to ~4.4% of the total Fe-bearing impurities initially present in the mineral. This Fe(III) removal by *Shewanella putrefaciens* CIP8040 resulted in an increase of whiteness by 10.1% and brightness by 3.6%. On the other hand, the removal efficiency of the other *Shewanella* strains ranges between 30.8 – 44.9mg of bioreducible Fe_2O_3 per 100g of kaolin (~2.9 – 4.28% bioreducible Fe_2O_3) and resulted in approximately 7.4% improvement in whiteness and 2.3% in brightness. The observation above was similar to observations made by Lee et

Comment [DM60]: Why is *S. loihica* different? Maybe divide this sentence into two sentences – one on the first 4 and the second on *S. loihica*.

al., (2002) where the amount of iron impurities in low grade kaolin decrease to 3.7 from 5.1 wt.% Fe₂O₃ after biotreatment with unidentified indigenous microbial cultures.

Moreover, *Shewanella loihica* was not able to couple oxidation of lactate to the reduction of Fe(III) in both kaolin and silica sand with only 0.08mg of bio-reducible Fe₂O₃ per 100g of kaolin (0.01% Fe₂O₃ of Fe-impurities removed). This bacterium is known to utilize lactate or formate as electron donor during anaerobic respiration (Nakamura et al., 2010; O'Loughlin et al., 2007). At the same time, studies have shown that *Shewanella loihica* is a psychrotolerant bacteria capable of growing at a temperature of 5°C or lower with a remarkable rate of growth at temperatures as low as 8°C and as high as 37°C. The bacterium has an optimal temperature requirement of 18°C (Gao et al., 2006; Roh et al., 2006). This low temperature requirement may support the reason why the bacteria was not able to support Fe(III) bio-reduction within the temperature limit in our system. Because of the low temperature requirement, this bacterial strain may not be commercially applicable at medium temperature but may be a useful candidate for a field study pilot scale experiment considering the low temperature climate in the UK.

In Chapter 5, apart from *S. loihica*, all the tested iron-reducing bacteria were able to reduce Fe(III) in silica sand (silica sand 2, from Oakamoor). *S. putrefaciens* CIP8040 and *S. oneidensis* have almost similar bio-leaching rates with an average of ~101mg of bio-reducible Fe₂O₃ per 100g of silica (~15.12% Fe₂O₃). *Shewanella algae* BrY was the most efficient reducer in silica sand 2 (Oakamoor) with a maximum iron removal of ~117.3mg of bio-reducible Fe₂O₃ per 100g of sand after 10 days. This is approximately equivalent to 17.6% of the total Fe-bearing impurities present in silica sand 2. Reduction of the ferric (Fe³⁺) fraction in chalk was also achieved using *Shewanella putrefaciens* CIP8040 (Chapter 4) with a very low amount of iron removed. Treatment with this iron reducing bacterium removed 9.15mg of bio-reducible Fe₂O₃ per 100g of chalk (approximately 8.3% of Fe-bearing mineral in the chalk) after 5 days bio-leaching. The colour properties did not improve, with a slight decrease in the whiteness below the initial value even though a portion of Fe(III) was leached.

Temperature was also observed to affect the rate of Fe(III) reduction (Chapter 3). For industrial pilot scale application, a temperature of around 30°C was identified as the ideal condition that enhances the rate of bioreduction. This growth temperature identified was also reported by O'Loughlin et al., (2007). The maximum bio-reducible Fe₂O₃ removed at 30°C was 67.63mg per 100g of kaolin (6.4% of Fe bearing impurities), and nearly around 41.5mg per 100g (3.9% of the Fe-bearing impurities) was removed at a temperature of 36°C after 5 days of bioreduction. The solid to liquid ratio (slurry density) also affected the rate of bioreduction in kaolin as seen in the small scale microcosm study (Chapter 3). It was observed that deploying more kaolin for a given liquid volume and constant bacterial biomass produced greater bioleaching rate and extent than using a smaller mineral mass. In addition, cell density has a great influence on the effectiveness of the bioleaching process in both kaolin (Chapter 3) and silica sand (Chapter 5). It was noticed that biotreating high mineral mass requires injection of high bacterial biomass because greater bioleaching is achieved in the presence of high cell numbers than in the presence of few bacterial cells. O'Loughlin (2008) made similar observations in his work on lepidocrocite where an increase in cell biomass was found to substantially affect the rate of lepidocrocite bioreduction.

In this work, variable lactate concentration data suggested that the rate and extent of Fe(III) reduction in both kaolin and silica sand directly depends on the concentration of lactate. The *Shewanella putrefaciens* CIP8040 response to different concentrations of electron donor was found to result in different rates and extents of Fe(III) bioreduction. More Fe(II) is leached in the presence of high concentration of electron donor. Although reduction of Fe(III) was observed at low concentration, the amount of Fe(II) leached was low. This scenario was also demonstrated in hydrous ferric oxide (HFO) reduction (Fredrickson et al., 2003) where the rate of reduction was influenced greatly by variation in electron donor concentration. It was therefore suggested that 10mM lactate was the ideal concentration required by *Shewanella putrefaciens* for achieving better bioreduction in kaolin and silica sand.

Comment [DM61]: What do you mean, high?

8.2: Effect of multiple cell injection during bioreduction

In Chapter 3, the effect of multiple cell injection in the presence of high and low electron donor was assessed for kaolin. At low concentrations of electron donor (0.5mM lactate), the

re-injection of metabolically active *Shewanella* cells resulted in rapid resumption of Fe(III) bioreduction after initial cessation (Jaisi et al., 2007b). This subsequently led to an increase in the absolute amount of Fe(II) concentration in the solution. This is an indication that fresh cells can transfer electrons to Fe(III) in the mineral after cessation of bioreduction from the initial cultures. Although the resumption in reduction was clearly apparent and has doubled the initial rate after re-inoculation of fresh *Shewanella* cells the amount of Fe(II) at the termination of experiment was very low due to the low concentration of lactate added to the system. The amount of iron removed after re-inoculation of fresh cells resulted in an increase in the whiteness by 5.5% and brightness by 0.5% only. However, at very high concentrations of lactate (5 – 20mM lactate), no rapid increase in Fe(III) reduction was noticed after multiple inoculation but a very slow and gradual increase in Fe(III) bioreduction with more Fe(II) measured on the first day of the experiment. This is because probably the greater part of Fe(III) was bioreduced at the initial state of the experiment. This resulted in an increase in the brightness by approximately 7.7% and brightness by 2%. For industrial application it is better to use high concentrations of lactate with a single inoculation than using multiple inoculations in the presence of higher or low concentrations of lactate. Similar results were also obtained when fresh cells were re-injected in silica sand (Chapter 5) containing low concentrations of lactate. A resumption of Fe(III) bioreduction was noticed but continued to progress linearly in cultures containing high concentrations of electron donor without any apparent lag period.

8.3: Effect of electron transfer mediators on the rate and extent of bioreduction

The effect of electron transfer mediators has been demonstrated using AQDS (anthraquinone-2,6-disulfonate – a humic acid analogue) for enhancing the rate of bioreduction. AQDS is designed to functionally mimic natural organic matter for transferring electron to Fe(III) bearing minerals (Royer et al., 2002). The compound plays a significant role in enhancing bioreduction of various metals, including Fe(III), by serving as a mediator between metals and microorganisms (Gu et al., 2005). The presence of this compound can rapidly increase the rate of Fe(III) reduction in iron oxide minerals (Royer et al., 2002; Lovley et al., 1998). In this work, AQDS was included in the system to stimulate and facilitate the transfer of electron from *Shewanella* cells to the surface of Fe(III) oxides and oxyhydroxides in kaolin and silica sand. The results demonstrate that AQDS is highly effective in enhancing

Comment [DM62]: What do you mean? This part of the sentence doesn't make sense.

bio-reduction by *Shewanella* strains. In addition, two natural organic matter additives (NOM 1 and NOM 2) were investigated for their electron shuttling potential. The outcome demonstrated that both NOM 1 and NOM 2 promote electron shuttling by enhancing and stimulating Fe(III) reduction using *Shewanella putrefaciens* CIP8040, with NOM 2 being identified as more efficient than NOM 1. Overall, biotreatment with AQDS was identified to yield a better result when compared with the two NOMs in kaolin and silica sand. The percentage of Fe removed in kaolin 3 (Melbur Yellow HCP) in the presence of AQDS (Chapter 3) was approximately 60mg of bio-reducible Fe_2O_3 per 100g of kaolin (5% of Fe-bearing impurities). This reduction resulted in the improvement of whiteness in the mineral by 8.27% and brightness by approximately 2%.

Comparatively, natural organic matter was observed to facilitate electron transfer in this work. Bio-reduction was evident when NOMs were added to some microcosms as an alternative to AQDS. A greater percentage of iron was removed using NOM; almost 56mg of bio-reducible Fe_2O_3 per 100g of kaolin (4.4% of Fe-bearing impurities) was effectively leached after biotreatment of kaolin 3 (Melbur Yellow HCP) in the presence of NOM 2. Significant amounts of iron were removed in the presence of NOM 2 but whiteness only improved by 1.6% and the brightness dropped below the initial value by 1.7%. Although more iron was removed using NOM 2 than with NOM 1 (45.5mg per 100g of kaolin) the whiteness after leaching in the presence of NOM 1 increased by 4.4% and brightness only increased by 0.2%, comparatively better than NOM 2. The kaolin material (Melbur Yellow HCP) is a material that has not been extensively treated. We assume that the natural organic matter, which is known to be a complex mixture of organic compounds (Gu et al., 2005), may be adsorbed and bind strongly on the surface of the mineral thereby decreasing the mineral (Kaolin 3) colour properties. Humic acids are known to be adsorbed onto mineral surfaces including kaolin thereby changing the mineral surface characteristics and reactivity (Qinyan et al., 2009). Biotreatment of kaolin 3 (Melbur Yellow HCP) may not be suitable in the presence of natural organic matter but may be satisfactory using AQDS.

In Chapter 5, one of the factors identified to influence effectiveness of electron shuttling potential of both AQDS and NOM in silica sand bio-reduction is the presence of high inoculation density. This observation was similarly reported by O'Loughlin, (2008) where

Inoculum density, concentration of electron shuttle added and reduction potential of the electron shuttling mediator were observed to greatly influence and enhance lepidocrocite bioreduction. Nevertheless, the percentage of Fe removed during bioleaching of silica sand 3 (King's Lynn), in the presence of AQDS, was approximately 86.1mg of Fe_2O_3 per 100g of sand (54.3% of the iron bearing impurities in the silica sand). Bioleaching of silica sand with NOM 2 effectively removed more iron. Around 97.9mg of bioavailable Fe_2O_3 per 100g of silica sand 2 was removed (equivalent to 59.3% of the total Fe-bearing impurities present in the silica). Although the initial rate of reduction was faster and high with the AQDS in the first day of the bioreduction, the extent of reduction was more in the presence of NOM after extending the period to about 15 days. Therefore AQDS is more effective for a shorter time frame period of bioleaching.

Similarly, *Shewanella putrefaciens* CIP8040 was able to couple reduction of Fe(III) in both silica sand and kaolin in the absence of any electron transfer mediator. As shown in Chapters 3 and 5, bioreduction in the absence of electron transfer mediator has successfully removed approximately 47.4mg of bio reducible Fe_2O_3 per 100g of kaolin 3 (Melbur Yellow HCP) within a period of five days (equivalent to 3.7% of the total Fe impurities present in the mineral). In silica sand 3 (King's Lynn), the amount of iron successfully removed by *Shewanella putrefaciens* CIP8040 in the absence of electron transport mediator accounted for approximate 47.6mg of bio reducible Fe_2O_3 per 100g of silica sand (almost 28% of the Fe-bearing mineral). It has been widely reported that in the absence of any extracellular electron transfer mediators such as quinones, dissimilatory iron-reducing bacteria such as *Shewanella* can reduce Fe(III) in minerals via direct contact or through enzymatic pathways (Cutting et al., 2009; Lloyd, 2003; Kostka et al., 1999a)

8.4: Bioleaching of chalk using *Pseudomonas mendocina* and *Desulfovibrio desulfuricans*

Growth tests in a synthetic medium using anaerobic *Pseudomonas mendocina* as one of the alternatives for bioleaching of chalk did not improve the colour properties; the colour index decreased below the initial value. The possible growth of this aerobic organism in chalk serving as the source of iron in Fe deficiency medium (FeDM) might suggest an indication of iron utilisation and was the only means used to assess iron uptake. *Pseudomonas*

mendocina and other microorganisms are known to require Fe at a very low concentration to support growth (Hersman et al., 2001). This may possibly explain why no colour increase was achieved even though bacterial growth was observed. Moreover, *Desulfovibrio desulfuricans*, a sulfate-reducing bacteria used as the third major alternative for possible precipitation of iron (Fe^{2+}) as FeS in chalk, has also not successfully improved the colour properties after bioleaching. The organism was able to precipitate Fe in the chalk as FeS because the characteristic dark FeS colouration was observed. The colour properties after bioleaching decreased far below the initial value because the washing process employed to separate FeS phase from the treated chalk was unsuccessful.

8.5: Comparison of iron removed from kaolin silica sand and carbonate (chalk)

The rate of iron reduction or the amount of bio reducible Fe_2O_3 leached from kaolin, silica sand and carbonate (chalk) were compared at the end of the experiments to understand how the different minerals respond to the bioleaching process. The results show a clearly distinct variation in the rate of iron removal from these minerals. *Shewanella putrefaciens* CIP8040 was able to effectively reduce more iron from kaolin than from silica sand and carbonate when the amount of Fe(III) reduced is expressed as concentration of Fe(II) in aqueous solution. In one way this variation could be related to the mass of mineral employed during bio reduction because more kaolin (20g) was bioleached than the silica sand (2.5g) used in the same volume of solution and cell suspension. It is obvious going by the mass of mineral used that there are more bio reducible Fe(III) in kaolin material to accept more electrons than present in the silica sand.

On the other hand, expressing the amount of iron bio reduced in terms of % Fe_2O_3 removed per gram of mineral material shows that more bio reducible Fe_2O_3 is effectively removed from silica sand compared to kaolin and carbonate material. Therefore it was clear that Fe(III) in the silica sand matrix was more susceptible to bacterial reduction than that in the kaolin. This observation could be related to the nature of how the iron-oxide impurities are mineralogically present or associated with the different minerals. For example iron impurities in the kaolinite are present as both structural and free Fe, but the free form of iron is more easily and readily attacked by bacteria than the structural iron because of their

low solubility (Chandrasekhar and Ramaswamy, 2006; Deer et al., 1999). Therefore the possibility of accessing and attacking the structural iron is very minimal. In contrast, iron-oxides in silica sand are mostly present as free mineral impurities coating the entire grain surface (Manukyan and Gabrielyan, 1999). This suggests that a greater percentage of the iron-oxide impurities can easily be accessed and leached out of the silica sand during bioreduction. In the carbonate, a greater portion of the iron impurity present is mostly ferrous and the *Shewanella* may have a limited access to bioreducible ferric iron present in the carbonates. This may possibly suggest the reason as to why only a tiny amount of iron was leached from carbonate.

8.6: Batch scale bioreactor experiments

This study has looked at the possibility of upscaling microcosm work to a large laboratory bioreactor experiment for the bioleaching of silica sand and kaolin for commercial benefit using *Shewanella*. Bioreduction of both silica sand and kaolin was successfully supported after upscaling in the presence of *Shewanella putrefaciens* CIP8040. Iron was effectively leached from all the three different kaolins used. The iron removed in kaolin 2 (Remblend) when expressed in weight by weight% of the mineral bioleached was approximately around 62.6mg of bioreducible Fe_2O_3 per 100g of kaolin (5.9% of the total Fe-bearing mineral). This was even more than the iron leached using the same kaolin material in small scale bioleaching experiment (46.6mg of bioreducible Fe_2O_3 per 100g) even though less kaolin mass was used. The treatment resulted in an increase in whiteness by 10.3% and brightness by 3.27%, closely similar to the values observed in the microcosm experiments. Similarly, biotreatment of kaolin 3 (Melbur Yellow HCP) effectively removed bioavailable Fe_2O_3 by 114mg per 100g of the mineral (8.9% of the total Fe impurities). The iron removed led to improvement of whiteness by 5.4% and brightness by 2.2% on day 5. Re-injection of *Shewanella* cells and further extension of the experiment to 10 days did not significantly result in resumption of any apparent bioreduction. This may be due to exhaustion of free iron or coating of Fe(II) on the mineral surface (Jaisi et al., 2007b). An increase in the brightness by 1.5% and whiteness by 6.7% was further achieved after extending the bioleaching period to 10 days. The results are in agreement with the microcosm experiments. In addition to these results, a successful third round bioreactor experiment

Comment [DM63]: Is it worth having a subheading here? If so, maybe the discussion chapter could have 2 or 3 subheadings.

with kaolin 4 (Melbur Yellow MGP) gave similar results to those for other kaolin materials. Bioleaching of this mineral removed 69.6mg of bio-reducible Fe_2O_3 per 100g of the mineral resulting in an increase in brightness of almost 1.8% and brightness of 8.2%.

The batch bioreactor experiments carried out in this piece of research also demonstrate the bio-reduction of silica sand at large scale. *Shewanella putrefaciens* CIP8040 has been able to couple reduction of iron in silica sand and effectively decreased the amount of iron present in the mineral. Bioleaching of silica sand in a large reactor is characterised by a drop in Fe(II) production after initially rapid Fe(III) reduction, which may suggest formation and precipitation of siderite (MacDonald et al., 2011). Varying amounts of iron were leached after bio-reduction of two different masses of silica in the same volume of solution. However, more iron was removed in large reactor experiments than in small scale microcosms. In addition, the length of time required using large scale bioreactors to reduce significant amounts of iron in silica sand was less than the time observed to be required in the small scale bioleaching experiment. For example, using a bioreactor about 89.03mg of bio-reducible Fe_2O_3 per 100g of silica sand was removed on day 4, but 86.1mg per 100g of silica sand was leached in microcosms experiment after 15 days. This suggests that upscaling the bioleaching process be appropriate for commercial benefit.

8.7: Impact of bioleaching on mineralogy

Partial destruction of kaolin platelets has occurred as seen from SEM investigation, but mineralogical assessment examined by analytical technique such as X-ray diffraction, Fourier transformed infrared spectroscopy reveals no major crystallographic change or significant alteration in the mineral framework after bio-reduction. Although bio-reduction was evident, the effect of bio-reduction may not necessarily have much impact on the mineral crystal structure. Iron oxides on the mineral surface or “free” iron are known to be more easily attacked by bacteria than structural iron because of its low solubility (Chandrasekhar and Ramaswamy, 2006). This was supported by the increase in the colour value a usually observed (signifying reduction of the surface iron rather than structural iron) after colour analysis of the kaolin material. Likewise bulk chemistry of kaolin confirmed by EDX and chemical assay using XRF both reveal decrease of Fe content after bio-reduction. Similarly,

Comment [DM64]: This could be a third section – entitled ‘impact on mineralogy’

no major changes were revealed by FTIR and XRD after bioreduction of silica sand. The bioleaching has no impact on the crystallinity of the mineral. The EDX analysis of the quartz grains and XRF data obtained reveals changes in the bulk chemical composition, with Fe content decreasing after reduction. Similarly biotreatment did not affect the chemistry of chalk because the mineralogy remains the same after biotreatment.

In general, bioleaching does not affect the crystal structure of the mineral and at the same time no crystalline by-products which may possibly affect the quality of the mineral were detected by any analytical technique. Although formation of crystalline by-products may not be completely ruled out, the bioreduction time frame may be too short for them to accumulate and build up in the system. For example, Mössbauer analysis of biotreated kaolin has revealed an increase in the Fe(III) doublet, which suggests possible retention of Fe(II) in the solid phase of kaolin which may promote mineral transformation to more crystalline Fe(II) oxide by-products (Hansel et al., 2004; Zachara et al., 2002). This might be important for industrial and commercial applications, because accumulation of a crystalline by-product may possibly have another negative impact on the mineral quality.

The work reported in this thesis has shown that dissimilatory iron reduction is an important process that can be used for the biorefinement of Fe(III)-containing minerals most particularly silica sand and clay minerals like kaolin. Microbiological refining of these iron bearing minerals should be considered for commercial pilot scale application. This is necessary because the large scale batch bioreactor experiments removed almost same or more iron bearing impurities compared with the corresponding small scale experiments. These appreciably improved the quality and colour properties of the initial material.

Comment [DM65]: Do you mean Fe(II) or Fe (III)? Check each time you use one or the other.

CHAPTER 9 : GENERAL CONCLUSION AND FUTURE WORK

9.1: GENERAL CONCLUSION

Industrial minerals such as kaolin, silica sand and carbonate minerals are rarely pure, containing certain Fe-bearing impurities (mainly Fe(III)oxide) present in the form of oxides and oxy-hydroxides that generally affect and limit their industrial application. Microbial removal of iron in these minerals could be a suitable way for improving their quality and industrial value considering the environmental, operational, economical and technological disadvantages posed by the convention chemical and physical methods widely used. However, iron impurities associated with carbonate are mostly ferrous, present in the form of siderite (FeCO_3), and require a different bioleaching approach.

The reduction of iron oxide impurities present in the kaolin, silica and carbonate (chalk) were investigated using different commercially available iron-reducing bacteria. To date, investigation of iron reduction using iron-reducing bacteria in a closed system were mostly conducted at small scale laboratory experiments. This study to the best of our knowledge was the first to use iron-reducing bacteria in a closed system large bioreactors for the bioreduction of iron bearing impurities present in industrial kaolin and silica sand.

All the commercially available iron-reducing bacteria tested in this research except *Shewanella loihica* were able to reduce and leach iron (III) in kaolin, silica sand and some portion of the ferric fraction in chalk, by coupling oxidation of lactate to anaerobic respiration. This anaerobic respiration is apparently one of the mechanisms by which the iron-reducing bacteria may reduce Fe(III) in many iron bearing minerals. Among the selected commercially available *Shewanella* strains used, *Shewanella putrefaciens* CIP8040 was the most efficient for the bioreduction of kaolin and *Shewanella algae* BrY was suitable for the

bio-reduction of silica sand in small scale experiments. The aerobic *Pseudomonas mendocina* used for the bio-leaching of chalk may be able to utilise iron in the carbonate to support growth. Although this organism is known to solubilise and transport iron into the cell from solid Fe-bearing phase, the amount of iron uptake resulting from mineral dissolution may be very low and hence not much improvement in the colour properties has resulted. In addition, the use of *Desulfovibrio desulfuricans*, a sulphate-reducing bacterium, has not been successful in improving the quality of the chalk even though the bacteria were able to precipitate iron in the mineral as FeS, giving a characteristic dark coloration.

Apart from assessing the potential of different *Shewanella* strains on the rate and extent of bio-reduction in kaolin and silica sand, other factors were identified to influence the rate and extent of the bio-leaching process in small scale experiments. For example, the rate and extent of Fe(III) reduction was observed to be dependent on temperature. A temperature of around 30°C was the identified optimal temperature required by *Shewanella putrefaciens* CIP8040 for effective bio-leaching although bio-leaching was also observed at elevated temperature of 36°C and at a low temperature of 20°C. The solid to liquid ratio (slurry density) is paramount in the bio-leaching process because deploying more mineral for a given liquid volume and constant bacterial biomass produces greater bio-leaching rate and extent than deploying a smaller mineral mass. Furthermore the overall rate of Fe(III) reduction depends also on the cell density in both kaolin and silica sand because substantial amounts of iron were removed in the presence high cell density than low cell density.

In addition, the rate and extent of bio-reduction directly depends on the concentrations of electron donor (lactate) present. More iron was removed in the presence of high concentration of lactate (10 -20mM) than in the presence of low concentration (0.1mM lactate). Moreover, addition of metabolically active cells after initial cessation of Fe(III) reduction was observed to rapidly increase the rate of reduction when a low concentration of electron donor (0.5mM lactate) was used with kaolin. But gradual and linear resumption of Fe(III) reduction was seen when a high concentration of electron donor (5 -20mm lactate) was added in experiments with kaolin and silica sand.

The effects of electron transfer mediators were demonstrated using AQDS (anthraquinone 2,6 disulphonate – a humic acid analogue) and natural organic matter (NOM). It was found that addition of AQDS greatly influenced and enhanced the overall rate and extent of bioreduction in comparison to experiments without AQDS. This is because the AQDS alleviates the need for *Shewanella* cells to establish a direct physical contact with the insoluble Fe(III) oxides in the mineral. Bioleaching of the three different kaolin materials in the presence of AQDS has generally increased the brightness and whiteness values thereby improving the optical properties of the mineral material. Similarly, the two natural organic matter (NOM) samples tested for their electron shuttling potential were also able to support electron transfer, and enhanced the bioreduction of Fe(III) in the presence of *Shewanella putrefaciens* CIP8040. The rate and extent of Fe(III) bioreduction varied amongst the two NOMs with NOM 2 appeared to be better than NOM 1. It was found out that biotreatment with the NOMs decreased the colour properties of kaolin 3 (Melbur Yellow HCP – a dirty non processed kaolin material), probably due to absorption of these compounds on mineral surfaces.

Importantly this research has successfully upscaled the bioleaching process after initial optimisation of small microcosm studies. Like in the small-scale bioreduction, *Shewanella putrefaciens* CIP8040 was able to anaerobically couple reduction of Fe(III) in kaolin and silica sand to the oxidation of lactate in the presence of anthraquinone-2,6-disulfonate serving as electron transport mediator. The solution chemistry in the reactor was observed to remain consistent throughout the experiment suggesting low accumulation of organic acids. The amount of iron leached was even more than or similar to the amount of iron bioleached in the small scale microcosms. Consequently, improvement of the colour values was achieved with an increase above the initial colour value. The colour improvement was consistent with what has been achieved in small scale microcosms. In general, the results from bioreactor indicated that more satisfying results could be achieved when bioleaching conditions are properly optimized.

For the carbonate material, no improvement in the colour properties was achieved, even though evidence of Fe utilisation by *Pseudomonas mendocina* was observed through monitoring growth by optical density. Moreover, subsequent bioleaching with *Desulfovibrio*

desulfuricans - a sulphate-reducing bacterium did not improve the colour properties of chalk, although the bacterium was observed to be able to leach Fe from the mineral, but the iron precipitated as a different iron phase (possibly iron sulfide).

The mineralogical assay using XRF and SEM-EDX has revealed decreases in the iron content after bioreduction in both kaolin and silica sand. Further assessment using other analytical techniques such as XRD and FTIR reveals that the observed bioreduction was mostly from the bacterial attack of the free surface iron(III) oxides but not the structural iron. This is because no major changes have occurred between the bioleached and the initial mineral material. In addition, the bioreduction does not cause formation of any apparent crystalline by-product. The bioreduction has not resulted in any unfavourable modification in the mineralogy of either kaolin or silica sand.

The work reported in this thesis has shown that dissimilatory iron reduction is an important process that can be used for the biorefinement of Fe(III)-containing minerals most particularly silica sand and clay minerals like kaolin. Microbiological refining of these iron bearing minerals should be considered for commercial pilot scale application. This is necessary because the large-scale batch bioreactor experiments removed almost the same or more iron bearing impurities compared with the corresponding small scale experiments. These appreciably improved the quality and colour properties of the initial material.

Comment [DM66]: Can you make any comment about the carbonate experiments, as a separate paragraph? Or do you prefer not to, given that they were only at small scale.

9.2: FUTURE WORK

This study has explored the possibility of using iron-reducing bacteria for the bioreduction of kaolin and silica sand, and part of the ferric fraction in chalk, but there are still few areas that may require further attention in order to optimise the bioleaching process for full commercial application and benefit, most specifically the bioreactor experiment. In view of the observations made in the course of this study, it will be useful if the following areas are given further attention:

- Experiments may be required with small-scale microcosms to further investigate the effect of different concentrations of electron transfer mediators (AQDS and NOM) in order to identify and unravel the ideal concentration that may be required for

optimal electron transfer to Fe(III) oxides in kaolin and silica sand. This is necessary because this research has only maintained a constant dose (concentration) of electron shuttling system (100µm). In addition batch experiments at different pH values should also be investigated in order to relate the effect of low and high hydrogen ion concentrations on the bioleaching process.

- Because of the low temperature requirements of *Shewanella loihica* which was lower than the temperature limit in our system, it will be highly recommended to consider further experiments at a temperature between 4°C and 15°C. In addition, it will be of industrial relevance to consider a field study pilot scale experiments considering the low temperature climate in the UK. This will provide better understanding on the different temperature response of this bacteria due to the outdoor temperature variations
- Only total organic carbon (TOC) was analysed, and the TOC equivalent of lactate calculated from the TOC data was used to understand the stoichiometry of lactate oxidation to Fe(III) reduction in the system. It is worthwhile to properly analyse the lactate and acetate turnover during the bioreduction process in order to better understand the stoichiometry of mineral Fe(III) respiration. This will allow a proper quantification of how much organic carbon was depleted relative to the amount of Fe(III) reduced by *Shewanella* cells.
- Although no improvement was achieved after bioleaching of chalk using sulfate-reducing bacteria even though evidence of iron probably precipitating as FeS was observed. It will therefore be useful to test different approaches for separating the dark phase of FeS formed by *Desulfovibrio desulfuricans* from the chalk mineral, such as the use of chelating agents like NTA or EDTA (ethylenediaminetetraacetic acid) during biotreatment. This may solubilise the dark phase which could then be removed easily. At the same time, further investigation is also needed to test and develop the bioleaching of carbonate with entirely different bacteria.

- Further experiments are required to be conducted using the large bioreactors for the bioleaching of kaolin and silica. It will be important to provide an improved mechanical stirrer that will keep the high density slurry of kaolin in suspension. This will allow for proper investigation and testing of different mineral to liquid ratio and cell to solid ratio, in order to optimise the bioleaching process at production scale. It may be possible that a large bacteria:solid ratio and/or lower solid:liquid ratio would be more appropriate at large scale.
- A new packed column bioreactor with flow-through system should be fabricated and tested for the bioleaching of silica sand. This will permit the bioleaching of large amounts of solid silica sand, because the silica sand tends to settle during the experiment at the bottom of the reactors due to its density. Because of this the reactors do not support bioleaching of large amounts of silica sand. Possible precipitation and formation of secondary mineralisation products were **inferred** due to sudden drop in ferrous iron during bio-reduction of silica sand. This should be further investigated to identify if there is siderite formation in the system.
- Part of the initial plan of this research was to isolate indigenous iron-reducing bacteria that may be present in the fresh kaolin and silica sand with the intention of comparing their iron reduction potential with the commercially available iron-reducing bacteria. This should be further tested to see if the indigenous iron reducers will produce better bioleaching of the mineral material.

Comment [DM67]: Inferred if deduced from solution compositional data; observed if identified as a solid product.

REFERENCES

- Ambikadevi, V. R. and Lalithambika, M. (2000) 'Effect of organic acids on ferric iron removal from iron-stained kaolinite', *Applied Clay Science*, 16, (3-4), pp. 133-145.
- Anderson, R. T., Rooney-Varga, J. N., Gaw, C. V. and Lovley, D. R. (1998) 'Anaerobic benzene oxidation in the Fe(III) reduction zone of petroleum-contaminated aquifers', *Environmental Science & Technology*, 32, pp. 1222 - 1229.
- Anton, K. and Terry, J. B. (2007) 'The surface physicochemistry and adhesiveness of *Shewanella* are affected by their surface polysaccharides', *Microbiology*, 159, pp. 1872-1883.
- Antonio, M. R., Tischler, M. L. and Witzcak, D. (2000) 'Extracellular iron-sulfur precipitates from growth of *Desulfovibrio desulfuricans*', *Material Research Society Symposium Proceedings*, 590, (33 - 38).
- Asmatulu, R. (2002) 'Removal of the discoloring contaminants of an East Georgia kaolin clay and its dewatering', *Turkish Journal of Engineering & Environmental Sciences*, 26, pp. 447-453.
- Atkins, P. and De Paula, J. (2010) 'Physical Chemistry', University Press: Oxford. New York., pp. 1 - 972.
- Bain, D. C., McHardy, W. J. and Lachowski, E. E. (1996) 'X-ray fluorescence spectroscopy and microanalysis', in Wilson, M.J. (Ed), 'Clay Mineralogy: Spectroscopic and Chemical Determinative Methods.', Oxford: Chapman & Hall, pp. 260 - 299.
- Banza, A. N., Quindt, J. and Gock, E. (2006) 'Improvement of the quartz sand processing at Hohenbocka', *International Journal of Mineral Processing*, 79, (1), pp. 76-82.
- Bide, T., Idoine, N. E., Brown, T. J. and Smith, K. (2010) 'United Kingdom Minerals Yearbook 2010, British Geological Survey,' Mineral and Waste Water Programme: Open Report OR/11/032, pp. 1 - 104.

- Bloodworth, A. J., Highley, D. E. and Mitchell, C. J. (1993) 'Industrial Minerals Laboratory Manual', (Technical Report WG/93/1; Keyworth, Nottingham, British Geological Survey.), pp. 1 - 72.
- Bond, D. R. and Lovley, D. R. (2005) 'Evidence of involvement of an electron shuttle in electricity generation by *Geothrix fermentans*', *Applied & Environmental Microbiology*, 71, pp. 2186 - 2189.
- Bonneville, S., Behrends, T. and Cappellen, P. V. (2009) 'Solubility and dissimilatory reduction kinetics of iron(III) oxyhydroxides: A linear free energy relationship', *Geochimica et Cosmochimica Acta*, 73, pp. 5273 - 5282.
- Bonneville, S., Behrends, T., Van Cappellen, P., Hyacinthe, C. and Roling, W. F. M. (2006) 'Reduction of Fe(III) colloids by *Shewanella putrefaciens*: A kinetic model ', *Geochimica et Cosmochimica Acta*, 70, pp. 5842 - 5854.
- Bonneville, S., Van Cappellen, P. and behrends, T. (2004) 'Microbial reduction of iron(III) oxyhydroxides: effects of mineral solubility and availability', *Chemical Geology*, 212, pp. 255 - 268.
- Bose, S., Hochella Jr, M. F., Gorby, Y. A., Kennedy, D. W., McCready, D. E., Madden, A. S. and Lower, B. H. (2009) 'Bioreduction of hematite nanoparticles by the dissimilatory iron reducing bacterium *Shewanella oneidensis* MR-1', *Geochimica et Cosmochimica Acta*, 73, (4), pp. 962-976.
- Bozal, N., Montes, M. J., Tudela, E., Jimenez, F. and Guinea, J. (2002) '*Shewanella frigidimarina* and *Shewanella livingstonensis* sp. nov. isolated from Antarctic coastal areas.', *International Journal of Systematic and Evolutionary Microbiology*, 52, pp. 195 - 205.
- Bristow, C. M. and Scott, P. W. (1998) 'Kaolinized Devonian Metasediments Adjacent to the St. Austell Granite Cornwall', *Geoscience in south-west England*, 9, (255 - 262).
- British Geological Survey, (2006) 'Limestone. Mineral Planning Factsheet. Office of the Deputy Prime Minister. British Geological Survey, access on 17/07/2011', (www.bgs.ac.uk/downloads/start.cfm?id=1361).
- British Geological Survey, (2006a) 'Silica sand. Mineral Planning Factsheet. Office of the Deputy Prime Minister: Creating Suitable Community. British Geological Survey. access on 16/06/08 at', , (http://www.mineralsuk.com/britmin/mpfsilica_sand.pdf).

- British Geological Survey, (2006b) 'Kaolin. Mineral Planning Factsheet. Office of the Deputy Prime Minister: Creating Sustainable Community. British Geological Survey, access on 16/06/2008', (<http://www.mineralsuk.com/britmin/mpfkaolin.pdf>).
- British Geological Survey, (2009a) 'Silica sand. Mineral Planning Factsheet. Community and Local Government. British Geological Survey, access on 17/03/2011', (www.bgs.ac.uk/downloads/start.cfm?id=1369).
- British Geological Survey, (2009b) 'Kaolin. Mineral Planning Factsheet. Communities and Local Government. British Geological Survey, access on 17/03/2011', (www.bgs.ac.uk/downloads/start.cfm?id=1362).
- Burgos, W. D., Fang, Y., Royer, R. A., Yeh, G.-T., Stone, J. J., Jeon, B.-H. and Dempsey, B. A. (2003) 'Reaction-based modeling of quinone-mediated bacterial iron(III) reduction', *Geochimica et Cosmochimica Acta*, 67, (15), pp. 2735-2748.
- Caccavo, F., Jr., Blakemore, R. P. and Lovley, D. R. (1992) 'A hydrogen-oxidizing Fe(III)-reducing microorganism from the Great Bay estuary, New Hampshire', *Appl. Environ. Microbiol.*, 58, pp. 3211 - 3216.
- Caccavo, F., Jr., Coates, J. D., Rossello-Mora, R. A., Ludwig, W., Schleifer, K. H., Lovley, D. R. and McInerney, M. J. (1996a) '*Geovibrio ferrireducens*, a phylogenetically distinct dissimilatory Fe(III)-reducing bacterium', *Archives of Microbiology*, 165, pp. 370 - 376.
- Caccavo, F., Jr. and Das, A. (2002) 'Adhesion of dissimilatory Fe(III)-reducing bacteria to Fe(III) minerals', *Geomicrobiology Journal*, 19, pp. 161 - 177.
- Caccavo, F., Jr., Frolund, B., Van Ommen Kloeke, F. and Nielsen, P. H. (1996b) 'Deflocculation of activated sludge by the dissimilatory Fe(III)-reducing bacterium *Shewanella algae* BrY', *Applied & Environmental Microbiology*, 62, pp. 1487 - 1490.
- Caccavo, F., Jr., Schamberger, P. C., Keiding, K. and Nielsen, P. H. (1997) 'Role of hydrophobicity in the adhesion of the dissimilatory Fe(III)-reducing *Shewanella algae* BrY to amorphous Fe(III) oxide.', *Applied & Environmental Microbiology*, 63, pp. 3837 - 3843.
- Cameselle, C., Ricart, M. T., Núñez, M. J. and Lema, J. M. (2003) 'Iron removal from kaolin. Comparison between "in situ" and "two-stage" bioleaching processes', *Hydrometallurgy*, 68, (1-3), pp. 97-105.

- Chandrasekhar, S. and Ramaswamy, S. (2002) 'Influence of mineral impurities on the properties of kaolin and its thermally treated products', *Applied Clay Science*, 21, (3-4), pp. 133-142.
- Chandrasekhar, S. and Ramaswamy, S. (2006) 'Iron minerals and their influence on the optical properties of two Indian kaolins', *Applied Clay Science*, 33, (3-4), pp. 269-277.
- Childers, S. E., Ciufo, S. and Lovely, D. R. (2002) '*Geobacter metallireducens* accesses insoluble Fe(III) oxide by chemotaxis', *Nature*, 416, pp. 767-769.
- Coates, J. D., Ellis, D. J., Gaw, C. V. and Lovley, D. R. (1999) '*Geothrix fermentans* gen. nov., sp. nov., a novel Fe(III)-reducing bacterium from a hydrocarbon-contaminated aquifer', *International Journal of Systematic Bacteriology* 49 pt 4, (4), pp. 1615 - 1622.
- Cooper, D. C., Picardal, F., Rivera, J. and Talbot, C. (2000) 'Zinc immobilization and magnetite formation via ferric oxide reduction by *Shewanella putrefaciens* 200', *Environmental Science & Technology*, 34, pp. 100 - 106.
- Cornell, R. M. and Schwertmann, U. (2003) 'The Iron Oxides: Structure, Properties, Reactions, Occurrence and Uses', (Revised and expanded edition). Weinheim, Wiley-VCH, pp. 1 - 664.
- Cummings, D. E., Caccavo, F., Jr., Fendorf, S. and Rosenzweig, R. F. (1999) 'Arsenic mobilization by the dissimilatory Fe(III)-reducing bacterium *Shewanella alga* BrY', *Applied & Environmental Microbiology*, 33, (723 - 729).
- Cummings, D. E., Snoeyenbos-West, O. L., Newby, D. T., Niggemeyer, A. M., Lovley, D. R., Achenbach, L. A. and Rosenzweig, R. F. (2003) 'Diversity of *Geobacteraceae* Species Inhabiting Metal-Polluted Freshwater Lakes Ascertained by 16S rDNA Analyses', *Microbial Ecology* 46, pp. 257 - 269.
- Cunningham, A. B., Gerlach, R., Sharp, R. R. and Caccavo, F., Jr. (2007) 'Effect of starvation on bacterial transport through porous media', *Advances in Water Resources*, 30, pp. 1583 - 1592.
- Cutting, R. S., Coker, V. S., Fellowes, J. W., Lloyd, J. R. and Vaughan, D. J. (2009) 'Mineralogical and morphological constraints on the reduction of Fe(III) minerals by *Geobacter sulfurreducens*', *Geochimica et Cosmochimica Acta*, 73, (14), pp. 4004-4022.

- Das, A. and Caccavo, F., Jr. (2001) 'Adhesion of the dissimilatory Fe(III) reducing bacterium *Shewanella alga* BrY to hydrous ferric oxide', *Current Microbiology*, 42, pp. 151 - 154.
- de Mesquita, L. M. S., Rodrigues, T. and Gomes, S. S. (1996) 'Bleaching of Brazilian kaolins using organic acids and fermented medium', *Minerals Engineering*, 9, (9), pp. 965-971.
- Deer, W. A., Howie, R. A. and Zussman, J. (1999) 'An Introduction to Rock - Forming Minerals; 2nd Edition', London: Longman, pp. 1 - 696.
- Department for Communities and Local Government, (1996) 'Minerals Planning Guidance 15: Provision of silica sand in England, access on 12/08/2011', www.communities.gov.uk/documents/planningandbuilding/.../155508.doc
- Dhungana, S., Anthony III, C. R. and Hersman, L. E. (2007) 'Effect of Exogenous Reductant on Growth and Iron Mobilization from Ferrihydrite by the *Pseudomonas mendocina* ymp Strain', *Applied & Environmental Microbiology*, 73, (10), pp. 3428 – 3430.
- Dhungana, S. and Crumbliss, A. L. (2005) 'Coordination Chemistry and Redox Processes in Siderophore-Mediated Iron Transport', *Geomicrobiology Journal*, 22, pp. 87-98.
- Dong, H., Kukkadapu, R. K., Fredrickson, J. K., Zachara, J. M., Kennedy, D. W. and Kostandarithes, H. M. (2003) 'Microbial Reduction of Structural Fe(III) in Illite and Goethite', *Environmental Science & Technology*, 37, (7), pp. 1268-1276.
- Du, F., Li, J., Li, X. and Zhang, Z. (2011) 'Improvement of iron removal from silica sand using ultrasound-assisted oxalic acid', *Ultrasonics Sonochemistry*, 18, (1), pp. 389-393.
- Fadrus, H. and Maly, J. (1975) 'Suppression of Iron(III) Interference in the Determination of Iron (II) in Water by the 1,10-Phenanthroline Method.', *Analyst*, 100, pp. 549 - 554.
- Finneran, K. T., Johnsen, C. V. and Lovley, D. R. (2003) '*Rhodoferax ferrireducens* sp. nov., a psychrotolerant, facultative anaerobic bacterium that oxidizes acetate with the reduction of Fe(III)', *International Journal of Systematic and Evolutionary Microbiology*, 53, pp. 1911 - 1916.
- Fischer, W. R. (1988) 'Microbiological reaction of iron in soils. In iron in soil and clay minerals.(Eds. J. W. Stucki, B.A. Goodman, and U. Schewertmann)', D. Reidel Publ. Co., pp. 715 - 748.
- Fredrickson, J. K., Kota, S., Kukkadapu, R. K., Liu, C. and Zachara, J. M. (2003) 'Influence of Electron Donor/Acceptor Concentrations on Hydrous Ferric Oxide (HFO) Bioreduction', *Biodegradation*, 14, (2), pp. 91-103.

- Fredrickson, J. K., Zachara, J. M., Kennedy, D. W., Dong, H., Onstott, T. C., Hinman, N. W. and Shu-mei, L. (1998) 'Biogenic iron mineralization accompanying the dissimilatory reduction of hydrous ferric oxide by a groundwater bacterium', *Geochimica et Cosmochimica Acta*, 62, pp. 3239 - 3257.
- Fredrickson, J. K., Zachara, J. M., Kukkadapu, R. K., Gorby, Y. A., Smith, S. C. and Brown, C. F. (2001) 'Biotransformation of Ni-substituted hydrous ferric oxides by an Fe(III)-reducing bacterium', *Environmental Science & Technology*, 35, pp. 703 - 712.
- Gao, H., Obraztova, A., Stewart, N., Popa, R., Fredrickson, J. K., Tiedje, J. M., Nealson, K. H. and Zhou, J. (2006) '*Shewanella loihica* sp. nov., isolated from iron-rich microbial mats in the Pacific Ocean', *International Journal of Systematic and Evolutionary Microbiology*, 56, (8), pp. 1911-1916.
- Gates, W. P., Jaunet, A.-M., Tessier, D., Cole, M. A., Wilkinson, H. T. and Stucki, J. W. (1998) 'Swelling and texture of iron-bearing smectites reduced by bacteria', *Clays and Clay Minerals*, 46, (5), pp. 487-497.
- Gebrehiwet, T. A. and Krishnamurthy, R. V. (2007) 'Isotopic and chemical investigations of Fe(III) reduction by *Shewanella putrefaciens* strain 200R', *Geobiology*, 5, pp. 391 - 399.
- Gorby, Y. A., Yanina, S., McLean, J. S., Rosso, K. M., Moyles, D., Dohnalkova, A., Beveridge, T. J., Chang, I. S., Kim, B. H., Kim, K. S., Culley, D. E., Reed, S. B., Romine, M. F., Saffarini, D. A., Hill, E. A., Shi, L., Elias, D. A., Kennedy, D. W., Pinchuk, G., Watanabe, K., Ishii, S., Logan, B., Nealson, K. H. and Fredrickson, J. K. (2006) 'Electrically conductive bacterial nanowires produced by *Shewanella oneidensis* strain MR-1 and other microorganisms', *Proceedings of the National Academy of Sciences*, 106, (23), pp. 9535.
- Granizo, M. L., Blanco-Varela, M. T. and Palomo, A. (2000) 'Influence of the starting kaolin on alkali-activated materials based on metakaolin. Study of the reaction parameters by isothermal conduction calorimetry', *Journal of Materials Science*, 35, (24), pp. 6309-6315.
- Gu, B. and Chen, J. (2003) 'Enhanced microbial reduction of Cr(VI) and U(VI) by different natural organic matter fractions', *Geochimica et Cosmochimica Acta*, 67, (19), pp. 3575-3582.
- Gu, B., Yan, H., Zhou, P., Watson, D. B., Park, M. and Istok, J. (2005) 'Natural Humics Impact Uranium Bioreduction and Oxidation', *Environmental Science & Technology*, 39, (14), pp. 5268-5275.

- Gunasekaran, S., Anbalagan, G. and Pandi, S. (2006) 'Raman and infrared spectra of carbonates of calcite structure', *Journal of Raman Spectroscopy*, 37, (9), pp. 892-899.
- Guo, M.-R., He, Q.-X., Li, Y.-M., Lu, X.-q. and Chen, Z.-l. (2010) 'Removal of Fe from Kaolin using Dissimilatory Fe(III)-Reducing Bacteria', *Clays and Clay Minerals*, 58, (4), pp. 515-521.
- Hansel, C. M., Benner, S. G., Nico, P. and Fendorf, S. (2004) 'Structural constraints of ferric (hydr)oxides on dissimilatory iron reduction and the fate of Fe(II)', *Geochimica et Cosmochimica Acta*, 68, (15), pp. 3217-3229.
- Hersman, L. E., Forsythe, J. H., Ticknor, L. O. and Maurice, P. A. (2001) 'Growth of *Pseudomonas mendocina* on Fe(III) (Hydr)Oxides', *Applied & Environmental Microbiology*, 67, (10), pp. 4448-4453.
- Hersman, L. E., Maurice, P. and Sposito, G. (1996) 'Iron acquisition from hydrous Fe(III)-oxide by an aerobic *Pseudomonas sp.*', *Chemical Geology*, 132, pp. 25 - 31.
- Hosseini, M. R., Pazouki, M., Ranjbar, M. and Habibian, M. (2007) 'Bioleaching of iron from highly contaminated Kaolin clay by *Aspergillus niger*', *Applied Clay Science*, 37, (3-4), pp. 251-257.
- Hyacinthe, C., Cappellen, P. V. and Bonneville, S. (2008) 'Effect of Sorbed Fe(II) on the initial Reduction Kinetics of 6-Line Ferrihydrite and Amorphous Ferric Phosphate by *Shewanella putrefaciens*', *Geomicrobiology*, 25, pp. 181 - 192.
- Industrial, M. (2009) 'Prices; Industrial Minerals', January 2009, pp. 72 - 73.
- Jaisi, D. P., Dong, H., Kim, J., He, Z. and Morton, J. P. (2007a) 'Nontronite particle aggregation induced by microbial Fe(III) reduction and exopolysaccharide production', *Clay and Clay Minerals*, 55, (1), pp. 96 - 107.
- Jaisi, D. P., Dong, H. and Liu, C. (2007b) 'Influence of biogenic Fe(II) on the extent of microbial reduction of Fe(III) in clay minerals nontronite, illite, and chlorite', *Geochimica et Cosmochimica Acta*, 71, (5), pp. 1145-1158.
- Jaisi, D. P., Dong, H. and Liu, C. (2007c) 'Kinetic Analysis of Microbial Reduction of Fe(III) in Nontronite', *Environmental Science & Technology*, 41, pp. 2437 - 2444.

- Jaisi, D. P., Dong, H. and Morton, J. P. (2008) 'Partitioning of Fe(II) in reduced nontronite (NAu-2) to reactive site: reactivity in terms of Tc(VII) reduction', *Clays and Clay Minerals*, 56, pp. 175 - 189.
- Kahraman, S., Önal, M., Sarlkaya, Y. and Bozdogan, I. (2005) 'Characterization of silica polymorphs in kaolins by X-ray diffraction before and after phosphoric acid digestion and thermal treatment', *Analytica Chimica Acta*, 552, (1-2), pp. 201-206.
- Kappler, A., Benz, M., Schink, B. and Brune, A. (2004) 'Electron shuttling via humic acids in microbial iron(III) reduction in a freshwater sediment', *FEMS Microbiology Ecology*, 47, pp. 85 - 92.
- Kato, C., Li, L., Nogi, Y., Nakamura, Y., Tamaoka, J. and Horikoshi, K. (1998) 'Extremely barophilic bacteria isolated from the Mariana Trench, Challenger Deep, at a depth of 11,000 meters', *Applied & Environmental Microbiology*, 64, pp. 1510 - 1513.
- Kazumi, J., Haggblom, M. M. and Young, L. Y. (1995) 'Degradation of monochlorinated aromatic compounds under iron-reducing conditions', *Applied & Environmental Microbiology*, 61, pp. 4069 - 4073.
- Kieft, T. L., Fredrickson, J. K., Onstott, T. C., Gorby, Y. A., Kostandarithes, H. M., Bailey, T. J., Kennedy, D. W., Li, S. W., Plymale, A. E., Spadoni, C. M. and Gray, M. S. (1999) 'Dissimilatory Reduction of Fe(III) and other Electron Acceptors by a *Thermus* Isolate', *Applied & Environmental Microbiology*, 63, (3), pp. 1241 - 1221.
- Konishi, Y., Ohno, K., Saitoh, N., Nomura, T., Nagamine, S., Hishida, H., Takahashi, Y. and Uruga, T. (2007) 'Bioreductive deposition of platinum nanoparticles on the bacterium *Shewanella algae*', *Journal of Biotechnology*, 128, (3), pp. 648-653.
- Kostka, J. E., Dalton, D., Skelton, H., Dollhopf, S. and Stucki, J. W. (2002) 'Growth of iron (III) reducing bacteria on clay minerals as the sole electron acceptor and a growth yield comparison on variety of oxidized iron form', *Applied & Environmental Microbiology*, 68, pp. 6256 - 6262.
- Kostka, J. E., Stucki, J. W., Nealson, K. H. and Wu, J. (1996) 'Reduction of structural Fe(III) in smectite by a pure culture of *Shewanella putrefaciens* strain MR-1', *Clays and Clay Minerals*, 44, (4), pp. 522-529.
- Kostka, J. E., Viehweger, H. R. and Stucki, J. W. (1999a) 'Respiration and Dissolution of Iron(III)-Containing Clay Minerals by Bacteria', *Environmental Science & Technology*, 33, pp. 3127-3133.

- Kostka, J. E., Wu, J., Nealson, K. H. and Stucki, J. W. (1999b) 'The impact of structural Fe(III) reduction by bacteria on the surface chemistry of smectite clay minerals', *Geochimica et Cosmochimica Acta*, 63, (22), pp. 3705-3713.
- Lagarec, K. and Rancourt, D. G. (1997) 'Extended Voigt-based analytic lineshape method for determining N-dimensional correlated hyperfine parameters distributions in Mössbauer spectroscopy.', *Nucl Instrum and Meth in Phys Res, B*, (129), pp. 266 - 280.
- Lee, E. Y., Cho, K. S., Ryu, H. W. and Chang, Y. K. (1999) 'Microbial Removal of Fe(III) Impurities from Clay Using Dissimilatory Iron Reducers', *Journal of Bioscience and Bioengineering*, 87, (3), pp. 397 - 399.
- Lee, E. Y., Cho, K. S. and Wook Ryu, H. (2002) 'Microbial refinement of kaolin by iron-reducing bacteria', *Applied Clay Science*, 22, pp. 47-53.
- Leonardo, M. R., Moser, D. P., Brantner, C. A., MacGregor, B. J., Paster, B. J., Stackebrandt, E. and Nealson, K. H. (1999) 'Shewanella pealeana sp. nov., a member of the microbial community associated with the accessory nidamental gland of the squid *Loligo pealei*', *International Journal of Systematic and Evolutionary Microbiology*, 49, pp. 1341 - 1351.
- Liu, C., Kota, S., Zachara, J. M., Fredrickson, J. K. and Brinkman, C. (2001) 'Kinetic analysis of the bacterial reduction of goethite', *Environmental Science & Technology*, 35, pp. 2482 - 2490.
- Lloyd, J. R. (2003) 'Microbial reduction of metals and radionuclides', *FEMS Microbiology Reviews*, 27, (2-3), pp. 411-425.
- Lloyd, J. R., Chesnes, J., Glasauer, S., Bunker, D. J., Livens, F. R. and Lovley, D. R. (2002) 'Reduction of actinides and fission products by Fe(III)-reducing bacteria', *Geomicrobiology Journal*, 19, pp. 103 - 120.
- Lobo, S. A. L., Melo, A. M. P., Carita, J. N., Teixeira, M. and Saraiva, L. M. (2007) 'The anaerobe *Desulfovibrio desulfuricans* ATCC 27774 grows at nearly atmospheric oxygen levels', *FEBS Letters*, 581, (3), pp. 433-436.
- Lovley, D. (2006) 'Dissimilatory Fe(III)- and Mn(IV)-Reducing Prokaryotes', in *The Prokaryotes*. pp. 635-658.
- Lovley, D. R. (1987) 'Organic matter mineralization with the reduction of ferric iron: A review', *Geomicrobiology Journal*, 5, (3-4), pp. 375 - 399.

- Lovley, D. R. (1991) 'Dissimilatory Fe(III) and Mn(IV) reduction', *Microbiological Reviews*, 55, pp. 259-287.
- Lovley, D. R. (1993) 'Dissimilatory Metal Reduction', *Annual Review of Microbiology*, 47, (1), pp. 263-290.
- Lovley, D. R. (1997) 'Microbial Fe(III) reduction in subsurface environment', *FEMS Microbiology Reviews*, 20, pp. 305-313.
- Lovley, D. R. (2000) 'Fe(III) and Mn(IV) reduction. In: D.R. Lovley (ed.), Environmental microbe-metal interactions', ASM Press, Washington, D.C., pp. 3-30.
- Lovley, D. R. (2001) 'Reduction of iron and humics in subsurface environment', *Subsurface Microbiology and Biogeochemistry*, pp. 193-217.
- Lovley, D. R., Baedecker, M. J., Lonergan, D. J., Cozzarelli, I. M., Phillips, E. J. and Siegal, D. I. (1989) 'Oxidation of aromatic contaminants coupled to microbial iron reduction', *Nature*, 339, pp. 297-299.
- Lovley, D. R., Coates, J. D., Blunt-Harris, E. L., Phillips, E. J. and Woodward, J. C. (1996) 'Humic substance as electron mediators for microbial respiration', *Nature*, 328, pp. 445-448.
- Lovley, D. R., Fraga, J. L., Blunt-Harris, E. L., Hayes, L. A., Phillips, E. J. P. and Coates, J. D. (1998) 'Humic Substances as a Mediator for Microbially Catalyzed Metal Reduction', *Acta hydrochimica et hydrobiologica*, 26, (3), pp. 152-157.
- Lovley, D. R., Giovannoni, S. J., White, D. C., Champine, J. E., Phillips, E. J., Gorby, Y. A. and Goodwin, S. (1993) '*Geobacter metallireducens* gen. nov. sp. nov., a microorganism capable of coupling the complete oxidation of organic compounds to the reduction of iron and other metals', *Archives of Microbiology* 159, (4), pp. 336-344.
- Lovley, D. R., Holmes, D. E., Nevin, K. P. and Poole. (2004) 'Dissimilatory Fe(III) and Mn(IV) Reduction', in *Advances in Microbial Physiology*. Vol. Volume 49 Academic Press, pp. 219-286.
- Lovley, D. R. and Lloyd, J. R. (2000) 'Microbes with a mettle for bioremediation', *Nature Biotechnology*, 18, pp. 600-601.

- Lovley, D. R., Phillips, E. J. P. and Lonergan, D. J. (1991) 'Enzymatic versus nonenzymatic mechanisms for Fe(III) reduction in aquatic sediments', *Environmental Science & Technology*, 25, pp. 1062 - 1067.
- Lovley, D. R. and Woodward, J. C. (1996) 'Mechanisms for chelator stimulation of microbial Fe(III)-oxide reduction', *Chemical Geology*, 132, (1-4), pp. 19-24.
- Luu, Y. S. and Ramsay, J. A. (2003) 'Review: microbial mechanisms of accessing insoluble Fe(III) as an energy source', *World Journal of Microbiology and Biotechnology*, 19, pp. 215 - 225.
- MacDonald, L. H., Moon, H. S. and Jaffé, P. R. (2011) 'The role of biomass, electron shuttles, and ferrous iron in the kinetics of *Geobacter sulfurreducens* mediated ferrihydrite reduction', *Water Research*, 45, (3), pp. 1049-1062.
- Manning, D. A. C. (1995) 'Introduction to Industrial Minerals', First Edition. Chapman and Hall, 2-6 Boundary Row, London., pp. 1 - 276.
- Manukyan, R. and Gabrielyan, D. (1999) 'Refinement of sand', *Glass and Ceramics*, 56, (1), pp. 14-15.
- Maurice, P. A., Lee, Y. J. and Hersman, L. E. (2000) 'Dissolution of Al-substituted goethites by an aerobic *Pseudomonas mendocina* var. bacteria', *Geochimica et Cosmochimica Acta*, 64, (8), pp. 1363-1374.
- Maurice, P. A., Vierkorn, M. A., Hersman, L. E. and Fulghum, J. E. (2001) 'Dissolution of well and poorly ordered kaolinites by an aerobic bacterium', *Chemical Geology*, 180, (1-4), pp. 81-97.
- Mockovciaková, A., Iveta, S., Jirí, S. and Ivana, K. (2008) 'Characterization of changes of low and high defect kaolinite after bioleaching', *Applied Clay Science*, 39, (3-4), pp. 202-207.
- Mortimer, R. J. G., Coleman, M. L. and Rae, J. E. (1997) 'Effect of bacteria on elemental composition of early diagenetic siderite: implications for palaeoenvironmental interpretations. ', *Sedimentology*, 44, (759 - 765).
- Mowla, D., Karimi, G. and Ostadnezhad, K. (2008) 'Removal of hematite from silica sand ore by reverse flotation technique', *Separation and Purification Technology*, 58, (3), pp. 419-423.

- Munch, J. C. and Ottow, J. C. G. (1983) 'Reductive transformation mechanism of ferric oxides in hydromorphic soils', *Ecological Bulletins*, 35, pp. 383 - 394.
- Murray, H. H. (2007) 'Applied Clay Mineralogy: Occurrences, Processing and Application of Kaolins, Bentonites, Palygorskite-Sepiolite, and Common Clays. Developments in Clay Sciences 2.', First Edition: Elsevier, Oxford., pp. 1 - 180.
- Myers, C. M. and Nealson, K. H. (1988) 'Bacterial manganese reduction and growth with manganese oxide as the sole electron acceptor', *Science*, 240, pp. 1319-1321.
- Myers, C. R. and Myers, J. M. (1997) 'Outer membrane cytochromes of *Shewanella putrefaciens* MR-1: spectral analysis, and purification of the 83-kDa c-type cytochromes', *Biochimica et Biophysica Acta*, 1326, pp. 307 - 318.
- Nakamura, R., Okamoto, A., Tajima, N., Newton, G. J., Kai, F., Takashima, T. and Hashimoto, K. (2010) 'Biological Iron-Monosulfide Production for Efficient Electricity Harvesting from a Deep-Sea Metal-Reducing Bacterium', *ChemBioChem*, 11, (5), pp. 643-645.
- Nealson, K., Belz, A. and McKee, B. (2002) 'Breathing metals as a way of life: geobiology in action', *Antonie van Leeuwenhoek*, 81, (1), pp. 215-222.
- Nealson, K. H. and Saffarini, D. (1994) 'Iron and Manganese in anaerobic respiration: Environmental significance. physiology, and regulation', *Annual Review of Microbiology*, 48, (311 - 343).
- Nevin, K. P. and Lovley, D. R. (2000a) 'Lack of Production of Electron-Shuttling Compounds or Solubilization of Fe(III) during Reduction of Insoluble Fe(III) Oxide by *Geobacter metallireducens*', *Applied & Environmental Microbiology*, 66, (5), pp. 2248-2251.
- Nevin, K. P. and Lovley, D. R. (2000b) 'Potential for Nonenzymatic Reduction of Fe(III) via Electron Shuttling in Subsurface Sediments', *Environmental Science & Technology*, 34, (12), pp. 2472-2478.
- Nevin, K. P. and Lovley, D. R. (2002a) 'Mechanism for Fe(III) reduction in sedimentary environment', *Geomicrobiology Journal*, 19, pp. 141 - 159.
- Nevin, K. P. and Lovley, D. R. (2002b) 'Mechanisms for Accessing Insoluble Fe(III) Oxide during Dissimilatory Fe(III) Reduction by *Geothrix fermentans*', *Applied & Environmental Microbiology*, 68, (5), pp. 2294-2299.
- Newman, D. K. and Kolter, R. (2000) 'A role for excreted quinones in extracellular electron transfer', *Nature*, 405, pp. 94 - 97.

- Norrish, K. and Chappell, B. W. (1967) 'X-ray Fluorescence Spectrography', in Zussman, J. (Ed) 'Physical Methods in Determinative Mineralogy', London and New York: Academic Press, pp. 161 - 214.
- O'Loughlin, E. J. (2008) 'Effect of Electron Transfer Mediators on the Bioreduction of Lepidocrocite (γ -FeOOH) by *Shewanella putrefaciens* CN32', *Environ. Sci. Technol.*, 42, pp. 6876 - 6882.
- O'Loughlin, E. J., Laresa-Casanova, P., Scherer, M. and Cook, R. (2007) 'Green Rust Formation from the Bioreduction of γ -FeOOH (Lepidocrocite): Comparison of Several *Shewanella* Species', *Geomicrobiology*, 24, pp. 211 - 230.
- O'Reilly, S. E., Furukawa, Y. and Newell, S. (2006) 'Dissolution and microbial Fe(III) reduction of nontronite (NAu-1)', *Chemical Geology*, 235, pp. 1 - 11.
- Park, D. H. and Kim, B. H. (2001) 'Growth Properties of the Iron-reducing Bacteria, *Shewanella putrefaciens* IR-1 and MR-1 Coupling to Reduction of Fe(III) to Fe(II)', *The Journal of Microbiology*, 39, (4), pp. 273-278.
- Petrovskis, E. A., Vogel, T. M. and Adriaens, P. (2004) 'Effect of electron acceptors and donors on transformation of tetrachloromethane by *Shewanella putrefaciens* MR-1', *FEMS Microbiology letters*, 121, pp. 357 - 363.
- Picardal, F., Arnold, R. G. and Huey, B. B. (1995) 'Effects of electron donor and acceptor conditions on reductive dehalogenation of tetrachloromethane by *Shewanella putrefaciens* 200', *Applied & Environmental Microbiology*, 61, pp. 8 -12.
- Popa, A., Sasca, V., Kiss, E. E., Marinkovic-Neducin, R., Bokorov, M. T. and Holclajtner-Antunovic, I. (2010) 'Studies in structural characterization of silica-heteropolyacids composites prepared by sol-gel method', *Material Chemistry and Physics*, 119, pp. 465 - 470.
- Postma, D. and Jakobsen, R. (1996) 'Redox zonation: equilibrium constrains on the Fe(III)/SO₄-reduction interface', *Geochim Cosmochim Acta*, 60, pp. 3169 - 3175.
- Prasad, M. S., Reid, K. J. and Murray, H. H. (1991) 'Kaolin: processing, properties and applications', *Applied Clay Science*, 6, (2), pp. 87-119.
- Psyrillos, A., Howe, J. H., Manning, D. A. C. and Burley, S. D. (1999) 'Geological controls on kaolin particle shape and consequences for mineral processing', *Clay Minerals*, 34, (1), pp. 193-208.

- Psyrillos, A., Manning, D. A. C. and Burley, S. D. (1998) 'Geochemical constraints on kaolinization in the St Austell Granite, Cornwall, England', *Journal of the Geological Society, London*, 155, pp. 829 - 840.
- Qinyan, Y., Li, Y. and Gao Baoyu. (2009) 'Impact factors and thermodynamic characteristics of aquatic humic acid loaded onto kaolin', *Colloid and Surfaces B: Biointerfaces*, 27, pp. 241 - 247.
- Rancourt, D. G. and Ping, J. Y. (1991) 'Voigt-based methods for arbitrary -shaped static hyperfine parameter distribution Mössbauer spectroscopy. ', *Nuclear Instruments and Methods in Physics Research, B*, (58), pp. 85 - 87.
- Reeves, G. M., Sims, I. and Cripps, J. C. (2006) 'Clay Materials Used in Construction.', Geological Society, London, Engineering Geology Special Publication, 21., pp. 1 - 525.
- Reguera, G., McCarthy, K. D., Mehta, T., Nicoll, J. S., Tuominen, M. T. and Lovley, D. R. (2005) 'Extracellular electron transfer via microbial nanowires', *Nature*, 435, (7045), pp. 1098-1101.
- Roden, E. E. (2003) 'Fe(III) oxide reactivity toward biological versus chemical reduction', *Environmental Science & Technology*, 37, (1319 - 1324).
- Roden, E. E. (2004) 'Analysis of long-term bacterial vs. chemical Fe(III) oxide reduction kinetics', *Geochimica et Cosmochimica Acta*, 68, (15), pp. 3205 - 3216.
- Roden, E. E. and Zachara, J. M. (1996) 'Microbial Reduction of Crystalline Iron(II) Oxides: Influence of Oxide Surface Area and Potential for Cell Growth', *Environmental Science & Technology*, 30, (1618 - 1628).
- Roh, Y., Gao, H., Vali, H., Kennedy, D. W., Yang, Z. K., Gao, W., Dohnalkova, A. C., Stapleton, R. D., Moon, J.-W., Phelps, T. J., Fredrickson, J. K. and Zhou, J. (2006) 'Metal Reduction and Iron Biomineralization by a Psychrotolerant Fe(III)-Reducing Bacterium, *Shewanella* sp. Strain PV-4', *Applied & Environmental Microbiology*, 72, (5), pp. 3236-3244.
- Rosenbaum, M. A., Bar, H. Y., Beg, Q. K., Segrè, D., Booth, J., Cotta, M. A. and Angenent, L. T. (2011) '*Shewanella oneidensis* in a lactate-fed pure-culture and a glucose-fed co-culture with *Lactococcus lactis* with an electrode as electron acceptor', *Bioresource Technology*, 102, (3), pp. 2623-2628.

- Royer, R. A., Burgos, W. D., Fisher, A. S., Jeon, B.-H., Unz, R. F. and Dempsey, B. A. (2002) 'Enhancement of Hematite Bioreduction by Natural Organic Matter', *Environmental Science & Technology*, 36, (13), pp. 2897-2904.
- Rusch, B., Hanna, K. and Humbert, B. (2010) 'Coating of quartz silica with iron oxides: Characterization and surface reactivity of iron coating phases', *Colloids and Surfaces A: Physicochemical and Engineering Aspects*, 353, (2-3), pp. 172-180.
- Russell, J. D. and Fraser, A. R. (1996) 'Infrared Method', in Wilson, M.J. (Ed) 'Clay Mineralogy: Spectroscopic and Chemical Determinative Methods', Oxford: Chapman & Hall, pp. 11 - 64.
- Ryu, H. W., Cho, K. S., Chang, Y. K., Kim, S. D. and Mori, T. (1995) 'Refinement of Low-Grade Clay by Microbial Removal of Sulfur and Iron Compounds Using *Thiobacillus ferrooxidans*', *Journal of Fermentation and Bioengineering*, 80, (1), pp. 46 -52.
- Schröder, I., Johnson, E. and de Vries, S. (2003) 'Microbial ferric iron reductases', *FEMS Microbiology Reviews*, 27, (2-3), pp. 427-447.
- Semple, K. and Westlake, D. (1987) 'Characterization of iron-reducing *Alteromonas putrefaciens* strains from oil field fluids', *Canadian Journal of Microbiology*, 33, pp. 366 - 371.
- Sengupta, P., Saikia, P. C. and Borthakur, P. C. (2008) 'SEM-EDX characterization of iron-rich kaolinite clay', *Journal of Scientific and Industrial Research*, 67, pp. 812 - 818.
- Stucki, J. W. (2006) 'Properties and behaviour of iron in clay minerals. In: Bergaya, F., Theng, B.G.K, Lagaly, G. (Eds)', *Hand book of clay science*, Elsevier, Amsterdam, pp. 429 - 482.
- Styriaková, I., Jablonovská, K., Mockovciaková, A., Bekéniyová, A., Styriak, I., Kraus, I., Osacký, M. and Lovás, M. (2010) 'Dissolution of iron from quartz sands by basin bioleaching under static in-situ conditions', *Hydrometallurgy*, 104, (3-4), pp. 443-447.
- Styriakova, I. and Styriak, I. (2000) 'Iron removal from kaolins by bacterial leaching.', *Ceramics - Silikaty*, 44, (4), pp. 135-141.
- Styriaková, I., Styriak, I., Kraus, I., Hradil, D., Grygar, T. and Bezďicka, P. (2003) 'Biodestruction and deferritization of quartz sands by *Bacillus* species', *Minerals Engineering*, 16, (8), pp. 709-713.

- Styriakova, I., Styriak, I. and Malachovsky, P. (2007) 'Nutrients enhancing the bacterial iron dissolution in the processing of feldspar raw materials.', *Ceramics - Silikaty*, 51, (4), pp. 202-209.
- Styriaková, I., Styriak, I., Malachovský, P., Vecera, Z. and Kolousek, D. (2007) 'Bacterial clay release and iron dissolution during the quality improvement of quartz sands', *Hydrometallurgy*, 89, (1-2), pp. 99-106.
- Sung, Y., Fletcher, K. E., Ritalahti, K. M., Apkarian, R. P., Ramos-Hernandez, N., Sanford, R. A., Mesbah, N. M. and Löffler, F. E. (2006) '*Geobacter lovleyi* sp. nov. Strain SZ, a Novel Metal-Reducing and Tetrachloroethene-Dechlorinating Bacterium.', *Applied and Environmental Microbiology*, 72, pp. 2775 - 2782.
- Tang, Y. J., Hwang, J. S., Wemmer, D. E. and Keasling, J. D. (2007) '*Shewanella oneidensis* MR-1 fluxome under various oxygen conditions', *Applied & Environmental Microbiology*, 73, pp. 718 - 729.
- Thandrup, B. (2000) 'Bacterial manganese and iron reduction in aquatic sediments', *Advances in Microbial Ecology*, 16, pp. 41 - 48.
- Turrick, C. E., Caccavo, F., Jr. and Tisa, L. S. (2003) 'Electron transfer from *Shewanella algae* BrY to hydrous ferric oxide is mediated by cell-associated melanin', *FEMS Microbiology letters*, 220, pp. 99 -104.
- Turrick, C. E., Tisa, L. S. and Caccavo, F., Jr. (2002) 'Melanin production and uses as a soluble electron shuttle for Fe(III) oxide reduction and as terminal electron acceptor by *Shewanella algae* BrY', *Applied & Environmental Microbiology*, 68, pp. 2436 - 2444.
- Urrutia, M. M., Roden, E. E., Fredrickson, J. K. and Zachara, J. M. (1998) 'Microbial and surface chemistry controls on reduction of synthetic Fe(III) oxide minerals by the dissimilatory iron-reducing bacterium *Shewanella alga* ', *Geomicrobiology* 15, pp. 269 - 291.
- Urrutia, M. M., Roden, E. E. and Zachara, J. M. (1999) 'Influence of aqueous and solid-phase Fe(II) complexants on microbial reduction of crystalline iron (III) oxides', *Environmental Science & Technology*, 33, pp. 4022 - 4028.
- Veglio, F., Passariello, B., Toro, L. and Marabini, A. M. (1996) 'Development of a Bleaching Process for a Kaolin of Industrial Interest by Oxalic, Ascorbic, and Sulfuric Acids: Preliminary Study Using Statistical Methods of Experimental Design.', *Industrial & Engineering Chemistry Research*, 35, pp. 1680 - 1687.

- Venkateswaran, K., Moser, D. P., Dollhopf, M. E., Lies, D. P., Saffarini, D. A., MacGregor, B. J., Ringelberg, D. B. and White, D. C. (1999) 'Polyphasic taxonomy of the genus *Shewanella* and description of *Shewanella oneidensis* sp. nov. ', *International Journal of Systematic Bacteriology*, 49, pp. 705 - 724.
- von Canstein, H., Ogawa, J., Shimizu, S. and Lloyd, J. R. (2008) 'Secretion of flavins by *Shewanella* species and their role in extracellular electron transfer', *Applied & Environmental Microbiology*, 74, pp. 615 - 623.
- Wilson, I. R. (2003) 'Current World Status of Kaolin from South-West England', *Geoscience in south-west England*, 10, pp. 417 - 423.
- Wilson, I. R. (2004) 'Kaolin and halloysite deposits of China', *Clay Minerals*, 39, (1 - 15).
- Zachara, J. M., Fredrickson, J. K., Li, S.-M., Kennedy, D. W., Smith, S. C. and Gassman, P. L. (1998) 'Bacterial reduction of crystalline Fe (super 3+) oxides in single phase suspensions and subsurface materials', *American Mineralogist*, 83, (11-12_Part_2), pp. 1426-1443.
- Zachara, J. M., Kukkadapu, R. K., Fredrickson, J. K., Gorby, Y. A. and smith, S. C. (2002) 'Biomining of Poorly Crystalline Fe(III) Oxides by Dissimilatory Metal Reducing Bacteria (DMRB)', *Geomicrobiology*, 19, pp. 170 - 207.
- Zegeye, A., Huguet, L., Abdelmoula, M., Carteret, C., Mullet, M. and Jorand, F. (2007) 'Biogenic hydroxysulfate green rust, a potential electron acceptor for SRB activity', *Geochimica et Cosmochimica Acta*, 71, (22), pp. 5450-5462.
- Zhao, H. L., Wang, D. X., Cai, Y. X. and Zhang, F. C. (2007) 'Removal of iron from silica sand by surface cleaning using power ultrasound', *Minerals Engineering*, 20, (8), pp. 816-818.

Davi

d

Man

ning

27/

04/

201

1

18:5

3

Mak

e

sure

you

use

the

sam

e

sam

ple

i/d

as in

the

text

!

Also

, in

this

tabl

e

set

it up

so

the

deci

mal

poin

ts

are

alig

ned
—
use
the
deci
mal
poin
t
tab

David Manning 27/04/2011 18:53

Is 'parked' the right word?

APPENDIX 1

Appendix 1.1: Selection of the most suitable iron reducing bacteria for leaching of kaolin

	Fe(II) mmol/L			CIP8040		
Days	1	2	3	Average	STD	Error
0	0.0000	0.0000	0.0000	0.0000	0.0000	0.0000
1	1.0895	1.1287	1.1679	1.1287	0.0392	0.0226
2	1.2464	1.3213	1.2892	1.2856	0.0376	0.0217
3	1.4069	1.3534	1.3855	1.3819	0.0269	0.0155
4	1.4212	1.3891	1.4497	1.4200	0.0303	0.0175
5	1.4604	1.4426	1.4782	1.4604	0.0178	0.0103

	Fe(II) mmol/L			CN32		
Days	1	2	3	Average	STD	Error
0	0.0000	0.0000	0.0000	0.0000	0.0000	0.0000
1	0.8862	0.7185	0.7827	0.7958	0.0846	0.0488
2	1.0930	0.9896	0.9432	1.0086	0.0767	0.0443
3	1.3142	1.2179	1.1109	1.2143	0.1017	0.0587
4	1.4105	1.3070	1.1822	1.2999	0.1143	0.0660
5	1.4426	1.4283	1.3463	1.4057	0.0520	0.0300

	Fe(II) mmol/L			<i>S. alga BrY</i>		
Days	1	2	3	Average	STD	Error
0	0.0000	0.0000	0.0000	0.0000	0.0000	0.0000
1	1.0053	1.0161	1.0740	1.0318	0.0369	0.0213
2	1.0993	1.1174	1.1246	1.1138	0.0130	0.0075
3	1.3597	1.1680	1.2005	1.2427	0.1026	0.0592
4	1.3307	1.3705	1.3633	1.3548	0.0212	0.0122
5	1.3886	1.4246	1.4248	1.4127	0.0208	0.0120
10	1.5658	1.5260	1.5405	1.5441	0.0201	0.0116

	Fe(II) mmol/L			<i>S. oneidensis</i>		
Days	1	2	3	Average	STD	Error
0	0.0000	0.0000	0.0000	0.0000	0.0000	0.0000
1	0.8570	0.8136	0.8353	0.8353	0.0217	0.0125
2	0.8895	0.8787	0.8895	0.8859	0.0063	0.0036
3	0.9438	0.8859	0.9112	0.9136	0.0290	0.0167
4	0.9800	0.9221	0.9474	0.9498	0.0290	0.0167
5	1.0016	0.9655	0.9293	0.9655	0.0361	0.0209
10	1.0306	0.9800	1.0053	1.0053	0.0253	0.0146

	Fe(II) mmol/L			<i>S. loihica</i>		
Days	1	2	3	Average	STD	Error
0	0.0000	0.0000	0.0000	0.0000	0.0000	0.0000
1	0.0017	0.0017	0.0016	0.0017	0.0001	0.0001
2	0.0020	0.0020	0.0021	0.0020	0.0001	0.0000
3	0.0020	0.0022	0.0023	0.0022	0.0002	0.0001
4	0.0021	0.0022	0.0024	0.0023	0.0001	0.0001
5	0.0023	0.0025	0.0026	0.0024	0.0002	0.0001

Appendix 1.2: Data from bioleaching of kaolin (Effect of cell/solid ratio)

	Fe(II) mmol/L		20g/2ml cells		
Days	1	2	Average	STD	Error
0	0.0000	0.0000	0.0000	0.0000	0.0000
1	0.1435	0.1575	0.1505	0.0099	0.0070
2	0.1505	0.1646	0.1575	0.0100	0.0070
3	0.1716	0.1786	0.1751	0.0050	0.0035
4	0.1822	0.2209	0.2015	0.0274	0.0194
5	0.1857	0.2279	0.2068	0.0299	0.0211
10	0.2103	0.2490	0.2297	0.0274	0.0194

	Fe(II) mmol/L		20g/4ml cells		
Days	1	2	Average	STD	Error
0	0.0000	0.0000	0.0000	0.0000	0.0000
1	1.1074	1.1356	1.1215	0.0199	0.0141
2	1.1180	1.1391	1.1286	0.0149	0.0106
3	1.1602	1.1778	1.1690	0.0124	0.0088
4	1.1884	1.2974	1.2429	0.0771	0.0545
5	1.2165	1.4030	1.3098	0.1319	0.0933
10	1.6035	1.6070	1.6053	0.0025	0.0018

	Fe(II) mmol/L		20g/7ml cells		
Days	1	2	Average	STD	Error
0	0.0000	0.0000	0.0000	0.0000	0.0000
1	1.1285	1.1285	1.1285	0.0000	0.0000
2	1.2306	1.2306	1.2306	0.0000	0.0000
3	1.3220	1.3959	1.3590	0.0523	0.0370
4	1.5370	1.5402	1.5386	0.0023	0.0016
5	1.5261	1.5543	1.5402	0.0199	0.0141
10	1.7513	1.7055	1.7284	0.0324	0.0229

	Fe(II) mmol/L		10g/2ml cells		
Days	1	2	Average	STD	Error
0	0.0000	0.0000	0.0000	0.0000	0.0000
1	0.5410	0.4847	0.5129	0.0398	0.0281
2	0.6395	0.6430	0.6413	0.0025	0.0018
3	0.6817	0.6923	0.6870	0.0075	0.0053
4	0.7451	0.7099	0.7275	0.0249	0.0176
5	0.9245	0.7591	0.8418	0.1169	0.0827
10	1.0828	0.9526	1.0177	0.0920	0.0651

	Fe(II) mmol/L		10g/4ml cells		
Days	1	2	Average	STD	Error
0	0.0000	0.0000	0.0000	0.0000	0.0000
1	0.5058	0.6219	0.5639	0.0821	0.0581
2	0.6993	0.7169	0.7081	0.0124	0.0088
3	0.7451	0.7943	0.7697	0.0348	0.0246
4	0.8190	0.9069	0.8629	0.0622	0.0440
5	0.8295	0.9315	0.8805	0.0721	0.0510
10	1.0300	1.0336	1.0318	0.0025	0.0018

	Fe(II) mmol/L		10g/7ml cells		
Days	1	2	Average	STD	Error
0	0.0000	0.0000	0.0000	0.0000	0.0000
1	0.6114	0.6219	0.6167	0.0075	0.0053
2	0.7029	0.6571	0.6800	0.0323	0.0229
3	0.8014	0.7345	0.7679	0.0473	0.0334
4	0.8788	0.7873	0.8330	0.0647	0.0457
5	0.9315	0.8014	0.8664	0.0920	0.0651
10	1.1497	1.1004	1.1251	0.0349	0.0247

Appendix 1.3: Effect of temperature on the bioreduction of kaolin

Average Fe(II)mmol/L					
Days	20°C	Days	30°C	Days	36°C
0	0.0019	0	0.0000	0	0.0000
1	0.0360	1	0.0496	1	0.0320
2	0.0411	2	0.0540	2	0.0350
3	0.0441	3	0.0597	3	0.0370
4	0.0454	4	0.0676	4	0.0410
5	0.0466	5	0.0676	5	0.0415
		12	0.0759	7	0.0430
				10	0.0440

Appendix 1.4: Data from bioreduction of kaolin using 0.1mM lactate.

Hours	Absorbance (0.1)			Fe ²⁺ (µg)			Fe(II) mmol/L			Average	STD	Error
	1	2	3	1	2	3	1	2	3			
0	0.0000	0.0000	0.0000	0.1111	0.1111	0.1111	0.0080	0.0080	0.0080	0.0080	0.0000	0.0000
2	0.0060	0.0090	0.0050	0.4444	0.6111	0.3889	0.0318	0.0438	0.0279	0.0345	0.0083	0.0048
4	0.0040	0.0090	0.0030	0.3333	0.6111	0.2778	0.0239	0.0438	0.0199	0.0292	0.0128	0.0074
6	0.0030	0.0100	0.0070	0.2778	0.6667	0.5000	0.0199	0.0477	0.0358	0.0345	0.0140	0.0081
8	0.0030	0.0090	0.0190	0.2778	0.6111	1.1667	0.0199	0.0438	0.0836	0.0491	0.0322	0.0186
10	0.0030	0.0190	0.0200	0.2778	1.1667	1.2222	0.0199	0.0836	0.0875	0.0637	0.0380	0.0219
12	0.0050	0.0190	0.0230	0.3889	1.1667	1.3889	0.0279	0.0836	0.0995	0.0703	0.0376	0.0217
14	0.0070	0.0190	0.0270	0.5000	1.1667	1.6111	0.0358	0.0836	0.1154	0.0783	0.0401	0.0231
18	0.0010	0.0100	0.0050	0.1667	0.6667	0.3889	0.0119	0.0477	0.0279	0.0292	0.0179	0.0104
34	0.0020	0.0120	0.0040	0.2222	0.7778	0.3333	0.0159	0.0557	0.0239	0.0318	0.0211	0.0122
38	0.0010	0.0110	0.0060	0.1667	0.7222	0.4444	0.0119	0.0517	0.0318	0.0318	0.0199	0.0115
42	0.0060	0.0130	0.0150	0.4444	0.8333	0.9444	0.0318	0.0597	0.0676	0.0531	0.0188	0.0109
58	0.0070	0.0130	0.0140	0.5000	0.8333	0.8889	0.0358	0.0597	0.0637	0.0531	0.0151	0.0087
82	0.0080	0.0160	0.0160	0.5556	1.0000	1.0000	0.0398	0.0716	0.0716	0.0610	0.0184	0.0106
106	0.0080	0.0230	0.0380	0.5556	1.3889	2.2222	0.0398	0.0995	0.1592	0.0995	0.0597	0.0345
130	0.0080	0.0310	0.0310	0.5556	1.8333	1.8333	0.0398	0.1313	0.1313	0.1008	0.0528	0.0305

Appendix 1.5: Data from bioreduction of kaolin using 0.3mM lactate.

	Absorbance			Fe ²⁺ (µg)			Fe (II) mmol/L					
Hours	1	2	3	1	2	3	1	2	3	Average	STD	Error
0	0.0000	0.0000	0.0000	0.1111	0.1111	0.1111	0.0080	0.0080	0.0080	0.0080	0.0000	0.0000
2	0.0130	0.0240	0.0220	0.8333	1.4444	1.3333	0.0597	0.1035	0.0955	0.0862	0.0233	0.0135
4	0.0120	0.0400	0.0330	0.7778	2.3333	1.9444	0.0557	0.1671	0.1393	0.1207	0.0580	0.0335
6	0.0160	0.0390	0.0440	1.0000	2.2778	2.5556	0.0716	0.1631	0.1830	0.1393	0.0594	0.0343
8	0.0150	0.0350	0.0520	0.9444	2.0556	3.0000	0.0676	0.1472	0.2149	0.1432	0.0737	0.0426
10	0.0280	0.0420	0.0470	1.6667	2.4444	2.7222	0.1194	0.1751	0.1950	0.1631	0.0392	0.0226
12	0.0200	0.0460	0.0560	1.2222	2.6667	3.2222	0.0875	0.1910	0.2308	0.1698	0.0739	0.0427
14	0.0320	0.0480	0.0560	1.8889	2.7778	3.2222	0.1353	0.1989	0.2308	0.1883	0.0486	0.0281
18	0.0480	0.0480	0.0600	2.7778	2.7778	3.4444	0.1989	0.1989	0.2467	0.2149	0.0276	0.0159
34	0.0440	0.0440	0.0500	2.5556	2.5556	2.8889	0.1830	0.1830	0.2069	0.1910	0.0138	0.0080
38	0.0450	0.0450	0.0650	2.6111	2.6111	3.7222	0.1870	0.1870	0.2666	0.2135	0.0459	0.0265
42	0.0370	0.0460	0.0540	2.1667	2.6667	3.1111	0.1552	0.1910	0.2228	0.1897	0.0338	0.0195
58	0.0300	0.0370	0.0560	1.7778	2.1667	3.2222	0.1273	0.1552	0.2308	0.1711	0.0535	0.0309
82	0.0310	0.0560	0.0440	1.8333	3.2222	2.5556	0.1313	0.2308	0.1830	0.1817	0.0497	0.0287
106	0.0470	0.0560	0.0660	2.7222	3.2222	3.7778	0.1950	0.2308	0.2706	0.2321	0.0378	0.0218
130	0.0510	0.0540	0.0550	2.9444	3.1111	3.1667	0.2109	0.2228	0.2268	0.2202	0.0083	0.0048

Appendix 1.6: Data from bioreduction of kaolin using 0.5mM lactate.

Hours	Absorbance			Fe ²⁺ (µg)			Fe (II) mmol/L			Average	STD	Error
	1	2	3	1	2	3	1	2	3			
0	0.0000	0.0000	0.0000	0.1111	0.1111	0.1111	0.0080	0.0080	0.0080	0.0080	0.0000	0.000
2	0.0290	0.0290	0.0260	1.7222	1.7222	1.5556	0.1233	0.1233	0.1114	0.1194	0.0069	0.0040
4	0.0600	0.0380	0.0440	3.4444	2.2222	2.5556	0.2467	0.1592	0.1830	0.1963	0.0453	0.0261
6	0.0650	0.0480	0.0560	3.7222	2.7778	3.2222	0.2666	0.1989	0.2308	0.2321	0.0338	0.0195
8	0.0650	0.0570	0.0630	3.7222	3.2778	3.6111	0.2666	0.2348	0.2586	0.2533	0.0166	0.0096
10	0.0660	0.0550	0.0720	3.7778	3.1667	4.1111	0.2706	0.2268	0.2944	0.2639	0.0343	0.0198
12	0.0690	0.0650	0.0740	3.9444	3.7222	4.2222	0.2825	0.2666	0.3024	0.2838	0.0179	0.0104
14	0.0840	0.0650	0.0620	4.7778	3.7222	3.5556	0.3422	0.2666	0.2547	0.2878	0.0475	0.0274
18	0.0850	0.0640	0.0810	4.8333	3.6667	4.6111	0.3462	0.2626	0.3302	0.3130	0.0444	0.0256
34	0.0830	0.0600	0.0790	4.7222	3.4444	4.5000	0.3382	0.2467	0.3223	0.3024	0.0489	0.0282
38	0.0710	0.0650	0.0470	4.0556	3.7222	2.7222	0.2905	0.2666	0.1950	0.2507	0.0497	0.0287
42	0.0830	0.0480	0.0540	4.7222	2.7778	3.1111	0.3382	0.1989	0.2228	0.2533	0.0745	0.0430
58	0.0510	0.0470	0.0610	2.9444	2.7222	3.5000	0.2109	0.1950	0.2507	0.2188	0.0287	0.0166
82	0.0530	0.0560	0.0600	3.0556	3.2222	3.4444	0.2188	0.2308	0.2467	0.2321	0.0140	0.0081
106	0.0690	0.0560	0.0670	3.9444	3.2222	3.8333	0.2825	0.2308	0.2745	0.2626	0.0279	0.0161
130	0.0890	0.0610	0.0710	5.0556	3.5000	4.0556	0.3621	0.2507	0.2905	0.3011	0.0565	0.0326

Appendix 1.7: Data from bioreduction of kaolin using 1mM lactate.

Hours	Absorbance			Fe ²⁺ (µg)			Fe (II) mmol/L			Average	STD	Error
	1	2	3	1	2	3	1	2	3			
0	0.0000	0.0000	0.0000	0.1111	0.1111	0.1111	0.0080	0.0080	0.0080	0.0080	0.0000	0.0000
2	0.0320	0.0360	0.0330	1.8889	2.1111	1.9444	0.1353	0.1512	0.1393	0.1419	0.0083	0.0048
4	0.0460	0.0500	0.0460	2.6667	2.8889	2.6667	0.1910	0.2069	0.1910	0.1963	0.0092	0.0053
6	0.0480	0.0690	0.0590	2.7778	3.9444	3.3889	0.1989	0.2825	0.2427	0.2414	0.0418	0.0241
8	0.0700	0.0730	0.0700	4.0000	4.1667	4.0000	0.2865	0.2984	0.2865	0.2905	0.0069	0.0040
10	0.0750	0.0810	0.0720	4.2778	4.6111	4.1111	0.3064	0.3302	0.2944	0.3104	0.0182	0.0105
12	0.0840	0.0850	0.0880	4.7778	4.8333	5.0000	0.3422	0.3462	0.3581	0.3488	0.0083	0.0048
14	0.0840	0.0840	0.0870	4.7778	4.7778	4.9444	0.3422	0.3422	0.3541	0.3462	0.0069	0.0040
18	0.0850	0.0900	0.0920	4.8333	5.1111	5.2222	0.3462	0.3661	0.3740	0.3621	0.0143	0.0083
34	0.0860	0.0950	0.0940	4.8889	5.3889	5.3333	0.3501	0.3860	0.3820	0.3727	0.0196	0.0113
38	0.0950	0.0790	0.0920	5.3889	4.5000	5.2222	0.3860	0.3223	0.3740	0.3608	0.0338	0.0195
42	0.0870	0.0840	0.0620	4.9444	4.7778	3.5556	0.3541	0.3422	0.2547	0.3170	0.0543	0.0314
58	0.0720	0.0910	0.0680	4.1111	5.1667	3.8889	0.2944	0.3700	0.2785	0.3143	0.0489	0.0282
82	0.0720	0.0510	0.0740	4.1111	2.9444	4.2222	0.2944	0.2109	0.3024	0.2692	0.0507	0.0293
106	0.0700	0.1030	0.0670	4.0000	5.8333	3.8333	0.2865	0.4178	0.2745	0.3263	0.0795	0.0459
130	0.0530	0.0820	0.0850	3.0556	4.6667	4.8333	0.2188	0.3342	0.3462	0.2997	0.0703	0.0406

Appendix 1.8: Data from blank microcosms during bioreduction of kaolin using 0.1 -1mM lactate.

Days	Blank	Fe ²⁺ (µg)	Fe(II) mmol/L
0	0.0000	0.1111	0.0080
2	0.0030	0.2778	0.0199
4	0.0020	0.2222	0.0159
6	0.0030	0.2778	0.0199
8	0.0020	0.2222	0.0159
10	0.0030	0.2778	0.0199
12	0.0040	0.3333	0.0239
14	0.0040	0.3333	0.0239
18	0.0030	0.2778	0.0199
34	0.0030	0.2778	0.0199
38	0.0050	0.3889	0.0279
42	0.0040	0.3333	0.0239
58	0.0070	0.5000	0.0358
82	0.0110	0.7222	0.0517
106	0.0100	0.6667	0.0477
130	0.0100	0.6667	0.0477

Appendix 1.9: Data from bioreduction of kaolin amended with acetate

Hours	Absorbance			Fe ²⁺ (µg)			Fe(II) mmol/L			Average	STD	Error
	1	2	3	1	2	3	1	2	3			
0	0.0000	0.0000	0.0000	0.1111	0.1111	0.1111	0.0080	0.0080	0.0080	0.0080	0.0000	0.0000
2	0.0270	0.0230	0.0390	1.6111	1.3889	2.2778	0.1154	0.0995	0.1631	0.1260	0.0331	0.0191
4	0.0340	0.0330	0.0460	2.0000	1.9444	2.6667	0.1432	0.1393	0.1910	0.1578	0.0288	0.0166
6	0.0400	0.0370	0.0530	2.3333	2.1667	3.0556	0.1671	0.1552	0.2188	0.1804	0.0338	0.0195
8	0.0500	0.0590	0.0570	2.8889	3.3889	3.2778	0.2069	0.2427	0.2348	0.2281	0.0188	0.0109
10	0.0500	0.0680	0.0590	2.8889	3.8889	3.3889	0.2069	0.2785	0.2427	0.2427	0.0358	0.0207
12	0.0510	0.0710	0.0560	2.9444	4.0556	3.2222	0.2109	0.2905	0.2308	0.2440	0.0414	0.0239
24	0.0410	0.0450	0.0390	2.3889	2.6111	2.2778	0.1711	0.1870	0.1631	0.1737	0.0122	0.0070
28	0.0390	0.0390	0.0380	2.2778	2.2778	2.2222	0.1631	0.1631	0.1592	0.1618	0.0023	0.0013
32	0.0420	0.0390	0.0390	2.4444	2.2778	2.2778	0.1751	0.1631	0.1631	0.1671	0.0069	0.0040
48	0.0350	0.0350	0.0640	2.0556	2.0556	3.6667	0.1472	0.1472	0.2626	0.1857	0.0666	0.0385
72	0.0450	0.0460	0.0530	2.6111	2.6667	3.0556	0.1870	0.1910	0.2188	0.1989	0.0173	0.0100
96	0.0620	0.0630	0.0590	3.5556	3.6111	3.3889	0.2547	0.2586	0.2427	0.2520	0.0083	0.0048
120	0.0520	0.0540	0.0520	3.0000	3.1111	3.0000	0.2149	0.2228	0.2149	0.2175	0.0046	0.0027
144	0.0500	0.0560	0.0600	2.8889	3.2222	3.4444	0.2069	0.2308	0.2467	0.2281	0.0200	0.0116
192	0.0500	0.0620	0.0670	2.8889	3.5556	3.8333	0.2069	0.2547	0.2745	0.2454	0.0348	0.0201
216	0.0210	0.0510	0.0400	1.2778	2.9444	2.3333	0.0915	0.2109	0.1671	0.1565	0.0604	0.0349
240	0.0160	0.0360	0.0370	1.0000	2.1111	2.1667	0.0716	0.1512	0.1552	0.1260	0.0471	0.0272
264	0.0250	0.0560	0.0750	1.5000	3.2222	4.2778	0.1074	0.2308	0.3064	0.2149	0.1004	0.0580
288	0.0230	0.0530	0.0650	1.3889	3.0556	3.7222	0.0995	0.2188	0.2666	0.1950	0.0861	0.0497
312	0.0180	0.0480	0.0570	1.1111	2.7778	3.2778	0.0796	0.1989	0.2348	0.1711	0.0813	0.0469
336	0.0200	0.0690	0.0550	1.2222	3.9444	3.1667	0.0875	0.2825	0.2268	0.1989	0.1004	0.0580
360	0.0150	0.0490	0.0680	0.9444	2.8333	3.8889	0.0676	0.2029	0.2785	0.1830	0.1068	0.0617

Appendix 1.10: Data from bioreduction of kaolin amended with *Shewanella putrefaciens* CIP8040 cells

Hours	Absorbance			Fe ²⁺ (µg)			Fe(II) mmol/L			Average	STD	Error
	1	2	3	1	2	3	1	2	3			
0	0.0000	0.0000	0.0000	0.1111	0.1111	0.1111	0.0080	0.0080	0.0080	0.0080	0.0000	0.0000
2	0.0330	0.0330	0.0300	1.9444	1.9444	1.7778	0.1393	0.1393	0.1273	0.1353	0.0069	0.0040
4	0.0460	0.0400	0.0420	2.6667	2.3333	2.4444	0.1910	0.1671	0.1751	0.1777	0.0122	0.0070
6	0.0530	0.0430	0.0410	3.0556	2.5000	2.3889	0.2188	0.1791	0.1711	0.1897	0.0256	0.0148
8	0.0590	0.0430	0.0480	3.3889	2.5000	2.7778	0.2427	0.1791	0.1989	0.2069	0.0326	0.0188
10	0.0570	0.0740	0.0440	3.2778	4.2222	2.5556	0.2348	0.3024	0.1830	0.2401	0.0599	0.0346
12	0.0470	0.0570	0.0530	2.7222	3.2778	3.0556	0.1950	0.2348	0.2188	0.2162	0.0200	0.0116
24	0.0430	0.0290	0.0370	2.5000	1.7222	2.1667	0.1791	0.1233	0.1552	0.1525	0.0279	0.0161
28	0.0410	0.0330	0.0370	2.3889	1.9444	2.1667	0.1711	0.1393	0.1552	0.1552	0.0159	0.0092
32	0.0420	0.0300	0.0340	2.4444	1.7778	2.0000	0.1751	0.1273	0.1432	0.1485	0.0243	0.0140
48	0.0520	0.0320	0.0430	3.0000	1.8889	2.5000	0.2149	0.1353	0.1791	0.1764	0.0399	0.0230
72	0.0450	0.0320	0.0380	2.6111	1.8889	2.2222	0.1870	0.1353	0.1592	0.1605	0.0259	0.0149
96	0.0540	0.0610	0.0590	3.1111	3.5000	3.3889	0.2228	0.2507	0.2427	0.2387	0.0143	0.0083
120	0.0410	0.0680	0.0690	2.3889	3.8889	3.9444	0.1711	0.2785	0.2825	0.2440	0.0632	0.0365
144	0.0360	0.0460	0.0510	2.1111	2.6667	2.9444	0.1512	0.1910	0.2109	0.1844	0.0304	0.0175
192	0.0490	0.0520	0.0510	2.8333	3.0000	2.9444	0.2029	0.2149	0.2109	0.2096	0.0061	0.0035
216	0.0610	0.0550	0.0540	3.5000	3.1667	3.1111	0.2507	0.2268	0.2228	0.2334	0.0151	0.0087
240	0.0430	0.0550	0.0510	2.5000	3.1667	2.9444	0.1791	0.2268	0.2109	0.2056	0.0243	0.0140
264	0.1300	0.1140	0.1130	7.3333	6.4444	6.3889	0.5252	0.4616	0.4576	0.4814	0.0380	0.0219
288	0.1260	0.1200	0.1160	7.1111	6.7778	6.5556	0.5093	0.4854	0.4695	0.4881	0.0200	0.0116
312	0.1210	0.1190	0.1150	6.8333	6.7222	6.5000	0.4894	0.4814	0.4655	0.4788	0.0122	0.0070
336	0.1260	0.1140	0.1120	7.1111	6.4444	6.3333	0.5093	0.4616	0.4536	0.4748	0.0301	0.0174
360	0.1200	0.1290	0.1180	6.7778	7.2778	6.6667	0.4854	0.5212	0.4775	0.4947	0.0233	0.0135

Appendix 1.11: Data from bioreduction of kaolin amended with kaolin midway of the experiments

Hours	Absorbance			Fe ²⁺ (µg)			Fe(II) mmol/L			Average	STD	Error
	1	2	3	1	2	3	1	2	3			
0	0.0000	0.0000	0.0000	0.1111	0.1111	0.1111	0.0080	0.0080	0.0080	0.0080	0.0000	0.0000
2	0.0240	0.0420	0.0330	1.4444	2.4444	1.9444	0.1035	0.1751	0.1393	0.1393	0.0358	0.0207
4	0.0470	0.0500	0.0480	2.7222	2.8889	2.7778	0.1950	0.2069	0.1989	0.2003	0.0061	0.0035
6	0.0600	0.0640	0.0510	3.4444	3.6667	2.9444	0.2467	0.2626	0.2109	0.2401	0.0265	0.0153
8	0.0740	0.0700	0.0610	4.2222	4.0000	3.5000	0.3024	0.2865	0.2507	0.2799	0.0265	0.0153
10	0.0650	0.0790	0.0540	3.7222	4.5000	3.1111	0.2666	0.3223	0.2228	0.2706	0.0499	0.0288
12	0.0660	0.0840	0.0520	3.7778	4.7778	3.0000	0.2706	0.3422	0.2149	0.2759	0.0638	0.0369
24	0.0340	0.0440	0.0330	2.0000	2.5556	1.9444	0.1432	0.1830	0.1393	0.1552	0.0242	0.0140
28	0.0350	0.0420	0.0350	2.0556	2.4444	2.0556	0.1472	0.1751	0.1472	0.1565	0.0161	0.0093
32	0.0340	0.0390	0.0390	2.0000	2.2778	2.2778	0.1432	0.1631	0.1631	0.1565	0.0115	0.0066
48	0.0390	0.0540	0.0430	2.2778	3.1111	2.5000	0.1631	0.2228	0.1791	0.1883	0.0309	0.0178
72	0.0380	0.0480	0.0380	2.2222	2.7778	2.2222	0.1592	0.1989	0.1592	0.1724	0.0230	0.0133
96	0.0460	0.0680	0.0370	2.6667	3.8889	2.1667	0.1910	0.2785	0.1552	0.2082	0.0635	0.0366
120	0.0570	0.0640	0.0530	3.2778	3.6667	3.0556	0.2348	0.2626	0.2188	0.2387	0.0222	0.0128
144	0.0520	0.0500	0.0740	3.0000	2.8889	4.2222	0.2149	0.2069	0.3024	0.2414	0.0530	0.0306
192	0.0420	0.0620	0.0660	2.4444	3.5556	3.7778	0.1751	0.2547	0.2706	0.2334	0.0512	0.0295
216	0.0310	0.0440	0.0600	1.8333	2.5556	3.4444	0.1313	0.1830	0.2467	0.1870	0.0578	0.0334
240	0.0320	0.0500	0.0570	1.8889	2.8889	3.2778	0.1353	0.2069	0.2348	0.1923	0.0513	0.0296
264	0.0470	0.0460	0.0840	2.7222	2.6667	4.7778	0.1950	0.1910	0.3422	0.2427	0.0862	0.0498
288	0.0400	0.0560	0.0630	2.3333	3.2222	3.6111	0.1671	0.2308	0.2586	0.2188	0.0469	0.0271
312	0.0360	0.0590	0.0650	2.1111	3.3889	3.7222	0.1512	0.2427	0.2666	0.2202	0.0609	0.0352
336	0.0420	0.0690	0.0540	2.4444	3.9444	3.1111	0.1751	0.2825	0.2228	0.2268	0.0538	0.0311
360	0.0350	0.0480	0.0600	2.0556	2.7778	3.4444	0.1472	0.1989	0.2467	0.1976	0.0497	0.0287

Appendix 1.12: Data from bio-reduction of kaolin not amended throughout the experiment.

Hours	Absorbance			Fe ²⁺ (µg)			Fe(II) mmol/L			Average	STD	Error
	1	2	3	1	2	3	1	2	3			
0	0.0000	0.0000	0.0000	0.1111	0.1111	0.1111	0.0080	0.0080	0.0080	0.0080	0.0000	0.0000
2	0.0410	0.0280	0.0350	2.3889	1.6667	2.0556	0.1711	0.1194	0.1472	0.1459	0.0259	0.0149
4	0.0350	0.0420	0.0310	2.0556	2.4444	1.8333	0.1472	0.1751	0.1313	0.1512	0.0222	0.0128
6	0.0520	0.0450	0.0430	3.0000	2.6111	2.5000	0.2149	0.1870	0.1791	0.1936	0.0188	0.0109
8	0.0660	0.0580	0.0340	3.7778	3.3333	2.0000	0.2706	0.2387	0.1432	0.2175	0.0663	0.0383
10	0.0780	0.0710	0.0410	4.4444	4.0556	2.3889	0.3183	0.2905	0.1711	0.2600	0.0782	0.0452
12	0.0860	0.0780	0.0530	4.8889	4.4444	3.0556	0.3501	0.3183	0.2188	0.2958	0.0685	0.0395
24	0.0420	0.0360	0.0340	2.4444	2.1111	2.0000	0.1751	0.1512	0.1432	0.1565	0.0166	0.0096
28	0.0420	0.0480	0.0370	2.4444	2.7778	2.1667	0.1751	0.1989	0.1552	0.1764	0.0219	0.0127
32	0.0410	0.0390	0.0300	2.3889	2.2778	1.7778	0.1711	0.1631	0.1273	0.1539	0.0233	0.0135
48	0.0440	0.0380	0.0360	2.5556	2.2222	2.1111	0.1830	0.1592	0.1512	0.1645	0.0166	0.0096
72	0.0340	0.0420	0.0340	2.0000	2.4444	2.0000	0.1432	0.1751	0.1432	0.1539	0.0184	0.0106
96	0.0650	0.0610	0.0380	3.7222	3.5000	2.2222	0.2666	0.2507	0.1592	0.2255	0.0580	0.0335
120	0.0560	0.0590	0.0380	3.2222	3.3889	2.2222	0.2308	0.2427	0.1592	0.2109	0.0452	0.0261
144	0.0560	0.0650	0.0600	3.2222	3.7222	3.4444	0.2308	0.2666	0.2467	0.2480	0.0179	0.0104
192	0.0500	0.0640	0.0680	2.8889	3.6667	3.8889	0.2069	0.2626	0.2785	0.2493	0.0376	0.0217
216	0.0590	0.0690	0.0710	3.3889	3.9444	4.0556	0.2427	0.2825	0.2905	0.2719	0.0256	0.0148
240	0.0500	0.0850	0.0770	2.8889	4.8333	4.3889	0.2069	0.3462	0.3143	0.2891	0.0730	0.0421
264	0.0340	0.0790	0.0690	2.0000	4.5000	3.9444	0.1432	0.3223	0.2825	0.2493	0.0940	0.0543
288	0.0370	0.0550	0.0550	2.1667	3.1667	3.1667	0.1552	0.2268	0.2268	0.2029	0.0414	0.0239
312	0.0390	0.0640	0.0540	2.2778	3.6667	3.1111	0.1631	0.2626	0.2228	0.2162	0.0501	0.0289
336	0.0340	0.0590	0.0570	2.0000	3.3889	3.2778	0.1432	0.2427	0.2348	0.2069	0.0553	0.0319
360	0.0370	0.0560	0.0500	2.1667	3.2222	2.8889	0.1552	0.2308	0.2069	0.1976	0.0386	0.0223

Appendix 1.13: Data from Blank microcosm in experiments amended with acetate, kaolin, *Shewanella* cells.

Hours	Blank	Fe2+ (µg)	Fe(II) mmol/L
0	0.0000	0.1111	0.0080
2	0.0030	0.2778	0.0199
4	0.0060	0.4444	0.0318
6	0.0070	0.5000	0.0358
8	0.0060	0.4444	0.0318
10	0.0080	0.5556	0.0398
12	0.0040	0.3333	0.0239
24	0.0020	0.2222	0.0159
28	0.0020	0.2222	0.0159
32	0.0030	0.2778	0.0199
48	0.0030	0.2778	0.0199
72	0.0020	0.2222	0.0159
96	0.0040	0.3333	0.0239
120	0.0060	0.4444	0.0318
144	0.0030	0.2778	0.0199
192	0.0060	0.4444	0.0318
216	0.0040	0.3333	0.0239
240	0.0030	0.2778	0.0199
264	0.0040	0.3333	0.0239
288	0.0050	0.3889	0.0279
312	0.0060	0.4444	0.0318
336	0.0050	0.3889	0.0279
360	0.0040	0.3333	0.0239

Appendix 1.14: Data from bioreduction of Kaolin 2 using 5mM lactate.

Days	Absorbance		Fe ²⁺ (µg)		Fe(II) mmol/L		Average	STD	Error
	1	2	1	2	1	2			
0	0.0000	0.0000	0.3164	0.3164	0.0227	0.0227	0.0227	0.0000	0.0000
1	0.1340	0.1550	7.8870	9.0734	0.5649	0.6498	0.6074	0.0601	0.0425
2	0.1550	0.1720	9.0734	10.0339	0.6498	0.7186	0.6842	0.0486	0.0344
3	0.1730	0.1810	10.0904	10.5424	0.7227	0.7550	0.7389	0.0229	0.0162
4	0.1820	0.1940	10.5989	11.2768	0.7591	0.8077	0.7834	0.0343	0.0243
5	0.1740	0.1880	10.1469	10.9379	0.7267	0.7834	0.7550	0.0401	0.0283
6	0.1620	0.2010	9.4689	11.6723	0.6782	0.8360	0.7571	0.1116	0.0789
7	0.1530	0.2120	8.9605	12.2938	0.6418	0.8805	0.7611	0.1688	0.1194
8	0.1520	0.1690	8.9040	9.8644	0.6377	0.7065	0.6721	0.0486	0.0344
9	0.1640	0.1890	9.5819	10.9944	0.6863	0.7874	0.7368	0.0715	0.0506
10	0.1890	0.1970	10.9944	11.4463	0.7874	0.8198	0.8036	0.0229	0.0162
11	0.1970	0.2140	11.4463	12.4068	0.8198	0.8886	0.8542	0.0486	0.0344
12	0.2290	0.1950	13.2542	11.3333	0.9493	0.8117	0.8805	0.0973	0.0688
13	0.1940	0.2080	11.2768	12.0678	0.8077	0.8643	0.8360	0.0401	0.0283
14	0.1860	0.2090	10.8249	12.1243	0.7753	0.8683	0.8218	0.0658	0.0465
15	0.1990	0.2130	11.5593	12.3503	0.8279	0.8845	0.8562	0.0401	0.0283
16	0.2020	0.2180	11.7288	12.6328	0.8400	0.9048	0.8724	0.0458	0.0324
17	0.2170	0.2160	12.5763	12.5198	0.9007	0.8967	0.8987	0.0029	0.0020
18	0.2170	0.2180	12.5763	12.6328	0.9007	0.9048	0.9027	0.0029	0.0020

Appendix 1.15: Data from bioreduction of Kaolin 2 using 10mM lactate.

Days	Absorbance		Fe ²⁺ (µg)		Fe(II) mmol/L		Average	STD	Error
	1	2	1	2	1	2			
0	0.0000	0.0000	0.3164	0.3164	0.0227	0.0227	0.0227	0.0000	0.0000
1	0.1500	0.1520	8.7910	8.9040	0.6296	0.6377	0.6337	0.0057	0.0040
2	0.1670	0.1740	9.7514	10.1469	0.6984	0.7267	0.7126	0.0200	0.0142
3	0.1910	0.1900	11.1073	11.0508	0.7955	0.7915	0.7935	0.0029	0.0020
4	0.1970	0.1970	11.4463	11.4463	0.8198	0.8198	0.8198	0.0000	0.0000
5	0.1860	0.2000	10.8249	11.6158	0.7753	0.8319	0.8036	0.0401	0.0283
6	0.1980	0.2010	11.5028	11.6723	0.8238	0.8360	0.8299	0.0086	0.0061
7	0.2050	0.2000	11.8983	11.6158	0.8522	0.8319	0.8420	0.0143	0.0101
8	0.2030	0.2130	11.7853	12.3503	0.8441	0.8845	0.8643	0.0286	0.0202
9	0.2130	0.2230	12.3503	12.9153	0.8845	0.9250	0.9048	0.0286	0.0202
10	0.2370	0.2250	13.7062	13.0282	0.9816	0.9331	0.9574	0.0343	0.0243
11	0.2290	0.2400	13.2542	13.8757	0.9493	0.9938	0.9715	0.0315	0.0223
12	0.2440	0.2500	14.1017	14.4407	1.0100	1.0342	1.0221	0.0172	0.0121
13	0.2550	0.2500	14.7232	14.4407	1.0545	1.0342	1.0444	0.0143	0.0101
14	0.2430	0.2340	14.0452	13.5367	1.0059	0.9695	0.9877	0.0258	0.0182
15	0.2380	0.2440	13.7627	14.1017	0.9857	1.0100	0.9978	0.0172	0.0121
16	0.2400	0.2490	13.8757	14.3842	0.9938	1.0302	1.0120	0.0258	0.0182
17	0.2410	0.2410	13.9322	13.9322	0.9978	0.9978	0.9978	0.0000	0.0000
18	0.2500	0.2340	14.4407	13.5367	1.0342	0.9695	1.0019	0.0458	0.0324

Appendix 1.16: Data from bioreduction of Kaolin 2 using 15mM lactate.

Days	Absorbance		Fe ²⁺ (µg)		Fe(II) mmol/L		Average	STD	Error
	1	2	1	2	1	2			
0	0.0000	0.0000	0.3164	0.3164	0.0227	0.0227	0.0227	0.0000	0.0000
1	0.1580	0.1580	9.2429	9.2429	0.6620	0.6620	0.6620	0.0000	0.0000
2	0.1690	0.1780	9.8644	10.3729	0.7065	0.7429	0.7247	0.0258	0.0182
3	0.1930	0.2010	11.2203	11.6723	0.8036	0.8360	0.8198	0.0229	0.0162
4	0.1880	0.2120	10.9379	12.2938	0.7834	0.8805	0.8319	0.0687	0.0486
5	0.2070	0.2140	12.0113	12.4068	0.8603	0.8886	0.8744	0.0200	0.0142
6	0.2070	0.2250	12.0113	13.0282	0.8603	0.9331	0.8967	0.0515	0.0364
7	0.2120	0.2210	12.2938	12.8023	0.8805	0.9169	0.8987	0.0258	0.0182
8	0.2170	0.2260	12.5763	13.0847	0.9007	0.9371	0.9189	0.0258	0.0182
9	0.2330	0.2440	13.4802	14.1017	0.9655	1.0100	0.9877	0.0315	0.0223
10	0.2240	0.2690	12.9718	15.5141	0.9290	1.1111	1.0201	0.1288	0.0910
11	0.2410	0.2620	13.9322	15.1186	0.9978	1.0828	1.0403	0.0601	0.0425
12	0.2540	0.2650	14.6667	15.2881	1.0504	1.0949	1.0727	0.0315	0.0223
13	0.2740	0.2760	15.7966	15.9096	1.1314	1.1395	1.1354	0.0057	0.0040
14	0.2590	0.2410	14.9492	13.9322	1.0707	0.9978	1.0342	0.0515	0.0364
15	0.2710	0.2650	15.6271	15.2881	1.1192	1.0949	1.1071	0.0172	0.0121
16	0.2700	0.2790	15.5706	16.0791	1.1152	1.1516	1.1334	0.0258	0.0182
17	0.2790	0.2820	16.0791	16.2486	1.1516	1.1637	1.1577	0.0086	0.0061
18	0.2800	0.2850	16.1356	16.4181	1.1556	1.1759	1.1658	0.0143	0.0101

Appendix 1.17: Data from bioreduction of Kaolin 2 using 20mM lactate.

Days	Absorbance		Fe ²⁺ (µg)		Fe(II) mmol/L		Average	STD	Error
	1	2	1	2	1	2			
0	0.0000	0.0000	0.3164	0.3164	0.0227	0.0227	0.0227	0.0000	0.0000
1	0.1610	0.1670	9.4124	9.7514	0.6741	0.6984	0.6863	0.0172	0.0121
2	0.1870	0.1850	10.8814	10.7684	0.7793	0.7712	0.7753	0.0057	0.0040
3	0.2020	0.2120	11.7288	12.2938	0.8400	0.8805	0.8603	0.0286	0.0202
4	0.2210	0.2140	12.8023	12.4068	0.9169	0.8886	0.9027	0.0200	0.0142
5	0.2190	0.2270	12.6893	13.1412	0.9088	0.9412	0.9250	0.0229	0.0162
6	0.2140	0.2290	12.4068	13.2542	0.8886	0.9493	0.9189	0.0429	0.0303
7	0.2280	0.2330	13.1977	13.4802	0.9452	0.9655	0.9553	0.0143	0.0101
8	0.2270	0.2420	13.1412	13.9887	0.9412	1.0019	0.9715	0.0429	0.0303
9	0.2420	0.2470	13.9887	14.2712	1.0019	1.0221	1.0120	0.0143	0.0101
10	0.2780	0.2700	16.0226	15.5706	1.1475	1.1152	1.1314	0.0229	0.0162
11	0.2690	0.2720	15.5141	15.6836	1.1111	1.1233	1.1172	0.0086	0.0061
12	0.2730	0.2700	15.7401	15.5706	1.1273	1.1152	1.1212	0.0086	0.0061
13	0.2860	0.2910	16.4746	16.7571	1.1799	1.2001	1.1900	0.0143	0.0101
14	0.2780	0.2820	16.0226	16.2486	1.1475	1.1637	1.1556	0.0114	0.0081
15	0.2870	0.2850	16.5311	16.4181	1.1840	1.1759	1.1799	0.0057	0.0040
16	0.2900	0.2890	16.7006	16.6441	1.1961	1.1921	1.1941	0.0029	0.0020
17	0.3000	0.3070	17.2655	17.6610	1.2366	1.2649	1.2507	0.0200	0.0142
18	0.3010	0.3210	17.3220	18.4520	1.2406	1.3215	1.2811	0.0572	0.0405

Appendix 1.18: Data from bioreduction of Kaolin 2 amended with different concentration of lactate (5 – 20mM)

Days	Blank	Fe ²⁺ (μ g)	Fe(II) mmol/L
0	0.0000	0.3164	0.0227
1	0.0010	0.3729	0.0267
2	0.0040	0.5424	0.0388
3	0.0060	0.6554	0.0469
4	0.0060	0.6554	0.0469
5	0.0050	0.5989	0.0429
6	0.0090	0.8249	0.0591
7	0.0050	0.5989	0.0429
8	0.0070	0.7119	0.0510
9	0.0060	0.6554	0.0469
10	0.0080	0.7684	0.0550
11	0.0090	0.8249	0.0591
12	0.0060	0.6554	0.0469
13	0.0040	0.5424	0.0388
14	0.0030	0.4859	0.0348
15	0.0040	0.5424	0.0388
16	0.0040	0.5424	0.0388
17	0.0020	0.4294	0.0308
18	0.0010	0.3729	0.0267

Appendix 1.19: Natural log of Fe(II) calculated from bioreduction of Kaolin 2 added with 0.1mM lactate.

Hours	Fe(II) mmol/L			LN[Fe(II)]			Average	STD	Error
	1	2	3	1	2	3			
0	0.0080	0.0080	0.0080	-4.8336	-4.8336	-4.8336	-4.8336	0.0000	0.0000
2	0.0318	0.0438	0.0279	-3.4473	-3.1289	-3.5808	-3.3857	0.2322	0.1341
4	0.0239	0.0438	0.0199	-3.7350	-3.1289	-3.9173	-3.5937	0.4128	0.2383
6	0.0199	0.0477	0.0358	-3.9173	-3.0418	-3.3295	-3.4296	0.4462	0.2576
8	0.0199	0.0438	0.0836	-3.9173	-3.1289	-2.4822	-3.1761	0.7187	0.4149
10	0.0199	0.0836	0.0875	-3.9173	-2.4822	-2.4357	-2.9451	0.8423	0.4863
12	0.0279	0.0836	0.0995	-3.5808	-2.4822	-2.3079	-2.7903	0.6901	0.3985
14	0.0358	0.0836	0.1154	-3.3295	-2.4822	-2.1595	-2.6571	0.6043	0.3489
18	0.0119	0.0477	0.0279	-4.4281	-3.0418	-3.5808	-3.6836	0.6988	0.4035
34	0.0159	0.0557	0.0239	-4.1405	-2.8877	-3.7350	-3.5877	0.6392	0.3691
38	0.0119	0.0517	0.0318	-4.4281	-2.9618	-3.4473	-3.6124	0.7470	0.4313
42	0.0318	0.0597	0.0676	-3.4473	-2.8187	-2.6935	-2.9865	0.4039	0.2332
58	0.0358	0.0597	0.0637	-3.3295	-2.8187	-2.7542	-2.9675	0.3152	0.1820
82	0.0398	0.0716	0.0716	-3.2242	-2.6364	-2.6364	-2.8323	0.3394	0.1959
106	0.0398	0.0995	0.1592	-3.2242	-2.3079	-1.8379	-2.4566	0.7050	0.4070
130	0.0398	0.1313	0.1313	-3.2242	-2.0302	-2.0302	-2.4282	0.6893	0.3980

Appendix 1.20: Natural log of Fe(II) calculated from bioreduction of Kaolin 2 added with 0.3mM lactate.

Hours	Fe(II) mmol/L			LN[Fe(II)]			Average	STD	Error
	1	2	3	1	2	3			
0	0.0080	0.0080	0.0080	-4.8336	-4.8336	-4.8336	-4.8336	0.0000	0.0000
2	0.0597	0.1035	0.0955	-2.8187	-2.2687	-2.3487	-2.4787	0.2972	0.1716
4	0.0557	0.1671	0.1393	-2.8877	-1.7891	-1.9714	-2.2161	0.5888	0.3399
6	0.0716	0.1631	0.1830	-2.6364	-1.8132	-1.6981	-2.0492	0.5117	0.2955
8	0.0676	0.1472	0.2149	-2.6935	-1.9158	-1.5378	-2.0490	0.5893	0.3402
10	0.1194	0.1751	0.1950	-2.1255	-1.7426	-1.6349	-1.8343	0.2579	0.1489
12	0.0875	0.1910	0.2308	-2.4357	-1.6555	-1.4663	-1.8525	0.5138	0.2967
14	0.1353	0.1989	0.2308	-2.0004	-1.6147	-1.4663	-1.6938	0.2757	0.1592
18	0.1989	0.1989	0.2467	-1.6147	-1.6147	-1.3996	-1.5430	0.1242	0.0717
34	0.1830	0.1830	0.2069	-1.6981	-1.6981	-1.5755	-1.6572	0.0708	0.0409
38	0.1870	0.1870	0.2666	-1.6766	-1.6766	-1.3221	-1.5584	0.2047	0.1182
42	0.1552	0.1910	0.2228	-1.8632	-1.6555	-1.5014	-1.6734	0.1816	0.1048
58	0.1273	0.1552	0.2308	-2.0610	-1.8632	-1.4663	-1.7968	0.3029	0.1749
82	0.1313	0.2308	0.1830	-2.0302	-1.4663	-1.6981	-1.7315	0.2835	0.1637
106	0.1950	0.2308	0.2706	-1.6349	-1.4663	-1.3072	-1.4695	0.1639	0.0946
130	0.2109	0.2228	0.2268	-1.5565	-1.5014	-1.4837	-1.5138	0.0379	0.0219

Appendix 1.21: Natural log of Fe(II) calculated from bio-reduction of Kaolin 2 added with 0.5mM lactate.

Hours	Fe(II) mmol/L			LN[Fe(II)]			Average	STD	Error
	1	2	3	1	2	3			
0	0.0080	0.0080	0.0080	-4.8336	-4.8336	-4.8336	-4.8336	0.0000	0.0000
2	0.1233	0.1233	0.1114	-2.0928	-2.0928	-2.1945	-2.1267	0.0588	0.0339
4	0.2467	0.1592	0.1830	-1.3996	-1.8379	-1.6981	-1.6452	0.2239	0.1292
6	0.2666	0.1989	0.2308	-1.3221	-1.6147	-1.4663	-1.4677	0.1463	0.0845
8	0.2666	0.2348	0.2586	-1.3221	-1.4492	-1.3524	-1.3745	0.0664	0.0383
10	0.2706	0.2268	0.2944	-1.3072	-1.4837	-1.2227	-1.3379	0.1332	0.0769
12	0.2825	0.2666	0.3024	-1.2641	-1.3221	-1.1960	-1.2607	0.0631	0.0364
14	0.3422	0.2666	0.2547	-1.0724	-1.3221	-1.3679	-1.2541	0.1590	0.0918
18	0.3462	0.2626	0.3302	-1.0608	-1.3371	-1.1079	-1.1686	0.1478	0.0853
34	0.3382	0.2467	0.3223	-1.0841	-1.3996	-1.1323	-1.2053	0.1700	0.0981
38	0.2905	0.2666	0.1950	-1.2363	-1.3221	-1.6349	-1.3978	0.2098	0.1211
42	0.3382	0.1989	0.2228	-1.0841	-1.6147	-1.5014	-1.4001	0.2794	0.1613
58	0.2109	0.1950	0.2507	-1.5565	-1.6349	-1.3836	-1.5250	0.1286	0.0742
82	0.2188	0.2308	0.2467	-1.5194	-1.4663	-1.3996	-1.4618	0.0600	0.0347
106	0.2825	0.2308	0.2745	-1.2641	-1.4663	-1.2926	-1.3410	0.1094	0.0632
130	0.3621	0.2507	0.2905	-1.0159	-1.3836	-1.2363	-1.2119	0.1851	0.1068

Appendix 1.22: Natural log of Fe(II) calculated from bio-reduction of Kaolin 2 added with 0.5mM lactate.

Hours	Fe(II) mmol/L			LN[Fe(II)]			Average	STD	Error
	1	2	3	1	2	3			
0	0.0080	0.0080	0.0080	-4.8336	-4.8336	-4.8336	-4.8336	0.0000	0.0000
2	0.1353	0.1512	0.1393	-2.0004	-1.8892	-1.9714	-1.9536	0.0577	0.0333
4	0.1910	0.2069	0.1910	-1.6555	-1.5755	-1.6555	-1.6289	0.0462	0.0267
6	0.1989	0.2825	0.2427	-1.6147	-1.2641	-1.4159	-1.4316	0.1759	0.1015
8	0.2865	0.2984	0.2865	-1.2501	-1.2093	-1.2501	-1.2365	0.0236	0.0136
10	0.3064	0.3302	0.2944	-1.1829	-1.1079	-1.2227	-1.1712	0.0583	0.0337
12	0.3422	0.3462	0.3581	-1.0724	-1.0608	-1.0269	-1.0534	0.0236	0.0136
14	0.3422	0.3422	0.3541	-1.0724	-1.0724	-1.0381	-1.0610	0.0198	0.0114
18	0.3462	0.3661	0.3740	-1.0608	-1.0050	-0.9835	-1.0164	0.0399	0.0231
34	0.3501	0.3860	0.3820	-1.0494	-0.9520	-0.9624	-0.9879	0.0535	0.0309
38	0.3860	0.3223	0.3740	-0.9520	-1.1323	-0.9835	-1.0226	0.0963	0.0556
42	0.3541	0.3422	0.2547	-1.0381	-1.0724	-1.3679	-1.1595	0.1813	0.1047
58	0.2944	0.3700	0.2785	-1.2227	-0.9941	-1.2783	-1.1650	0.1506	0.0869
82	0.2944	0.2109	0.3024	-1.2227	-1.5565	-1.1960	-1.3251	0.2008	0.1160
106	0.2865	0.4178	0.2745	-1.2501	-0.8728	-1.2926	-1.1385	0.2311	0.1334
130	0.2188	0.3342	0.3462	-1.5194	-1.0959	-1.0608	-1.2254	0.2552	0.1474

Appendix 1.23: Bioreduction of Kaolin 2 comparing effect of electron shuttling system

	(AQDS)	Absorbance	Fe ²⁺ (μg)		Fe(II) mmol/L				
Days	1	2	1	2	1	2	Average	STD	Error
0	0.0000	0.0000	0.2500	0.2500	0.0179	0.0179	0.0179	0.0000	0.0000
1	0.0870	0.0960	4.6000	5.0500	0.3295	0.3617	0.3456	0.0228	0.0161
2	0.1260	0.1390	6.5500	7.2000	0.4691	0.5157	0.4924	0.0329	0.0233
3	0.1600	0.1710	8.2500	8.8000	0.5909	0.6303	0.6106	0.0279	0.0197
4	0.1610	0.1820	8.3000	9.3500	0.5944	0.6697	0.6321	0.0532	0.0376
5	0.1850	0.1890	9.5000	9.7000	0.6804	0.6947	0.6876	0.0101	0.0072

	(NOM 1)	Absorbance	Fe ²⁺ (μg)		Fe(II) mmol/L				
Days	1	2	1	2	1	2	Average	STD	Error
0	0.0000	0.0000	0.2500	0.2500	0.0179	0.0179	0.0179	0.0000	0.0000
1	0.0920	0.1030	4.8500	5.4000	0.3474	0.3868	0.3671	0.0279	0.0197
2	0.1230	0.1090	6.4000	5.7000	0.4584	0.4082	0.4333	0.0355	0.0251
3	0.1320	0.1480	6.8500	7.6500	0.4906	0.5479	0.5192	0.0405	0.0286
4	0.1530	0.1500	7.9000	7.7500	0.5658	0.5551	0.5604	0.0076	0.0054
5	0.1750	0.1740	9.0000	8.9500	0.6446	0.6410	0.6428	0.0025	0.0018

	(NO NOM)	Absorbance	Fe ²⁺ (μg)		Fe(II) mmol/L				
Days	1	2	1	2	1	2	Average	STD	Error
0	0.0000	0.0000	0.2500	0.2500	0.0179	0.0179	0.0179	0.0000	0.0000
1	0.0730	0.0760	3.9000	4.0500	0.2793	0.2901	0.2847	0.0076	0.0054
2	0.0840	0.1110	4.4500	5.8000	0.3187	0.4154	0.3671	0.0684	0.0483
3	0.1280	0.1200	6.6500	6.2500	0.4763	0.4476	0.4620	0.0203	0.0143
4	0.1560	0.1560	8.0500	8.0500	0.5765	0.5765	0.5765	0.0000	0.0000
5	0.1720	0.1650	8.8500	8.5000	0.6338	0.6088	0.6213	0.0177	0.0125

Days	Blank	Fe ²⁺ (μg)	Fe(II) mmol/L
0	0.0000	0.2500	0.0179
1	0.0050	0.5000	0.0358
2	0.0050	0.5000	0.0358
3	0.0090	0.7000	0.0501
4	0.0020	0.3500	0.0251
5	0.0070	0.6000	0.0430

Appendix 1.24: Bioreduction of Kaolin 3 comparing effect of electron shuttling system

Days	Absorbance NOM 1			Fe2+(μg)			Fe(II) mmol/L			average	STD	Error
	1	2	3	1	2	3	1	2	3			
0	0.0000	0.0000	0.0000	0.2500	0.2500	0.2500	0.0179	0.0179	0.0179	0.0179	0.0000	0.0000
1	0.0920	0.1160	0.1190	4.8500	6.0500	6.2000	0.3474	0.4333	0.4440	0.4082	0.0530	0.0306
2	0.1260	0.1200	0.1580	6.5500	6.2500	8.1500	0.4691	0.4476	0.5837	0.5001	0.0732	0.0422
3	0.1350	0.1500	0.1680	7.0000	7.7500	8.6500	0.5013	0.5551	0.6195	0.5586	0.0592	0.0342
4	0.1610	0.1850	0.1990	8.3000	9.5000	10.2000	0.5944	0.6804	0.7305	0.6685	0.0688	0.0397
5	0.1670	0.2160	0.1990	8.6000	11.0500	10.2000	0.6159	0.7914	0.7305	0.7126	0.0891	0.0514

Days	Absorbance NOM 2			Fe2+(μg)			Fe(II) mmol/L			average	STD	Error
	1	2	3	1	2	3	1	2	3			
0	0.0000	0.0000	0.0000	0.2500	0.2500	0.2500	0.0179	0.0179	0.0179	0.0179	0.0000	0.0000
1	0.1740	0.1380	0.1440	8.9500	7.1500	7.4500	0.6410	0.5121	0.5336	0.5622	0.0691	0.0399
2	0.2000	0.1560	0.1860	10.2500	8.0500	9.5500	0.7341	0.5765	0.6840	0.6649	0.0805	0.0465
3	0.2060	0.1960	0.1920	10.5500	10.0500	9.8500	0.7556	0.7198	0.7055	0.7269	0.0258	0.0149
4	0.2560	0.2040	0.2240	13.0500	10.4500	11.4500	0.9346	0.7484	0.8201	0.8344	0.0939	0.0542
5	0.2750	0.2260	0.2150	14.0000	11.5500	11.0000	1.0027	0.8272	0.7878	0.8726	0.1144	0.0660

	Absorbance (AQDS)			Fe2+(µg)			Fe(II) mmol/L					
Days	1	2	3	1	2	3	1	2	3	average	STD	Error
0	0.0000	0.0000	0.0000	0.2500	0.2500	0.2500	0.0179	0.0179	0.0179	0.0179	0.0000	0.0000
1	0.2000	0.2250	0.2010	10.2500	11.5000	10.3000	0.7341	0.8236	0.7377	0.7651	0.0507	0.0293
2	0.2230	0.2270	0.2500	11.4000	11.6000	12.7500	0.8165	0.8308	0.9132	0.8535	0.0522	0.0301
3	0.2280	0.2390	0.2500	11.6500	12.2000	12.7500	0.8344	0.8738	0.9132	0.8738	0.0394	0.0227
4	0.2540	0.2180	0.2620	12.9500	11.1500	13.3500	0.9275	0.7986	0.9561	0.8941	0.0839	0.0485
5	0.2590	0.2500	0.2590	13.2000	12.7500	13.2000	0.9454	0.9132	0.9454	0.9346	0.0186	0.0107

	Absorbance (No ES)			Fe2+(µg)			Fe(II) mmol/L					
Days	1	2	3	1	2	3	1	2	3	average	STD	Error
0	0.0000	0.0000	0.0000	0.2500	0.2500	0.2500	0.0179	0.0179	0.0179	0.0179	0.0000	0.0000
1	0.1160	0.1340	0.1370	6.0500	6.9500	7.1000	0.4333	0.4978	0.5085	0.4799	0.0407	0.0235
2	0.1480	0.1570	0.1520	7.6500	8.1000	7.8500	0.5479	0.5801	0.5622	0.5634	0.0161	0.0093
3	0.1780	0.1710	0.1940	9.1500	8.8000	9.9500	0.6553	0.6303	0.7126	0.6661	0.0422	0.0244
4	0.1940	0.1770	0.2070	9.9500	9.1000	10.6000	0.7126	0.6517	0.7592	0.7078	0.0539	0.0311
5	0.1830	0.2170	0.2070	9.4000	11.1000	10.6000	0.6732	0.7950	0.7592	0.7425	0.0626	0.0361

Days	Blank	Fe2+(µg)	Fe(II) mmol/L
0	0.0000	0.2500	0.0179
1	0.0030	0.4000	0.0286
2	0.0040	0.4500	0.0322
3	0.0050	0.5000	0.0358
4	0.0080	0.6500	0.0466
5	0.0090	0.7000	0.0501

Appendix 1.25: Bioreduction of Kaolin 3 and Kaolin 4: relative importance of biogenic and abiotic factors.

	Absorbance			Fe ²⁺ (µg)			Fe(II) mmol/L			Bleached + cell		
Days	1	2	3	1	2	3	1	2	3	Average	STD	Error
0	0.0000	0.0000	0.0000	0.3164	0.3164	0.3164	0.0227	0.0227	0.0227	0.0227	0.0000	0.0000
1	0.1380	0.1180	0.1170	8.1130	6.9831	6.9266	0.5811	0.5001	0.4961	0.5258	0.0479	0.0277
2	0.1300	0.1900	0.1890	7.6610	11.0508	10.9944	0.5487	0.7915	0.7874	0.7092	0.1390	0.0803
3	0.2050	0.1880	0.1830	11.8983	10.9379	10.6554	0.8522	0.7834	0.7631	0.7996	0.0467	0.0269
4	0.1910	0.1990	0.1820	11.1073	11.5593	10.5989	0.7955	0.8279	0.7591	0.7942	0.0344	0.0199
5	0.1710	0.1910	0.1970	9.9774	11.1073	11.4463	0.7146	0.7955	0.8198	0.7766	0.0551	0.0318
7	0.2080	0.2870	0.2340	12.0678	16.5311	13.5367	0.8643	1.1840	0.9695	1.0059	0.1629	0.0941
10	0.2730	0.3280	0.3020	15.7401	18.8475	17.3785	1.1273	1.3499	1.2447	1.2406	0.1113	0.0643

	Absorbance			Fe ²⁺ (µg)			Fe(II) mmol/L			Bleached/no cell/sterile		
Days	1	2	3	1	2	3	1	2	3	average	Std	Error
0	0.0000	0.0000	0.0000	0.3164	0.3164	0.3164	0.0227	0.0227	0.0227	0.0227	0.0000	0.0000
1	0.0030	0.0030	0.0030	0.4859	0.4859	0.4859	0.0348	0.0348	0.0348	0.0348	0.0000	0.0000
2	0.0030	0.0030	0.0070	0.4859	0.4859	0.7119	0.0348	0.0348	0.0510	0.0402	0.0093	0.0054
3	0.0020	0.0070	0.0040	0.4294	0.7119	0.5424	0.0308	0.0510	0.0388	0.0402	0.0102	0.0059
4	0.0050	0.0060	0.0080	0.5989	0.6554	0.7684	0.0429	0.0469	0.0550	0.0483	0.0062	0.0036
5	0.0040	0.0040	0.0070	0.5424	0.5424	0.7119	0.0388	0.0388	0.0510	0.0429	0.0070	0.0040
7	0.0030	0.0090	0.0030	0.4859	0.8249	0.4859	0.0348	0.0591	0.0348	0.0429	0.0140	0.0081
10	0.0030	0.0040	0.0070	0.4859	0.5424	0.7119	0.0348	0.0388	0.0510	0.0415	0.0084	0.0049

Days	Absorbance			Fe ²⁺ (µg)			Fe(II) mmol/L			Bleached/no cell/unsterile		
	1	2	3	1	2	3	1	2	3	Average	STD	Error
0	0.0000	0.0000	0.0000	0.3164	0.3164	0.3164	0.0227	0.0227	0.0227	0.0227	0.0000	0.0000
1	0.0030	0.0050	0.0060	0.4859	0.5989	0.6554	0.0348	0.0429	0.0469	0.0415	0.0062	0.0036
2	0.0040	0.0030	0.0040	0.5424	0.4859	0.5424	0.0388	0.0348	0.0388	0.0375	0.0023	0.0013
3	0.0040	0.0020	0.0060	0.5424	0.4294	0.6554	0.0388	0.0308	0.0469	0.0388	0.0081	0.0047
4	0.0120	0.0050	0.0040	0.9944	0.5989	0.5424	0.0712	0.0429	0.0388	0.0510	0.0176	0.0102
5	0.0350	0.0110	0.0050	2.2938	0.9379	0.5989	0.1643	0.0672	0.0429	0.0914	0.0642	0.0371
7	0.0160	0.0090	0.0180	1.2203	0.8249	1.3333	0.0874	0.0591	0.0955	0.0807	0.0191	0.0110
10	0.0230	0.0260	0.0100	1.6158	1.7853	0.8814	0.1157	0.1279	0.0631	0.1022	0.0344	0.0199

Days	Absorbance			Fe ²⁺ (µg)			Fe(II) mmol/L			Unbleached + cell		
	1	2	3	1	2	3	1	2	3	Average	STD	Error
0	0.0000	0.0000	0.0000	0.3164	0.3164	0.3164	0.0227	0.0227	0.0227	0.0227	0.0000	0.0000
1	0.2500	0.4510	0.3130	14.4407	25.7966	18.0000	1.0342	1.8476	1.2892	1.3903	0.4160	0.2402
2	0.2550	0.3650	0.3320	14.7232	20.9379	19.0734	1.0545	1.4996	1.3660	1.3067	0.2284	0.1319
3	0.4640	0.4130	0.3450	26.5311	23.6497	19.8079	1.9002	1.6938	1.4187	1.6709	0.2416	0.1395
4	0.4160	0.3710	0.4020	23.8192	21.2768	23.0282	1.7059	1.5239	1.6493	1.6264	0.0932	0.0538
5	0.3590	0.4790	0.4610	20.5989	27.3785	26.3616	1.4753	1.9609	1.8880	1.7747	0.2619	0.1512
7	0.5670	0.5170	0.4890	32.3503	29.5254	27.9435	2.3169	2.1146	2.0013	2.1443	0.1599	0.0923
10	0.4810	0.4920	0.4680	27.4915	28.1130	26.7571	1.9690	2.0135	1.9164	1.9663	0.0486	0.0281

Days	Absorbance			Fe ²⁺ (μg)			Fe(II) mmol/L			Unbleached/no cell/sterile		
	1	2	3	1	2	3	1	2	3	Average	STD	Error
0	0.0000	0.0000	0.0000	0.3164	0.3164	0.3164	0.0227	0.0227	0.0227	0.0227	0.0000	0.0000
1	0.0010	0.0010	0.0010	0.3729	0.3729	0.3729	0.0267	0.0267	0.0267	0.0267	0.0000	0.0000
2	0.0010	0.0010	0.0020	0.3729	0.3729	0.4294	0.0267	0.0267	0.0308	0.0281	0.0023	0.0013
3	0.0040	0.0010	0.0060	0.5424	0.3729	0.6554	0.0388	0.0267	0.0469	0.0375	0.0102	0.0059
4	0.0040	0.0040	0.0080	0.5424	0.5424	0.7684	0.0388	0.0388	0.0550	0.0442	0.0093	0.0054
5	0.0040	0.0050	0.0150	0.5424	0.5989	1.1638	0.0388	0.0429	0.0834	0.0550	0.0246	0.0142
7	0.0060	0.0080	0.0080	0.6554	0.7684	0.7684	0.0469	0.0550	0.0550	0.0523	0.0047	0.0027
10	0.0040	0.0030	0.0090	0.5424	0.4859	0.8249	0.0388	0.0348	0.0591	0.0442	0.0130	0.0075

Days	Absorbance			Fe ²⁺ (μg)			Fe(II) mmol/L			Unbleached/ no cell/unsterile		
	1	2	3	1	2	3	1	2	3	average	Std	Error
0	0.0000	0.0000	0.0000	0.3164	0.3164	0.3164	0.0227	0.0227	0.0227	0.0227	0.0000	0.0000
1	0.0020	0.0030	0.0050	0.4294	0.4859	0.5989	0.0308	0.0348	0.0429	0.0361	0.0062	0.0036
2	0.0020	0.0040	0.0030	0.4294	0.5424	0.4859	0.0308	0.0388	0.0348	0.0348	0.0040	0.0023
3	0.0020	0.0010	0.0050	0.4294	0.3729	0.5989	0.0308	0.0267	0.0429	0.0334	0.0084	0.0049
4	0.0140	0.0080	0.0080	1.1073	0.7684	0.7684	0.0793	0.0550	0.0550	0.0631	0.0140	0.0081
5	0.0190	0.0060	0.0100	1.3898	0.6554	0.8814	0.0995	0.0469	0.0631	0.0699	0.0269	0.0156
7	0.0230	0.0120	0.0100	1.6158	0.9944	0.8814	0.1157	0.0712	0.0631	0.0834	0.0283	0.0164
10	0.0180	0.0140	0.0230	1.3333	1.1073	1.6158	0.0955	0.0793	0.1157	0.0968	0.0182	0.0105

APPENDIX 2

Appendix 2.1: Selection of the most suitable iron reducing bacteria for leaching of silica sand

	Average Fe(II) mmol/L								
Days	<i>S. loihica</i>	STD	Error	<i>S. oneidensis</i>	STD	Error	<i>S. alga BrY</i>	STD	Error
0	0.0187	0.0000	0.0000	0.0187	0.0000	0.0000	0.0187	0.0000	0.0000
1	0.0065	0.0014	0.0008	0.2784	0.0106	0.0061	0.2567	0.0512	0.0296
2	0.0087	0.0012	0.0007	0.3157	0.0297	0.0172	0.3411	0.0061	0.0035
3	0.0112	0.0013	0.0008	0.3314	0.0290	0.0167	0.3796	0.0312	0.0180
4	0.0126	0.0011	0.0006	0.3362	0.0257	0.0149	0.4218	0.0074	0.0043
5	0.0151	0.0014	0.0008	0.3712	0.0104	0.0060	0.4411	0.0034	0.0020
10				0.3953	0.0201	0.0116	0.4592	0.0156	0.0090

Fe(II) mmol/L			
Day	CIP8040	SD	Error
0	0.0187	0.0000	0.0000
1	0.3085	0.0316	0.0183
3	0.3303	0.0050	0.0029
5	0.3520	0.0057	0.0033
9	0.3956	0.0125	0.0072
12	0.4125	0.0104	0.0060
15	0.4246	0.0115	0.0066

Appendix 2.2: Bioreduction of silica sand comparing effect of electron shuttling system and volume of cell suspension added.

Day	Absorbance (AQDS)			Fe2+(µg)			Fe(II) leached mmol/L			3.5ml of cells		
	1	2	3	1	2	3	1	2	3	Average	STD	Error
0	0.0000	0.0000	0.0000	0.2500	0.2500	0.2500	0.0179	0.0179	0.0179	0.0179	0.0000	0.0000
1	0.0230	0.0380	0.0270	1.4000	2.1500	1.6000	0.1003	0.1540	0.1146	0.1229	0.0278	0.0161
3	0.0290	0.0700	0.0440	1.7000	3.7500	2.4500	0.1218	0.2686	0.1755	0.1886	0.0743	0.0429
5	0.0420	0.0750	0.0550	2.3500	4.0000	3.0000	0.1683	0.2865	0.2149	0.2232	0.0595	0.0344
8	0.0450	0.0780	0.0630	2.5000	4.1500	3.4000	0.1791	0.2972	0.2435	0.2399	0.0592	0.0342
11	0.0610	0.0850	0.0650	3.3000	4.5000	3.5000	0.2363	0.3223	0.2507	0.2698	0.0460	0.0266
15	0.0650	0.0890	0.0710	3.5000	4.7000	3.8000	0.2507	0.3366	0.2722	0.2865	0.0447	0.0258

Day	Absorbance (AQDS)			Fe2+(µg)			Fe(II) leached mmol/L			7ml of cells		
	1	2	3	1	2	3	1	2	3	Average	STD	Error
0	0.0000	0.0000	0.0000	0.2500	0.2500	0.2500	0.0179	0.0179	0.0179	0.0179	0.0000	0.0000
1	0.0500	0.0700	0.0680	2.7500	3.7500	3.6500	0.1970	0.2686	0.2614	0.2423	0.0394	0.0228
3	0.0750	0.0750	0.0720	4.0000	4.0000	3.8500	0.2865	0.2865	0.2757	0.2829	0.0062	0.0036
5	0.0790	0.0810	0.0770	4.2000	4.3000	4.1000	0.3008	0.3080	0.2936	0.3008	0.0072	0.0041
8	0.0910	0.0840	0.0830	4.8000	4.4500	4.4000	0.3438	0.3187	0.3151	0.3259	0.0156	0.0090
11	0.0940	0.0890	0.0870	4.9500	4.7000	4.6000	0.3545	0.3366	0.3295	0.3402	0.0129	0.0075
15	0.0970	0.0930	0.0890	5.1000	4.9000	4.7000	0.3653	0.3509	0.3366	0.3509	0.0143	0.0083

Day	Absorbance (NOM 2)			Fe2+(µg)			Fe(II) leached mmol/L			7ml of cells		
	1	2	3	1	2	3	1	2	3	average	STD	Error
0	0.0000	0.0000	0.0000	0.2500	0.2500	0.2500	0.0179	0.0179	0.0179	0.0179	0.0000	0.0000
1	0.0390	0.0370	0.0450	2.2000	2.1000	2.5000	0.1576	0.1504	0.1791	0.1623	0.0149	0.0086
3	0.0460	0.0500	0.0520	2.5500	2.7500	2.8500	0.1826	0.1970	0.2041	0.1946	0.0109	0.0063
5	0.0680	0.0630	0.0660	3.6500	3.4000	3.5500	0.2614	0.2435	0.2543	0.2531	0.0090	0.0052
8	0.0900	0.0870	0.0700	4.7500	4.6000	3.7500	0.3402	0.3295	0.2686	0.3127	0.0386	0.0223
11	0.0960	0.0920	0.0920	5.0500	4.8500	4.8500	0.3617	0.3474	0.3474	0.3521	0.0083	0.0048
15	0.1060	0.1020	0.0980	5.5500	5.3500	5.1500	0.3975	0.3832	0.3688	0.3832	0.0143	0.0083

Day	Absorbance (NOM 2)			Fe2+(µg)			Fe(II) leached mmol/L			3.5ml Cells		
	1	2	3	1	2	3	1	2	3	average	STD	Error
0	0.0000	0.0000	0.0000	0.2500	0.2500	0.2500	0.0179	0.0179	0.0179	0.0179	0.0000	0.0000
1	0.0430	0.0390	0.0400	2.4000	2.2000	2.2500	0.1719	0.1576	0.1611	0.1635	0.0075	0.0043
3	0.0480	0.0460	0.0550	2.6500	2.5500	3.0000	0.1898	0.1826	0.2149	0.1958	0.0169	0.0098
5	0.0610	0.0610	0.0590	3.3000	3.3000	3.2000	0.2363	0.2363	0.2292	0.2340	0.0041	0.0024
8	0.0650	0.0660	0.0700	3.5000	3.5500	3.7500	0.2507	0.2543	0.2686	0.2578	0.0095	0.0055
11	0.0750	0.0770	0.0750	4.0000	4.1000	4.0000	0.2865	0.2936	0.2865	0.2889	0.0041	0.0024
15	0.0770	0.0770	0.0790	4.1000	4.1000	4.2000	0.2936	0.2936	0.3008	0.2960	0.0041	0.0024

Appendix 2.3: Bioreduction of silica sand comparing effect of NOM 1, NOM2, AQDS and No Electron shuttle/ volume of cell suspension added.

Days	Absorbance (NOM 1)			Fe2+(µg)			Fe(II) leached mmol/L			Average	STD	Error
	1	2	3	1	2	3	1	2	3			
0	0.0000	0.0000	0.0000	0.2500	0.2500	0.2500	0.0179	0.0179	0.0179	0.0179	0.0000	0.0000
1	0.0230	0.0240	0.0220	1.4000	1.4500	1.3500	0.1003	0.1038	0.0967	0.1003	0.0036	0.0021
3	0.0250	0.0280	0.0240	1.5000	1.6500	1.4500	0.1074	0.1182	0.1038	0.1098	0.0075	0.0043
5	0.0500	0.0320	0.0400	2.7500	1.8500	2.2500	0.1970	0.1325	0.1611	0.1635	0.0323	0.0186
9	0.0510	0.0410	0.0410	2.8000	2.3000	2.3000	0.2005	0.1647	0.1647	0.1767	0.0207	0.0119
12	0.0520	0.0450	0.0450	2.8500	2.5000	2.5000	0.2041	0.1791	0.1791	0.1874	0.0145	0.0084
15	0.0620	0.0470	0.0470	3.3500	2.6000	2.6000	0.2399	0.1862	0.1862	0.2041	0.0310	0.0179

Days	Absorbance (NOM 2)			Fe2+(µg)			Fe(II) leached mmol/L			Average	STD	Error
	1	2	3	1	2	3	1	2	3			
0	0.0000	0.0000	0.0000	0.2500	0.2500	0.2500	0.0179	0.0179	0.0179	0.0179	0.0000	0.0000
1	0.0240	0.0240	0.0270	1.4500	1.4500	1.6000	0.1038	0.1038	0.1146	0.1074	0.0062	0.0036
3	0.0340	0.0390	0.0310	1.9500	2.2000	1.8000	0.1397	0.1576	0.1289	0.1420	0.0145	0.0084
5	0.0500	0.0470	0.0580	2.7500	2.6000	3.1500	0.1970	0.1862	0.2256	0.2029	0.0204	0.0118
9	0.0520	0.0490	0.0500	2.8500	2.7000	2.7500	0.2041	0.1934	0.1970	0.1981	0.0055	0.0032
12	0.0510	0.0540	0.0580	2.8000	2.9500	3.1500	0.2005	0.2113	0.2256	0.2125	0.0126	0.0073
15	0.0500	0.0540	0.0550	2.7500	2.9500	3.0000	0.1970	0.2113	0.2149	0.2077	0.0095	0.0055

	Absorbance (AQDS)			Fe2+(μ g)			Fe(II) leached mmol/L					
Days	1	2	3	1	2	3	1	2	3	Average	STD	Error
0	0.0000	0.0000	0.0000	0.2500	0.2500	0.2500	0.0179	0.0179	0.0179	0.0179	0.0000	0.0000
1	0.0350	0.0140	0.0180	2.0000	0.9500	1.1500	0.1432	0.0680	0.0824	0.0979	0.0399	0.0231
3	0.0420	0.0330	0.0250	2.3500	1.9000	1.5000	0.1683	0.1361	0.1074	0.1373	0.0305	0.0176
5	0.0420	0.0290	0.0410	2.3500	1.7000	2.3000	0.1683	0.1218	0.1647	0.1516	0.0259	0.0150
9	0.0570	0.0540	0.0440	3.1000	2.9500	2.4500	0.2220	0.2113	0.1755	0.2029	0.0244	0.0141
12	0.0560	0.0540	0.0460	3.0500	2.9500	2.5500	0.2184	0.2113	0.1826	0.2041	0.0189	0.0109
15	0.0650	0.0570	0.0510	3.5000	3.1000	2.8000	0.2507	0.2220	0.2005	0.2244	0.0252	0.0145

	Absorbance (No. E. Shuttle)			Fe2+(μ g)			Fe(II) leached mmol/L					
Days	1	2	3	1	2	3	1	2	3	Average	STD	Error
0	0.0000	0.0000	0.0000	0.2500	0.2500	0.2500	0.0179	0.0179	0.0179	0.0179	0.0000	0.0000
1	0.0210	0.0190	0.0120	1.3000	1.2000	0.8500	0.0931	0.0859	0.0609	0.0800	0.0169	0.0098
3	0.0300	0.0360	0.0350	1.7500	2.0500	2.0000	0.1253	0.1468	0.1432	0.1385	0.0115	0.0066
5	0.0350	0.0370	0.0300	2.0000	2.1000	1.7500	0.1432	0.1504	0.1253	0.1397	0.0129	0.0075
9	0.0490	0.0480	0.0370	2.7000	2.6500	2.1000	0.1934	0.1898	0.1504	0.1779	0.0238	0.0138
12	0.0510	0.0480	0.0420	2.8000	2.6500	2.3500	0.2005	0.1898	0.1683	0.1862	0.0164	0.0095
15	0.0440	0.0470	0.0500	2.4500	2.6000	2.7500	0.1755	0.1862	0.1970	0.1862	0.0107	0.0062

Day	Blank	Fe2+(μg)	Fe(II) leached mmol/L
0	0.0000	0.2500	0.0179
1	0.0030	0.4000	0.0286
3	0.0030	0.4000	0.0286
5	0.0010	0.3000	0.0215
8	0.0020	0.3500	0.0251
11	0.0010	0.3000	0.0215
15	0.0020	0.3500	0.0251

Days	Blank	Fe2+(μg)	Fe(II) leached mmol/L
0	0.0000	0.2500	0.0179
1	0.0020	0.3500	0.0251
3	0.0030	0.4000	0.0286
5	0.0010	0.3000	0.0215
9	0.0010	0.3000	0.0215
12	0.0000	0.2500	0.0179
15	0.0000	0.2500	0.0179

Appendix 2.4: Data from bioreduction of silica sand amended with different concentration of lactate (1– 15mM)

Hours	Absorbance		Fe2+(µg)		Fe(II) leached mmol/L		1mM	STD	Error
	1	2	1	2	1	2	Average		
0	0.0000	0.0000	0.1111	0.1111	0.0080	0.0080	0.0080	0.0000	0.0000
2	0.0080	0.0080	0.5556	0.5556	0.0398	0.0398	0.0398	0.0000	0.0000
6	0.0090	0.0040	0.6111	0.3333	0.0438	0.0239	0.0338	0.0141	0.0099
8	0.0100	0.0070	0.6667	0.5000	0.0477	0.0358	0.0418	0.0084	0.0060
24	0.0110	0.0120	0.7222	0.7778	0.0517	0.0557	0.0537	0.0028	0.0020
48	0.0190	0.0160	1.1667	1.0000	0.0836	0.0716	0.0776	0.0084	0.0060
72	0.0160	0.0140	1.0000	0.8889	0.0716	0.0637	0.0676	0.0056	0.0040
96	0.0170	0.0140	1.0556	0.8889	0.0756	0.0637	0.0696	0.0084	0.0060
120	0.0180	0.0140	1.1111	0.8889	0.0796	0.0637	0.0716	0.0113	0.0080
144	0.0210	0.0160	1.2778	1.0000	0.0915	0.0716	0.0816	0.0141	0.0099
168	0.0400	0.0360	2.3333	2.1111	0.1671	0.1512	0.1592	0.0113	0.0080
192	0.0410	0.0330	2.3889	1.9444	0.1711	0.1393	0.1552	0.0225	0.0159
216	0.0430	0.0330	2.5000	1.9444	0.1791	0.1393	0.1592	0.0281	0.0199
240	0.0370	0.0430	2.1667	2.5000	0.1552	0.1791	0.1671	0.0169	0.0119
264	0.0460	0.0450	2.6667	2.6111	0.1910	0.1870	0.1890	0.0028	0.0020
288	0.0450	0.0450	2.6111	2.6111	0.1870	0.1870	0.1870	0.0000	0.0000
312	0.0480	0.0480	2.7778	2.7778	0.1989	0.1989	0.1989	0.0000	0.0000
360	0.0400	0.0450	2.3333	2.6111	0.1671	0.1870	0.1771	0.0141	0.0099
432	0.0470	0.0480	2.7222	2.7778	0.1950	0.1989	0.1970	0.0028	0.0020
504	0.0490	0.0470	2.8333	2.7222	0.2029	0.1950	0.1989	0.0056	0.0040
576	0.0510	0.0480	2.9444	2.7778	0.2109	0.1989	0.2049	0.0084	0.0060
648	0.0670	0.0510	3.8333	2.9444	0.2745	0.2109	0.2427	0.0450	0.0318

	Absorbance		Fe2+(µg)		Fe(II) leached mmol/L		5mM		
Hours	1	2	1	2	1	2	Average	STD	Error
0	0.0000	0.0000	0.1111	0.1111	0.0080	0.0080	0.0080	0.0000	0.0000
2	0.0130	0.0080	0.8333	0.5556	0.0597	0.0398	0.0497	0.0141	0.0099
6	0.0120	0.0110	0.7778	0.7222	0.0557	0.0517	0.0537	0.0028	0.0020
8	0.0160	0.0140	1.0000	0.8889	0.0716	0.0637	0.0676	0.0056	0.0040
24	0.0160	0.0180	1.0000	1.1111	0.0716	0.0796	0.0756	0.0056	0.0040
48	0.0180	0.0200	1.1111	1.2222	0.0796	0.0875	0.0836	0.0056	0.0040
72	0.0400	0.0360	2.3333	2.1111	0.1671	0.1512	0.1592	0.0113	0.0080
96	0.0290	0.0240	1.7222	1.4444	0.1233	0.1035	0.1134	0.0141	0.0099
120	0.0320	0.0360	1.8889	2.1111	0.1353	0.1512	0.1432	0.0113	0.0080
144	0.0300	0.0350	1.7778	2.0556	0.1273	0.1472	0.1373	0.0141	0.0099
168	0.0380	0.0390	2.2222	2.2778	0.1592	0.1631	0.1611	0.0028	0.0020
192	0.0390	0.0360	2.2778	2.1111	0.1631	0.1512	0.1572	0.0084	0.0060
216	0.0350	0.0360	2.0556	2.1111	0.1472	0.1512	0.1492	0.0028	0.0020
240	0.0490	0.0520	2.8333	3.0000	0.2029	0.2149	0.2089	0.0084	0.0060
264	0.0550	0.0640	3.1667	3.6667	0.2268	0.2626	0.2447	0.0253	0.0179
288	0.0440	0.0670	2.5556	3.8333	0.1830	0.2745	0.2288	0.0647	0.0458
312	0.0780	0.0590	4.4444	3.3889	0.3183	0.2427	0.2805	0.0535	0.0378
360	0.0590	0.0580	3.3889	3.3333	0.2427	0.2387	0.2407	0.0028	0.0020
432	0.0690	0.0640	3.9444	3.6667	0.2825	0.2626	0.2726	0.0141	0.0099
504	0.0670	0.0600	3.8333	3.4444	0.2745	0.2467	0.2606	0.0197	0.0139
576	0.0730	0.0670	4.1667	3.8333	0.2984	0.2745	0.2865	0.0169	0.0119
648	0.0640	0.0690	3.6667	3.9444	0.2626	0.2825	0.2726	0.0141	0.0099

	Absorbance		Fe2+(µg)		Fe(II) leached mmol/L		10mM		
Hours	1	2	1	2	1	2	Average	STD	Error
0	0.0000	0.0000	0.1111	0.1111	0.0080	0.0080	0.0080	0.0000	0.0000
2	0.0070	0.0090	0.5000	0.6111	0.0358	0.0438	0.0398	0.0056	0.0040
6	0.0090	0.0090	0.6111	0.6111	0.0438	0.0438	0.0438	0.0000	0.0000
8	0.0150	0.0110	0.9444	0.7222	0.0676	0.0517	0.0597	0.0113	0.0080
24	0.0170	0.0140	1.0556	0.8889	0.0756	0.0637	0.0696	0.0084	0.0060
48	0.0170	0.0150	1.0556	0.9444	0.0756	0.0676	0.0716	0.0056	0.0040
72	0.0180	0.0200	1.1111	1.2222	0.0796	0.0875	0.0836	0.0056	0.0040
96	0.0290	0.0310	1.7222	1.8333	0.1233	0.1313	0.1273	0.0056	0.0040
120	0.0310	0.0310	1.8333	1.8333	0.1313	0.1313	0.1313	0.0000	0.0000
144	0.0360	0.0340	2.1111	2.0000	0.1512	0.1432	0.1472	0.0056	0.0040
168	0.0440	0.0430	2.5556	2.5000	0.1830	0.1791	0.1810	0.0028	0.0020
192	0.0460	0.0430	2.6667	2.5000	0.1910	0.1791	0.1850	0.0084	0.0060
216	0.0470	0.0510	2.7222	2.9444	0.1950	0.2109	0.2029	0.0113	0.0080
240	0.0560	0.0570	3.2222	3.2778	0.2308	0.2348	0.2328	0.0028	0.0020
264	0.0550	0.0570	3.1667	3.2778	0.2268	0.2348	0.2308	0.0056	0.0040
288	0.0650	0.0680	3.7222	3.8889	0.2666	0.2785	0.2726	0.0084	0.0060
312	0.0640	0.0630	3.6667	3.6111	0.2626	0.2586	0.2606	0.0028	0.0020
360	0.0720	0.0680	4.1111	3.8889	0.2944	0.2785	0.2865	0.0113	0.0080
432	0.0760	0.0760	4.3333	4.3333	0.3104	0.3104	0.3104	0.0000	0.0000
504	0.0750	0.0750	4.2778	4.2778	0.3064	0.3064	0.3064	0.0000	0.0000
576	0.0780	0.0810	4.4444	4.6111	0.3183	0.3302	0.3243	0.0084	0.0060
648	0.0800	0.0790	4.5556	4.5000	0.3263	0.3223	0.3243	0.0028	0.0020

	Absorbance		Fe2+(µg)		Fe(II) leached mmol/L		15mM		
Hours	1	2	1	2	1	2	Average	STD	Error
0	0.0000	0.0000	0.1111	0.1111	0.0080	0.0080	0.0080	0.0000	0.0000
2	0.0140	0.0110	0.8889	0.7222	0.0637	0.0517	0.0577	0.0084	0.0060
6	0.0100	0.0110	0.6667	0.7222	0.0477	0.0517	0.0497	0.0028	0.0020
8	0.0130	0.0140	0.8333	0.8889	0.0597	0.0637	0.0617	0.0028	0.0020
24	0.0160	0.0130	1.0000	0.8333	0.0716	0.0597	0.0657	0.0084	0.0060
48	0.0180	0.0150	1.1111	0.9444	0.0796	0.0676	0.0736	0.0084	0.0060
72	0.0200	0.0230	1.2222	1.3889	0.0875	0.0995	0.0935	0.0084	0.0060
96	0.0300	0.0330	1.7778	1.9444	0.1273	0.1393	0.1333	0.0084	0.0060
120	0.0350	0.0370	2.0556	2.1667	0.1472	0.1552	0.1512	0.0056	0.0040
144	0.0380	0.0430	2.2222	2.5000	0.1592	0.1791	0.1691	0.0141	0.0099
168	0.0540	0.0480	3.1111	2.7778	0.2228	0.1989	0.2109	0.0169	0.0119
192	0.0540	0.0480	3.1111	2.7778	0.2228	0.1989	0.2109	0.0169	0.0119
216	0.0520	0.0500	3.0000	2.8889	0.2149	0.2069	0.2109	0.0056	0.0040
240	0.0630	0.0550	3.6111	3.1667	0.2586	0.2268	0.2427	0.0225	0.0159
264	0.0630	0.0640	3.6111	3.6667	0.2586	0.2626	0.2606	0.0028	0.0020
288	0.0640	0.0660	3.6667	3.7778	0.2626	0.2706	0.2666	0.0056	0.0040
312	0.0700	0.0670	4.0000	3.8333	0.2865	0.2745	0.2805	0.0084	0.0060
360	0.0730	0.0740	4.1667	4.2222	0.2984	0.3024	0.3004	0.0028	0.0020
432	0.0750	0.0730	4.2778	4.1667	0.3064	0.2984	0.3024	0.0056	0.0040
504	0.0800	0.0820	4.5556	4.6667	0.3263	0.3342	0.3302	0.0056	0.0040
576	0.0830	0.0810	4.7222	4.6111	0.3382	0.3302	0.3342	0.0056	0.0040
648	0.0880	0.0850	5.0000	4.8333	0.3581	0.3462	0.3521	0.0084	0.0060

Hours	Blank	Fe2+(µg)	Fe(II) leached mmol/L
0	0.0000	0.1111	0.0080
2	0.0050	0.3889	0.0279
6	0.0030	0.2778	0.0199
8	0.0020	0.2222	0.0159
24	0.0040	0.3333	0.0239
48	0.0040	0.3333	0.0239
72	0.0050	0.3889	0.0279
96	0.0020	0.2222	0.0159
120	0.0030	0.2778	0.0199
144	0.0060	0.4444	0.0318
168	0.0050	0.3889	0.0279
192	0.0050	0.3889	0.0279
216	0.0080	0.5556	0.0398
240	0.0040	0.3333	0.0239
264	0.0060	0.4444	0.0318
288	0.0070	0.5000	0.0358
312	0.0060	0.4444	0.0318
360	0.0040	0.3333	0.0239
432	0.0100	0.6667	0.0477
504	0.0080	0.5556	0.0398
576	0.0080	0.5556	0.0398
648	0.0110	0.7222	0.0517

Appendix2.5: Natural log of average Fe(II) calculated from bioreduction of silica sand added with different lactate concentration (1 – 15mM)

	1mM lactate		5mM lactate		10mM lactate		15mM lactate	
Hours	Average Fe(II) mmol/L	Ln[Fe(II)]	Average Fe(II) mmol/L	Ln[Fe(II)]	Average Fe(II) mmol/L	Ln[Fe(II)]	Average Fe(II) mmol/L	Ln[Fe(II)]
0	0.0080	-4.8336	0.0080	-4.8336	0.0080	-4.8336	0.0080	-4.8336
2	0.0398	-3.2242	0.0497	-3.0010	0.0398	-3.2242	0.0577	-2.8526
6	0.0338	-3.3867	0.0537	-2.9241	0.0438	-3.1289	0.0497	-3.0010
8	0.0418	-3.1754	0.0676	-2.6935	0.0597	-2.8187	0.0617	-2.7859
24	0.0537	-2.9241	0.0756	-2.5823	0.0696	-2.6645	0.0657	-2.7234
48	0.0776	-2.5563	0.0836	-2.4822	0.0716	-2.6364	0.0736	-2.6090
72	0.0676	-2.6935	0.1592	-1.8379	0.0836	-2.4822	0.0935	-2.3697
96	0.0696	-2.6645	0.1134	-2.1768	0.1273	-2.0610	0.1333	-2.0152
120	0.0716	-2.6364	0.1432	-1.9432	0.1313	-2.0302	0.1512	-1.8892
144	0.0816	-2.5063	0.1373	-1.9858	0.1472	-1.9158	0.1691	-1.7772
168	0.1592	-1.8379	0.1611	-1.8254	0.1810	-1.7090	0.2109	-1.5565
192	0.1552	-1.8632	0.1572	-1.8504	0.1850	-1.6873	0.2109	-1.5565
216	0.1592	-1.8379	0.1492	-1.9024	0.2029	-1.5949	0.2109	-1.5565
240	0.1671	-1.7891	0.2089	-1.5659	0.2328	-1.4577	0.2427	-1.4159
264	0.1890	-1.6660	0.2447	-1.4077	0.2308	-1.4663	0.2606	-1.3447
288	0.1870	-1.6766	0.2288	-1.4750	0.2726	-1.2999	0.2666	-1.3221
312	0.1989	-1.6147	0.2805	-1.2711	0.2606	-1.3447	0.2805	-1.2711
360	0.1771	-1.7313	0.2407	-1.4241	0.2865	-1.2501	0.3004	-1.2026
432	0.1970	-1.6248	0.2726	-1.2999	0.3104	-1.1700	0.3024	-1.1960
504	0.1989	-1.6147	0.2606	-1.3447	0.3064	-1.1829	0.3302	-1.1079
576	0.2049	-1.5852	0.2865	-1.2501	0.3243	-1.1261	0.3342	-1.0959
648	0.2427	-1.4159	0.2726	-1.2999	0.3243	-1.1261	0.3521	-1.0437

APPENDIX 3

Appendix 3.1: Temperature, Ph, Redox potential data from Kaolin 2 bioreactor experiment

Date	Time	Blank reactor pH	Blank reactor redox	Biotreated reactor pH	Biotreated reactor redox	Blank reactor Temp	Blank reactor Temp
18-Jan-11	00:00	-4.216	-1.595	-4.437	-1.594	31.2	31.2
18-Jan-11	08:00	-4.22	-1.595	-4.439	-1.594	31.3	31.3
18-Jan-11	16:00	-4.225	-1.595	-4.444	-1.594	31.3	31.2
19-Jan-11	00:00	-4.229	-1.595	-4.449	-1.594	31.3	31.2
19-Jan-11	08:00	-4.222	-1.595	-4.367	-1.849	31.2	31.4
19-Jan-11	16:00	-4.805	-2.168	-4.739	-3.505	30.5	30.4
20-Jan-11	00:00	-4.585	-2.665	-5.036	-6.194	31.1	30.1
20-Jan-11	08:00	-4.533	-2.877	-5.013	-6.219	31.1	29.8
20-Jan-11	16:00	-4.531	-2.935	-4.955	-6.185	30.8	29.6
21-Jan-11	00:00	-4.527	-2.975	-4.895	-6.168	30.9	29.7
21-Jan-11	08:00	-4.526	-2.995	-4.877	-6.155	31.1	29.8
21-Jan-11	16:00	-4.524	-3.036	-4.838	-6.086	31.2	30.2
22-Jan-11	00:00	-4.525	-3.039	-4.807	-6.216	30.3	29.4
22-Jan-11	08:00	-4.528	-3.057	-4.777	-6.076	31	29.9
22-Jan-11	16:00	-4.53	-3.078	-4.756	-5.776	31.1	30.1
23-Jan-11	00:00	-4.532	-3.089	-4.748	-5.772	31.1	30
23-Jan-11	08:00	-4.535	-3.097	-4.743	-5.745	31.2	30
23-Jan-11	16:00	-4.538	-3.106	-4.741	-5.707	31.2	30
24-Jan-11	00:00	-4.542	-3.095	-4.728	-5.709	31.2	30
24-Jan-11	08:00	-4.546	-3.091	-4.721	-5.692	31.2	30
24-Jan-11	16:00	-4.547	-2.979	-4.717	-5.65	31.4	30.2
25-Jan-11	00:00	-4.535	-3.069	-4.258	-3.551	31.1	30.9
25-Jan-11	08:00	-4.541	-3.116	-4.065	-2.064	31.2	31.2
25-Jan-11	16:00	-4.543	-3.128	-3.992	-1.864	31	31
26-Jan-11	00:00	-4.549	-3.136	-3.954	-1.788	31.1	31
26-Jan-11	08:00	-4.555	-3.138	-3.956	-1.76	31.1	31

Appendix 3.2: Temperature, Ph, Redox potential data from kaolin 3 bioreactor experiment.

Date	Time	Blank reactor pH	Blank reactor Redox	Biotreated reactor pH	Biotreated reactor Redox	Blank reactor Temp	Biotreated reactor Temp
27-Jan-11	00:00	-5.037	-2.82	-5.946	-1.594	31.8	31.7
27-Jan-11	08:00	-5.167	-2.829	-6.027	-1.594	31.8	31.7
27-Jan-11	16:00	-4.799	-2.809	-5.076	-2.333	31.8	30.4
28-Jan-11	00:00	-4.765	-2.849	-5.283	-5.978	30.9	30.1
28-Jan-11	08:00	-4.713	-2.951	-5.318	-6.02	31.1	30.3
28-Jan-11	16:00	-4.67	-3.214	-5.245	-6.276	31.3	30.4
29-Jan-11	00:00	-4.656	-3.3	-5.277	-5.542	31.3	30.4
29-Jan-11	08:00	-4.635	-3.345	-5.192	-6.604	31.2	30.3
29-Jan-11	16:00	-4.619	-3.365	-5.134	-6.62	31.4	30.5
30-Jan-11	00:00	-4.609	-3.369	-5.039	-6.573	31.4	30.5
30-Jan-11	08:00	-4.604	-3.371	-5.04	-6.629	31.3	30.4
30-Jan-11	16:00	-4.599	-3.381	-5.064	-6.618	31.6	30.7
31-Jan-11	00:00	-4.596	-3.383	-5.053	-6.081	31.4	30.6
31-Jan-11	08:00	-4.593	-3.396	-5.231	-5.883	31.4	30.6
31-Jan-11	16:00	-4.588	-3.398	-5.319	-6.033	31.1	30.3
01-Feb-11	00:00	-4.589	-3.403	-5.261	-5.863	31.4	30.5
01-Feb-11	08:00	-4.587	-3.413	-5.259	-5.745	31.3	30.4
01-Feb-11	16:00	-4.587	-3.423	-5.236	-5.315	31.6	30.7
02-Feb-11	00:00	-4.592	-3.428	-5.23	-4.784	31.2	30.3
02-Feb-11	08:00	-4.592	-3.426	-5.082	-5.114	31.2	30.3
02-Feb-11	16:00	-4.592	-3.444	-5.067	-5.355	31.3	30.4
03-Feb-11	00:00	-4.592	-3.45	-5.058	-5.447	31.2	30.4
03-Feb-11	08:00	-4.592	-3.455	-5.022	-5.651	31.1	30.4
03-Feb-11	16:00	-4.594	-3.458	-5.018	-5.708	30.8	30.4

04-Feb-11	00:00	-4.599	-2.902	-4.978	-5.529	34.6	34.1
04-Feb-11	08:00	-4.6	-2.676	-4.953	-5.328	38.1	37.3
04-Feb-11	16:00	-4.896	-3.401	-5.046	-5.385	31.2	30.3
05-Feb-11	00:00	-4.844	-2.926	-5.034	-5.286	30.4	30
05-Feb-11	08:00	-4.78	-2.905	-4.979	-5.253	32.3	31.9
05-Feb-11	16:00	-4.73	-3.365	-4.973	-5.286	32.2	32
06-Feb-11	00:00	-4.695	-3.523	-4.983	-5.348	30	29.7
06-Feb-11	08:00	-4.676	-3.55	-4.99	-5.356	28.7	28.4
06-Feb-11	16:00	-4.661	-3.547	-4.786	-4.433	27.6	27.2
07-Feb-11	00:00	-4.655	-3.49	-4.335	-2.227	30.4	30.1
07-Feb-11	08:00	-4.646	-3.466	-4.261	-1.963	31.5	31.3
07-Feb-11	16:00	-4.636	-3.445	-4.25	-1.891	32.4	32.3

Appendix 3.3: Temperature, Ph, Redox potential data from kaolin 4 bioreactor experiment.

Date	Time	Blank reactor pH	Blank reactor redox	Biotreated reactor pH	Biotreated reactor redox	Blank reactor Temp	Biotreated reactor Temp
01-Mar-11	00:00	-5.268	-1.691	-5.948	-1.594	31.7	31.7
01-Mar-11	08:00	-5.317	-1.729	-6.102	-1.594	31.6	31.6
01-Mar-11	16:00	-5.066	-2.575	-5.314	-1.67	30	29.6
02-Mar-11	00:00	-4.954	-2.925	-5.266	-6.027	30.6	29.3
02-Mar-11	08:00	-4.813	-2.967	-5.277	-5.128	31.3	29.9
02-Mar-11	16:00	-4.721	-3.128	-5.214	-5.237	31.2	30.6
03-Mar-11	00:00	-4.7	-3.173	-5.072	-5.417	31.3	30.8
03-Mar-11	08:00	-4.697	-3.222	-5.099	-5.112	31.3	30.8
03-Mar-11	16:00	-4.705	-3.255	-5.13	-5.371	31.1	30.5
04-Mar-11	00:00	-4.713	-3.282	-5.46	-5.563	31.3	30.6
04-Mar-11	08:00	-4.722	-3.296	-5.496	-5.503	31.2	30.4
04-Mar-11	16:00	-4.732	-3.317	-5.462	-5.69	31.2	30.5
05-Mar-11	00:00	-4.743	-3.332	-5.428	-5.3	31.2	30.4
05-Mar-11	08:00	-4.754	-3.341	-5.387	-5.231	31.1	30.3
05-Mar-11	16:00	-4.764	-3.356	-5.361	-5.246	31.1	30.3
06-Mar-11	00:00	-4.775	-3.364	-5.336	-5.196	31.1	30.4
06-Mar-11	08:00	-4.784	-3.373	-5.305	-5.156	31.1	30.4
06-Mar-11	16:00	-4.794	-3.382	-5.274	-5.081	31.2	30.5
07-Mar-11	00:00	-4.802	-3.39	-5.243	-5.061	31.2	30.5
07-Mar-11	08:00	-4.809	-3.4	-5.214	-5.05	31.1	30.4
07-Mar-11	16:00	-4.82	-3.414	-4.971	-4.437	31.3	30.7
08-Mar-11	00:00	-4.826	-3.425	-4.5	-2.387	31.1	30.8
08-Mar-11	08:00	-4.832	-3.433	-4.524	-2.125	31.2	30.9
08-Mar-11	16:00	-4.835	-3.446	-4.568	-2.005	31.2	31
09-Mar-11	00:00	-4.84	-3.451	-4.602	-1.928	31.2	30.9
09-Mar-11	08:00	-4.845	-3.449	-4.64	-1.874	31.2	30.9
09-Mar-11	16:00	-4.85	-3.457	-4.68	-1.838	31.2	30.9

Appendix 3.4: Temperature, Ph, Redox potential data from silica sand (140g) bioreactor experiment

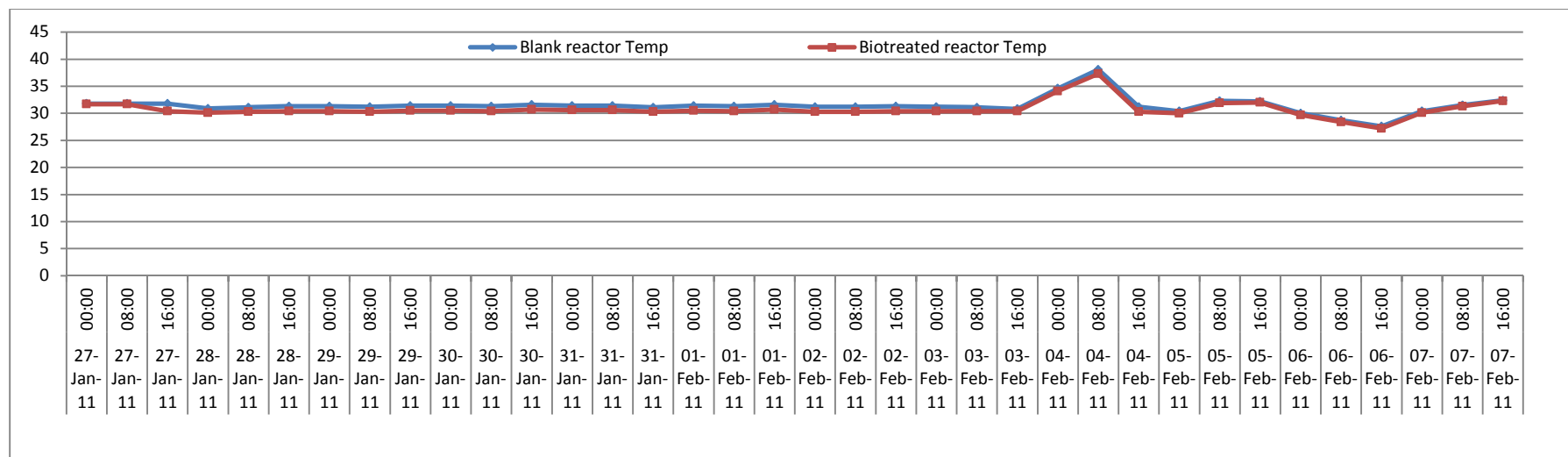
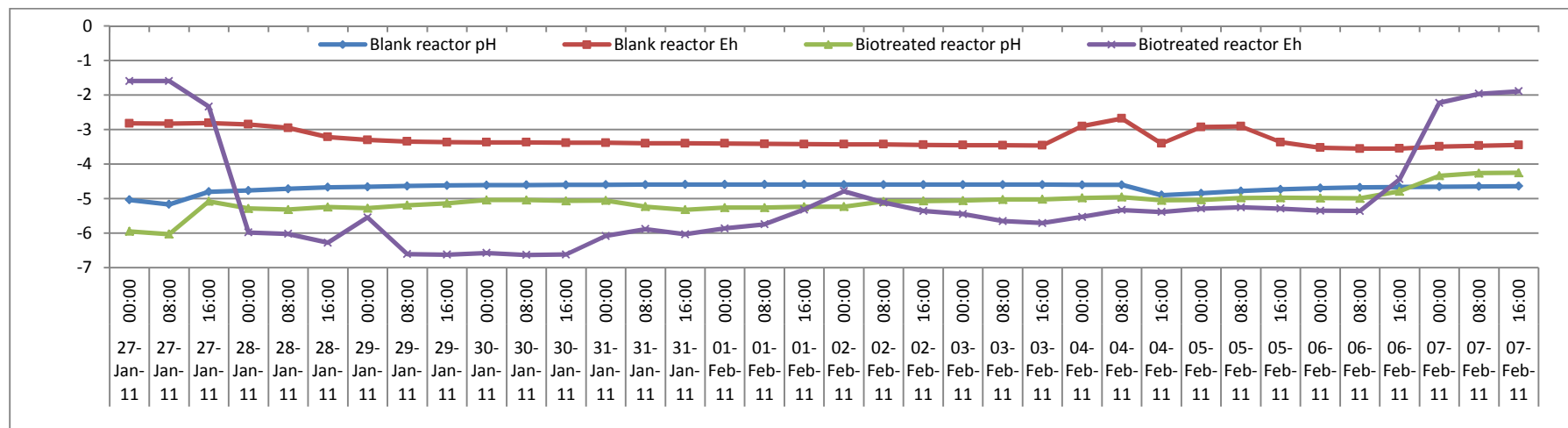
Date	Time	Blank reactor pH	Blank reactor redox	Biotreated reactor pH	Biotreated reactor redox	Blank reactor Temp	Biotreated reactor Temp
08-Feb-11	00:00	-3.33	-2.937	-3.343	-1.594	33.2	33.1
08-Feb-11	08:00	-3.335	-2.957	-3.673	-1.594	33	33
08-Feb-11	16:00	-4.871	-3.471	-4.699	-1.594	31.7	31.5
09-Feb-11	00:00	-4.833	-3.907	-4.86	-6.159	32.5	32.2
09-Feb-11	08:00	-4.745	-3.704	-4.865	-6.105	35	34.8
09-Feb-11	16:00	-4.685	-3.234	-4.902	-5.989	36.1	35.8
10-Feb-11	00:00	-4.652	-3.247	-4.932	-6.103	34.7	34.4
10-Feb-11	08:00	-4.638	-3.155	-4.942	-6.039	34.1	33.6
10-Feb-11	16:00	-4.629	-3.183	-4.968	-6.101	33.8	33.5
11-Feb-11	00:00	-4.622	-3.338	-4.986	-5.766	33.8	33.5
11-Feb-11	08:00	-4.615	-3.51	-4.992	-5.607	33.4	33
11-Feb-11	16:00	-4.607	-3.63	-4.943	-5.533	33.3	33
12-Feb-11	00:00	-4.603	-3.75	-4.881	-5.446	35.3	35
12-Feb-11	08:00	-4.592	-3.813	-4.847	-5.37	34.2	33.8
12-Feb-11	16:00	-4.586	-3.854	-4.807	-5.446	34.2	33.7
13-Feb-11	00:00	-4.58	-3.866	-4.764	-5.148	34.1	33.7
13-Feb-11	08:00	-4.575	-3.868	-4.722	-5.443	33.7	33.3
13-Feb-11	16:00	-4.571	-3.863	-4.67	-5.602	34	33.5
14-Feb-11	00:00	-4.566	-3.845	-4.637	-5.787	33.8	33.3
14-Feb-11	08:00	-4.561	-3.843	-4.661	-5.932	33.7	33.2
14-Feb-11	16:00	-4.558	-3.833	-4.693	-6.055	34.2	33.9
15-Feb-11	00:00	-4.551	-3.828	-4.789	-6.06	34.6	34.2
15-Feb-11	08:00	-4.546	-3.831	-4.796	-6.173	34.5	34.1
15-Feb-11	16:00	-4.539	-3.816	-4.82	-5.701	34.3	34
16-Feb-11	00:00	-4.535	-3.829	-4.838	-5.305	32.9	32.6
16-Feb-11	08:00	-4.538	-3.828	-4.846	-5.125	32.6	32.2

16-Feb-11	16:00	-4.538	-3.838	-4.844	-4.998	32.4	32
17-Feb-11	00:00	-4.538	-3.846	-4.847	-4.965	32	31.7
17-Feb-11	08:00	-4.54	-3.855	-4.858	-4.882	31.4	31.1
17-Feb-11	16:00	-4.54	-3.856	-4.892	-4.88	31.1	30.7
18-Feb-11	00:00	-4.545	-3.858	-4.906	-4.91	31.9	31.6
18-Feb-11	08:00	-4.546	-3.86	-4.92	-5.027	32.1	31.7
18-Feb-11	16:00	-4.513	-3.578	-4.792	-4.858	32.7	32.4
19-Feb-11	00:00	-4.487	-3.446	-4.636	-5.129	31.6	31.4
19-Feb-11	08:00	-4.502	-3.36	-4.586	-5.182	30.6	30.3
19-Feb-11	16:00	-4.479	-3.502	-4.548	-5.349	30.3	30
20-Feb-11	00:00	-4.5	-3.426	-4.517	-5.401	30.5	30.1
20-Feb-11	08:00	-4.483	-3.428	-4.53	-5.496	30.8	30.5
20-Feb-11	16:00	-5.062	-3.244	-4.499	-2.439	31.2	31.1
21-Feb-11	00:00	-5.282	-3.315	-4.908	-1.607	34.6	34.6
21-Feb-11	08:00	-5.376	-3.367	-4.924	-1.666	36	35.9
21-Feb-11	16:00	-5.019	-3.064	-4.909	-1.645	31.1	30.6

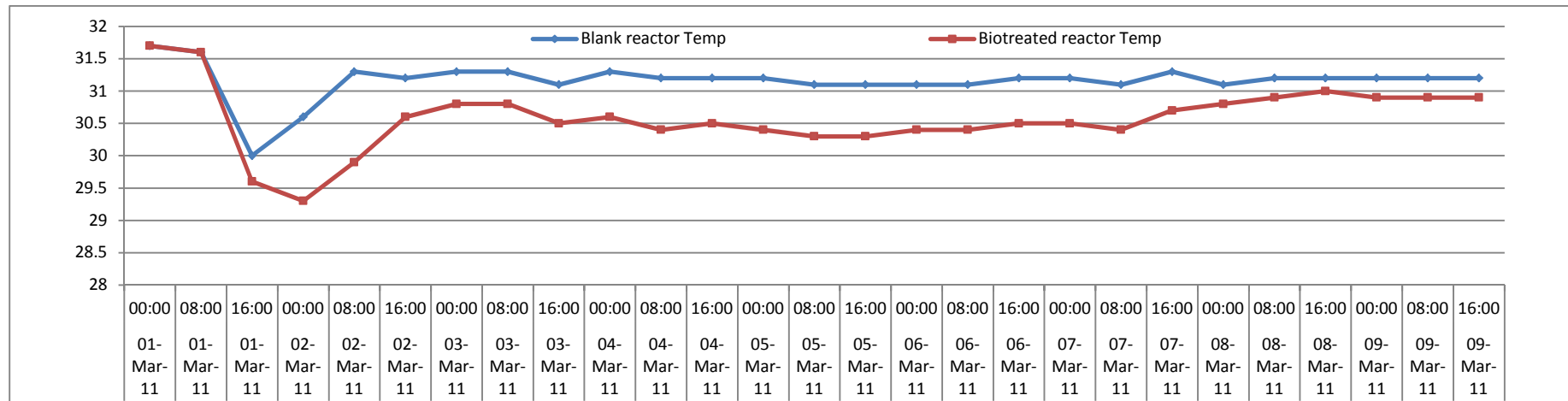
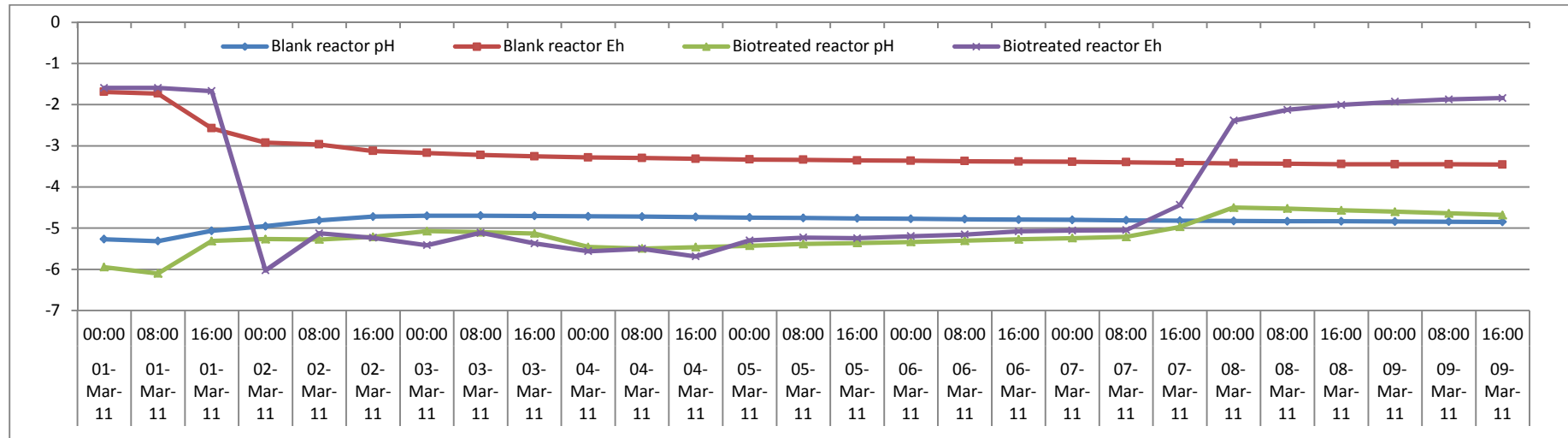
Appendix 3.5: Temperature, Ph, Redox potential data from silica sand (70g) bioreactor experiments

Date	Time	Blank reactor pH	Blank reactor redox	Biotreated reactor pH	Biotreated reactor redox	Blank reactor Temp	Biotreated reactor Temp
21-Feb-11	00:00	-5.282	-3.315	-5.908	-1.607	34.6	34.6
21-Feb-11	08:00	-5.376	-3.367	-6.024	-1.666	36	35.9
21-Feb-11	16:00	-5.019	-3.064	-5.309	-1.645	31.1	30.6
22-Feb-11	00:00	-4.974	-4.29	-5.504	-5.663	31.1	30.1
22-Feb-11	08:00	-4.871	-4.209	-5.48	-5.115	31.1	29.9
22-Feb-11	16:00	-4.813	-4.122	-5.35	-5.044	31.4	30.4
23-Feb-11	00:00	-4.783	-3.983	-5.135	-4.987	31.3	30.8
23-Feb-11	08:00	-4.763	-3.661	-5.055	-5.071	31.4	30.9
23-Feb-11	16:00	-4.747	-3.2	-5.032	-5.093	31.4	30.9
24-Feb-11	00:00	-4.731	-3.051	-4.976	-5.102	31.3	30.7
24-Feb-11	08:00	-4.726	-3.14	-4.948	-5.102	31.2	30.7
24-Feb-11	16:00	-4.714	-3.355	-4.911	-5.111	31.3	30.8
25-Feb-11	00:00	-4.708	-3.565	-4.873	-5.107	31.2	30.7
25-Feb-11	08:00	-4.706	-3.696	-4.837	-5.08	31.2	30.7
25-Feb-11	16:00	-4.698	-3.769	-4.827	-5.088	31.2	30.7
26-Feb-11	00:00	-4.695	-3.801	-4.819	-5.078	31.2	30.7
26-Feb-11	08:00	-4.691	-3.833	-4.814	-5.068	31.2	30.7
26-Feb-11	16:00	-4.687	-3.856	-4.811	-5.039	31.2	30.7
27-Feb-11	00:00	-4.679	-3.86	-4.857	-5.05	31.2	30.8
27-Feb-11	08:00	-4.676	-3.857	-4.861	-5.039	31.3	30.9
27-Feb-11	16:00	-4.669	-3.841	-4.848	-4.998	31.4	30.9
28-Feb-11	00:00	-4.661	-3.82	-4.837	-5.003	31.3	30.8
28-Feb-11	08:00	-4.657	-3.837	-4.901	-4.841	31.2	30.7
28-Feb-11	16:00	-4.778	-3.621	-5.35	-3.799	31.3	30.9
01-Mar-11	00:00	-5.268	-2.891	-5.948	-1.594	31.7	31.7
01-Mar-11	08:00	-5.317	-2.829	-6.102	-1.594	31.6	31.6
01-Mar-11	16:00	-5.066	-2.575	-5.314	-1.67	30.3	29.6

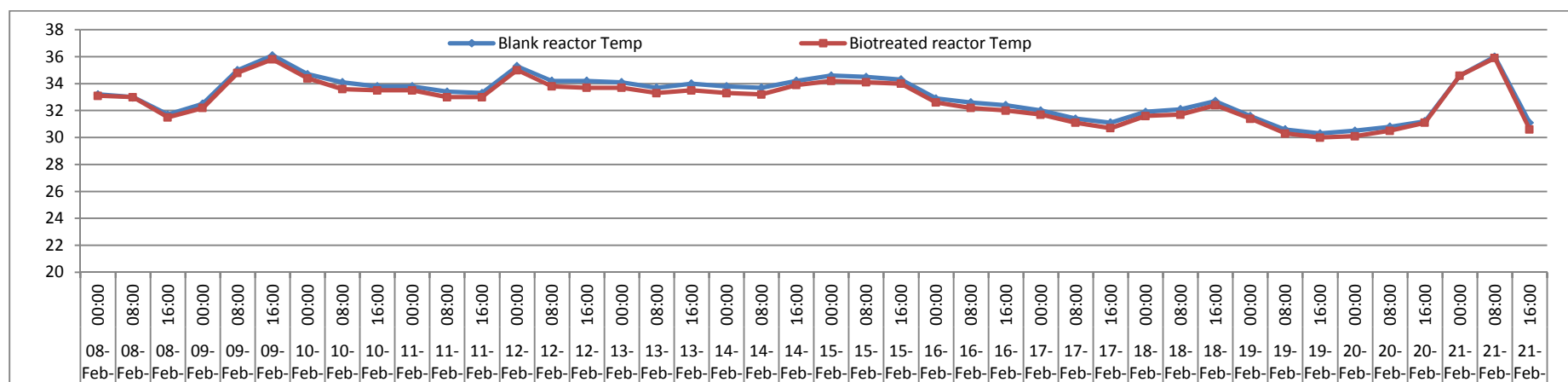
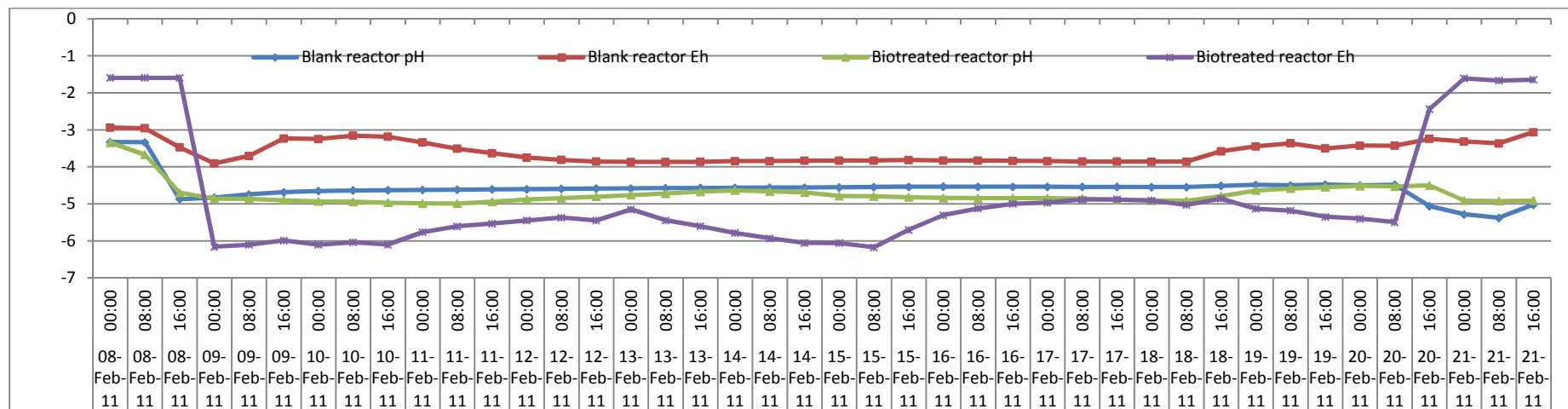
Appendix 3.6: Time profile of pH, Redox potential (Eh) and Temperature plots in Kaolin 3 from 27/Jan/2011 to 06/Jan/2011



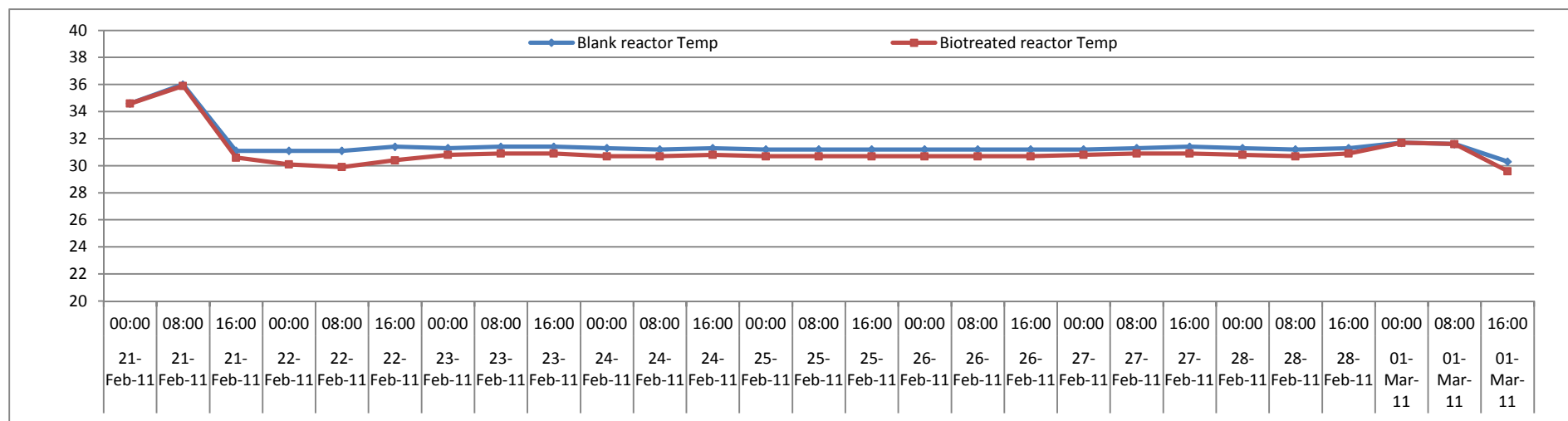
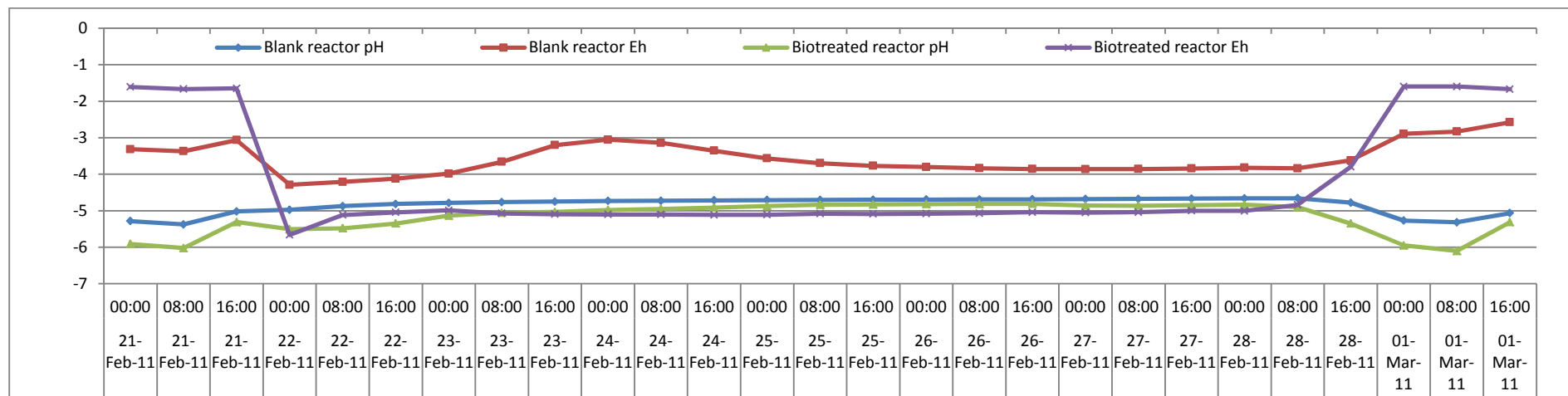
Appendix 3.7: Time profile of pH, Redox potential (Eh) and Temperature plots in Kaolin 4 from 01/Mar/2011 to 07/Mar/2011



Appendix 3.8: Time profile of pH, Redox potential (Eh) and Temperature plots in silica sand (140g) from 08/Feb/2011 to 20/Feb/2011



Appendix 3.9: Time profile of pH, Redox potential (Eh) and Temperature plots in silica sand (70g) from 21/Feb/2011 to 28/Feb/2011



Appendix 3.10: Large scale experiments for the bio-reduction of kaolin (4.5L reactors)

Days	Absorbance		Fe ²⁺ (μg)		Fe(II) leached mmol/L		Kaolin 2 (Reactor)		Error
	1	2	1	2	1	2	Average	STD	
0	0.0000	0.0000	0.3164	0.3164	0.0227	0.0227	0.0227	0.0000	0.0000
1	0.0480	0.0730	3.0282	4.4407	0.2169	0.3180	0.2675	0.0715	0.0506
2	0.0920	0.0890	5.5141	5.3446	0.3949	0.3828	0.3889	0.0086	0.0061
3	0.1080	0.0980	6.4181	5.8531	0.4597	0.4192	0.4394	0.0286	0.0202
4	0.1150	0.1360	6.8136	8.0000	0.4880	0.5730	0.5305	0.0601	0.0425
5	0.1190	0.1280	7.0395	7.5480	0.5042	0.5406	0.5224	0.0258	0.0182

Days	Abs (Blank)	Fe ²⁺ (μg)	Fe(II) mmol/L
0	0.0000	0.3164	0.0227
1	0.0040	0.5424	0.0388
2	0.0070	0.7119	0.0510
3	0.0100	0.8814	0.0631
4	0.0060	0.6554	0.0469
5	0.0050	0.5989	0.0429

Days	Absorbance		Fe ²⁺ (μg)		Fe(II) leached mmol/L		Kaolin 3 (Reactor)		Error
	1	2	1	2	1	2	Average	STD	
0	0.0000	0.0000	0.3164	0.3164	0.0227	0.0227	0.0227	0.0000	0.0000
1	0.1590	0.1790	9.2994	10.4294	0.6660	0.7470	0.7065	0.0572	0.0405
2	0.1460	0.1520	8.5650	8.9040	0.6134	0.6377	0.6256	0.0172	0.0121
3	0.1610	0.1770	9.4124	10.3164	0.6741	0.7389	0.7065	0.0458	0.0324
4	0.1890	0.2350	10.9944	13.5932	0.7874	0.9736	0.8805	0.1316	0.0931
5	0.2250	0.2360	13.0282	13.6497	0.9331	0.9776	0.9553	0.0315	0.0223
7	0.2050	0.2180	11.8983	12.6328	0.8522	0.9048	0.8785	0.0372	0.0263
8	0.2100	0.2060	12.1808	11.9548	0.8724	0.8562	0.8643	0.0114	0.0081
10	0.2170	0.2350	12.5763	13.5932	0.9007	0.9736	0.9371	0.0515	0.0364

Days	Abs (Blank)	Fe ²⁺ (μg)	Fe(II) mmol/L
0	0.0000	0.3164	0.0227
1	0.0330	2.1808	0.1562
2	0.0340	2.2373	0.1602
3	0.0320	2.1243	0.1521
4	0.0220	1.5593	0.1117
5	0.0280	1.8983	0.1360
7	0.0280	1.8983	0.1360
8	0.0210	1.5028	0.1076
10	0.0240	1.6723	0.1198

Days	Absorbance		Fe ²⁺ (µg)		Fe(II) leached mmol/L		Kaolin 4 (Reactor)		Error
	1	2	1	2	1	2	Average	STD	
0	0.0000	0.0000	0.3164	0.3164	0.0227	0.0227	0.0227	0.0000	0.0000
1	0.0980	0.0950	5.8531	5.6836	0.4192	0.4071	0.4131	0.0086	0.0061
2	0.1250	0.1210	7.3785	7.1525	0.5285	0.5123	0.5204	0.0114	0.0081
3	0.1370	0.1500	8.0565	8.7910	0.5770	0.6296	0.6033	0.0372	0.0263
4	0.1360	0.1450	8.0000	8.5085	0.5730	0.6094	0.5912	0.0258	0.0182
5	0.1370	0.1490	8.0565	8.7345	0.5770	0.6256	0.6013	0.0343	0.0243
6	0.1420	0.1340	8.3390	7.8870	0.5972	0.5649	0.5811	0.0229	0.0162

Days	Abs (Blank)	Fe ²⁺ (µg)	Fe(II)mmol/L
0	0.0000	0.3164	0.0227
1	0.0130	1.0508	0.0753
2	0.0130	1.0508	0.0753
3	0.0150	1.1638	0.0834
4	0.0150	1.1638	0.0834
5	0.0140	1.1073	0.0793
6	0.0110	0.9379	0.0672

Appendix 3.11: Large scale experiments for the bioreduction of silica sand (4.5L reactors)

Day	Absorbance		Fe ²⁺ (µg)		Fe(II) leached mmol/L		140g silica sand		
	1	2	1	2	1	2	Average	STD	Error
0	0.0000	0.0000	0.3164	0.3164	0.0227	0.0227	0.0227	0.0000	0.0000
1	0.0620	0.0710	3.8192	4.3277	0.2735	0.3100	0.2917	0.0258	0.0182
3	0.0970	0.0890	5.7966	5.3446	0.4152	0.3828	0.3990	0.0229	0.0162
5	0.0730	0.0880	4.4407	5.2881	0.3180	0.3787	0.3484	0.0429	0.0303
7	0.0570	0.0510	3.5367	3.1977	0.2533	0.2290	0.2412	0.0172	0.0121
9	0.0460	0.0490	2.9153	3.0847	0.2088	0.2209	0.2149	0.0086	0.0061
10	0.0420	0.0550	2.6893	3.4237	0.1926	0.2452	0.2189	0.0372	0.0263

Days	Abs (Blank)	Fe ²⁺ (µg)	Fe(II)mmol/L
0	0.0000	0.3164	0.0227
1	0.0060	0.6554	0.0469
3	0.0080	0.7684	0.0550
5	0.0030	0.4859	0.0348
7	0.0050	0.5989	0.0429
9	0.0030	0.4859	0.0348
10	0.0040	0.5424	0.0388

Day	Absorbance		Fe2+ μg		Fe(II) leached mmol/L		70g of silica sand		Error
	1	2	1	2	1	2	Average	STD	
0	0.0000	0.0000	0.3164	0.3164	0.0227	0.0227	0.0227	0.0000	0.0000
1	0.0700	0.0620	4.2712	3.8192	0.3059	0.2735	0.2897	0.0229	0.0162
2	0.0740	0.0790	4.4972	4.7797	0.3221	0.3423	0.3322	0.0143	0.0101
3	0.1190	0.1140	7.0395	6.7571	0.5042	0.4839	0.4941	0.0143	0.0101
4	0.1370	0.1040	8.0565	6.1921	0.5770	0.4435	0.5102	0.0944	0.0668
5	0.0760	0.0750	4.6102	4.5537	0.3302	0.3261	0.3282	0.0029	0.0020
6	0.0780	0.0590	4.7232	3.6497	0.3383	0.2614	0.2998	0.0544	0.0384
7	0.0760	0.0620	4.6102	3.8192	0.3302	0.2735	0.3019	0.0401	0.0283

Days	Blank	Fe2+ (μg)	Fe(II)mmol/L
0	0.0000	0.3164	0.0227
1	0.0010	0.3729	0.0267
2	0.0020	0.4294	0.0308
3	0.0010	0.3729	0.0267
4	0.0000	0.3164	0.0227
5	0.0010	0.3729	0.0267
6	0.0010	0.3729	0.0267
7	0.0000	0.3164	0.0227

APPENDIX 4

Appendix 4.1: Data from bioreduction of ferric fraction of carbonate (chalk)

Days	Fe(II)mmol/L				
	CIP8040_10g	Error	CIP8040_20g	Error	Blank
0	0.0000	0.0000	0.0000	0.00000	0.00000
1	0.0766	5.40E-03	0.1391	7.56E-03	2.93E-03
2	0.0989	5.75E-03	0.1892	9.08E-03	3.31E-03
3	0.1086	5.66E-03	0.2172	6.24E-03	3.99E-03
4	0.1127	5.87E-03	0.2394	9.08E-03	4.42E-03
5	0.1231	0.0124	0.2547	7.55E-03	4.42E-03

Days	Average Fe(II) mmol/L						
	With AQDS	STD	With NTA	STD	With AQDS & NTA	STD	Blank
0	0.0748	0.0000	0.0748	0.0000	0.0748	0.0000	
1	0.0795	0.0113	0.0860	0.0070	0.0827	0.0057	0.0748
2	0.0860	0.0052	0.0879	0.0074	0.0841	0.0057	0.0781
3	0.0869	0.0057	0.0897	0.0080	0.0855	0.0057	0.0785
4	0.0874	0.0063	0.0911	0.0069	0.0911	0.0076	0.0795
5	0.0930	0.0141	0.0944	0.0092	0.0930	0.0070	0.0818

Appendix 4.2: Bioleaching of carbonate using *P. mendocina*

<i>P. mendocina</i>	
Day	Abs(600nm)
0	0.000
2	0.126
4	0.177
5	0.301
6	0.425
8	0.507
10	0.609
12	0.649
15	0.631

APPENDIX 5

Appendix 5.1: Total organic carbon data determined from bioleaching of silica sand added with different lactate concentrations (1 – 15mM)

Microcosm experiment				1mM lactate		
Day	IC mg/L	TC mg/L	TOC mg/L	TOC (mmol/L)	TOC predicted in mg/L	TOC predicted in (mmol/L)
1	2.591	71.51	68.91	1.91	36	1
5	2.131	74.47	72.33	2.01	36	1
9	1.128	81.60	80.47	2.24	36	1
18	2.241	81.63	79.38	2.21	36	1
27	4.232	83.90	79.66	2.21	36	1

Microcosm experiment				5mM lactate		
Day	IC mg/L	TC mg/L	TOC mg/L	TOC (mmol/L)	TOC predicted in mg/L	TOC predicted in (mmol/L)
1	1.262	207.2	205.9	5.72	180	5
5	0.327	223.1	222.7	6.19	180	5
9	4.229	217.9	213.6	5.93	180	5
18	0.535	207.9	207.3	5.76	180	5
27	4.983	211.5	206.5	5.74	180	5

Microcosm experiment				10mM lactate		
Day	IC mg/L	TC mg/L	TOC mg/L	TOC (mmol/L)	TOC predicted in mg/L	TOC predicted in (mmol/L)
1	1.992	383.3	381.3	10.59	360	10
5	0.000	378.6	378.6	10.52	360	10
9	1.092	378.2	377.1	10.48	360	10
18	6.378	387.1	380.7	10.58	360	10
27	0.192	371.8	371.6	10.32	360	10

Microcosm experiment				15mM lactate		
Day	IC mg/L	TC mg/L	TOC mg/L	TOC (mmol/L)	TOC predicted in mg/L	TOC predicted in (mmol/L)
1	0.218	582.7	582.4	16.18	540	15
5	1.502	582.9	581.3	16.15	540	15
9	0.152	564.5	564.3	15.68	540	15
18	2.932	573.2	570.2	15.84	540	15
27	0.891	574.9	574.0	15.94	540	15

Microcosm experiment				Blank (10mM)		
Day	IC mg/L	TC mg/L	TOC mg/L	TOC (mmol/L)	TOC predicted in mg/L	TOC predicted in (mmol)
1	0.530	360.5	359.9	10.00	360	10
5	0.000	354.3	354.3	9.84	360	10
9	0.000	357.2	357.2	9.92	360	10
18	0.000	353.8	353.8	9.83	360	10
27	0.000	353.0	353.0	9.81	360	10

Appendix 5.2: Total organic carbon data determined from bioleaching of kaolin added with different lactate concentrations (5 – 20mM)

Microcosm experiment			5mM lactate		TOC predicted in mg/L	TOC predicted in (mmol)
Day	IC mg/L	TC mg/L	TOC mg/L	TOC (mmol/L)		
2	1.495	218.6	217.1	6.0306	180	5
5	0.721	205.0	204.2	5.6722	180	5
10	1.160	192.7	191.5	5.3194	180	5
13	1.646	193.0	191.3	5.3139	180	5
18	0.715	187.8	187.0	5.1944	180	5

Microcosm experiment			10mM lactate		TOC predicted in mg/L	TOC predicted in (mmol)
Day	IC mg/L	TC mg/L	TOC mg/L	TOC (mmol/L)		
2	0.000	376.5	376.5	10.4583	360	10
5	0.822	368.2	367.3	10.2028	360	10
10	0.189	347.8	347.6	9.6556	360	10
13	0.000	344.0	344.0	9.5556	360	10
18	0.000	332.2	332.2	9.2278	360	10

Microcosm experiment			15mM		TOC predicted in mg/L	TOC predicted in (mmol)
Day	IC mg/L	TC mg/L	TOC mg/L	TOC (mmol/L)		
2	2.939	528.3	525.3	14.5917	540	15
5	2.483	529.2	526.7	14.6306	540	15
10	0.000	499.5	499.5	13.8750	540	15
13	0.000	496.7	496.7	13.7972	540	15
18	0.0144	470.6	469.5	13.0417	540	15

Microcosm experiment			20mM			
Day	IC mg/L	TC mg/L	TOC mg/L	TOC (mmol/L)	TOC predicted in mg/L	TOC predicted in (mmol/L)
2	0.673	724.2	723.5	20.0972	720	20
5	0.000	700.7	700.7	19.4639	720	20
10	0.000	670.4	670.4	18.6222	720	20
13	0.000	665.1	665.1	18.4750	720	20
18	0.000	628.9	628.9	17.4694	720	20

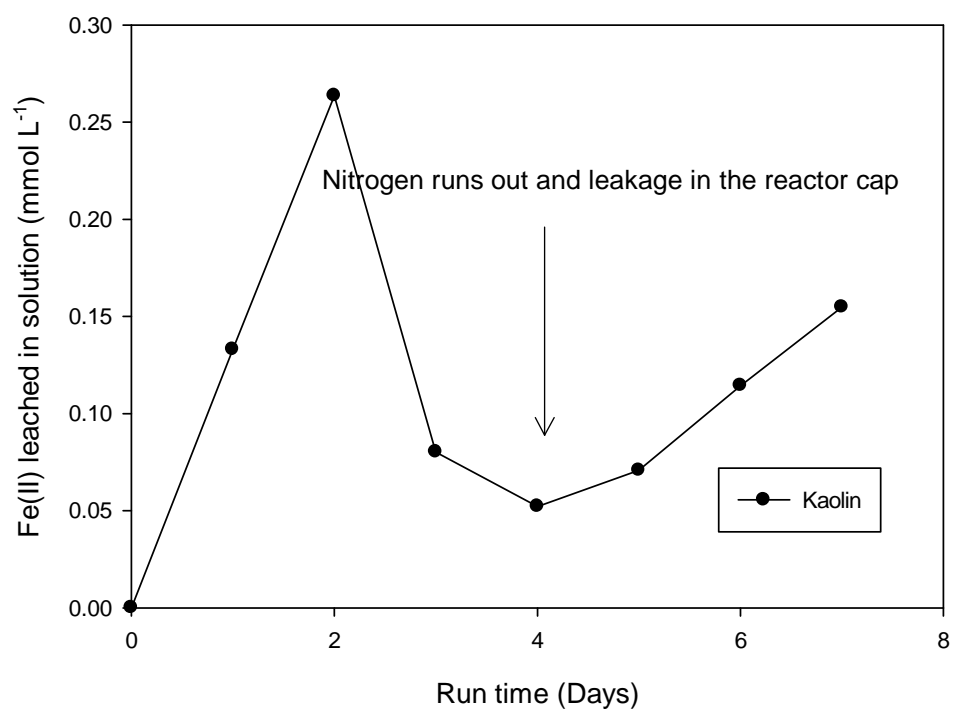
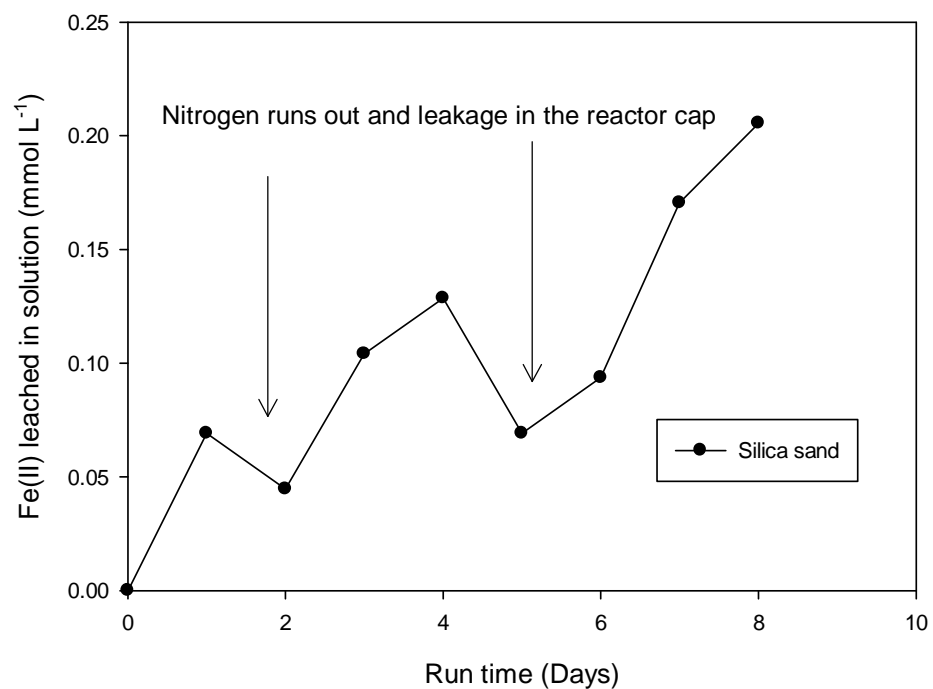
Microcosm experiment			Blank (20mM)			
Day	IC mg/L	TC mg/L	TOC mg/L	TOC (mmol/L)	TOC predicted in mg/L	TOC predicted in (mmol)
2	1.238	759.1	757.8	21.050	720	20
5	0.000	709.5	709.5	19.708	720	20
10	0.000	707.4	707.4	19.650	720	20
13	0.000	705.7	705.7	19.603	720	20
18	1.487	704.6	703.1	19.531	720	20

Appendix 5.3: Total organic carbon data determined from bioleaching of kaolin added with different lactate concentrations (0.1 – 1mM)

Microcosm experiment after 130 hours						
Lactate concentration	IC mg/L	TC mg/L	TOC mg/L	TOC predicted in mg/L	TOC (mmol/L)	TOC Predicted in (mmol/L)
0.1 mM	1.735	22.58	20.84	3.6	0.5789	0.1
0.3 mM	1.19	33.45	32.26	10.8	0.8961	0.3
0.5 mM	2.156	39.83	37.67	18	1.0464	0.5
1.0 mM	2.467	57.12	54.65	36	1.5181	1
Blank (1.0mM)	0.704	39.43	38.72	36	1.0756	1

APPENDIX 6

Appendix 6.1: Preliminary bioreactor result run at room temperature



Appendix 6.2: small scale microcosms experiment with silica sand and kaolin.



Appendix 6.3: Running preliminary experiment at room temperature using 4.5L bioreactor.



Appendix 6.4: Running Experiment for the bioreduction of kaolin in a constant temperature room (30°C).



Appendix 6.5: Running experiment for the bioreduction of silica sand in a controlled temperature room.

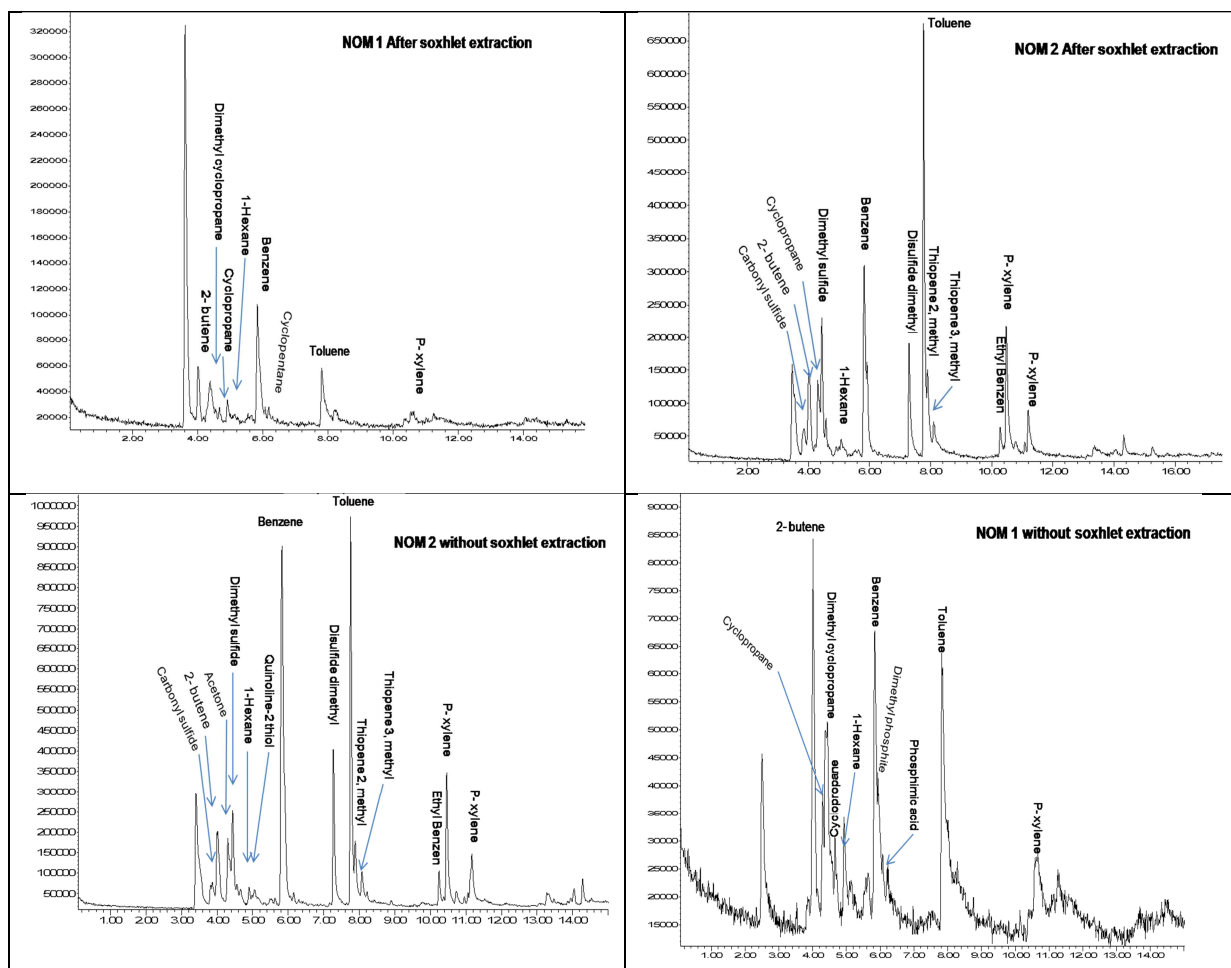


APPENDIX 7

Appendix 7.1: Analyses of kaolin and carbonate standards provided by the industrial partners and comparison of measured L*, a*, b*, ISO Brightness and Whiteness values with the supplied values

Reference	Analysis at	L*	A*	B*	ISO Brightness	Yellowness
GCL53.13	NCL	83	3.53	8.85	53.25	21.3
GCL53.13	WBB	82.95	3.6	9.3	52.73	22.23
<i>Difference</i>		<i>0.05</i>	<i>-0.07</i>	<i>-0.45</i>	<i>0.52</i>	<i>-0.93</i>
GCL58.39	NCL	85.6	4.24	10.15	56.57	23.85
GCL58.39	WBB	87.26	3.8	9.5	60.25	21.84
<i>Difference</i>		<i>-1.66</i>	<i>0.44</i>	<i>0.65</i>	<i>-3.68</i>	<i>2.01</i>
GCL58.75	NCL	86.06	4.1	9.92	57.62	23.18
GCL58.75	WBB	86.89	4	9.7	59.39	22.42
<i>Difference</i>		<i>-0.83</i>	<i>0.1</i>	<i>0.22</i>	<i>-1.77</i>	<i>0.76</i>
GCL60.34	NCL	86.55	3.81	9.13	59.28	21.37
GCL60.34	WBB	87.15	3.7	9	60.5	20.96
<i>Difference</i>		<i>-0.6</i>	<i>0.11</i>	<i>0.13</i>	<i>-1.22</i>	<i>0.41</i>
GCL78.08	NCL	93.71	1.38	5.6	77.67	11.71
GCL78.08	WBB	93.19	1.7	5.9	76.21	12.53
<i>Difference</i>		<i>0.52</i>	<i>-0.32</i>	<i>-0.3</i>	<i>1.46</i>	<i>-0.82</i>
GCL80.99	NCL	94.66	1.29	4.83	80.72	10.13
GCL80.99	WBB	94.65	1.4	5.1	80.56	10.7
<i>Difference</i>		<i>0.01</i>	<i>-0.11</i>	<i>-0.27</i>	<i>0.16</i>	<i>-0.57</i>
Remblend	NCL	92.61	-0.15	6.18	74.9	11.71
Remblend	Imerys	93	-0.19	6.05	75.9	8.8
<i>Difference</i>		<i>-0.39</i>	<i>0.04</i>	<i>0.13</i>	<i>-1</i>	<i>2.91</i>
Snowcal 45	NCL	95.48	0.41	3.04	84.87	
Snowcal 45	Omya	96.3	1.4	4.2	84.4	
<i>Difference</i>		<i>-0.82</i>	<i>-0.99</i>	<i>-1.16</i>	<i>0.47</i>	

Appendix 7.2: Analysis of natural organic matter (NOM 1 and NOM 2) using GC-MS



Appendix 7.3: Elemental analysis of NOM 1 and NOM 2

Sample	% Carbon	% Hydrogen	% Nitrogen
NOM 1	1.62	0.00	0.00
NOM 2	19.05	0.77	0.63